“Studies on a Xerohalophyte - *Suaeda* sp. to decode its molecular adaptations under harsh environmental conditions using proteomics, ionomics and metabolomics approaches”

Thesis submitted to Jawaharlal Nehru University
for award of the degree of

DOCTOR OF PHILOSOPHY

S. WUNGRAMPHA

Stress Physiology and Molecular Biology Laboratory

School of Life Sciences

JAWAHARLAL NEHRU UNIVERSITY

New Delhi – 110067

India

2019

Jawaharlal Nehru University
जवाहरलाल नेहरू विश्वविद्यालय
School of Life Sciences
जीवन विज्ञान संस्थान (एसएलएस)
New Delhi- 110067, India / नई दिल्ली – 110067, भारत
Tel.: +91-11-26704530, 26704512

Certificate

This is to certify that the research work embodied in the thesis entitled "**Studies on a Xerohalophyte - *Suaeda* sp. to decode its molecular adaptations under harsh environmental conditions using proteomics, ionomics and metabolomics approaches**" is the original work of the candidate for the partial fulfilment of the requirement for the award of the degree of **Doctor of Philosophy** and has been carried out in the School of Life Sciences (SLS), Jawaharlal Nehru University, New Delhi, India.

This work is original and has not been submitted so far in part or full, for the award of any degree or diploma of any other university.

Candidate
S. Wungrampha

13/7/19

Dean
Professor K. Natarajan
School of Life Sciences
Jawaharlal Nehru University
New Delhi- 110067
India

12/July 2019

Supervisor
Professor Ashwani Pareek
School of Life Sciences
Jawaharlal Nehru University
New Delhi- 110067
India

Acknowledgement

Nothing comes easy in life; for the fruit of labour is always sweet.

Never had I dreamt for such a day to come in my life. Science was always a passion and biology always my dream. However, not even in my wildest dreams did I imagine to plunged myself into the pursuit for getting a philosophy of doctorate in the field of plant molecular biology. Getting involved into the scientific community not only broaden my understanding on the principles of life but also opened my beliefs on the purpose of life -*we indeed are more than just our genes*. Each of us have a purpose, i.e. to fulfil our dreams and pursue to become a good human being in this chaotic world. To bring me to this understanding of the philosophy of life and also to the world of science, several people are involved. And I felt this is the right platform to thank few of them.

Firstly, I would like to thank my supervisor, *Professor Ashwani Pareek*. He not only opened his lab to let me do my PhD research work but also welcomed me to pursue after my dreams by accepting me as I was. Naïve was I back then when I requested him to teach me the alphabet of plant's stress biology. He not only taught me what stress physiology is all about but, also made me learned several other principles that will not only make me a good biologist but also ease my path in my future professional life. The height I have attained today has so much to do because of him. Along with him, I also would like to thank his better half, *Dr. Sneh Lata Singla-Pareek*. She along with Prof. Pareek helped me several times in solving issues related to my research. They also gave me the opportunity to present my research work in several platforms ranging from national to international conferences moreover they taught me how to present my work to be a winner of the audience.

Secondly, I would like to thank *Professor Govindjee*. He was one of the reasons why I chose to be in the field of plant biology. Back then in 2012 i.e. during my Master's days, the School of Life Sciences in JNU, Professor Govindjee came here as a visiting faculty and taught us plant physiology with special focus on photosynthesis. Since then I got fascinated with photosynthesis and the whole plant kingdom. He also gave me the chance to visit his home in Urbana (2015) for a week during the initial years of my PhD and showed me around the laboratories in UIUC and explained to me some of the work done there. That further added for my passion to do research.

I also would like to thank the CIF staffs, especially *Amar Chand* for helping me in all the works related to instrumentation. *Mr. Manu, Dr. Sandeep* and *Dr. Ajay* from AIRF also have helped me in several of my works. I also would like to thank *Mr. Manoj* from the cash section who helped me in clearing the bills for my field work. The staffs from SLS are amazing and they have helped me in all my administrative work. Special thanks to the eflora.com community who helped me in identifying the species (*Suaeda fruticosa*) with which I did my research.

I would like to thank my team in JNU. Without them, my scientific pursue will be like sailing in the rough sea alone. *Mr. Ramesh* was very helpful in all aspects of my work in the lab. He not only maintained the lab clean but also helped in arranging equipment necessary for my experiments. During my thesis writing, his tea in the lab saved a lot of my time. I would like to thank *Dr. Jeremy*, he not only came along with me for my field work but also shaped my thesis by correcting and giving scientific inputs. *Dr. Rohit* also helped me in completing my

field work studies and also in writing research articles. I would like to thank *Dr. Ramsong* and his wife *Dari* for their friendships which goes beyond the four corners of this lab. It is such friendship that refreshes my mind and motivated me to work persistently in the lab. Dr. Priyanka, Dr. Ashutosh and Mrs. Chhaya also were very helpful friends in the lab, I am grateful to them I would also like to specially thank Khalid, Jayram, Deepti, Anjali and Lokendar for being around when I needed them.

A special thanks to *Mr. Rathore* without him, my field work would have been unimaginable. He was the only one who accompanied me to the field in the middle of nowhere, where heat and loneliness were our only friends. Without any hesitation, he always comes along with me three times a year for the past six years. Together with him, we sacrificed our sleep harvesting the samples and spent the whole 24 hours talking everything under the sun. I would like to wish him the best in life. I also would like to thank all the staff workers there in the Sambhar lake. I might not remember their names but, most of their faces will always be there in my heart whenever I look back at the days and nights spent there.

I would like to thank some of my friends beyond the walls of SLS. *Nathan, Solomon* and *James* are my brothers from different parents. Through thick and thin, they were always there for me. They made my stay in JNU very memorable. I thank God for this beautiful friendship that we all shared which will last a lifetime. The JNUCF community was my strongest support in making me understand the purpose of life. For which, I am always thankful. I also would like to thank *Rossilla* for her constant emotional support. She might have joined late in my pursue to this present work but her presence in my life have boosted me in several ways.

Last but not the least, I would like to thank the most important people in my life, without whom I could never reach where I am now, that is none other than my loving mom and dad. Words cannot express neither feelings can tell how much I owed them for their constant support. Without them, this work is next to impossible. Thank you very much.

Finally, all glory and honour belonged to God, the almighty Father in heaven.

S. Wungrampha

Dedicated to my parents

Table of Contents

Chapter 1

Introduction

In the near future, food and nutritional security are projected to be the greatest problems for the mankind. As per the FAO report (2018), in between 2014 and 2016, about 11% of the total population (accounting to roughly 800 million people) could not meet their daily dietary needs (Dillard, 2019). Further, the UN report (2013) states that the world population is expected to reach up to 10 billion by 2050. To add to the complexity of the situation, agricultural land being used for cultivation is declining rapidly with time. Further, degradation of arable land due to factors such as soil salinization (Shashid et al., 2018; Xie et al., 2019), heavy metal deposition (Jacob et al., 2018), increasing soil alkalinity (Bourrié et al., 2018), drought (Yin et al., 2018), ot flooding (Burn and Whitfield, 2018) has increased over the years (Pareek et al., 2010). Therefore, there is an urgent need to come up with solution(s) to increase the food production by 70% by the year by 2050 and that too by minimizing the use of fresh water (UN news, 2013; Raiten and Combs, 2019).

Under field condition, plants are often subjected to several stress that hinder their growth and development (Joshi et al., 2016; Nongpiur et al., 2016). These stresses can be broadly classified into two categories; biotic or abiotic stress. Biotic stress is caused due to the living organisms such as bacteria, virus, nematodes, insects and fungus. On the other hand, abiotic stress is manifested through physical factors such as high temperature, drought, salinity, and cold (Pareek et al., 2010). Among the various abiotic stresses, salinity stress is one of the stress that has led to severe losses in agricultural lands (Munns and Tester, 2008). Soil salinization is potentially considered irreversible, the effect of which spreads not only on the land but also on the water bodies leading to a severe decline in vegetation around it (Munns and Gilliham, 2015). Several reports regarding soil salinization leading to the loss in agricultural land, vegetation and

economy have come up in recent year (cf. Qadir et al., 2014; UN report, 2014; Vargas et al., 2018; FAO report, 2018). However, a sustainable solution to the problem is still debatable.

Plants, believed to have originated from the fresh water charophycean green algae (Graham et al., 2000), can broadly be categorized into glycophytes and extremophiles depending on their tolerance capacity to tolerate the stress. *Glycophytes* are the plants that are adapted to healthy soils and require fresh water to complete their life cycle. These plants are susceptible to stress and adverse environments, thereby compromising their growth and productivity. On the other hand, *extremophiles* are the plants that are well adapted to the extreme soil/environmental conditions which are quite detrimental to most of the plants (Flowers and Colmers, 2008; Wungrampha et al., 2018).

Halophytes are a special group of plant species comprising nearly 2% of terrestrial plants which can tolerate and complete their life cycle at salinity equivalent to the seawater (Kosova et al., 2013). These group of plant species are widely distributed in the coastal regions, marshy land, swamps and saline semi-deserts (Glenn and Brown, 1999). Tolerance to salinity is a common trait in plants; however, the threshold level of salinity is higher for halophytes than that of glycophytes (Barbour, 1970; Glenn and Brown, 1999; Kosova et al., 2013). Under salinity, plants are exposed to two forms of stress; an early and quick osmotic shock which results due to declining soil water potential followed by ionic stress as salt ions of sodium and chloride enter the plant. This situation leads to a marked disturbances in the cellular homeostasis in plants as salt ions hinder the uptake of essential minerals such as K^+, $Ca^{2+,}$ and Mn^{2+} (Das et al., 2015; Nongpiur et al., 2016, 2019). Some of the anatomical, physiological and molecular response of plants towards salinity, both in glycophytes and halophytes, are described in Wungrampha et al. (2018).

With soil salinization increasing every day, research on halophytes has increased over the years. Several laboratories around the globe have reported

these plants to be a useful for “allele mining” for stress responsive genes (Amtmann, 2009; Flowers et al., 2010; Abideen et al., 2011; Bita and Gerats, 2013). Halophytes are also considered as a group of plant species that hold the genetic resources for developing plants/crops that are tolerant to various abiotic stress (Flower and Colmer, 2015).

1.1 The objective of the proposed work

In recent years, several studies related to understanding the physiology of stress responses (both in glycophytes and halophytes) have been carried out in diverse plant species such as rice (Lakra et al., 2018; Kazerani et al., 2019; Lakra et al., 2019), Arabidopsis (Joshi et al., 2016, 2018; Kudo et al., 2019), tobacco (Purty et al., 2008; Gosa et al., 2019), mustard (Nazir et al., 2019), and halophytes such as *Aeluropus lagopoides* (Barhoumi 2019), *Salvadora persica* (Tounekti et al., 2018), *Suaeda salsa* (Liu et al., 2018), *Mesembryanthemum crystallinum* (Mahmood et al., 2019) and *Atriplex halimus* (Bankaji et al., 2019). In addition, several reports on “allele mining” to dissect more favorable allelic variations of a candidate gene that controls key agronomic traits for potential crop improvement have been done (Kumar et al., 2010; Joshi et al., 2016; Ogawa et al., 2018; Joshi et al., 2018; Inukai et al., 2019). As discussed, halophytes are a group of special plant species that can tolerate a wide range of abiotic and biotic stress with their anatomical, physiological and molecular adaptions (more details on mode of adaptations in halophytes is discussed in Chapter 2). Therefore, several reports on allele mining are available from halophytes (Ogawa et al., 2018; Alqahtani et al., 2019; Bhalaniet al., 2019; Newete et al., 2019) for crop improvement. With this background knowledge, we formulated our work towards understanding the stress physiology of a xero-halophyte that can tolerate not only high salinity but also extremely high temperature. This xero-halophyte is identified as *Suaeda fruticosa* that grows naturally on the bank of Sambhar Salt Lake in Rajasthan (detailed study of the plant and the lake is presented in Chapter 3). The lake is situated in the Thar Desert and receives little or no rain. The temperature in the

area reaches up to 50^{o}C during the peak summer. The water from the lake is used to extract potable salt for human consumption. *Suaeda fruticosa* could tolerate the extreme salinity and temperature of the Lake. To further understand the mode of adaptations that *S. fruticosa* favours both at the molecular and physiological levels, we put forward the following questions:

1. *What are the physiological and anatomical features of the plant which enable S. fruticosa to survive under extreme conditions?*
2. *How is that the plant is able to continue photosynthesis even under extremes of temperature, alkalinity and salinity in soil?*
3. *Since there are large variations in the environmental conditions during the day and across the seasons, what are the changes in the proteome, metabolome and ionome of the plants as affected by these variations?*
4. *Can we develop holistic understanding based on the "OMICS" studies to decode the molecular mechanism associated with stress tolerance in this xerohalophyte?*

The present thesis is an attempt to answer these questions through experimental approaches.

Chapter 2

Review of literature

2.1 Introduction

Plants convert energy from sunlight to chemical energy through photosynthesis that gets converted to food and feeds the world. Thousands of plant species have evolved over million of years and have got adapted to diverse environments such as extreme temperature, drought, high concentrations of salt. Based on their habitats plants are broadly' classified into' two categories, i.e., glycophytes and extremophiles. *Glycophytes* are the plants that grow on healthy soils and require fresh water to complete their life cycle. These plants are highly susceptible to water stress and other adverse environments, which results in compromising their growth and productivity. On the other hand, *extremophiles* are plants that are well adapted to extreme soil/environmental conditions that are detrimental to most of the other organisms on earth. Extremophiles are further categorized as *halophytes* (capable of surviving under high salt concentrations), *acidophiles* (adapted to acidic conditions; pH <3), *thermophiles* (adapted to high temperature), *hypoliths* (lives underneath rocks in deserts), *metallotolerant* (thriving in presence of high concentration of metals like Cu, Zn, Ni, *etc*.), *oligotrophs* (surviving in low-nutrient soils), *cryophiles* (capable of surviving under extreme low temperature) and *xerophytes* (adapted to environment with very little water, like desert).

The sessile nature of plants is one of the primary reasons for their exposure to various stresses under natural conditions (Wungrampha et al., 2018), of which, salinity is one of the most significant abiotic stress that leads to loss of arable land (Munns & Gilliham, 2015). A report from the UN (2014) states that roughly 20% and 2.1% of irrigated and dry cultivable land are affected by salinity, respectively. Further, between 1990 to 2010, salinization of soil has

increased from 45.5 to 62 million hectares and has brought an annual economic loss of 27 billion USD (Qadiret al., 2014). At cellular level, salinity causes severe physiological and molecular imbalances (Figure 2.1), which further disturbs the vital process of seed germination, photosynthesis, respiration and ultimately results in reduced crop yield (Purty et al., 2008; Joshi et al., 2016).

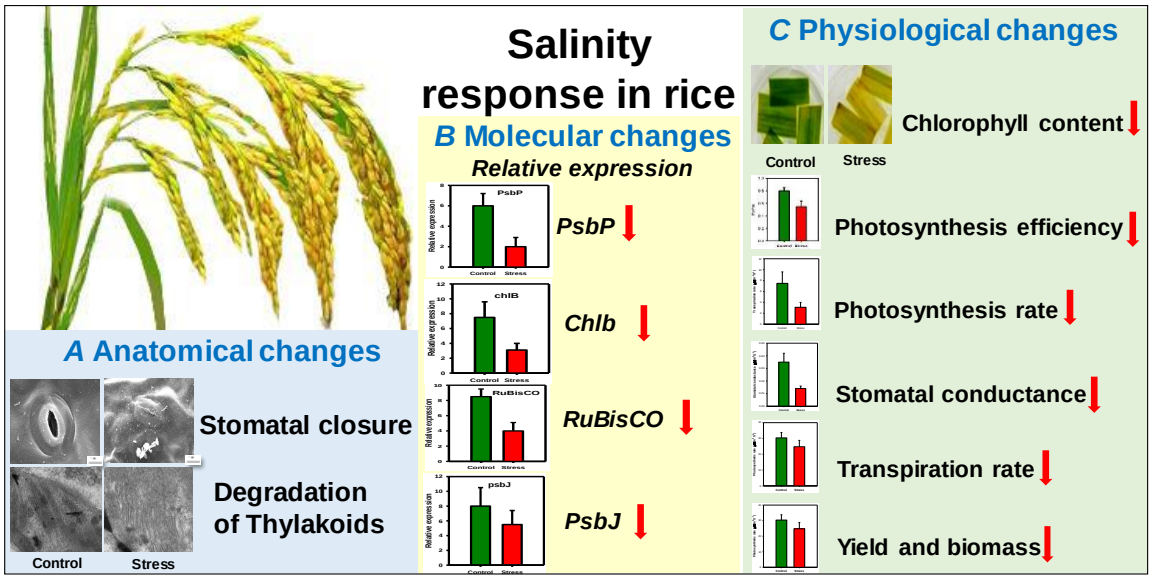

Figure 2.1: Schematic diagram showing representative changes at the anatomical, molecular, and physiological levels in glycophytes such as rice. In plants, changes in anatomical level result in the closure of stomata and degradation of the thylakoid membrane. At the same time, cumulative molecular studies have established the influence of salinity in down-regulating the genes involved in the process of photosynthesis such as photosystem II subunit P (*PsbP*), light-independent protochlorophyllide reductase (*chlB*), Ribulose 1, -5 Bisphosphate Carboxylase/Oxygenase (*RuBisCO*) and Photosystem II extrinsic subunit (*psbJ*). Changes at the physiological level in glycophytes result in a decrease in chlorophyll content, photosynthesis efficiency, photosynthesis rate, stomatal conductivity, and transpiration rate. A reduction in yield and biomass reflects the cumulative result of these changes. Reactive Oxygen Species (ROS) have been found to accumulate under many abiotic stresses in plants, including salinity. A thorough understanding of this process would help in raising plants for the dry and saline conditions.

The effect of salinity on plants comprises of osmotic and ionic stresses. Initially, plants sense a quick osmotic shock as the soil water potential becomes lower than that of the plant. This results in physiological drought of the plant cells.

Secondly, as ionic salts such as Na^+ and Cl^- enters the plant, the ion homeostasis gets disturbed which further hinders the uptake of other essential minerals like K^+, $Ca^{2+,}$ and Mn^{2+} (Das et al., 2015; Nongpiur et al., 2016). Excess Na^+, generally referred to as sodium toxicity, results in marginal yellowing in leaves followed by progressive necrosis. Similarly, excess Cl^- causes premature yellowing and leaf necrosis (Cassaniti et al., 2009). A brief description of the effects of salinity at the anatomical, molecular, and physiological levels in glycophytes is shown in Figure 2.1.

2.2 Salinity and halophytes

Tolerance to saline conditions is a common trait for all plants; however, it is the tolerance threshold that categorizes them into glycophytes or halophytes. In general, plants that cannot survive on >0.5 % of salt concentration are called as glycophytes and plants that can grow well in the saline soils are categorized as halophytes (Figure 2.2a). These plants display vast diversity for their salt tolerance threshold. Whereas some members of this group can grow well in slightly saline soils, others can tolerate salt concentrations equivalent to seawater Halophytes constitute about 2% of the terrestrial plants and are widely distributed in the coastal regions, marshy land, swamps and saline semi-deserts (Barbour, 1970; Glenn & Brown, 1999; Kosova et al., 2013).

The earliest fossil records of the land plants (spores and plant parts) date back to roughly 470 million years; however,evidence for recognizable plants date back to ~40 million years (Flowers et al., 2010). Characean, a slimy filamentous green sea alga, considered the closest relative to higher plants. It can survive both in saline and fresh water (Chapman & Buchheim, 1992). Available molecular evidence suggests that embryophytes evolved about 450 million years ago. By this time, the sea had turned slightly saline. Therefore, the exact time of origin of halophytes is debatable (Chapman & Buchheim, 1992; Flowers et al., 2010). The ability of halophytes to grow in both saline and healthy soils has enabled them to flourish well in diverse environments. These plants have their

representation in almost all the taxonomic groups of plants, ranging from non-vascular bryophytes (Sabovljević & Sabovljević, 2007) to vascular angiosperms (Barbour, 1970). However, the salt tolerance level of these plants varies to a large extent among various plant groups. Dicot halophytes generally require ~250 mM salt concentration for optimal growth and germination, whereas, halophytes from monocotyledons, gymnosperms or mosses usually are sensitive to very high salt concentrations. Though these plants are adapted to flourish in saline environments, germinating seeds and young seedlings of several of them are susceptible to salinity and even ~50 mM salt concentration can compromise seed germination (Flowers et al., 1986; Bell & O'Leary, 2003; Flowers & Colmer, 2008).

Mangrove forests occupy the coastal intertidal zones at low altitudes and harbor diverse plant species ranging from shrubs to tall trees. These plants are sensitive to the saline environment in their early stages of development but require salt for growth and propagation at the later stage (maturity). Therefore, these plants are classified into facultative and obligate halophytes (Wang et al., 2011). Nearly 70% of the Asian population depends on coastal vegetation for food (seafood) and coastal forests for wood and timber, of which contribution of mangroves is enormous. In addition to economic benefits, mangroves have several environmental advantages like coastal resilience (natural shield against extreme conditions like cyclones, ecological disasters or coastal soil erosion), provide habitat for a variety of animals and plants, act as a sink for the pollutants and also contribute in organic/inorganic mineral cycles. Mangroves are also known for large-scale carbon fixation and sedimentation, and the rate of carbon fixation can be as high as 200 gcm^{-2} (Alongi, 2014). Sedimentation of carbon by mangroves never attains saturation level due to its continuous sedimentation and vertical accretion (Hoberg, 2011; Lang'at et al., 2014; Sandilyan & Kathiresan, 2014; Sakho et al., 2015).

With respect to their habitat, mangroves can either be: *true mangroves*, that harbor at the coastal region and do not extend into the terrestrial communities, or mangroves associates, that are distributed in terrestrial and littoral zones (Liang et al., 2008). Mangroves are further classified as red, white, black, or bottom-wood, depending on their salinity tolerance levels and adaptation mechanism and operative in them. Red mangroves are uniquely adapted to saline conditions via developing a prop root system for anchoring firmly at the sandy soil of lower inter-tidal and sub-tidal region of the shore. These also are salt excluder species, deposit excess salt in the leaves and fruits. Black mangroves occupy the area just after the red mangroves towards the inland. These are uniquely adapted to their surrounding by developing pneumatophores root system (Figure 2.2b). In contrast to the above types, white mangroves are found in the marsh area, and bottom-wood mangroves occupy the upland fringes of mangroves habitation. These are considered as mangroves associates as they don't have the morphological features, like root aeration, salt balancing, vivipary, *etc*., that a true mangrove has (http://www.sms.si.edu/irlspec/Mangroves.htm) (accessed 22.11.18).

2.3 Classification of halophytes

Since the earliest reports on halophytes(Crozier, 1892; Barnes, 1898), significant efforts have been made to define and classify halophytes, recently reviewed by Grigore et al. (2014). Broadly, halophytes can be classified into various categories depending upon the level of salinity tolerance, mechanism of salinity tolerance, uses as cash-crops or their remediation ability.

2.3.1 Based on the level of salinity tolerance and requirement of saline environment for growth and propagation, halophytes have been categorized into three groups.

i) Habitat-indifferent/supporting halophytes: Plants of this group are capable of growing in the saline environment but do not show optimal

growth. These plants can be classified as tolerant in comparison to glycophytes, e.g. *Chenopodium glaucum, Myosurusminimus, Potentilla anserina*, etc.

ii) Facultative halophytes: These plants can thrive well at both low and moderately high salt concentrations, e.g. mangroves, *Glaux maritima, Plantago maritima, Aster tripodium*, etc.

iii) Obligate halophytes: These plants require higher salt concentration for their normal growth and development. Though they can grow in freshwater/low salt conditions, their growth is not optimal, and several of them are unable to complete their lifespan in freshwater conditions, e.g. *Atriplex halimus*, *Mesembryanthemum crystallinum*, etc. (Barbour, 1970; Sabovljević & Sabovljević, 2007; Wang et al., 2011; Hasanuzzaman et al., 2014).

2.3.2 Based on the mechanism of salinity tolerance, halophytes can be classified into the following categories.

i) Succulent: These plants can store salt in the vacuole and accumulate a large amount of water in the cytoplasm of the leaf cells. Accumulation of salts helps the plant to maintain the negative turgor pressure needed for water-mineral absorption from the saline soil. Storage of a large amount of water in the plasma membrane also helps to keep the salt concentration low and diluted, e.g. *Aloe vera, Cactus, Suaeda sp*., etc.

ii) Absalztypen: These plants have salt glands and salt pockets on the surface of the leaf and/or shoot. They accumulate salt in the salt pockets that help to maintain turgor pressure and excrete the excess salt through salt glands, e.g. *Tamarix aphylla*.

iii) Root filtered type: These plants have a special non-metabolic salt filtration system in the roots that filters the solution efficiently to prevent the

passage of excess ions to the xylem. The filtration system is made up of lipid membrane and phosphatidylcholine (phospholipid linked to choline), e.g. red mangroves. Some plants deposit lignin or suberin in the endodermal root cells, and their Casparian strips are closer to the root tip. These plants also filter the soil solution effectively for salts, e.g. *Prosopis*.

iv) Divergent-halophytes: These are plants that are grouped under halophytes because of their salinity tolerance level but cannot be categorized into any of the categories as mentioned above. The salt that is absorbed along with the mineral water in these plants gets accumulated in the tissues, but by the time the salt concentration attains a threshold value of tolerance, it completes its life cycle, e.g. *Juncus gerardii* (Sabovljević & Sabovljević, 2007).

2.3.3 Based on the commercial uses, halophytes can be placed in the following four categories.

i) Vegetable crops: Several species of halophytes are consumed for centuries by humans, especially living in coastal regions, e.g. *Salicornia* sp., *Portulaca oleracea, Crithmum maritimum, Aster tripolium*. Several other plants are being explored as sea vegetables/food such as *Batis maritima, Sarcocornia sp., Plantago coronopus, Mertensia maritima, Atriplex prostrate, Salsola soda, Crambe maritima*, and *Chenopodium quinoa*. These plants hold a promising future for sustainable agriculture without the use of fresh water and arable land (Ventura & Sagi, 2013; Ventura et al., 2015).

ii) Oilseeds/Bio-energy crops: Halophytes are being explored for their use as a source of renewable energy (Sharma et al. 2016). Oilseed crops like *Salicornia bigelovii* and *Kosteletzkya pentacarpos* can be used for biodiesel production, whereas, halophytes that produce a large amount of

lignocellulosic biomass like *Tamarix* sp. can be used for the production of ethanol or other forms of liquid biofuels (Ventura & Sagi, 2013).

iii) Fodder crops: Though salt accumulation reduces the nutritional value, several strategies are being explored to use halophytes as fodder. Few halophytic grasses restrict salt deposition/entry in the leaf and maintain low Na^+/K^+ ratio, which provides higher caloric value for foraging animals. Some of these grasses are also rich in proteins, e.g. *Atriplex* sp., *Salicornia bigelovii*, etc. (Ventura et al., 2015).

iv) Medicinal crops: Halophytes are rich in bioactive compounds like vitamins, carotenoids, terpenes, glycosides, polyunsaturated fatty acids, and phenolic compounds, and are well known for accumulation of anti-oxidizing agents, Reactive Oxygen Species (ROS) scavengers (Duarte et al., 2013) and readymade catabolic products (Werner & Witte, 2011). Several of them that includes *Mesembryanthemum edule*, *Crithmum maritimum, Salicornia sp., Aster tripolium, Salicornia herbacea, Plantago major* and *Zygophyllum album* are being used either traditionally and/or in the modern medical industry (Ksouri et al., 2012; Ventura et al., 2015).

2.3.4 Based on their capability to remediate saline soils, halophytes have been categorized into three groups.

i) Accumulators: These plants absorb salt from the saline soil and accumulate it in the vacuoles or other specialized organs. Because of high salt concentration in the above-ground biomass, they may not be appropriate for use as forage or development of value-added products, but these are highly preferred to remediate the saline soil, e.g. *Atriplex sp., Spartina alterniflora*, and *Amarix petandra*.

ii) Excluders: Plants of this group have developed various mechanisms to exclude/filter salts from entering into the plant tissues, e.g. *Rhizophora* sp. and *Prosopis* sp.

iii) Conductors: Plants belonging to this group absorb salts along with water from the saline soil but do not store absorbed salt in the plant organs. These plants transport the salts to the exposed surface of above ground biomass, from where it is dispersed with the winds. These plants are preferred for soil remediation, e.g. *Tamarix aphylla, Avicennia marina*, etc. (Yensen & Biel, 2006; Grigore et al., 2014).

2.4 Adaptations in halophytes

Adaptation is foremost for survival of a species and includes the traits that have evolved through natural selection. Charles Darwin theory on the survival of the fittest solely depends on adaptive fitness. It is only through adaptation that any species can occupy and flourish in its ecological niche overcoming the natural selection. It may take only a few years or even up to thousands of years for a plant species to establish an adaptive trait that helps it to survive in the changing environment. Adaptive changes that involve permanent modification of structural features, genetic adjustments, and are heritable can be described as long-term adaptations. On the other hand, the temporary changes in the structure/physiology that are not inherited are described as short-term adaptations (Duarte & Ferreira, 1995). When growing in the same unfavorable environment, various plant species share a common trait of physiological responses such as high root:shoot ratio, low photosynthetic activity, low tissue turnover, stunted or slow growth rate, etc. This phenomenon of common physiological responses by several species growing in the same unfavorable environment is called Stress Resistance Syndrome (SRS). Growth trait and SRS are physiologically linked, and therefore any alteration in the growth traits will show pleiotropic effects on SRS, thereby leading to the evolution of new species that perform better in response to a new environment (Chapin III et al., 1993).

Adaptations of halophytes in response to environmental conditions can be categorized into morphological, physiological, and genetic adjustments. Details of these adaptations are presented in the following section.

2.4.1 Morphological adaptations

Morphological features of an organism are the first visible characters and are attained through adaptation to occupy its ecological niche. For example, plants that occupy the savannas usually have longer root systems to absorb water, thick bark to survive during a forest fire, and a smaller number of leaves to reduce water loss. The arctic plants have shallow root systems to penetrate the thin layer of soil, reduced leaf area and number (for the conservation of water), short and clustered architecture and grow very close to the ground to resist the cold. The morphological features that halophytes have developed over millions of years of evolution for their survival in the extreme environment are as follows:

2.4.1.1 Succulent features

For survival under arid conditions through retaining water, some plants have developed the ability to store water in their body parts like shoots, roots and/or leaves (Figure 2.2c) and are categorized as succulents. Further, depending upon the organ used for water storage, these can be categorized as leaf, stem and caudiciform (base/trunk/root) type of succulent (Nyffeler et al., 2008). During the favorable conditions, succulents store a massive amount of water and nutrients in their tissues and are used for growth and metabolism during unfavorable conditions (Williams et al., 2014). In succulent leaves, a specialized parenchymatous tissue is present beneath the photosynthetically active chlorenchymatous tissue, which stores water (Chiang et al., 2013). In plants like Cacti and Agave, the two layers are separated spatially, which gives rise to an electrical analog character of capacitance. This arrangement reduces the rate of transpiration up to 34% and 37% respectively. Several of these plants have developed specific adaptation in their metabolism, i.e. Crassulacean Acid

Metabolism is discussed in section 3.2.5. To maintain an efficient hydraulic system in the succulent organs, these plants have developed three-dimensional (3D) venation pattern. 3D venations have evolved several times via distinct developmental pathways. It reorganizes the internal leaf distances and maintains sufficient vein density for efficient transport of water and minerals, and their storage across the leaf to be used during the dry season (Chiang et al., 2013; Griffiths, 2013).

2.4.1.2 Salt glands

The salt gland is a special tissue present on the epidermis of the halophytes that helps the plant in exporting excess salt ion from its tissue to the surface at the expense of energy. Structurally, it is made up of three types of cells; the collecting cells, which connect directly to the mesophyll cells; the stalk and the secretory cells, which directly excrete the salts from its pores (Figure 2.2c). Whereas these glands predominantly secrete sodium and chloride ions (Tan et al., 2013), there are reports that these glands are also capable of removing divalent ions like calcium (Ca^{2+}) and magnesium (Mg^{2+}), e.g. *Tamarix aphylla* (Thomson et al., 1969). In some halophytes like *Aegiceras corniculatum* and *Avicennia marina*, salt glands not only excrete excess salt but also help in water uptake during salinity. In these plants, increasing soil salinity from 50 to 500 mM leads to an increase in uptake of water to 90% (Tan et al., 2013).

2.4.1.3 Vesiculated trichomes

Trichomes (Trichos, the Greek word for hair) are small hairy epidermal cell outgrowths present on the surface of stem and leaf. These outgrowths result from the process of endo-reduplication (Hulskamp, 2004), which is a special type of cell cycle where the mitotic pathway is switched on, leading to continuous DNA replication without cell division. This process ultimately leads to polyploidy (Yoshizumi et al., 2006). Trichomes can be unicellular or multicellular. Broadly, trichomes are categorized into two types, glandular or non-glandular. The

glandular trichomes secrete a mixture of chemicals like essential oils, phenols, and phenol oxidizing enzymes (polyphenol oxidase) and acysugar that help the plants in combating pests and insects (Peter & Shanower, 1998). These secretions also protect the plants from various environmental stress conditions like UV, heat, and cold (Hulskamp, 2004).

Halophytes have evolved a unique type of trichome structures, which is made up of a stalk and a sphere-shaped bladder cell. These are called as vesiculated trichomes. The stalk can be unicellular to multicellular, whereas, the bladder is unicellular (Figure 2.2e). During development, the bladder cells increase its size more than the stalk and attain a big size. It has a large vacuole and small cytoplasm. The cytoplasm contains small vesicles that are hydrolyzed at a later stage (Smaoui et al., 2011). These trichomes sequester the excessive salt in the vacuoles within the bladder cells. Upon attaining a certain threshold of salt concentration, bladder cells rupture and release the salt to the external environment. The movement of salt from the stalk to the bladder cell is through a symplastic movement along the plasmodesmata. Several vesiculated trichomes vary with the developmental stage of the plant organs. The younger leaf has more vesicular trichomes than the older leaves. The number of trichomes also increases in response to the increase in salt concentration, high light intensity, and aeration on the leaf surface (Smaoui et al., 2011).

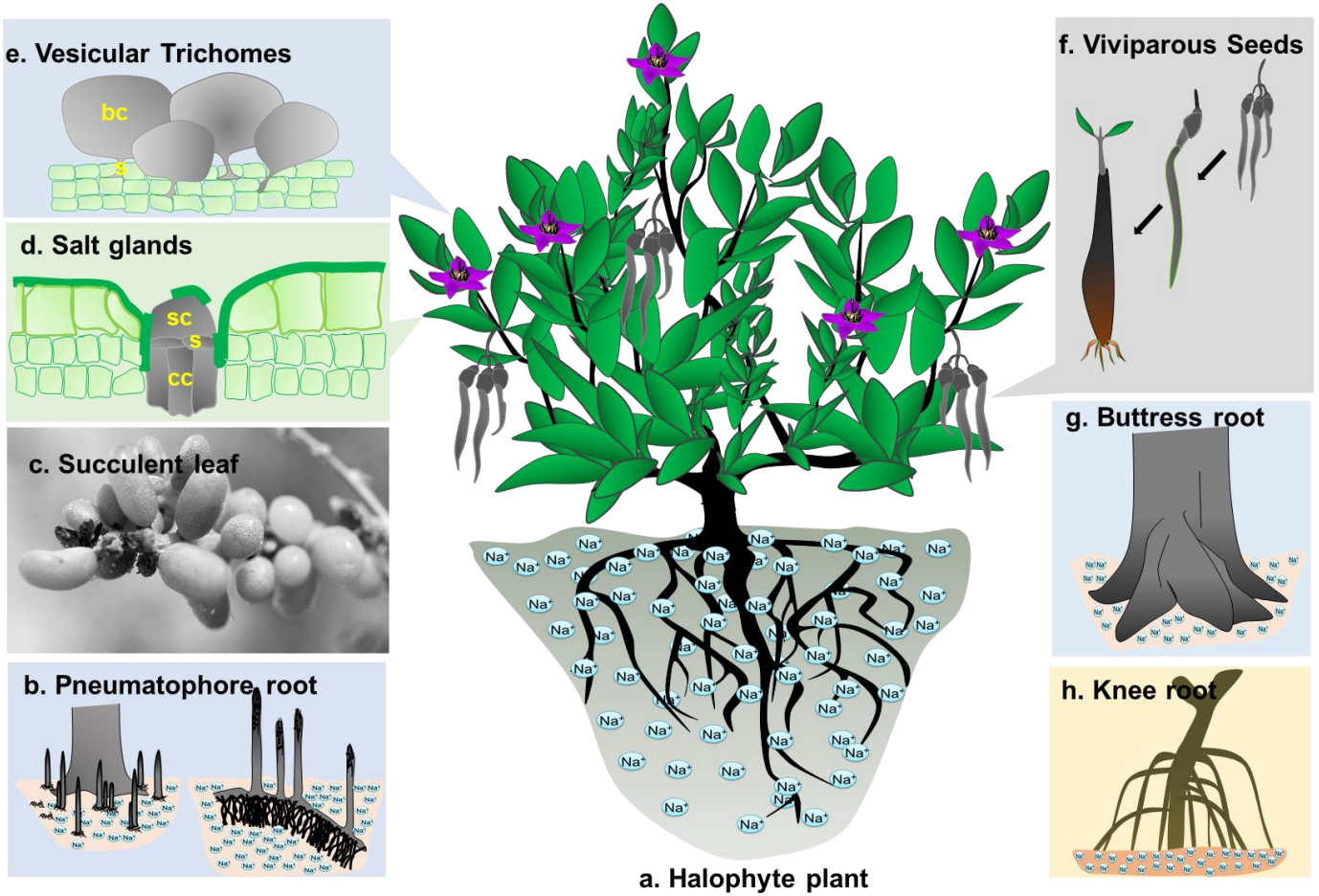

Figure 2.2: Morphological adaptation in Halophyte. (a) A model halophyte. (b) Pneumatophore root (c) Succulent leaf (d) Salt gland comprises of three types of cells; the collecting cells (cc), the stalk (s), and the secretory cells (sc). (e) Vesiculated trichomes which are made of the stalk (s) and a sphere-shaped bladder cell (bc). (f) Viviparous seeds. The seeds germinate before abscission from the parent plants. (g) Buttress root (h) Knee root

2.4.1.4 Vivipary

The phenomenon of seed germination before abscission from the parent plants is called vivipary (Figure 2.2f). It can be categorized as true or pseudo-vivipary. If the plantlets are formed as a result of *in situ* germination of seeds formed through the sexual reproduction, it is called as true vivipary, e.g. members of Poaceae, mangroves like *Bruguiera gymnorrhiza*, *Rhizophora mangle* and *Avicennia marina*. It is predominant in the marine habitats. In these species, the embryo does not enter into the dormant phase, and even if it does, it is only for a short time. It reduces the resting period of the seeds, which germinate when still in the fruit attached to the parent plant. The size of the plantlets at the time of their separation from the parent plant varies among species (Vega & Rúgolo de Agrasar, 2006). This phenomenon protects embryos from the harsh saline environment of the soil (Cota-Sanchez et al., 2007). On the other hand, several plants develop vegetative buds that grow to form plantlets as a result of asexual reproduction, called as pseudo-vivipary e.g. *Agave, Posidonia, Polygonum*, and *Phormium*. Plants having the pseudo-vivipary type of asexual reproduction are more common in alpine, temperate and arid habitats, which helps in the conservation of advantageous gene combinations useful for the plant to tolerate stress conditions or adapt to harsh environments (Vega & Rúgolo de Agrasar, 2006). Several woody mangroves, though are tolerant to salinity at maturity but are sensitive to saline soils at seed germination and seedling stage. These plants have evolved vivipary to overcome this sensitivity and therefore, their seedlings do not face the saline soils. The seeds of these plants have large propagules for storage of nutrients and salts, which enables it to propagate in high salt water. In obligate halophytes, the storage salt from the propagules is used during germination when grown under fresh water (Wang et al., 2011).

2.4.1.5 Dimorphic seeds

Seed dimorphism is a phenomenon of developing two types of phenologically different seeds from a plant at the same time. Some of the halophytes employ

production of dimorphic seeds to escape the saline environment during germination and may help in their dispersal too. Mangroves, that are in direct contact with the sea water, encounter a constant change in their microenvironment. For example, high tides deposit more salts in these regions that increase the salinity levels while during the rainy season, salinity levels decline because of the rainwater pouring in. The similar phenomenon is also observed in the saline desert soil. Production of dimorphic seeds helps the plants to propagate themselves in the changing environmental cycle (Khan & Bilquees, 1998). *Atriplex triangularis* (Khan et al., 1998), *Arthrocnemum indicum* (Khan & Bilquees, 1998), *Suaeda splendens* (Redondo-Gomez et al., 2008) and *Suaeda aralocaspica* (Wang et al., 2008) are a few examples which produce distinct dimorphic seeds. These plants produce brown and black colour. Black seeds are sensitive to salinity, temperature, and high light intensity, and undergo a dormancy period, a phenomenon generally known as the "Cautious" germination strategy (Gutterman, 1993). In contrast, brown seeds are heavier and can germinate quickly. These seeds can tolerate a wide range of environmental conditions. They can germinate even at the salt concentration as high as 1000 mM (Khan & Bilquees, 1998). This phenomenon is known as “Opportunistic” germination strategy (Gutterman, 1993).

2.4.1.6 Root modifications

In the coastal regions, seawater deposits a high amount of salt that compromises the growth of microorganisms in the soil. Waterlogging is another common feature of the coastal soils. Increased salinity and waterlogging leads to depletion of oxygen content in the soils and causes physiological drought and hypoxia. These conditions ultimately can lead to rotting of roots, spreading of diseases, and low yield (Barrett-Lennard, 2003; Hayashi et al., 2013). Plants growing in these areas have evolved to develop a unique root system “pneumatophore” that help the plant to conquer salinity and hypoxia (Figure 2.2b). Pneumatophores are modifications of the roots that grow upwards, against the gravity, and protrude

out from the soil for aeration, e.g. *Sonneratia alba* (Krauss et al., 2003). Spongy tissue structures "lenticels" are present on the surface of pneumatophores that help in gas exchange (Purnobasuki & Siuzuki, 2005). Apart from nutritional uptake, mangrove roots need to hold fast themselves on the soft wet ground and therefore, have developed several modifications. Some of the examples include buttress roots, prop roots, or knee roots. Whereas buttress roots are the large shallow roots that are spread around the primary root (Figure 2.2g), prop roots arise from the stem to support the plant to hold fast on the ground, e.g. *Rhizophora mangle* (Ellison & Farbsworth, 1990). Knee roots are the superficial root forms like an elbow or knee (Figure 2.2h), e.g. *Bruguiera gymnorrhiza* (McCusker, 1971). In all the systems, the root hangs in the air to get direct air from the atmosphere (http://www.wettropics.gov.au/mangroves-info) (accessed 22.10.18).

2.4.2 Physiological adaptations

Halophytes have developed several physiological and/or biochemical strategies that help plants to flourish well in saline soils. Most of these strategies target regulatory control to maintain the desired osmotic pressure (Koyro et al., 2013). This includes accumulation of organic/inorganic molecules in the vacuole, storing water in the vacuole, depositing compatible solutes in the cytoplasm, osmolyte accumulation, compartmentalization of toxic ions or release of free radical scavengers in the cytoplasm (Figure 2.3a) (Binzel et al., 1988; Glenn & Brown, 1999). A comparative schematic diagram of halophytes and glycophytes under abiotic stress are given in Figure 2.2. The major physiological adaptations of halophyte are discussed here.

2.4.2.1 Ion inclusion and exclusion

Maintenance of ionic balance at a certain threshold level is essential for plant growth and development. Under saline conditions, plants accumulate ionic salts like Na^+ and Cl^- ions in the cytoplasm in large amount that causes ionic

imbalance. Excess Na^+ in the leaf causes stomatal closure that leads to a reduction in transpiration rate. Na^+ also interferes with several K^+-cofactor enzymes and inhibit K^+ metabolism. It also displaces the membrane-bound Ca^{2+}, which is important for cell signaling, This results in elevation of Na^+/K^+ ratio in the cell which further leads to activation of caspase-like molecules having role in programmed cell death (Duarte et al., 2013). Accumulation of toxic salt further hinders the uptake of useful mineral ions like K^+, Mg^{2+}, and Ca^{2+} (Khan et al., 2000).

For glycophytes, accumulating Na^+ above the average threshold level of 90-120 $\mu molg^{-1}$ fresh weight is considered toxic and known to cause several physiological and mechanical imbalances (Figure 2.3b) (Fortmeier and Schubert, 1995; Nublat et al., 2001). But, halophytes have evolved several barriers to check the entry of excess Na^+ and Cl^- (Sabovljević and Sabovljević, 2007). Some endogenous plant growth promoting rhizobacteria (PGPR) associated with halophytes secrete exopolysaccharides that not only neutralizes the cation but also helps in forming a biofilm that restricts the entry of excess Na^+ in the plant tissues (Qin et al., 2016). Halophytes maintain high K^+/Na^+ ratio in the cytoplasm, which inturn blocks the entry of more salts into the cytoplasm, a mechanism known as ion exclusion (Koyro et al., 2011). In plants, water uptake and movement occur from higher water potential to lower water potential. An increased concentration of salts in the soil reduces its water potential and therefore, interferes with the water uptake by the plants. To enable water absorption from the ground that has low water potential, halophytes adapt a unique “ionic inclusion mechanism” wherein; it accumulates excess NaCl in the cell vacuoles. Whereas such a high concentration of salt in the cytoplasm is toxic (Türkan & Demiral, 2009), transport and storage of these salts in vacuole help to lower the water potential of the cell. *Suaeda maritima* possess large vacuole, which occupies nearly 77% of the mesophyll cell and enables salt storage up to 500 mM concentration (Hasanuzzaman et al., 2014). Lower water potential in the cell as compared to the soil helps in water uptake the by plant tissues (Koyro et

al., 2011). Some of the excess salts are also deposited in the pocket/bladder gland present in the shoots. Accumulation of salts in the tissues reduces the turgor pressure by lowering the water potential of the halophytes more than that of the soil, which in turn helps in water and mineral uptake even under the high saline environment (Hasegawa et al., 2000; Khan et al., 2000).

2.4.2.2 Accumulation of metabolites and osmolytes

To maintain the osmotic balance, plants accumulate various organic compounds in their cells. These molecules also called osmolites are not charged and do not interfere with the general metabolic processes of the cell. They protect the membrane structure and regulate the osmotic balance within the cell. Some of these molecules are hydrophobic in nature and act as osmoprotectants by enveloping around the proteins, organelles, and cell membrane (Huchzermeyer et al., 2004). Most common osmolytes include proline, sugars and glycine (Huchzermeyer et al., 2004; Koyro, 2006; Ramakrishna & Ravishankar, 2011).

In response to salinity stress, plants trigger the accumulation of proline to very high concentrations, which in turn help plants to tolerate salinity stress. Proline is an efficient quencher of O_2^- and therefore, acts as a strong antioxidant molecule. It has been observed thatexogenous supply of proline improves the antioxidative activity of some enzymes and help the plant to adapt to saline conditions (Hoque et al., 2008; Ahmed et al., 2010; Deivanai et al., 2011). The level of proline accumulation is directly linked to abiotic stress, such as salinity or heat. In response to salinity levels of ~600 mM, proline accumulation increases by 70 and 100 fold in Mediterranean halophytes, *Inula crithmoides*, and *Plantago crassifolia*, respectively (Pardo-Domènech et al., 2015). Aquatic halophytes like *Ruppia megacarpa, Ruppia polycarpa*, and *Ruppia tuberose* accumulate high

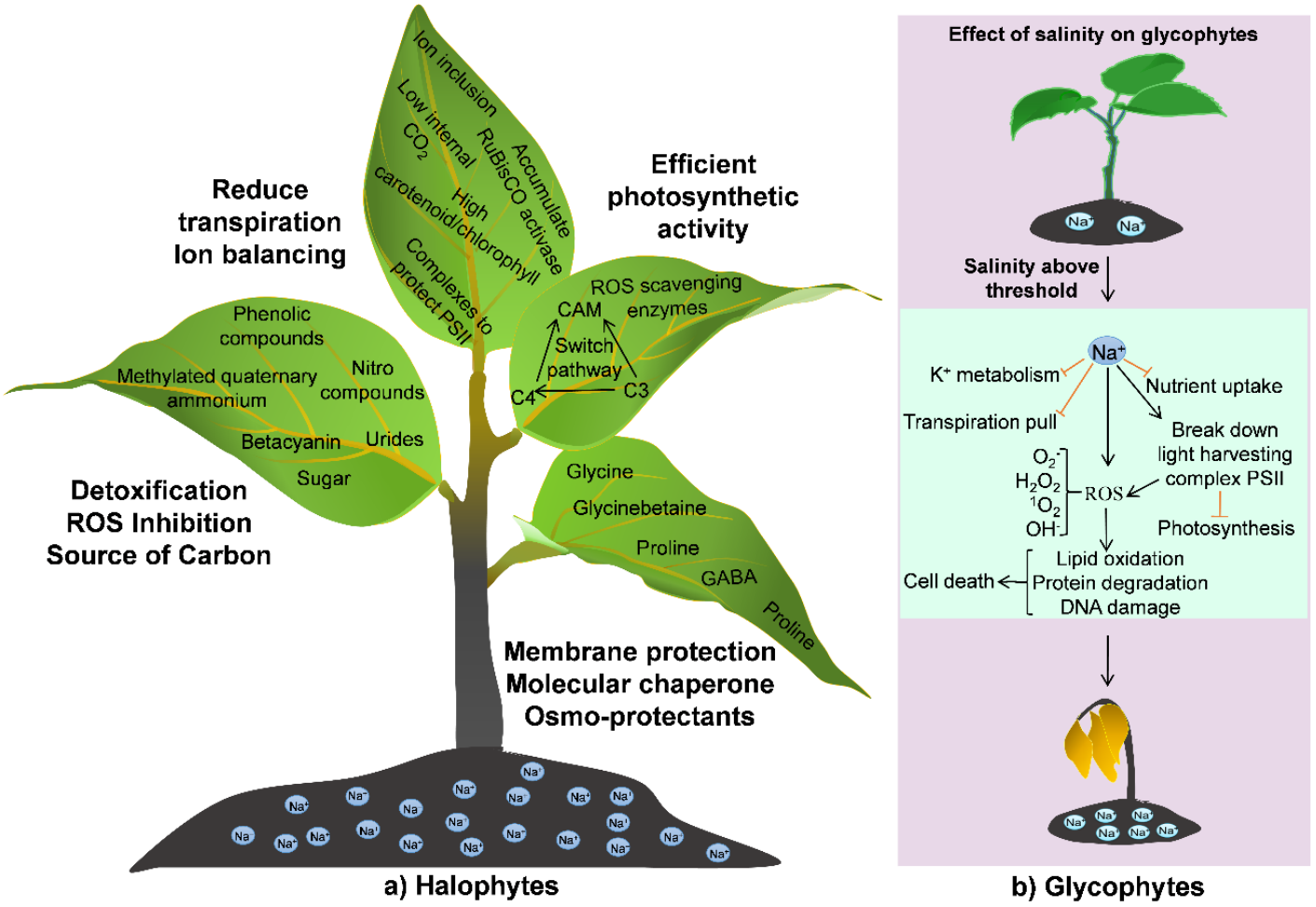

Figure 2.3: Comparative physiological response in halophyte and glycophyte plants. a) Model of a halophyte plant showing physiological adaptations to salinity. b) Model of a glycophyte plant showing effects of salinity on its various physiological aspects.

amount of organic solute (proline) in the cytosol to protect itself from salinity-induced damage. It is estimated that the organic proline solute occupies ~50% of the total solutes in the cytoplasm (Brock, 1981). In *Triglochin maritima*, the dry shoot weight has 10-20% proline constituting maximum amino acid from the pool (Steward & Lee, 1974).

An elevated amount of glycine, a quaternary ammonium compound, leads to enhanced tolerance to abiotic stress. These metabolites help in stabilizing complex proteins by intervening in transcription and translation machinery. Indirectly, it also induces H_2O_2 signaling by enhancing catalase expression (Park et al., 2007). Under stress, glycine is accumulated in large concentration in the chloroplast, where it protects the thylakoid membrane and enhance the photosynthetic activity (Ashraf and Foolad, 2007). Further, it has been reported to play a significant role in the recovery of plants from photoinhibition caused by high light and salinity (Holmstrom et al., 2000). In *Suaeda fruticosa* and *Inula crithmoides*, accumulation of glycine in response to salinity stress can reach up to 500 $\mu molg^{-1}$ and 300 $\mu molg^{-1}$of dry weight, respectively (Gil et al., 2014).

Further, it has been reported that the tolerance threshold of the plants that accumulate glycine is much higher as compared to the plants that accumulate proline in response to salinity stress (Gil et al., 2014). *Atriplex griffithii* accumulates glycine betaine, a quaternary ammonia compound in the cytoplasm which acts as an osmoprotectant as well as balances the osmotic pressure build-up by the salt (Khan et al., 2000). The plant produces anthocyanin under light stress and betacyanin under salt, thermal and anoxia conditions. In halophytes like *Halimione portulacoides, Sarcocornia fruticosa*, and *Sueda salsa*, a large amount of betacyanin is released that helps in detoxification and scavenging ROS (Duarte et al., 2013). Phenolic compounds, tocopherol, carotenoids, vitamins, or polyphenols are other compatible solutes that help plants to detoxify the ROS. Tocopherol and carotenoids protect the lipid membrane by reducing

the fatty acyl peroxy radicals through chemical scavenging and/or physical quenching (Reginato et al., 2014).

Several soluble sugars like sucrose, glucose, or fructose also accumulate in plants in response to salinity conditions. These sugar metabolites help the plants under various stress conditions like salinity cold and drought. Further, they regulate gene expression and signaling during stress (Yuanyuan et al., 2009). The principal function of soluble sugars is to act as a metabolic source of energy for plants. Under environmental stress, large sugar molecules, such as sucrose, break down to glucose and fructose for metabolic use. Some of these smaller molecules are inter-converted to sugar hormones that further help in regulation of gene expression and cell signaling. Low sugar levels in leaves lead to an up-regulation of photosynthesis and promotion of carbohydrate synthesis (Rosa et al., 2009). Fructan, a carbohydrate, osmotically balances the plants by converting to hexose under dehydration and freezing. Raffinose, a family of the oligosaccharides, protects the membrane by acting as free radical scavenger under high salinity stress (Krasensky & Jonak, 2012). High level of sugars and polyols are detected in most of the halophytes under any level of salinity. Unlike the dicot halophytes, the monocots store a high amount of sugars as an osmoprotectant, mainly sucrose that constitutes up to 50-80% of the total soluble sugars. In mangroves, high accumulation of polyols such as mannitol, pinitol or inositol, has been reported (Gil et al., 2013).

2.4.2.3 Accumulation of readymade catabolic products

Several halophytes like *Salicornia* sp., *Thellungiella halophila*, accumulate readymade catabolic products in its shoot that help them to adapt to high saline and low nutritional soil (Kant et al., 2008; Ventura et al., 2010). Soluble nitrogen (up to 250 mM) and various forms of nitro-compounds such as ureides, methylated quaternary ammonium compounds or imino acid accumulate in the cytosol (Steward & Rhodes, 1978). Ureides are the major nitrogen-transportable compounds (allantoin and allantoate) in plants. These are rich in nitrogen

(4N:4C) and are very advantageous to plants as they minimize the loss of photosynthetic carbon energy product in transporting nitrogen from roots to shoots. Many plants accumulate ureides in response to stress like salinity, senescence, and high NH_4 concentrations to supply nitrogen (Zrenner et al., 2006; Ventura et al., 2010).

2.4.2.4 Regulation of Reactive oxygen species

Reactive oxygen species (ROS) describes a group of reactive molecules and/or free radicals that are derived from molecular oxygen. These molecules are produced as a by-product from various metabolic reactions in the cell and act as molecular messengers. Some of the common ROS that is found in the plants include superoxide anion (O_2^-), hydrogen peroxide (H_2O_2), singlet oxygen ($^1O_2$) and hydroxyl radicals (OH^-) (Mittler et al., 2004; Asada, 2006; Sharma et al., 2012). When produced in excess, ROS leads to oxidation of lipids and carbohydrates, protein denaturation, pigments breakdown and/or DNA damage and may ultimately result in cell death (Bose et al., 2014; Reginato et al., 2014).

Stress escalates the production of ROS that helps to maintain cellular homeostasis of the plant (Foyer, 2005; Sharma et al., 2012; Reginato et al., 2014). Under salinity, there is substantial impairment of energy that hinders the flow of electrons to the quinone pool of electron transport chain in photosynthesis. This occurs due to the dissipation of high energy at the light harvesting complex, PSII and limits CO_2 fixation. The free energy and electrons ultimately lead to the production of ROS (Mittler et al., 2004; Duarte et al., 2013). In several halophytes, the production of ROS decreases drastically under long-term salinity stress. In response to salinity stress, halophytes activate superoxide dismutase (SOD) that converts the superoxides to less toxic ROS molecules like H_2O_2, or an ordinary molecule, O_2 (Jithesh et al., 2006; Bose et al., 2014; Reginato et al., 2014). In *Sarcocornia fruticosa*, increased level of SOD and H_2O_2 is also accompanied by increased levels of glutathione peroxidase (GPx) enzyme. This enzyme helps in detoxifying the H_2O_2 molecules by breaking them

down into water molecules. It also helps in reducing the lipid hyperoxides to its corresponding alcohol (Duarte et al., 2013).

2.4.2.5 Photosynthesis efficiency

Plant growth and biomass are directly linked to photosynthesis and its activity. Based on the type of sugar molecule synthesized for storage during photosynthesis, plants can be categorized into three groups, C_3, C_4, and CAM (Crassulacean Acid Metabolism). In C_3 plants, RuBisCO catalysis the carboxylation of ribulose-1,5-bisphosphate to two molecules of three carbon compound (3-Phosphoglycerate), through a process known as Calvin-Benson-Bassham cycle (CBB cycle) or TCA cycle or citric acid cycle (Bassham et al., 1950). RuBisCO can also add O_2 instead of CO_2, called oxygenase reaction, leading to the production of phosphoglycolate that doesn't have any metabolic role and plant has to clear it through photorespiration. Photorespiration is an energy demanding process which decreases the photosynthetic efficiency of plants up to 40% in response to high temperature and drought (Leegood, 2007; Gowik & Westhoff, 2011). C_4 system is more efficient for carbon assimilation as the CO_2 is concentrated at the site of RuBisCO in the mesophyll cells where further carboxylation takes place. Consequently, the oxygenase reaction and photorespiration are minimized in these plants (Gowik & Westhoff, 2011). In CAM plants, the stomata opens during night, capture the CO_2 for assimilation and store it in the vacuole in the form of four carbon molecules such as malate. During daytime, malate undergoes decarboxylation, making CO_2 available to RuBisCO (Nimmo, 2000). Further, CAM plants facilitate uptake of water and its movement between tissues via generation of osmotic gradients by accumulating solutes. C_3 carbon assimilation pathway is highly prone to oxidative stress due to ROS activity. Some C_3 halophytes have developed an extraordinary developmentally-programmed regulatory mechanism to switch its carbon assimilation pathways to C_4 or CAM, in response to stress. This helps the plant in reducing ROS production and hence protects it under stress conditions (Bose et

al., 2014). *Mesembryanthemum crystallinum* (C_3 plant) switches to CAM, and *Atriplex lentiformis*, (C_3 plant) switches to the C_4 pathway in response to salinity stress (Adams et al., 1992; Yen et al., 2001; Winter & Holtum, 2007; Bose et al., 2014). Similarly, *Portulaca oleracea*, which is a C_4 plant, switches to the CAMpathway under salinity stress conditions (Bose et al., 2014) for better and efficient energy metabolism.

Under salinity stress, the osmotic pressure of the soil decreases and causes an ionic imbalance in the plants (as discussed in section 3.2.1). This compromises the integrity of the light-harvesting complex photosystem II (PSII). To protect PSII, the excess energy is dissipated into heat by forming zeaxanthin, a process known as the xanthophyll cycle (Duarte et al., 2013). Halophytes have evolved several modifications for their efficient energy use. They regulates photosynthesis under stress by minimizing stomatal conductivity and transpiration pull without compromising the uptake of minerals. Unlike glycophytes, the internal CO_2 concentration is kept at a minimum to reduce the salt loading in the leaves; this enables the plant to balance the salts at a sub-toxic level. Further, some halophytes maintain high carotenoid/chlorophyll ratio that regulates electron flow and quantum yield to protect the system from photoinhibition, e.g. *Plantago coronopus* (Koyro, 2006). *Porteresia coarctata*, a close relative of rice, has developed a specialized mechanism to maintain a higher photosynthetic rate under stress (Bose et al., 2014). It has a relatively high expression of RuBisCO activate enzyme as well as the larger subunit of RuBisCO. In addition to this, a 33 kDa Mn-stabilizing protein (MIPS, L-myoinositol 1-phosphate synthase) accumulates at high levels. *P. coarctata* uses MIPS to stabilize other protective protein molecules that bind to the oxygen releasing complex of PSII. It also shows increased expression of the CP47 protein in chlorophyll a/b, subunit IV protein of the PSII that helps in stabilizing D1 of PSII and cross-linking of ferredoxin-$NADP^+$ oxidoreductase enzyme respectively (Bose et al., 2014).

2.4.3 Molecular and genetic adaptations

Plants exhibit stress tolerance trait through adaptations to diverse environments via natural selection. These environmental adaptations lead to changes in allelic/gene frequency of a species and are directly reflected in the genetic makeup of the species. These genetic modifications are fine-tuned over the thousands of years of evolution and lead to the directional evolution of species (Hoffmann & Hercus, 2000; Hoffmann & Willi, 2008; Nevo, 2011). It is through the modification of the acquired heritable molecular construct that enables an organism to be fit under the stress environment (Hasegawa et al., 2000). Traits that help a species to adapt to an environment are functionally conserved across species adapted in the same environment, thereby leading to parallel or convergent evolution. Several molecules that regulate the expression of genes at the level of transcription, translation and post-translational modifications have been identified in recent years in isolated studies (Pandey and Somssich, 2009; Agarwal et al., 2013; Gupta and Huang, 2014). However, most of the phenotypic variations in response to environmental stress, are usually controlled by multiple genes; therefore, interval mapping of the variants is performed to identify the quantitative genes. This quantitative mapping is collectively known as the QTL (Quantitative Trait Loci) mapping (Orgogozo et al., 2006). Several QTLs controlling specific traits in plants like plant height (Heidari et al., 2012), biomass and yield (Suji et al., 2012; Tripathi et al., 2012; Serba et al., 2015), resistance to powdery mildew (Asad et al., 2014), flag leaf length/width, panicle diameter/length or number of tillers (Lim et al., 2014) have been identified.

Salinity stress is often followed/accompanied by osmotic stress; therefore, identifying the appropriate gene(s) for salinity tolerance is complicated due to its multigenic regulatory control. Several independent studies have been performed for the identification of candidate genes responsible for salinity tolerance, and many have been identified that regulate salinity tolerance. Members of a few gene families like NHX, SOS, NAC, DREB, and HKT have been suggested to

play a vital role in salinity tolerance in plants (Gupta and Huang, 2014; Katschnig et al., 2015). Several attempts have been made to improve salinity tolerance in crop plants in the recent past without much success (Colmer et al., 2005; Ashraf and Akram, 2009). However, heterologous expression of several genes of halophytic origin has resulted in improved salinity tolerance (Miyama and Hanagata, 2007; Sultana et al., 2012; Joshi et al., 2013; Rozema and Schat, 2013). A comprehensive list of genes that resulted in salinity tolerance in heterologous systems is provided in Table 2.1. Though most of the heterologous expression studies have been performed in tobacco and Arabidopsis, few have been expressed in actual crops like rice, alfalfa, cotton, and *Jatropha*. SaNHX1, a gene encoding for vacuolar Na^+/H^+ antiporter from *Spartina anglica*, was expressed in rice and have been shown to improve salinity tolerance (Lan et al., 2011). Lv et al. (2008) reported the heterologous expression of H^+-PPase gene TsVP from *Thellungiella halophila* in *Gossypium hirsutum.* Transgenic plants displayed significant tolerance as compared to wild-type plants. Jha et al. (2013) expressed SbNHX1 from *Salicornia brachiata* in *Jatropha* and reported that transgenic *Jatropha* plants performed better than wild-type plants in up to 200 mM of NaCl concentrations. Similarly, several other genes like SiBADH and SiCMO from *Suaeda sp*., AhDREB1 from *Atriplex hortensis*, ThCYP1 from *Thellungiella halophila*, SbNHX1 from *Salicornia brachiata*, have been expressed in *Nicotiana tabacum* and reported to enhance salinity tolerance (Li et al., 2003a; Shen et al., 2003; Chen et al., 2007; Lv et al., 2008; Wu et al., 2008; Jha et al., 2013). Based on the available genetic data for salinity tolerance, regulatory mechanisms could be categorized as follows:

Modification/variation of the homologous genes, a simple variation in the sequence of the gene by addition and/or deletion mutation alters the response of the protein. PcMIPS from *Porteresia coarctata* that encodes for L-myo-Inositol-1-phosphate synthase is an excellent example of such variations. PcMIPS has a distinct variation of 37 amino acids that lies between 174 and 210 amino acid

chain as that of *Oryza sativa* MIPS gene. This variation is responsible for tolerance to salinity (Majee et al., 2004).

Gene duplication and gene ontology (GO) profiling has revealed that halophytes show more inclination towards duplication of ion transport-related genes. Few genes like HKT, NHX, and CBL show tandem duplication in halophytes as compared to their counter glycophyte species and have been reported to be the crucial genes for salinity tolerance (Dassanayake et al., 2011; Oh et al., 2012; Wu et al., 2012).

Epigenetic modification is a phenomenon of changing the activity of heritable genes without altering the sequence of DNA. Under salinity stress, halophytes like, *Mesembryanthemum crystallinum* shows hypermethylation of CpNpG sequence of the nuclear genome. This modification is coupled with the switchover from C_3 to the CAM pathway (Dassanayake et al., 2011; Oh et al., 2012). *Chloris virgata* shows root-specific methylation under salinity and alkali stress (Cao et al., 2012). Similarly, *Zygophyllum dumosum* shows post-translational methylation of H3 protein when it is grown at the wet ground. Mangroves also show hypomethylation of DNA when they are grown under saline condition (Golldack et al., 2011).

2.5 Available genetic and omics-based resources of halophytes

In recent years, several novel technologies like genomics, transcriptomics, proteomics, metabolomics, etc., have been developed that are providing ample opportunities to understand the biology of a living organism. Omics, in general, is used for data acquisition in a high throughput manner and its analysis to understand the biological processes. They produce system scale data, which is very helpful to understand the molecular and genetic control of plant functions.

2.5.1 Whole Genome Sequencing

Eutrema salsugineum (formerly known as *Thellungiella halophila*), a member of the Brassicaceae family is an excellent model system for studying salinity tolerance. It can tolerate extreme cold or saline conditions and therefore, can play a crucial role in understanding the molecular mechanisms of salt tolerance. Yang et al. (2013) generated the whole genome sequence for this plant and is available at phytozome (http://phytozome.jgi.doe.gov/pz/#!info?alias=Org_Esalsugineum) (accessed 11.07.19). Analysis has revealed that about 51.4% of its genome comprises of repetitive DNA elements and 26,351 protein-coding genes have been predicted from the ~ 243 Mb genome assemblies. *Thellungiella parvula*, another member of the Brassicaceae that is phylogenetically close to Arabidopsis, is an extremophile and a good model system (Amtmann et al., 2005; Amtmann, 2009), and can play a crucial role in understanding the biology of salinity tolerance in plants. Both Arabidopsis and *T. parvula* have common features like the rosette size, the time required for vernalization, time period of developmental stages and its genome size. It can tolerate extreme cold, heat, and salinity up to 500 mM concentration (http://thellungiella.org/index.php) (accessed 11.07.19). Two independent research groups (Dassanayake et al., 2011; Oh et al., 2012) have generated the whole genome sequence of *T. purvula*, independently. Oh et al. (2010) have predicted 28,901 protein-coding genes from the 140 Mb genomic sequence (available in NCBI, accession number SRA026763). They further compared the genome sequence of *T. parvula* with the orthologous of Arabidopsis and BAC (bacterial artificial chromosome) sequence of *T. halophila*. The analysis revealed that there is sequence conservation among the three related species. It is also found that *T. parvula* has multiple sequence repeats resulting in 30% shorter DNA segments as compared to *T. halophila*. *Thellungiella salsuginea* is another extremophile that belongs to family Brassicaceae and is frequently used for salinity tolerant studies. Wu et al. (2012) have generated whole genome sequence for *T. salsuginea* and predicted 28,457

protein-coding genes from ~ 223 Mbp genome assemblies. Also, they have identified several genes related to cation transport and abscisic acid signaling. *Salicornia sp*. belongs to a group of succulent halophytes and is widely distributed along the coastal and marshy area. They are cultivated widely because of their high protein and oil content. Whole genome sequencing and assembly for *Salicornia sp*. is underway at Centre for Desert Agriculture, King Abdullah University of Science and Technology, Saudi Arabia (https://pag.confex.com/pag/xxi/webprogram/Paper8088.html) (accessed 16.11.16). Similarly, *T. halophilea* salt-tolerant relative of Arabidopsis with the very similar genetic construct and morphological features are also being sequenced at the University of Arizona (http://xwang.openwetware.org/Research.html) (accessed 16.11.16). These genomic resources are critical for investigating and understanding the salinity-based defense mechanisms.

Table 2.1: List of the stress-responsive genes isolated from halophytes and characterized through heterologous expression

S/ No	Name of the gene	Source	Possible function(s)	Heterologos Host	Reference
1	*AcPMP3*	*Aneurolepidiumchinense*	Prevent Na^+ entry	Yeast	Inada et al. (2005)
2	*AeMDHAR*	*Acanthus ebracteatus*	ROS scavenger	Rice	Sultana et al. (2012)
3	*AgNHX1*	*Atriplex gmelini*	Na^+/H^+ antiporter	Rice	Ohta et al. (2002)
4	*AgNHX1*	*Atriplex gmelini*	Na^+/H^+ antiporter	Yeast	Hamada et al. (2001)
5	*AhDREB1*	*Atriplex hortensis*	Transcription factor	Tobacco	Shen et al. (2003)
6	*AhProT1*	*Atriplex hortensis*	Proline transporter	Arabidopsis	Shen et al. (2002)
7	*AlNHX*	*Aeluropus littoralis*	Na^+/H^+ antiporter	Tobacco	Zhang et al. (2008)
8	*AlSAP*	*Aeluropus littoralis*	E3 ubiquitin ligase activity	Rice	Saad et al. (2012)
9	*AlSAP*	*Aeluropus littoralis*	E3 ubiquitin ligase activity	Tobacco	Saad et al. (2010)
10	*AmDHAR*	*Avicennia maritima*	Monodehydroascorbate	Tobacco	Kavitha et al. (2010)

			reductase		
11	*AnNIP1;1*	*Atriplex nummularia*	Glycerol transporter	Yeast	Cabello-Hurtado and Ramos (2004)
12	*AnNIP1;2*	*Atriplex nummularia*	Glycerol transporter	Yeast	Cabello-Hurtado and Ramos(2004)
13	*Bg70*	*Bruguiera gymnorhiza*	Salinity tolerance	Arabidopsis	Ezawa and Tada (2009)
14	*cyc 02*	*Catharanthus roseus*	Salinity tolerance	Arabidopsis	Ezawa and Tada (2009)
15	*HcNHX1*	*Halostachys caspica*	Na^+/H^+ antiporter	Arabidopsis	Guan et al. (2011)
16	*HcVHA-B*	*Halostachys caspica*	pumps H^+	Arabidopsis	Hu et al. (2012)
17	*HcVP1*	*Halostachys caspica*	pumps H^+	Arabidopsis	Hu et al. (2012)
18	*KcMS*	*Kandelia candel*	Triterpene biosynthesis	Yeast	Basyuni et al. (2006)
19	*LbDREB*	*Limonium bicolor*	Transcription factor	Tobacco	Ban et al. (2011)
20	*NtCIPK2*	*Nitraria tangutorum*	Signalling complex	*E. coli*	Zheng et al. (2014)
21	*pAPX*	*Salicornia brachiata*	Ascorbate peroxidase biosynthesis	Arabidopsis	Tiwari et al. (2014)
22	*PcINO1*	*Porteresia coarctata*	Myo-inositol biosynthesis	Yeast	Dasidar et al. (2006)
23	*PINO1*	*Porteresia coarctata*	Myo-inositol biosynthesis	Tobacco	Majee et al. (2004)
24	*PutHKT2;1*	*Puccinellia tenuiflora*	pumps H^+	Yeast and Arabidopsis	Ardie et al. (2009)
25	*SaINO1*	*Spartina alterniflora*	Myo-inositol biosynthesis	Arabidopsis	Joshi et al. (2013)
26	*SaNHX1*	*Spartina anglica*	pumps H^+	Rice	Lan et al.(2011)
27	*SaVHAc1*	*Spartina alterniflora*	H^+ transport	Rice	Baisakh et al. (2012)
28	*SbASR-1*	*Salicornia brachiata*	Abscisic acid (ABA) responsive signalling	Groundnut	Tiwari et al. (2015)
29	*SbASR-1*	*Salicornia brachiata*	Abscisic acid (ABA) responsive signalling	Tobacco	Jha et al. (2012a)
30	*SbGSTU*	*Salicornia brachiata*	Glutathione S-transferase biosynthesis	Tobacco	Jha et al. (2011)

31	*SbMT-2*	*Salicornia brachiata*	Metallothioneins biosynthesis	Tobacco	Chaturvedi et al. (2014)
32	*SbNHX1*	*Salicornia brachiata*	Na^+/H^+ antiporter	Jatropha	Jha et al. (2013)
33	*SbpAPX*	*Salicornia brachiata*	Ascorbate peroxidase biosynthesis	Tobacco	Singh et al. (2014b)
34	*SbpAPX*	*Salicornia brachiata*	Ascorbate peroxidase biosynthesis	Peanut	Singh et al. (2014a)
35	*SbSOS1*	*Salicornia brachiata*	Stress signaling	Tobacco	Yadav et al. (2012)
36	*ScVP*	*Suaeda corniculata*	pumps H^+	Arabidopsis	Liu et al. (2011)
37	*SeCMO*	*Salicornia europaea*	Choline monooxygenase	Tobacco	Wu et al. (2010)
38	*SeLCY*	*Salicornia europaea*	b-Lycopene Cyclase	Arabidopsis	Chen et al. (2011)
39	*SeNHX1*	*Salicornia europaea*	Na^+/H^+ antiporter	Tobacco	Zhou et al.(2008)
40	*SlBADH*	*Suaeda liaotungensis*	Betaine aldehyde dehydrogenase	Tobacco	Li et al. (2003b)
41	*SlCMO*	*Suaeda liatungensis*	Choline monooxygenase	Tobacco	Li et al. (2003a)
42	*SsNHX1*	*Salsola soda*	Na^+/H^+ antiporter	Alfalfa	Li et al. (2011a)
43	*SsPP*	*Suaeda salsa*	Vacuolar proton pumping pyrophosphatase	Arabidopsis	Guo et al. (2006)
44	*SsVP*	*Suaeda salsa*	pumps H^+	Arabidopsis	Guo et al. (2006)
45	*ThCYP1*	*Thellungiella halophila*	Stress signaling	Tobacco	Chen et al. (2007)
46	*ThGSTZ1*	*Tamarix hispida*	Glutathione transferase biosynthesis	Arabidopsis	Yang et al. (2014)
47	*ThHAK5*	*Thellungiella halophila*	K+ transporter	Yeast	Alemán et al. (2009)
48	*ThIPK2*	*Thellungiella halophila*	Signalling molecules	Brassica	Zhu et al. (2009)
49	*ThNHX1*	*Thellungiella halophila*	Na^+/H^+ antiporter	Arabidopsis	Wu et al. (2008)
50	*ThVHAc1*	*Tamarix hispida*	pumps H^+	Yeast	Gao et al. (2010)
51	*ThZFL*	*Tamarix hispida*	Transcription factor	Tobacco	An et al. (2011)
52	*TrNHX1*	*Trifolium repens*	pumps H^+	Yeast	Tang et al. (2009)

53	*TsCBF1*	*Thellungiella halophila*	Transcription factor	Maize	Zhang et al. (2010)
54	*TsVP*	*Thellungiella halophila*	pumps H^+	Yeast and Tobacco	Gao et al. (2006)
55	*TsVP*	*Thellungiella halophila*	pumps H^+	Maize	Li et al. (2008)
56	*TsVP*	*Thellungiella halophila*	pumps H^+	Cotton	Lv et al. (2008)
57	*ZmVHA-B1*	*Zostera marina*	pumps H^+	Yeast	Alemzadeh et al. (2006)
58	*ZmVP1*	*Zoysia matrella*	pumps H^+	Arabidopsis	Chen et al. (2015)

2.5.2 Gene expression studies and cDNA libraries of halophytes

Several EST datasets and cDNA libraries have been generated for halophytes and are listed in Table 2.2. *Mesembryanthemum crystallinum*is commonly known as the ice plant and belongs to the *Aizoaceae* family. To identify genes that regulate its ability to switch from C_3 to CAM, an EST dataset was generated from the leaf of well-watered plants and plants grown in saline soil. Altogether9733 ESTs were characterized (Kore-eda et al., 2004). Analyzing the EST reveals that genes encoding for enzymes of the CAM pathway, ion homeostasis, osmoprotectant biosynthesis enzymes, and stress-related proteins showed 2-12 folds change in response to stress. Genes encoding for light harvesting complex and photosystem complex (C_3 pathway components) showed down-regulation by four folds. Gene encoding the proteins for RuBisCO was also down-regulated by seven-folds (Michalowski & Bohnert, 1992; Kore-eda et al., 2004). Circadian gene expression analysis for 24 hours of the CAM induction in *Mesembryanthemum crystallinum* showed that the putative genes display a phase shift of the mRNA abundance after CAM induction (Cushman et al., 2008).

Porteresia coarctata, a wild relative model plant of rice, is widely used to understand salinity and submergence tolerance. Garg et al. (2014) have generated a sizeable transcriptomic dataset for *Porteresia* using Illumina platform. The dataset consists of 375 million high-quality reads that were

assembled into 1,52,367 unique transcripts with an average length of 795 bp. Likewise, three subtractive cDNA libraries of Pokkali, a rice genotype that is naturally salt tolerant has been constructed by Kumari et al. (2009). Through subtractive hybridization, they generated a pool of 1194 ESTs that were induced under salinity stress.

Similarly, Zhang et al. (2014a) have generated large-scale transcriptomic data for a perennial herbaceous, *Karelinia caspica*, which belongs to family *Asteraceae*. It is tolerant to salinity, drought, cold, heat and is also resistant to pests. High-quality sequences were assembled, leading to the identification of 2,87,159 non-redundant transcript with an average length of 652 bp. Large-scale transcript datasets (~80 million reads) have been generated for *Salicornia europaea* shoots in response to salinity stress (Ma et al., 2013). Tsukagoshi et al. (2015) analyzed the RNA-seq from the roots of five-day-old seedling *Mesembryanthemum crystallinum* under different levels of salinity. This RNA was further converted into cDNA library and was sequenced using paired end model from the two ends. Of the 84 million paired read sequences assembled, 53,516 contigs that has 67 M bp sequence was obtained. RNA-Seq of 126,235 unigene that has 36,511 CDS from a forage herb *Achnatherum splendens* has also been identified by Liu et al. (2016).

Suppression Subtractive Hybridization (SSH) has been used for the identification of differentially expressed genes from halophytes in response to salt stress. Zouari et al. (2007) used SSH on cDNA libraries generated from root and leaf samples of *Aeluropus littoralis*. Similarly, Fu et al. (2005) generated SSH libraries for *Aegiceras corniculatum* and identified several ESTs that uniquely expressed in response to salt stress. cDNA libraries for *Thellungiella halophila* in response to various stress condition including salinity, freezing, and ABA treatment have also been generated. These cDNAs have been named as RTFL (RIKEN *Thellungiella halophila* Full-length), and a pool of about 20,000 cDNA

clones is available (http://www.brc.riken.go.jp/lab/epd/Eng/) (accessed 16.11.16) (Taji et al., 2008).

Table 2.2: List of representative transcriptomics-based studies in halophytes

S/ No	Species	Technique used	Reference
1	*Achnatherum splendens*	*De novo* Transcriptome	Liu et al. (2016)
2	*Aegiceras corniculatum*	Suppression Subtraction Hybridization	Fu et al. (2005)
3	*Aeluropus littorali*	Suppression Subtraction Hybridization	Zouari et al. (2007)
4	*Atriplex canescens*	Expressed Sequence Tag	Li et al. (2014)
5	*Avicennia marina*	Expressed Sequence Tag	Mehta et al. (2005)
6	*Halogeton glomeratus*	Transcriptome through Illumina sequencing	Wang et al. (2004)
7	*Ipomoea imperati*	Transcriptome through Illumina sequencing	Reid et al. (2016)
8	*Karelinia caspica*	Transcriptome through Illumina sequencing	Zhang et al. (2014a)
9	*Limonium bicolor*	Transcriptome through Illumina paired-end sequencing	Yuan et al. (2016)
10	*Limonium sinense*	Expressed Sequence Tag	Chen et al. (2007)
11	*Mesembryanthemum crystallinum*	Expressed Sequence Tag	Kore-eda et al.(2004)
		cDNA library	Michalowski and Bohnert (1992)
		RNA-Seq	Tsukagoshi et al. (2015)
12	*Millettia pinnata*	Transcriptome through Illumina sequencing	Huang et al. (2012)
13	*Porteresia coarctata*	*De novo* Transcriptome	Garg et al. (2014)
14	*Puccine lliatenuiflora*	Expressed Sequence Tag	Wang et al. (2007)
15	*Salicornia brachiata*	Expressed Sequence Tag	Jha et al.(2009)
16	*Salicornia europaea*	Transcriptome using Illumina HiSeqTM 2000	Ma et al. (2013)
17	*Spartina alterniflora*	Transcriptome using 454/GS-FLX and cDNA library	Bedre et al. (2016)
18	*Sporobolus virginicus*	Transcriptome through Illumina sequencing	Yoshizumi et al. (2006)
19	*Suaeda fruticosa*	*De Novo* Transcriptome	Diray-Arce et al. (2015)

20	*Suaeda glauca*	Transcriptome through Illumina HiSeq 2500	Jin et al. (2016)
21	*Suaeda salsa*	Expressed Sequence Tag	Zhang et al. (2001)
22	*Thellungiella halophila*	Expressed Sequence Tag	Wang et al. (2004)
		Suppression Subtraction Hybridization and Enrich cDNA	Taji et al. (2008)
23	*Thellungiella parvula*	Expressed Sequence Tag	Oh et al. (2010)
24	*Thellungiella salsuginea*	*De novo* Transcriptome	Lee et al. (2013)

2.5.3 Proteomics Studies

Several proteins related to salinity tolerance in halophytes have been identified using various proteomics techniques like 2D electrophoresis, LCMS-MS, iTRAQ, Phosphoproteome, electrospray, and Triple Quadrupole time-of-flight (TOF)-MS MS (Barkla et al., 2012; Krishnamurthy et al., 2014; Cheng et al., 2015) and are listed in Table 2.3. Askari et al. (2006) analyzed *Suaeda aegyptiaca* seedlings treated with various levels of salinity conditions through 2D-PAGE and identified 102 spots that showed a significant response to salt treatments. Relevant categories of differentially expressed protein in this data set include copper/zinc superoxide dismutase, dehydroascorbate reductase, quinine oxidoreductase, putative glutathione peroxidase, stromal ascorbate peroxidase, and peroxiredoxin like protein. Jha et al. (2012b) generated a 2D-PAGE based proteomic dataset of *Salicornia brachiata* in response to salinity and have identified a large number of differentially expressed proteins that includes storage proteins, a protein associated with energy metabolism and signaling protein. Proteomics of *Sesuvium portulacastrum* in response to a range of salinity (0-1000 mM) treatment for 30 days showed that major responsive proteins belong to photosynthesis regulatory proteins, ATP synthesizing proteins, ion binding and protein regulatory proteins (Yi et al., 2014). Similarly, several other 2D-based proteomic studies have highlighted the importance of signal transduction proteins, scaffolding and assembly-related proteins, proteins involved in ion

homeostasis and metabolic regulators (Pang et al., 2010; Wang, Xe et al., 2013; Vera-Estrella et al., 2014). Proteomic profiles in mangroves like *Bruguiera gymnorhiza* or *Kandelia candel* have highlighted the proteins involved in osmotic balancing, ionic compartmentalization, and energy metabolism, as crucial regulators of salinity tolerance (Tada & Kashimura, 2009; Wang et al., 2014). Zhu et al. (2012) found that *Bruguiera gymnorhiza* under mild salinity of 200 mM, showed up-regulation of photosynthesis-related proteins and osmotic balancer. With increasing salinity levels (500 mM), proteins involved in protein degradation, scaffolding, and cell organization were up-regulated too.

Recently, proteomic studies related to chloroplast proteome of halophyte species have also been reported (Fan et al., 2011; Wang et al., 2013). Proteome analysis of the chloroplast from *Kandelia candel* showed that proteins related to light-dependent reaction are up-regulated under mild and high salinity. Plastoglobuli that maintain the membrane fluidity and integrity were also up-regulated (Wang et al., 2013). Organelle proteomic datasets (chloroplast proteome) have been generated in response to varying salinity levels for *Salicornia europaea*. Ninety differentially expressed proteins were identified that included photosynthetic proteins such as CP29 and CP47 (an antennae molecule in PSII), chlorophyll a/b binding molecules, light harvesting molecule of PSII and PSI (Fan et al., 2011).

Table 2.3: List of representative proteomics-based studies in halophytes

S/no	Species	Technique	Reference
1	*Aeluropus lagopoides*	2D-PAGE and LC-MS	Sobhanian et al. (2010)
2	*Avicennia officinali*	2D-PAGE and nano-LC-MS/MS	Krishnamurthy et al. (2014)
3	*Beta vulgaris L.*	2D-PAGE	Wakeel et al. (2011)
4	*Bruguiera gymnorhiz*	2D-PAGE	Tada and Kashimura (2009); Zhu et al. (2012)
5	*Cakile maritima*	2D-PAGE	Debez et al. (2012)
6	*Halogeton glomeratus*	2D-PAGE	Wang et al. (2015)

7	*Kandelia candel*	iTRAQ (LC-ESI-MS/MS)	Wang et al. (2013)
		2D-PAGE	Wang et al. (2015)
8	*Mesembryanthemum crystallinum*	Shotgun peptide sequencing (LC-MS/MS)	Barkla et al. (2012)
		2D- DIGE	Barkla et al. (2016)
9	*Nitrarias phaerocarpa*	2D-PAGE	Chen et al. (2012)
10	*Porteresia coarctata*	2D-PAGE	Sengupta and Majumder (2009)
11	*Puccine lliatenuiflora*	Electrospray Quadrupole Time-of-Flight (ESI-Q-TOF-MS)	Yu et al. (2011)
12	*Salicornia brachiata*	2D-PAGE	Jha et al. (2012b)
13	*Salicornia europaea*	2D-PAGE	Wang et al. (2007); Wang et al. (2009)
		Nano LC-MS	Fan et al. (2011)
14	*Sesuvium portulacastrum*	2D-DIGE	Yi et al. (2014)
15	*Suaeda aegyptiaca*	2D-PAGE	Askari et al. (2006)
16	*Suaeda salsa*	2D-PAGE	Li et al. (2011b)
17	*Tangut nitraria*	Triple Quadrupole time-of-flight (TOF)-MS	Cheng et al. (2015)
18	*Thellungiella halophila*	2D-PAGE	Pang et al. (2010); Wang et al. (2013); Vera-Estrella et al. (2014)
		Phosphoproteome	Jun et al. (2010)
		iTRAQ (LC-MS)	Pang et al. (2010)
		LC-MS/MS	Vera-Estrella et al. (2014)

2.6 Industrial and agronomic applications of halophytes

About 6% of the world's total land and about one-third of the total irrigated land are affected by salinity. It has been estimated that the significant loss of crop yield is due to salinity. With the changing climatic patterns, this figure is expected to go up in the near future (Flowers et al., 2010). Numerous efforts have been devoted to understand the mechanism of salinity tolerance and identify genes/genetic components that regulate them. As discussed in this chapter,

plants have evolved several mechanisms to adapt to saline environments. While several genetic components controlling salt tolerance have been identified, we are far from engineering our crops for salt tolerance (Flowers, 2004; Zhang et al., 2014b). Multigenic inheritance for salinity tolerance is the main reason for the failure in breeding salt tolerant species (Flowers et al., 2010). However, halophytes are an excellent experimental system to dissect out the genetic control of salt tolerance and can play a crucial role in engineering food/feed crops for salinity tolerance. As discussed earlier, several halophytes species have been identified as a model system and, currently, these plants are being explored for genetic and genomic resources.

Identifying, domesticating, and harvesting cash-crops-halophytes (CCHs) has attracted the attention of the scientific community. Several CCHs that provide food, feed, and chemicals (industrial, pharmaceutical and plastics), and can be used for landscaping, ornamental, CO_2-sequestration, industrial raw material, unconventional irrigation, environment protection, and wildlife support have been identified (Koyro et al., 2014). Halophytes like *Salicornia sp.* and *Crithmum maritimum* are being used for centuries by humans as food in the coastal regions of the world. However, because of limited freshwater resources, there is intense interest in halophytes-based agriculture, and significant efforts have been made in this direction worldwide (Ventura et al., 2015). Several halophytes like *Salicorniasp*., *Aster tripolium*, *Atriplex nummularia*, *Crithmum maritimum, Crambe maritima, Beta maritima,* and *Portulaca oleracea* are either used or being explored for their potential to serve as food, forage or for industrial purposes (Hendricks & Bushnell, 2008; Gago et al., 2011; Anderson, 2014; Ventura et al., 2015). *Salicornia sp*. and *Sarcocornia sp*. are rich in mineral nutrients like calcium, potassium, iron, carbohydrates, and proteins. These plants also have high levels of antioxidants like ascorbic acid, polyphenolic compounds, polyols, and β-carotene (Hasegawa et al., 2000; Ventura & Sagi, 2013). *Chenopods sp*., *Distich lisspicata* (Saltgrass), and *Salicornia bigelovii* contain high crude protein and sulfur that help ruminate cattle. High antioxidants present

in this fodder crops in the form of vitamin A and E not only protects the plants but, also act as a precursor of the minerals for the cattle (Bustan et al., 2005; Norman et al., 2013; Ventura et al., 2015). Several of them are being explored for high nutritional potential, osmolytes or secondary metabolites like sugars, antioxidants, amino acids, *etc.*

Many halophytes like *Suaeda maritima*, *Sueda portulacastrum*, *Ipomoea pescaprae*, *Suaeda esteroa*, *Salicornia bigelovii* and *Atriplex barclayana* have shown a promising way for leaching out the minerals from aquaculture tank (Brown et al., 1999; Ayyappan et al., 2013). These plants have a high rate of evapotranspiration and have the ability to take up minerals from salty water and nutrient deficit soil (Brown et al., 1999). Recent studies show that decomposing halophytes like *Suaeda*, *Salicornia*, using phosphobacteria like *Bacillus megaterium*, results in a rapid increase in soil microflora such as fungi, bacteria. Further, they enrich the soil with essential enzymes like urease, cellulase, and alkaline phosphatase (Balakrishnan et al., 2007; Ayyappan et al., 2013) and are used as bio-fertilizers. *Spartina alterniflora* is grown in the marsh and coastal region and can grow in the areas with salinity levels partially higher than the seawater. This can reduce atmospheric CO_2, tolerate oil spill, support vast biodiversity and bioremediation, reduce toxic minerals like Pd and Cd (Koyro et al., 2014).

Halophytes also have huge potential in the biofuel industry. Carl Hodges, an atmospheric physicist from the University of Arizona, proposed seawater harvesting along the coastal line of the red sea. The 10,000 acres seawater forest in Massawa, Eritrea was planted with *Salicornia sp.* (sea asparagus) and other halophytes. This is the first example of commercial-scale farming with sea water. The primary objective was to grow halophytes for seed oils for bioenergy (Shillinger & Globe, 2001). Besides, woody stems of these halophytes could be used for fire woods, building material (timbers), edible seeds and forage. Though this project was terminated because of political disturbances in the region,

several other initiatives for growing halophytes for bioenergy have been started, and huge investments have been made in this direction (Sharma et al., 2016). Other halophytes like *Halopyrummu cronatum*, *Desmostachya bipinnata*, *Phragmites karka*, *Panicum turgidum*, and *Typha domingensis* are grown as a crop for the production of bio-ethanol crops. The high content of cellulose (~30%), hemicellulose (~33%) and little lignin (<10%) can be a good source of lignocelluloses biomass for ethanol production (Abideen et al., 2011; Abideen et al., 2012; Koyro et al., 2014). Sharma et al. (2016) have listed several halophytes that are being used or can be used for biofuel generation. Some of the halophytes that are potential for biofuel development are listed in Table 2.4. Green lab, NASA, is exploring and developing *Salicornia virginica* (grown widely), *Salicornia bigelovii* (high lipid) and *Salicornia euphoraea* (tall and broad) for biofuel and food production (Bomani et al., 2011). The sustainable aviation department of Boeing is focusing on halophytes after getting some breakthrough preliminary data for production of biofuels (http://cleantechnica.com/2014/01/27/boeing-bio-fuel-breakthrough-big-deal/) (accessed 16.11.16). Another group of Sustainable Bioenergy Research Consortium (SRBC), Abu Dhabi are also testing halophytes for its potential in producing biofuels (http://www.gizmag.com/halophyte-aviation-bio-fuel-desert-plants/30583/) (accessed 22.10.18).

Table 2.4: List of halophyte species assessed for their oil and lignocellulosic biomass yields

S/No	Plant	Family	Quantity	Tested range of tolerance in NaCl	Reference
Halophytes primarily used for oil extraction from seeds					
1	*Kosteletzkya virginica*	Malvaceae	17% (Dry Weight)	500 mM	Guo et al. (2006)
2	*Alhagi maurorum*	Papilionaceae	21.9% (Dry Weight)	600 mM	Abideen et al, (2012)
3	*Suaeda salsa*	Amaranthaceae	22% (Dry Weight)	200 mM	Mo and Li. (2010)

4	*Kosteletzkya pentacarpos*	Malvaceae	18-22% (Dry Weight)	200 mM	Ventura et al. (2015)
5	*Cressacretica*	Convolvulaceae	22.3% (Dry Weight)	850 mM	Weber et al. (2007)
6	*Halopyrum mucronatum*	Poaceae	22.7% (Dry Weight)	Seawater	Weber et al. (2007)
7	*Haloxylonstocksii*	Amaranthaceae	22.7% (Dry Weight)	500 mM	Weber et al. (2007)
8	*Arthrocnemum macrostachyum*	Amaranthaceae	25% (Dry Weight)	400 mM	Weber et al. (2007)
9	*Suaeda fruticosa*	Amaranthaceae	25% (Dry Weight)	400 mM	Shahi et al. (2013)
10	*Suaeda glauca*	Amaranthaceae	25% (Dry Weight)	200 mM	Du et al. (2009)
11	*Salicornia bigelovii*	Amaranthaceae	30% (Dry Weight)	400 mM	Weber et al. (2007)
12	*Helianthus annuus*	Asteraceae	35-52% (Dry Weight)	400 mM	Chen and He. (2011)
13	*Ricinus communis*	Euphorbiaceae	47-55% (Dry Weight)	400 mM	Zhou et al. (2010)
14	*Suaeda aralocaspica*	Amaranthaceae	30% (Dry Weight)	800 mM	Wang et al, (2012)
15	*Crithmum maritimum*	Apiaceae	45% (Dry Weight)	200 mM	Atia et al, (2010)
16	*Descurainaia sophia*	Brassicaceae	44.17% (Dry Weight)	400 mM	Peng et al. (1997)
17	*Allenrolfea occidentialis*	Amaranthaceae	14% (Dry Weight)	600 mM	Weber et al. (2007)
18	*Atriplex heterosperma*	Amaranthaceae	15.8% (Dry Weight)	600 mM	Weber et al. (2007)
19	*Halogeton glomeratus*	Amaranthaceae	24.7% (Dry Weight)	800 mM	Weber et al. (2007)
20	*Atriplex rosea*	Amaranthaceae	12.9% (Dry Weight)	1000 mM	Weber et al. (2007)
21	*Kochia scoparia*	Amaranthaceae	9.7% (Dry Weight)	1000 mM	Weber et al. (2007)
22	*Sarcobatus vermiculatus*	Sarcobataceae	17.5% (Dry Weight)	400 mM	Weber et al. (2007)
23	*Suaeda torreyana*	Amaranthaceae	25.25% (Dry Weight)	400 mM	Weber et al. (2007)
24	*Kosteletzkya virginica*	Malvaceae	30% (Dry Weight)	100 mM	He et al. (2003)
Halophytes primarily used for lignocellulosic biomass					
25	*Suaeda monoica*	Amaranthaceae	10.67% cellulose, 11.33% hemicellulose and 2.33% lignin	400 mM	Abideen et al. (2012)
26	*Arthrocnemum indicum*	Amaranthaceae	11.33% cellulose, 13.00%	800 mM	Abideen et al. (2012)

			hemicellulose and 7% lignin		
27	*Calotropis procera*	Apocynaceae	12.33% cellulose, 11.00% hemicellulose and 5% lignin	200 mM	Abideen et al. (2012)
28	*Tamarix indica*	Tamaricaceae	12.17% cellulose, 24.67% hemicellulose and 3.33% lignin	500 mM	Abideen et al. (2012)
29	*Ipomea pes-caprae*	Convolvulaceae	12.67% cellulose, 17% hemicellulose and 5.33% lignin	200 mM	Abideen et al. (2012)
30	*Sporobolus ioclados*	Poaceae	15.33% cellulose, 30.67% hemicellulose and 2% lignin	500 mM	Abideen et al. (2012)
31	*Aerva javanica*	Amaranthaceae	15.67% cellulose, 13.33% hemicellulose and 6.33% lignin	200 mM	Abideen et al. (2012)
32	*Achnatherumsplendens*	Poaceae	16.7% lignin	600 mM	Xian-Zhao et al. (2012)
33	*Dichanthium annulatum*	Poaceae	19% cellulose, 24.33% hemicellulose and 7% lignin	200 mM	Abideen et al. (2012)
34	*Salvadora persica*	Salvadoraceae	22% cellulose, 13.33% hemicellulose and 7% lignin	600 mM	Abideen et al, (2012)
35	*Eleusine indica*	Poaceae	22% cellulose, 29.67% hemicellulose and 7% lignin	200 mM	Abideen et al. (2012)
36	*Cenchrus ciliaris*	Poaceae	22.67% cellulose, 23.17% hemicellulose and 7% lignin	200 mM	Abideen et al. (2012)
37	*Chloris barbata*	Poaceae	25.33% cellulose,	200 mM	Abideen et al. (2012)

			23% hemicellulose and 8.33% lignin		
38	*Urochondra setulosa*	Poaceae	25.33% cellulose, 25% hemicellulose and 6.33% lignin	1000 mM	Abideen et al. (2012)
39	*Lasiurus scindicus*	Poaceae	24.67% cellulose, 29.67% hemicellulose and 6% lignin	400 mM	Abideen et al. (2012)
40	*Desmostachya bipinnata*	Poaceae	26.67% cellulose, 24.68% hemicellulose and 6.67% lignin	500 mM	Abideen et al. (2012)
41	*Phragmites karka*	Poaceae	26% cellulose, 29% hemicellulose and 10.33% lignin	500 mM	Abideen et al. (2012)
42	*Typha domingensis*	Poaceae	26.33% cellulose, 38.67% hemicellulose and 4.67% lignin	100 mM	Abideen et al. (2012)
43	*Aeluropus lagopoides*	Poaceae	26.67% cellulose, 29.33% hemicellulose and 7.67% lignin	750 mM	Abideen et al. (2012)
44	*Panicum turgidum*	Poaceae	28% cellulose, 27.97% hemicellulose and 6% lignin	200 mM	Abideen et al. (2012)
45	*Halopyrummu cronatum*	Poaceae	37% cellulose, 28.67% hemicellulose and 5% lignin	Seawater	Abideen et al. (2012)
46	*Panicum virgatum*	Poaceae	45% cellulose, 31% hemicellulose and 12%	200 mM	Abideen et al. (2012)

			lignin		
47	*Phragmites australis*	Poaceae	50% cellulose, 17% lignin	400 mM	Ming et al. (2010)
48	*Suaeda fruticosa*	Amaranthaceae	8.67% cellulose, 21% hemicellulose and 4.67% lignin	400 mM	Abideen et al. (2012)
49	*Salsolaim bricata*	Amaranthaceae	9% cellulose, 18.33% hemicellulose and 2.67% lignin	600 mM	Abideen et al. (2012)
50	*Miscanthus* spp.	Poaceae	40-60% cellulose, 20-40% hemicellulose and 10-30% lignin	200 mM	Brosse et al. (2012)
51	*Paspalum paspaloides*	Poaceae	20.33% cellulose, 33% hemicellulose and 2.33% lignin	200 mM	Abideen et al. (2012)

During evolution, halophytes not only have evolved to combat high salinity but also have developed the mechanisms to tolerate heavy metals (Shevyakova et al., 2003; Lefevre et al., 2009; Nedjimi & Daoud, 2009). These plants can be used to reclaim or clean up the saline soil or soil polluted with heavy metals (Manousaki & Kalogerakis, 2011b; Manousaki & Kalogerakis, 2011a).This process is called as phytoremediation. Phytoremediation can be discussed under four categories, i.e. Phytostabilization, phytoextraction, phytoexcretion, and phytodesalination

Phytostabilization refers to the reduction in the movement of heavy metals in the soil. Metal tolerant plants are ideal for this purpose. Halophytes like *Nerium oleander*, *Mesembryanthemum crystallinum*, and *Atriplex halimus* are resistant to lead (Pb) and cadmium (Cd). Growing these halophytes stabilize the heavy metals from leaching to the environment, protect contaminated soil from wind

and water erosion, and alter the chemical environment around the plant roots (Manousaki & Kalogerakis, 2011b; Manousaki & Kalogerakis, 2011a).

Phytoextraction refers to the uptake of toxic metals/elements/salts from the soil/water through plant roots and translocation to the above-ground aerial biomass. Heavy metal-tolerant halophyte species like *Atriplex halimus* and *Tamarix smyrnensis*, which absorb metals (Cd or Pb) and accumulate in their tissues, can be used for phytoextraction.

Phytoexcretion refers to the secretion of salts/metals from the aerial parts of the plant through excretory organs like salt glands or trichomes. *Tamarix smyrnensis* has salt glands on the surface of the leaf, which excretes not only excess salt but also heavy metals like Pd, Cd, and Zn also. *Armeria maritima*, *Avicennia marina*, and *Avicennia germinans* are known to excrete Cd and Pb from the glandular trichomes (Kadukova et al., 2008; Manousaki et al., 2008; Manousaki & Kalogerakis, 2011b; Manousaki & Kalogerakis, 2011a).

Phytodesalination refers to the removal of salts from the saline soil by growing halophytes that can accumulate very high salt concentration in the above ground parts of the plant. Halophytes like *Leptochloa fusca*, *Suaeda calceoliformis*, *Sesuvium portulacastrum*, *Suaeda maritima*, *Tamarix smyrnensis,* and *Atriplex halimus* deposit the excess salt at glandular trichomes or salt glands or deposit inside the vacuole of the leaf. These plants gradually reduce the level of soil salinity, sodicity, and decrease the pH (Manousaki & Kalogerakis, 2011b; Hasanuzzaman et al., 2014).

Halophytes like *Acacia modesta*, *Acacia nilotica*, *Phoenix sylvestris*, *Tamarix articulate*, *Cressa cretica*, *Zizyphus maurtiana*, *Calotropis procera*, and *Withania coagulans* have been known for their medicinal value in treating stomach pain, diarrhea, flu, cough, diabetes, asthma, and cancer. Significant private investments have been made to explore the potential of halophytes for the pharmaceutical industry too (Priyashree et al., 2010; Khan et al., 2011).

Besides, several halophytes can potentially be used for ornamental and landscaping purposes.

2.7 Future prospects

World population is expected to touch nine billion by 2050, and therefore, there is an urgent need to increase our agricultural produce by over 70% (Anderson, 2014). It is estimated that about 62 million ha agriculture land is already salinized and this is continuously increasing. Over the last two decades, about 20 million ha irrigated land has been salinized. Rapid depletion of arable land due to soil salinization is one of the most common problems for agriculture in arid and semi-arid regions worldwide. In this situation, halophyte-based saline agriculture has enormous potential as it can be done on the saline lands using saline water. Also, there are over 800 million hectares of saline land along the coastal regions of the world that can be used for saline agriculture.

Halophytes with their potential to grow in the saline environment are promising candidates for saline agriculture (Xian-Zhao et al., 2012). Though studies are limited, the potentiality of using halophytes for saline agriculture is being explored and is gaining momentum. In coastal areas, seawater or brackish water are used for irrigating halophytes food crops. This helps to minimize the use of fresh water that has declined to 2.5% of the total water of this planet (Gul &Khan, 2003; Ventura et al., 2015). Halophytes have been tested for their potential to reclaim the saline soils, and results are very promising. *Suaeda fruticosa* has been reported to remove 504 kg of salt from one hectare of land in four months (Ravindran et al., 2007). Recent developments and opportunities in this area are reviewed elsewhere (Hasanuzzaman et al., 2014). Use of halophytes for reclaiming the saline soils can have a significant impact on agriculture with enormous ecological and environmental benefits.

Halophytes are an important natural genetic resource that can help us to understand the mechanism of salinity tolerance and hence can unlock the door to

engineering existing crops for salinity tolerance. Identification of novel genes responsible for salinity tolerance and higher biomass yields and their transfer to glycophytic crops can transform these crops to tolerate high salt concentrations. Several studies carried out in recent past have established the usefulness of this approach (Kumari et al., 2009; Joshi et al., 2016; Soda et al., 2016; Joshi et al., 2018; Soda et al., 2018). Therefore, there is an urgent need for significant efforts from the scientific community and substantial investment from public/private partnerships to generate funding for developing genetic and genomic resources for model halophytes.

Large-scale research on halophytes is still limited as the standard parameters for cultivating halophytes have not been established. So far, there are only a few species like *Salicornia bigelovii,* for which breeding program has been successfully setup, and progress has been made for the production of oilseeds (Ventura et al., 2015). Several other halophytes have been identified that can have a significant impact on food/feed/fuel production but a lot more need to be done. Further, very little is known about the potential pathogens of the halophytes and how these plants will respond when grown on a large scale. Thus, there are certain limitations that must be overcome before the dream of halophyte agriculture could be realized. To achieve this, concerted efforts of the scientific community including taxonomists, breeders, and molecular biologist, will be required for the identification, characterization, and domestication of halophytes that have never been grown in agricultural settings. With the increasing population, decreasing availability of arable land and freshwater for sustainable development of the agriculture sector, saline agriculture can emerge as one of the sustainable solutions.

Chapter 3

Suaeda fruticosa and its natural habitat

3.1 Introduction

Diversity in India is not only confined to ethnicity, culture, and religion but is also defined by its vast topography and climatic variations. Arguably, India is considered to have the most diverse climatic conditions compared to all the countries with a similar land mass/area (Attri & Tyagi, 2010). Climatic variations range from tropical in the south to temperate in the northern Himalayas. The northern hemisphere, which is on the higher elevation, receive sustainable snows during winter; the southern as well as the northeastern regions receive heavy rainfall whereas the central part which has the Thar desert receive little or almost no rain throughout the year (Singh, 1971). Broadly, the climatic variations in India can be categorized into six major divisions, namely; a) tropical rain forest b) tropical savannah, c) tropical and subtropical steppe, d) tropical desert, e) tropical semi-arid steppe, and g) mountainous climate (https://www.mapsofindia.com/maps/india/climaticregions.htm).

Two seasonal monsoons strongly influence the climatic factor in India. Firstly, the cold wind from the northern latitudes from January to June and secondly, the reverse wind bringing rain from the south-western region. The later contributes up to 75% of the annual rainfall in India, from June to September (Attri & Tyagi, 2010). Two physical factors hugely influence seasonal variations in India, which are the Himalayas and the Thar desert (Singh, 1971; Böhner, 2006). The Himalayan mountain range acts as a barrier from the frigid katabatic wind coming from the Central Asian continent. This makes the northern states of India such as Delhi, Utter Pradesh, Haryana and Punjab warmer than most of the land with similar latitudes in the subcontinental part of Asia (Böhner, 2006; Attri & Tyagi, 2010). The two physical barriers also contribute to the significant

variations in the rainfall received in India. The state of Rajasthan wherein the Thar desert is located is mostly dry and receive an average annual rainfall of 13 cm during its short 20 days of monsoon. Whereas, in Mawsynram, Meghalaya of the northeast region located at the Himalayan ranges receive an average annual rainfall of 1141 cm during its 180 days of monsoon (Attri & Tyagi, 2010).

Similar to how the annual rainfall across India varies, the average temperature also does vary in the entire region. Between 1981-2015, the maximum average temperature across the county was recorded during May and June (35.08^{o}C and 34.48^{o}C respectively), and minimum during December and January (13.09^{o}C and 12.16^{o}C respectively) (Viswanath & Ramachandran, 2018). The average annual temperature across India (23.65^{o}C) might not be as high as Dallol, Ethiopia which recorded 34.4^{o}C (Burt, 2014), but if considered regionally, the average annual temperature crossedabove 27.5^{o}C along the coastal line and few other regions such as Gandhinagar and Bhubaneshwar. On the contrary, along the extreme northern region of India as well as few places of the northeastern region such as Gangtok, Itanagar and Shillong experienced an annual average temperature that is lower than 20^{o}C (https://www.mapsofindia.com/maps/india/india-map-annualtemperature.jpg). A report from the Indian meteorological department, Govt. of India stated that almost all the states in India are experiencing an increase in average annual temperature (Rathore *et al.*, 2013).

In India, with the varied climatic conditions (environment heterogenicity), several diversities of vegetation are found. Some of the significant categories of vegetation are; **a)** tropical evergreen rain forest which is found mostly at the northeastern region and the Western Ghats (Richards, 1952; Bhuyan *et al.*, 2003). **b)** deciduous forest located at the low line of the Himalayas and other states such as West Bengal, Orissa, Karnataka, and Jharkhand (Murali & Sukumar, 1993). **c)** dry deciduous forest found along the central Deccan plateau and few other places such as Rajasthan, Punjab, Haryana, and Utter Pradesh

(Bagchi *et al.*, 2003). **d)** mountain forest found at the hills of Himalayas (Singh & Singh, 1987). **e)** tidal/mangroves along the coastal line and Sundarbans (Gupta & Khandelwal, 1989). **f)** desert forest found majorly in Rajasthan and some part of Gujarat (Singh & Rathod, 2002).

There are four major deserts in India, **a)** the cold mountain desert also called the Spiti Valley cold desert in the trans-Himalayas (https://whc.unesco.org/en/tentativelists/6055/), **b)** the white salt desert in Rann of Kutch, Gujarat,**c)** the Deccan thorn scrub forest, and **d)** the sandy desert also called the Thar desert in Rajasthan (Nath, 2012; Kane, 2018).Of these, the Thar desert, which also is known as the great Indian desert is the largest, covering an area of 2,00,000 km^2. The desert is also the 18^{th} largest in the world spreading across the states of Rajasthan, Gujarat, Haryana, and Punjab (https://www.beautifulworld.com/asia/india/thar-desert/). This dessert is also home to the famous Sambhar Salt Lake in Rajasthan which also is the largest inland salt producing lake in India.

In this present chapter, we measured soil pH and electrical conductivity of the soil, which is a measure of soil salinity, around Sambhar Salt Lake in Rajasthan. We choose the eastern side of the Lake as it represents the sites where salts are produced commercially. Measurements of the soil samples collected at various depths were done for three seasons, i.e. post-monsoon, winter and summer. We observed that the soil pH and salinity were lowest during post-monsoon (~8.3 and 50 dSm^{-1}) and gradually increased during summer (~9.55 and 60 dSm^{-1}). The atmospheric temperature of the lake area was also measured for all the three seasons for three consecutive years. In addition, photosynthetically active radiation (PAR) that falls on the surface of the Lake was also measured. We also identified some plant species that were seen growing in the area.

3.2. Material and Methods

3.2.1. *Plant material and study conditions*

For choosing the best plant for our analysis, a pilot survey was conducted at Sambhar Salt Lake (India's largest inland salt extraction site within the Thar desert) located in the middle of the Aravali schists, India (26°58' N, and 75°5' E). After observing some plants growing in the area, the site was monitored for a year to identify plant(s) that could survive during all the three seasons viz. post-monsoon, winter and summer. The specific site for all the experiments was selected to be towards the east side of the lake, which also is the area where the salts are being extracted since time unknown.

3.2.2. Histology, scanning electron microscopy (SEM) and Energy-dispersive X-ray spectroscopy analysis (EDXRF)

Leaf samples of *S. fruticosa* collected from each season were fixed in 0.1M phosphate buffer (pH 7.2) containing 2.5 % glutaraldehyde. For histology analysis, fixed samples were then processed, cross-sectioned, stained with 0.05 % toluidine blue, viewed and photographed using a Nikon Eclipse Ti-S Inverted Microscope. For SEM, fixed samples were processed at the Advanced Instrumentation Research Facility, Jawaharlal Nehru University, New Delhi and viewed under JEOL JSM-6360 SEM. From the same section of the leaf, few portions were used to view the presence of Na^+ ion using SEM coupled with Energy-dispersive X-ray spectroscopy

3.2.3. Soil pH and electrical conductivity (EC) measurements

Three replicates of soil samples, from top to 60 cm depth, with intervals of every 10 cm, were collected from the rhizosphere of *S. fruticosa* for every season, i.e. post-monsoon, winter and summer. The soils were dried at 60^0C and then crushed to small size of about 2 mm, which were then mixed and dissolved in deionized water and 0.01 M $CaCl_2$ solution with 1:5 (weight/weight) ratio

separately (Gillman & Sumpter, 1986). The mixtures were then left for shaking at 220 rpm overnight, and filtered using Whatman filter paper 40 (GE Healthcare). Soil pH, as well as the electrical conductivity (EC), were measured in both deionized water as well as 0.01 M $CaCl_2$ solutions, which was later averaged, as described by Laslett *et al.*(1897). The pH of the solution was measured using Control Dynamics pH meter (model no. APX 175 E/C), and the EC was measured using Handheld meter Cond 340i.

3.2.4. Temperature recording

To measure the atmospheric temperature the recorders were kept at three levels viz. plant's canopy level, middle level and ground level. The temperature recorded by the three devices were then averaged for two plants. Temperature for three consecutive years, i.e. 2015, 2016 and 2017 during the three different seasons was measured using Lascar-EasyLog Temperature and Humidity USB Data Logger (EL-USB-2+) at intervals of every 30 minutes on the days of harvesting the samples.

3.2.5. Photosynthetic active radiation (PAR) measurement

LX-101A Lux Meter (HTC Instruments, India) was used to measure the PAR around the Lake area. Measurements were done at ground as well as the canopy level of the *Suaeda fruticosa* growing around the Lake at every 30 minutes time interval between sunrise, i.e. 05:00 hours until sunset, i.e. 20:00 hours. The values obtained from the ground, as well as the canopy level, were then averaged to get the average PAR that the shrubs receive.

3.3. Results

3.3.1. Sambhar Salt Lake –the site of experiment

Next to China and USA, India is the third largest producer of potable salt in the world (http://saltcomindia.gov.in/industry_india.html?tp=Salt). There are four

primary sources of salt production in India; sea brine, lake brine, sub-soil brine, and rock salt deposit, of which, sea brine/water holds the maximum source. According to the Salt Commission of India (http://www.saltcomindia.gov.in/), there are six primary inland salt producing units that are functioning presently; Sambhar Lake, Nawa, Rajas, Kuchhaman, Sujangarh and Phalodi, of which, Sambhar Lake is the largest producing unit.

'Sambhar Salt Lake' is located 360 m above the sea level and expands up to an area of roughly 225 km^2 within the Thar desert in the middle of the Aravali schists, India (26°58'-27°2' N, 75°5' -75°13' E) (Figure 3.1). The lake has an average depth of 1 m and receives roughly an annual rainfall of 50 cm (Swain *et al.*, 1983; Yadav, 1997; Yadav & Sarin, 2009). However, during its short monsoon, rainfall reaches up to 100-500 mm (Sinha & Raymahashay, 2004). Apart from the minimum rains, it receives annually, seasonal streams such as from Khandel, Kharain, Mendha and Roopangarh which contribute to its water table (Roy, 1999). A study using radio-labeled isotopes of oxygen suggested that the lake is a terminal one wherein, the water conserved during the monsoon is balanced by evaporation during the winter season leaving almost negligible water during the summer period (Ramesh et al., 1993; Yadav, 1997). Salts such as NaCl, Na_2CO_3, and Na_2SO_4 are found most predominantly in the lake. The environment around the lake area is presumed to be oxidative in nature as pungent smell which arises due to the emission of H_2S was not observed in the area (Yadav and Sarin, 2009).

Annually, a gross production of 2×10^5 tons NaCl has been reported from Sambhar Lake. For this purpose, water from the lake and the brine from shallow subsurface is let to evaporate for the salt extraction towards the eastern side of the lake (Figure 3.1 and 3.2a). Wind and electrical energy is used to pump the water towards the extraction site for its evaporation (Yadav and Sarin, 2009). The salts are then transported by local railways (Figure 3.2b) to the processing site

and then marketed commercially by the name *Hindustan salt* by Hindustan Salt Ltd., a Government of India enterprise (http://www.indiansalt.com/product.htm).

Figure 3.1: Aerial view of Sambhar Lake. The picture was captured using Google Earth (https://www.google.com/intl/en_in/earth/) on 29-10-18 at 14:15 hours. The Lake covers an area of about 225 km^2 located in the middle of the Thar desert. Several small villages harbor on its bank. The saline water from the lake leaches out into the surrounding villages destroying almost all vegetations. The white portion in the image shows the dried sandy bank which is composed mostly of salt.

The deposition of such a high amount of salt in the lake has attracted several scientists over the last century, for which, three hypotheses have been put forward; **a)** dissolution of halite bed from the basin of the great ancient relict Tethys sea (Godbole, 1952) **b)** evaporation of the brine water containing salts originated from the disintegration of halite rock (Aggarwal, 1951) **c)** deposition of salt-laden aerosol around the lake from the Gulf of Kutch brought by aeolian transportation through monsoon winds (Holland & Christie, 1909). A new hypothesis suggesting the existence of present paleo-river above the stream trapped during the past has been also put forward by Roy (1999). However, the actual reasons for the salt deposition remains debatable. Apart from oxidized salt, heavy metal isotopes of U^{234} (Yadav & Sarin, 2009) and other minerals such

as nitrate, phosphate, and silicate (Jakher *et al.*, 1990) have been reported in abundance, in and around the lake area.

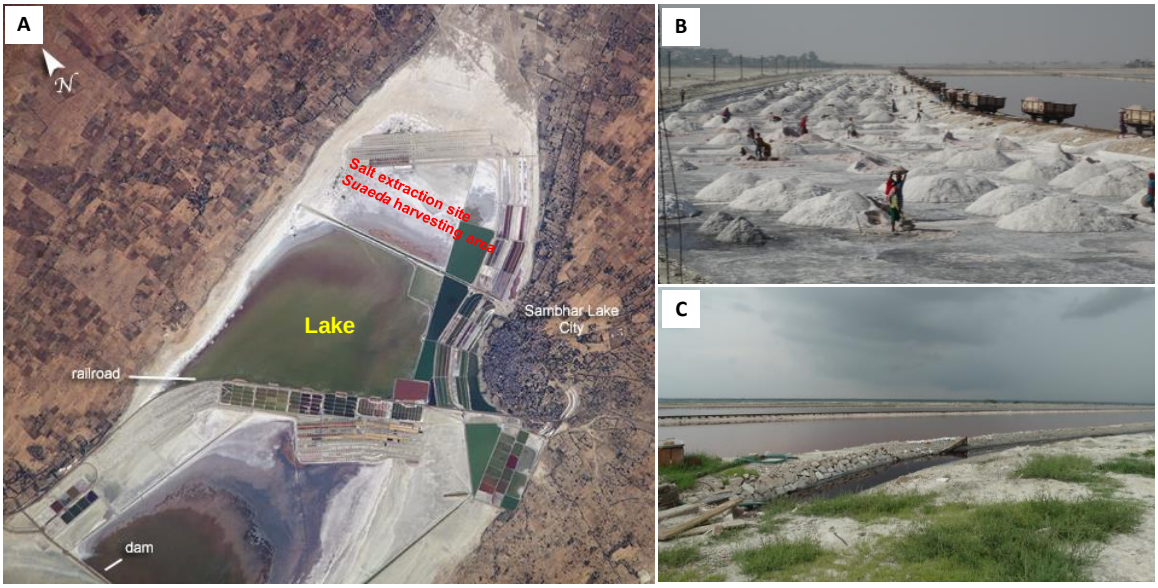

Figure 3.2: Aerial view of the salt extraction site and the activity around the Sambhar Salt Lake, Rajasthan. A) The Satellite view image of the site wherein the salts are extracted from Salt Lake in Rajasthan (*Pic: Earth Observatory, NASA*). Brine water is brought from the lake for evaporation towards the eastern side of the lake through water pumps. The closest village around the salt extraction site is the Sambhar village for which the name of the Lake is derived. The village is situated about 70 km away from the capital city Jaipur of Rajasthan. B) The area is dry for almost the entire seasons; however, it is driest during summer and winter. The brine that is brought from the lake deposits a large amount of salt after it gets evaporated. The salts were then collected, transported using rail engine for further processing. C). It is during the short monsoon that rainwater fills the lake. During this season, maximum vegetations can also was seen as rain flushes away the extra salts on the bank of the lake.

3.3.2. Temperature recordings at the salt extraction site across different seasons

Temperature for the three different seasons viz. post-monsoon, winter, and summer were recorded for the three consecutive years, i.e. 2015, 2016, and 2017 (Figure. 3.3). During the post-monsoon season, maximum temperature of 40.37 between 11:00 to 14:00 hours was recorded in the year 2015 while the minimum logged temperature was 26 between 04:00 to 06:00 hours.

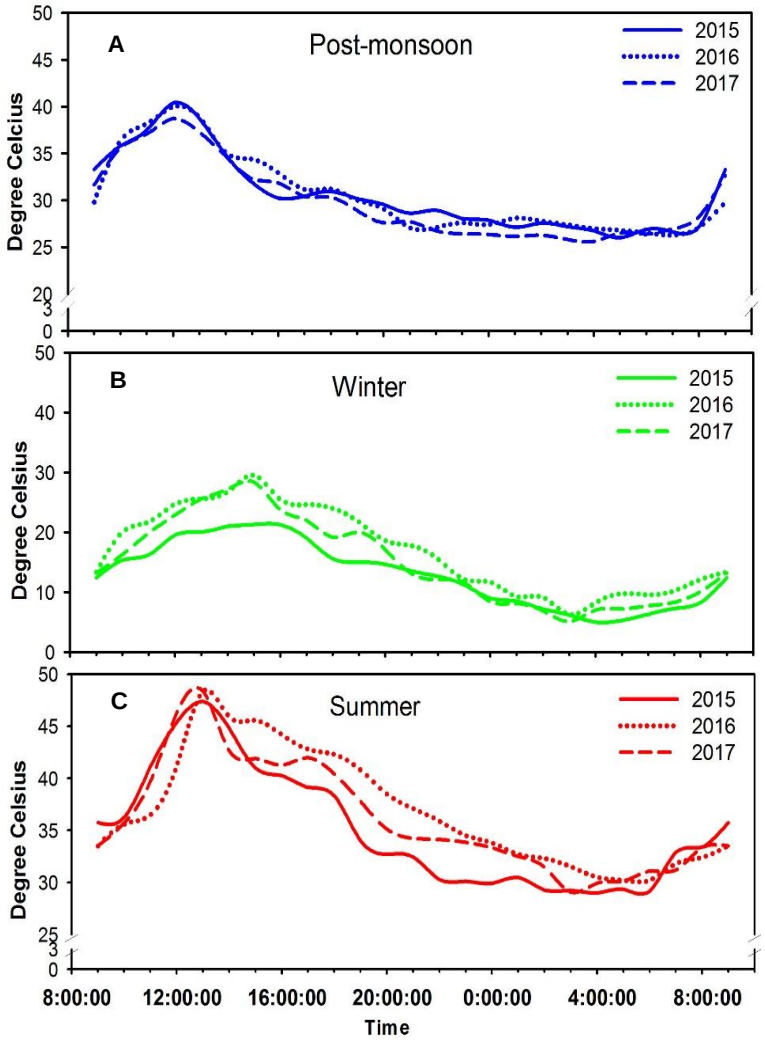

Figure 3.3: Recording of temperature during three seasons, i.e., post-monsoon, winter and summer of the salt extraction site of Sambhar Lake. The recordings were done for three consecutive years, i.e. 2015, 2016, and 2017 from the salt extraction site. A) The temperature recorded for three consecutive years during post-monsoon season. B) The temperature recorded for three consecutive years during peak winter season. C). The temperature recorded for three consecutive years during peak summer season.

However, the maximum average temperature was 39.7 ± 0.9ºC and minimum was 26.7 ± 0.34ºC (Figure. 3.3a). During the relatively short winter season, the temperature recorded during the day does not cross beyond 30ºC. But at night, the temperature dropped to about 6.7 ± 1.6ºC at around 04:00 hours (Figure. 3.3b). During the summer season, the temperature increases sharply

from about 30^{o}C at 08:00 hours to 47.4 ± 1.7^{o}C at 12:00 noon. At around 00:00 hour to 04:00 hours, the temperature decreases to about 28^{o}C (Figure. 3.3c). Since the temperature recordings were done for three years, it could also be concluded that there were not drastic fluctuations in the temperature within the three years period. Further the diurnal variations in temperature during the day in a particular season were almost similar during the three years of our experimentation. However, the seasonal variations could be scored in the temperature quite evidently.

3.3.3. Electrical conductivity and pH of the soil around the salt extraction site

Soil properties such as color and texture indicated that sandy-clay soil is predominant at the study site. Electrical conductivity (EC) and pH of the soil samples collected from various depths around the salt extraction site were measured for the three different seasons (Figure. 3.4).

The electrical conductivity of the soil was found to be extremely high throughout the seasons. EC was found to be the lowest during the post-monsoon season as a result of the rain flushing away the salt, thereby reducing the conductivity of the soil to ~35 dSm^{-1} (Figure. 3.4). During winter and summer, as the area gets dried up and salts began to precipitate, this is when the EC reached up to ~55 dSm^{-1} and ~65 dSm^{-1}, respectively. EC of the soil was seen to vary along the depth of the soil. Where it was seen to be the highest at the top soil level which attained 65 dSm^{-1} during summer. During post-monsoon and winter, the EC between the depth of 40 cm till 60 cm were found to be same. This could be due to the leaching of water from the lake towards the rhizosphere, which does not happen during summer when the lake is quite dry.

The pH of the soil was also seen to be very high throughout the seasons. The pH during post-monsoon and winter was observed to be similar ranging between 8.3 to 9.0 along the depth. However, during summer, the soil has the

highest pH ranging from 9 to 9.6 across the depth up to 60 cm. Maximum pH was observed at 50 cm depth attaining 9.59 during the summer season.

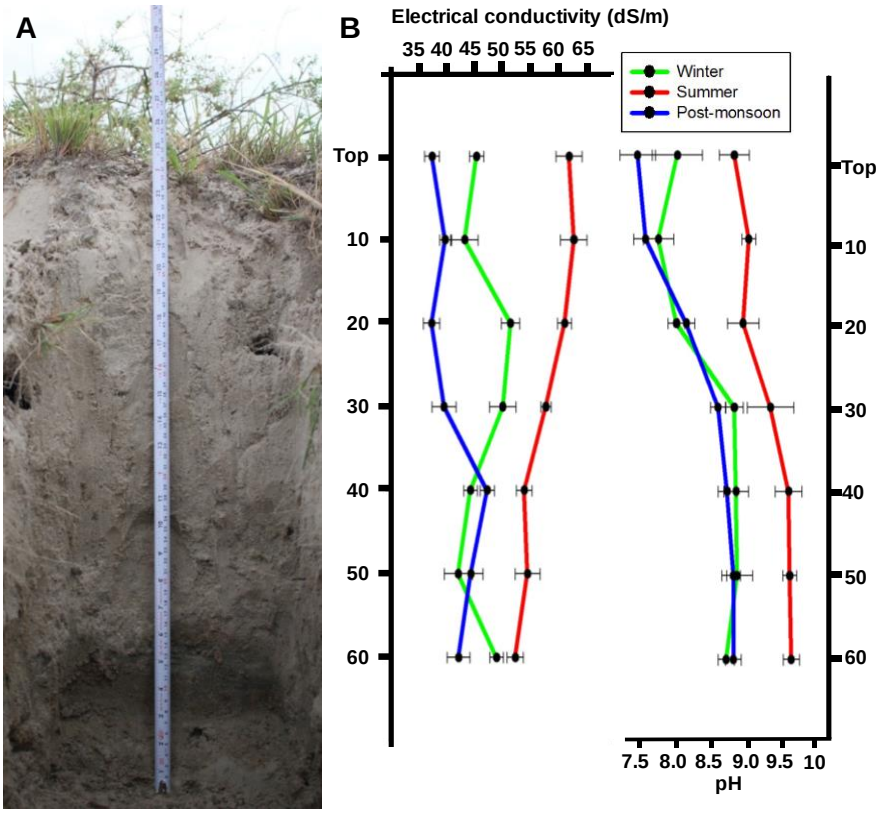

Figure 3.4: Electrical conductivity (EC) and pH of the soil recorded during three seasons, i.e., post-monsoon, winter, and summer at the salt extraction site in Sambhar Lake. Soil collected from various depths, i.e. topsoil, 10 cm, 20 cm, 30 cm, 40 cm, 50 cm, and 60 cm depth, around the lake were analyzed for their electrical conductivity and pH. A) Soil profile for which the parameters were analyzed. B) EC and pH of the soil at various depths at the place of experimentation as recorded during three different seasons.

Overall, our results indicated very high EC and high pH during the summer season. Taken together, these observations suggest that the three seasons impart two significant combinations of stresses to all the plants surviving at the site. During summer seasons, plants are subjected to high temperature and salinity stress, whereas during winter, plants are exposed to cold and salinity stress. The most optimum season for the plant, with respect to soil salinity,

alkalinity and atmospheric temperature, was observed to be during post-monsoon season.

3.3.4. Measurements of the photosynthetically active radiation at the salt extraction site

The maximum photosynthetically active radiation (PAR) (which is measured indirectly through the measurement of light intensity) on a clear day at the site was measured to be 1,600 µmol photons $m^{-2}s^{-1}$ between 10:00 hrs. to 15:00 hrs. as measured with LX-101A Lux Meter (Figure. 3.5). At this site, there was light from ~ 05:00 hrs. to ~ 20:00 hrs., before and after which the light intensity falls to nearly zero (dark).

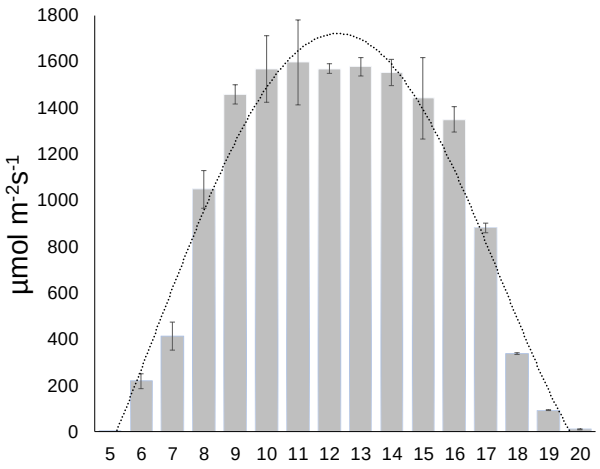

Figure 3.5: Light intensity of Sambhar lake from dawn to dusk as on February of 2018 during the experimental period.

3.3.5. Predominant vegetation around the salt extraction site

Due to the sandy and highly saline nature of the soil, vegetation around the lake was very scanty. However, during the post-monsoon season, as the rain flushes away the excess salt, some shrubs were found to grow around the area (Figure. 3.6). Although the water that pours into the lake during monsoon is less saline as compared to the brine water from the lake, salinity in and around the Lake

remains very high for any glycophyte to grow and therefore, halophytes predominate this region. Some of the halophytes that were found around the lake area were *Heliotropium curassavicum*, *Suaeda fruticosa*, *Aloe vera, Eleusine compressa*, *Sesuvium sesuvioides*, and *Chloris virgate*. Of these, *Suaeda fruticosa, Eleusine compressa,* and *Chloris virgate* were found to be most abundant.

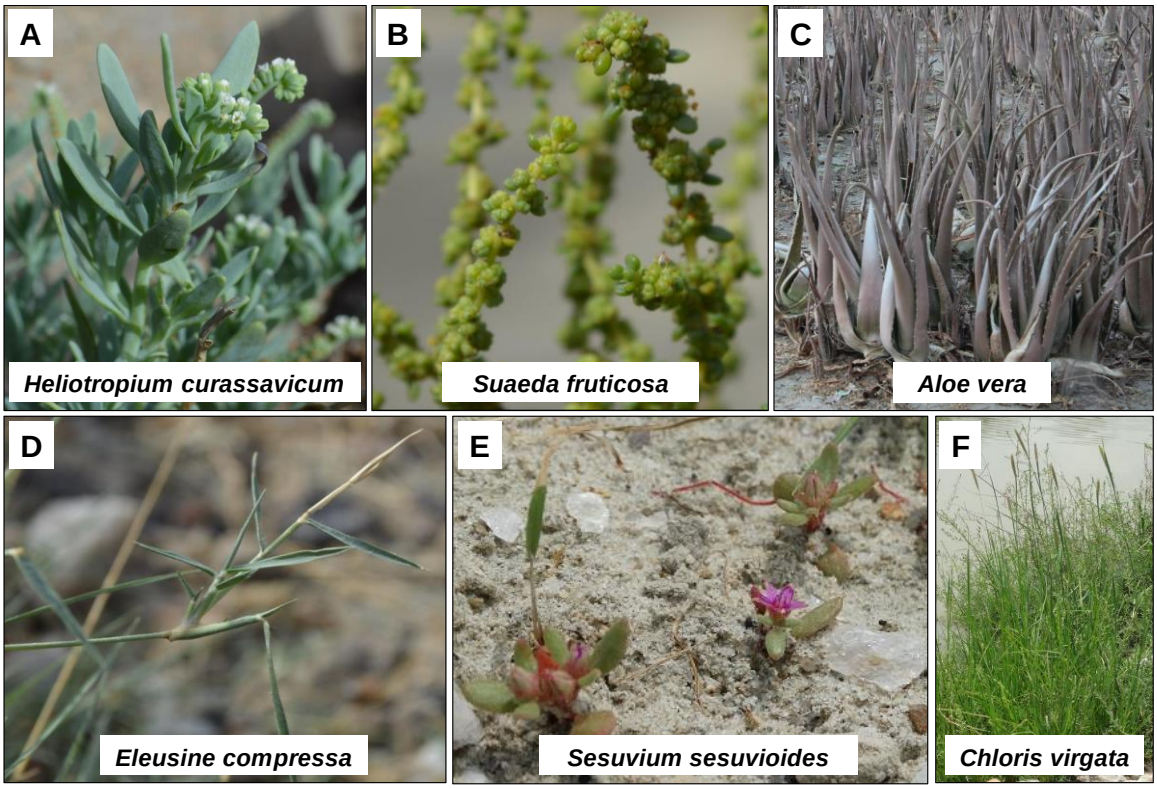

Figure 2.3: Flora found in and around the salt extraction site of Sambhar Lake. Halophytes such as *Heliotropium curassavicum*, *Suaeda fruticosa*, *Aloe vera*, *Eleusine compressa*, *Sesuvium sesuvioides*, and *Chloris virgate* were seen to grow in and around the salt extraction site, most of which flourished well during post-monsoon seasons as the water in the lake increases and salinity decreases. These plants complete their life cycle before the harsh summer sets in.

Monsoon period in the lake area is very short. It can be as short as 20 days receiving about 100-500 mm of rain during the season (Sinha and Raymahashay, 2004). In addition to a minimum or no rainfall, temperature around the area almost reaches 50^{o}C during summer and remains at an average

of 35^{o}C throughout the year. Salinity also remains high throughout the year (Upasani and Desai, 1990; Krishna et al., 2014). These harsh factors contribute to the minimum diversity of flora around the lake. Due to the severe climatic conditions, not all the halophytes that were found in the lake (Figure. 3.6) could survive throughout the year, i.e. post-monsoon, winter and summer. However, *Suaeda fruticosa* was seen to grow during all the seasons, although its growth and development reduces during winter and almost to none during summer (Figure. 3.7).

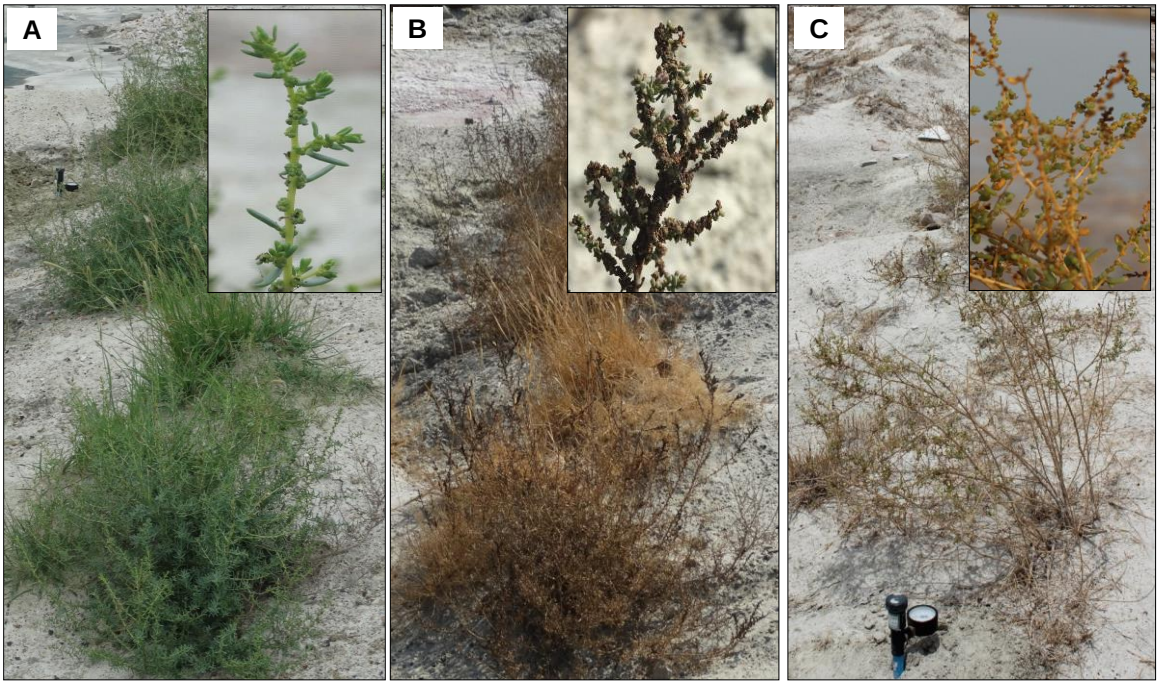

Figure 3.7: *Suaeda fruticosa* (L.) Forssk. growing in the salt lake area during the different seasons. Morphology of *S. fruticosa* changed along the season under the influence of the environment around it. The plants were green and healthiest during post-monsoon. During winter, turgid and reddish leaves were seen to develop along with mature seeds that are ready for dispersal through wind or other physical factors. Highly succulent leaves were seen to develop during summer as the temperature and salinity is maximum. A) *Suaeda fruticosa* as seen during post-monsoon. B) *Suaeda fruticosa* as seen during winter. And, C) *Suaeda fruticosa* as seen during summer season growing in its natural habitat.

3.3.6. Overview of *Suaeda fruticosa*

The plant genus *Suaeda* (family Chenopodiaceae) consists of about 110 species spreading around the coastal tropic as well as the sub-tropical areas. Most of the species are annual halophytes growing in saline or alkaline wetlands and dessert by developing succulent leaf (Fisher et al., 1997). Physiological and biochemical analysis of this genus reveals the presence of both C_3 and C_4 photosynthesis pathway wherein, during dry and high saline environment, C_4 species are seen growing predominantly over C_3 even though both can coexist (Fisher *et al.*, 1997).

Table 3.1: General characteristics of *S. fruticosa*; its classification and salient features. The table is modified from collective information obtained from

- http://www.efloras.org/florataxon.aspx?flora_id=5&taxon_id=242100197;
- https://wikivisually.com/wiki/Suaeda_fruticosa;
- http://www.theplantlist.org/tpl1.1/record/kew-2483984;
- http://flora.org.il/en/plants/SUAFRU/;
- https://pfaf.org/user/Plant.aspx?LatinName=Suaeda+fruticosa;
- http://www.efloraofgandhinagar.in/herb/suaeda-fruticosa.

Classification	
Kingdom	Plantae
Superdivision	Spermatophytes
Division	Angiospermae
Class	Dicotyledoneae
Family	Amaranthaceae formally known as Chenopodiaceae
Subfamily	Suaedoideae
Genus	Suaeda
Species	Fruticosa
Common name	Shrubby sea-blight
Phyllotaxy	
Leaf arrangement	Alternate arrangement with one leaf per node
Leaf type	Terete or cylindrical
Leaflet margin	Other
Stipule	Absent
Natural habitation and distribution	
Habitat	Sandy desert, saline soil and thermophilic

Chorotype	Sundanian
Salt resistance	Halophytic which can grow in salinity up to 65 dSm^{-1}
Synantroph	Obligate and natural
Distribution	Cape Verde, the Mediterranean region, the Canary Islands and the coasts of northern Africa, France, and south-eastern England, the Atlantic coasts of southern Spain and Portugal, the Arabian Peninsula, the Horn of Africa, Afghanistan, Iran, and the Indian sub-continent.
Floral and reproduction	
Tepal	Five fused green color tepal
Stigma	Three
Stamen	Five
Style	Three
Sexuality and reproductive morphology	Hermaphrotide
Sporangia/Seed homogeneity	Homogenous
Shape	Drum-shaped
Size	1.5 mm in wide
Flowering time	September to May
Propagation	Sexual by developing smooth black seeds
Plant structure	
Life form (Raunkiaer)	Chamaephyte
Size	Shrub growing up to 1-2 m in height
Leaf and branching	Densely branched and somewhat woody at the base
Feature	Pale green during early days which gradually turns grey
Spinescence	Absent
Succulence	Leaf succulent
Summer Shedding	Perennating

In India, four species of *Suaeda* have been listed in the efloraofindia database (https://sites.google.com/site/efloraofindia/species/a---l/a/amaranthaceae/suaeda), one of which includes *Suaeda fruticosa*. *Suaeda fruticosa* (L.) Forssk. is an evergreen succulent obligate halophyte shrub that grows to about 1m in height. It is usually seen to flourish well in sandy, alkaline and highly saline soil (https://www.pfaf.org/USER/Plant.aspx?LatinName=Suaeda+fruticosa) and produce numerous seeds. Flowering began from September till May

(http://flora.org.il/en/plants/SUAFRU/) and are pollinated by insects (Entomophily) and ants (Myrmecophily) (Figure. 3.8).

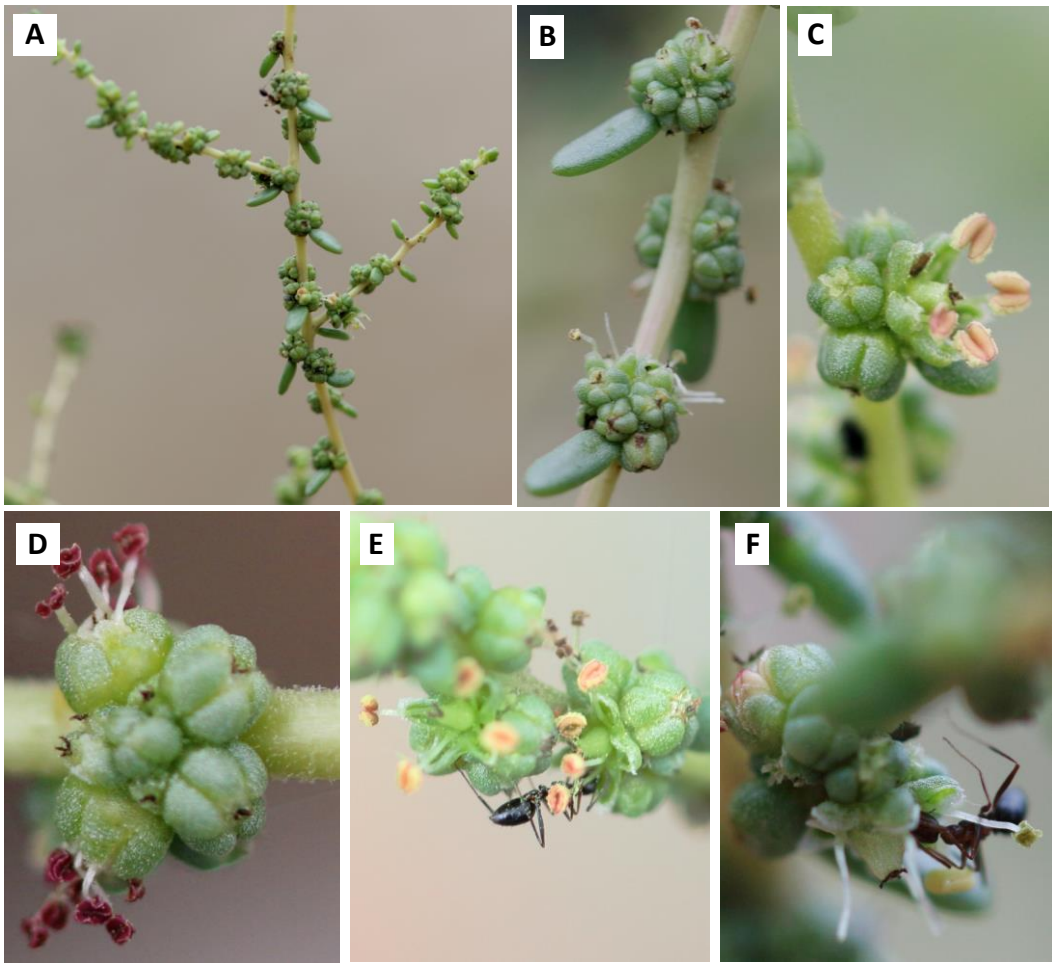

Figure 3.8: Reproductive phase of *S. fruticosa*. Flowers were found to be clustered tightly around the leaf axis arranged alternatively on the node. Most of the flowers are bisexual, drum-shaped with a width of about 1.5 mm. All five succulent tepals are fused. Pollinations is either through insects or ants; but occur mostly through ants, as the population of insects in the desert or saline environment are less. A & B) cluster of flowers arranged around the leaf. C & D) close up picture of the flower. E & F) Ongoing pollination by ant.

S. fruticosa is widely cultivated for its seeds that contain high edible oil (Weber et al., 2007), fodders for animals (Towhidi et al., 2011), medicinal uses such as for the treatment of hypoglycaemia (Benwahhoud et al., 2001), anophthalmia (Bennani-Kabchi et al., 1999) and hypolipidaemia (Chopra et al.,

1986). It is also used in bioremediation (Bareen & Tahira, 200) to remove heavy metals from the soil as well as in phytoremediation (Khan et al., 2009) to remove excess salt from the soil (Hameed et al., 2012). This plant can tolerate salt as high as 1000mM NaCl; however, its optimum growth is seen between 200-400 mM (Khan et al., 2000).

3.3.7. Histology and morphological features of leaves of S. fruticosa

The annual halophyte *S. fruticosa* was seen to develop different morphological features that are directly affected by the environmental factors surrounding it (Figure. 3.9). Germination happens at the beginning of July as rain flushes away the excess salt. By the end of August or early September (post-monsoon), mature plants were seen growing all over the bank of the salt extraction site. Leaves were long, narrow and dark green in color. SEM images indicated that the cells lining the surface of the leaf are large and irregularly-shaped and are accompanied by a number of stomata (Figure. 3.9a-c). Underneath these large cells of the epidermis lie a number of cell layers that make up the hypodermis (Figure. 3.9d).

As winter sets in, the lusty green *S. fruticosa* plant gradually turns brown (Figure. 3.9e). Succulent leaves began to develop, and the lusty green leaves gradually changed to reddish brown. Cells lining the surface of the leaf appear shrunken (Figure. 3.8f-g), a drastic change in stomatal density as well as its structure as compared to leaves collected during post-monsoon was observed. Matured seeds, ready to be dispersed, were seen all over the spikes. Succulent leaves gradually began to develop. By the time summer sets in, the leaves were lesser in number, smaller in size, turned dullish green and became highly succulent (Figure. 3.9i). SEM images showed that the cells lining the leaf surface were smaller in size and regularly-shaped (Figure. 3.9j-k). Stomata appeared to be more in number as compared to the other two seasons i.e. post-monsoon and winter. Significant changes in the anatomy of the leaves were also observed during summer. A single-layered hypodermis replaces the multi-layered

hypodermis as seen in the post-monsoon season leaf, and cells making up the pith (central vascular bundle) were larger than that during post-monsoon (Figure. 3.9l). These dramatic changes in structure and anatomy of *S. fruticosa* leaf may be a result of the plant's responses to several abiotic stresses which it is experiencing during these seasons.

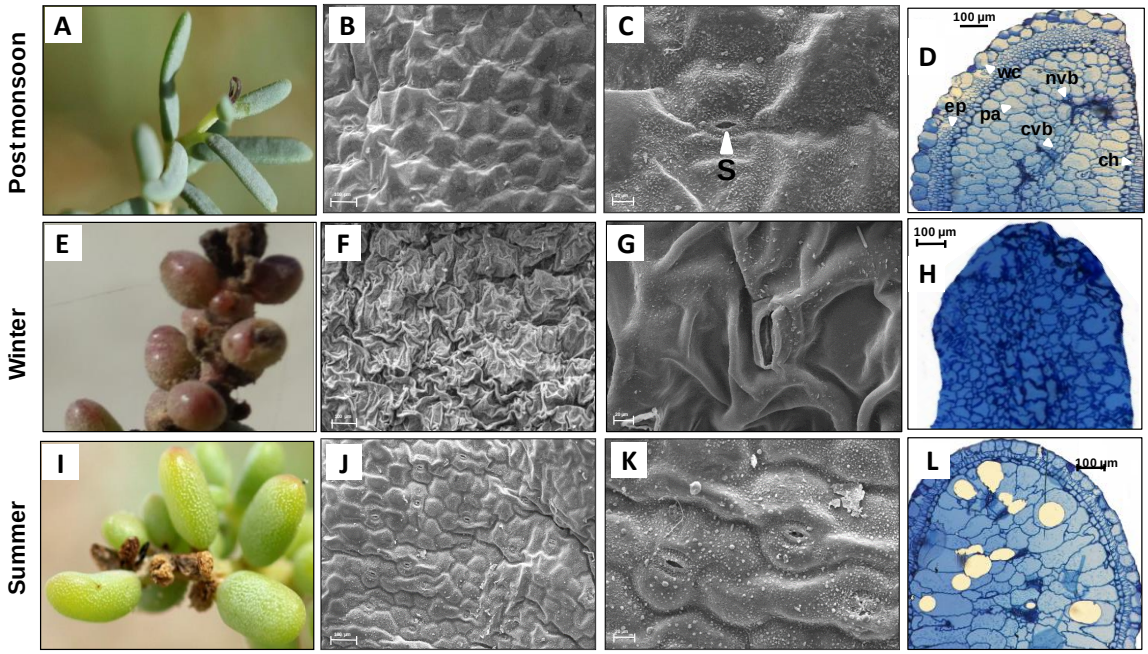

Figure 3.9: SEM and light microscopy images of leaves of *S. fruticosa*: The topographical and anatomical features of leaves were viewed using SEM and light microscopy. A) Eye view of leaves during post-monsoon. B) Surface topography of leaves during post-monsoon. C) View of stomata of leaves during post-monsoon. D) Cross section of the leaf during post-monsoon as view through light microscope after staining with toluidine blue. E) Eye view of leaves during winter. F) Surface topography of leaves during winter. G) View of stomata of leaves during winter. H) Cross section of the leaf during winter as view through light microscope after staining with toluidine blue. I) Eye view of leaves during summer. J) Surface topography of leaves during summer. K) View of stomata of leaves during summer. L) Cross section of the leaf during summer as view through light microscope after staining with toluidine blue. In the cross-section view, epidermis (ep) with window cells (wc), chlorenchyma (ch), net of peripheral vascular bundles (nvb), parenchyma (pa) and central vascular bundle (cvb) were clearly visible.

3.3.8. Ionic measurements in epidermal cells and mesophyll cells using Scanning electron microscopes-energy disperse X-ray (SEM-EDX) in leaves of S. fruticosa

As described above, the morphology and the anatomy of the leaf of *S. fruticosa* changes with the change in the environment and seasons. The level of salinity in the soil also was seen to change along with the seasons wherein, salinity was highest during summer; however, it was relatively lower during the post-monsoon season. To further check the levels of salt accumulated on the surface as well as the mesophyll layers of the leaves in *S. fruticosa*, SEM-EDX was done with the leaf harvested during the three seasons (Figure. 3.10)

During post-monsoon seasons, as salinity and soil pH are relatively the lowest, the amount of Na^+ ions that are accumulated on the leaf also was found to be relatively the lowest. On the epidermal layer, the concentration of Na^+ ions were found to be 2.5 ± 0.2% of the total ions whereas, in the mesophyll cells, the concentration was found to be 4.5 ± 0.6 % which is roughly double the amount that was detected in the epidermal layer (Figure. 3.10a-c). During winter and summer season, as salinity in and around the lake increases, the amount of Na^+ accumulating in the leaves of *S. fruticosa* also increases. During winter, 3.39 ± 0.31% and 6.5 ± 1.1% of the total ions were detected in the epidermal and mesophyll layers were of Na^+ ions (Figure 3.10d-f).

During summer, the concentration of Na^+ ions increased drastically both at the epidermal as well as the mesophyll layer as compared to that during post-monsoon and winter. At the epidermal layer, the concentration of Na^+ ions were found to be 27.8 ± 3.29% while 9.5 ± 1.7% Na^+ was detected in the mesophyll layer (Figure. 3.10g-i).

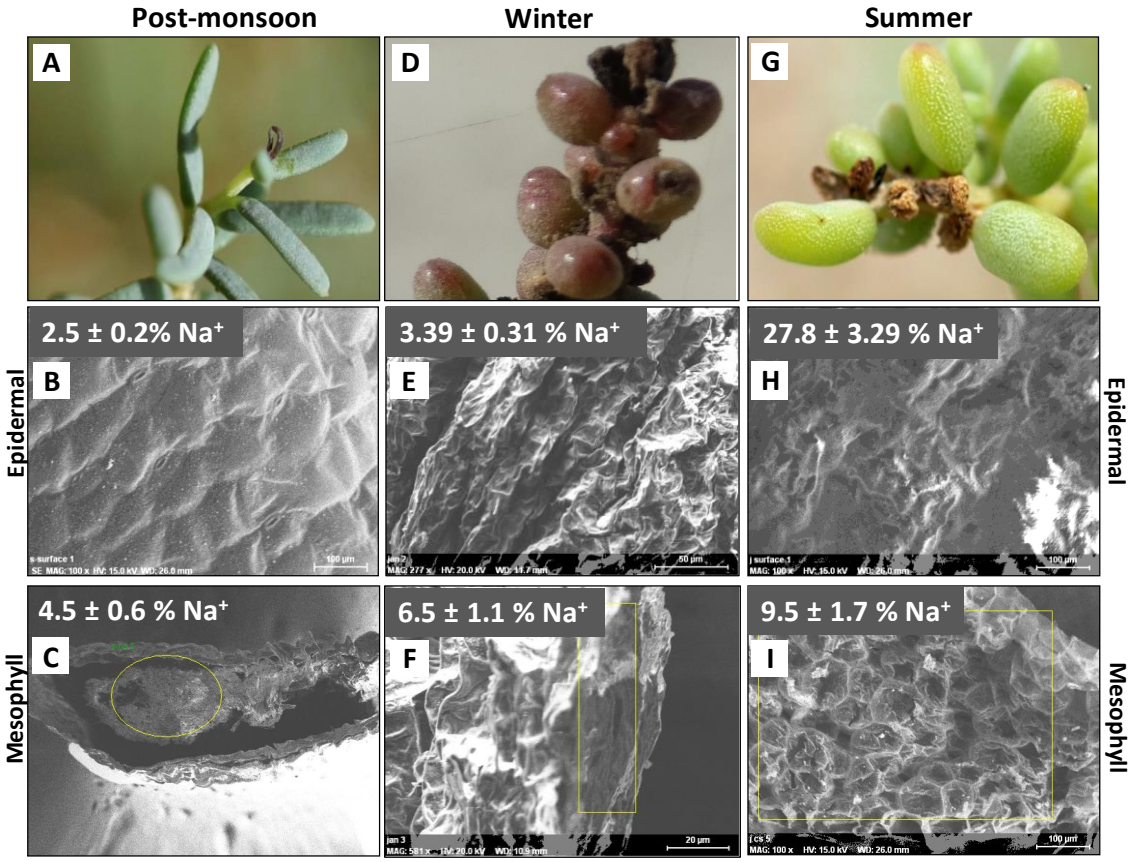

Figure 3.10: SEM-EDX analysis of sodium ions in the leaves of *S. fruticosa*: The concentration of Na^+ ions on the epidermal as well as the mesophyll layers of the *S. fruticosa* leaf was viewed using SEM-EDX. A-C) Percentage concentration of Na^+ ions on the epidermal and mesophyll layer of *S. fruticosa* leaf harvested during post-monsoon. D-F) Percentage concentration of Na^+ ions on the epidermal and mesophyll layers of *S. fruticosa* leaf harvested during winter. G-I) Percentage concentration of Na^+ ions on the epidermal and mesophyll layer of *S. fruticosa* leaf harvested during the summer season.

3.4 Discussion

The pattern of vegetation, as well as the diversity of the flora available in a particular niche, depend primarily on the environmental condition as well as the microclimate of the area (Ricklefs, 1977; Gao *et al.*, 2017). India, spreading to an area of 3.3 million km^2 (http://world.bymap.org/LandArea.html), is home to diverse vegetation due to its vast environmental diversity. In his short letter, Ricklefs (1977) hypothesized that local soil heterogenicity and microenvironment

which is caused due to physical factors and geographical differences underlie the diversity of a tree species in a forest canopy (Ricklefs, 1977). Environmental heterogenicity can be due to heterogeneity in rainfall, availability of water, temperature, and topography. These diversities are known to be among the significant factors for species diversity (Davidar et al., 2007; Stein et al., 2014; Stein and Kreft, 2015). Over the past century (1901-2004), India has faced several climatic disasters such as a) cold wave, fog, snowstorms and avalanches, (b) hailstorm, thunderstorm and dust storms, (c) heat wave, (d) tropical cyclones and tidal waves, (e) floods, heavy rain and landslides, and (f) droughts, which have caused severe losses in terms of economy, live stocks and agriculture products (De et al., 2005). Environmental heterogenicity can also be brought about due to natural disasters as well as species (biological) invasion (Ricciardi et al., 2011). Bhuyan et al. (2003) identified several diverse tree species that are distributed along undisturbed, mildly disturbed, and disturbed area by human habitation in Arunachal Pradesh. Towards the southern part of India, Joseph et al. (2008) observed that maximum diversity of vegetation is found in relatively higher elevated area with the lower annual temperature, which get the highest annual rainfall. Similarly, Prasad et al. (2008) have identified the changes in vegetation of the Western Ghats due to environmental heterogenicity.

The Northern Himalaya spreading up to the northeastern states and the Thar desert towards the western Ghats contributes significantly as natural environmental heterogenicity in India (Gupta and Khandelwal, 1989; Bagchi et al., 2003; Attri & Tyagi, 2010; Nath, 2012; Kane, 2018). Several types of dry, deciduous and tropical forest are found in India which majorly is due to the two-physical barriers i.e. the Himalayas and Thar desert (Gupta & Khandelwal, 1989; Bagchi et al., 2003; Kane, 2018). Arguably, the hot and dry great Indian desert, also known as the Thar desert, has the minimum vegetation across all the forest in India (Attri and Tyagi, 2010). It is in this desert that Sambhar Lake, the largest inland salt extraction site in India, is located.

In search of a plant that not only is tolerant to salinity and drought but also to high temperature and cold weather, vegetation in and around the Sambhar Lake were scored in the present work. Sambhar Lake is known for its high production of potable salt, and besides, the Lake also experience a temperature as high as 50^{o}C during summer and as low as 2^{o}C temperature during winter (Upasani and Desai, 1990; Krishna et al., 2014). Any vegetation that can complete its life cycle under such an adverse condition can be the answer to the quest of a dominant tolerant species for isolation of genetic components for crop improvement. A study of the physical environmental parameters around the Lake such as the electrical conductivity, pH, atmospheric temperature and photosynthetically active radiations was conducted during three different seasons viz., post-monsoon, winter and summer. The atmospheric temperature was recorded for three consecutive years for all different seasons. Along with the physical environmental factors, vegetations in and around the Lake was also observed for all the seasons.

Krishna et al., (2014) listed a few grassland shrubs growing around the saline area of Sambhar lake such as *Sporobolus virginicus*, *Eleusine compressa*, *Cressa cretica*, *Aeluropus lagopoides*, and *Suaeda fruticosa.* Not all that was listed by the group was found, but in our study, halophytes such as *Heliotropium curassavicum*¸ *Aloe vera,* and *Sesuvium sesuvioides* were seen abundantly in the area.

Most of the halophytes growing at the site were short-lived and believed to complete their life cycle before winter or summer sets in. This could be a mode of escaping the saline environment by dispersing the seeds and completing their life cycle before the harsh onset of weather. Some halophytes such as *Atriplex triangularis*, *Arthrocnemum indicum*, *Suaeda aralocaspica*, *Suaeda fruticosa*, and *Suaeda splendens* are known to develop a strategy referred to as *caution germination* strategy, wherein, the seeds dispersed during the favorable *conditions germinates* only when the salinity around its rhizosphere decreases

(Khan and Gul, 1998; Khan et al., 1998; Redondo-Gomez et al., 2008; Wang et al., 2008). The same strategy could have been adopted by those that were seen around the site. However, of all the annual halophytes growing in the area, *Suaeda fruticosa* was seen to grow throughout the year during all the season, i.e., post-monsoon, winter and summer irrespective of the temperature, salinity, and pH level around it (Figure. 3.11).

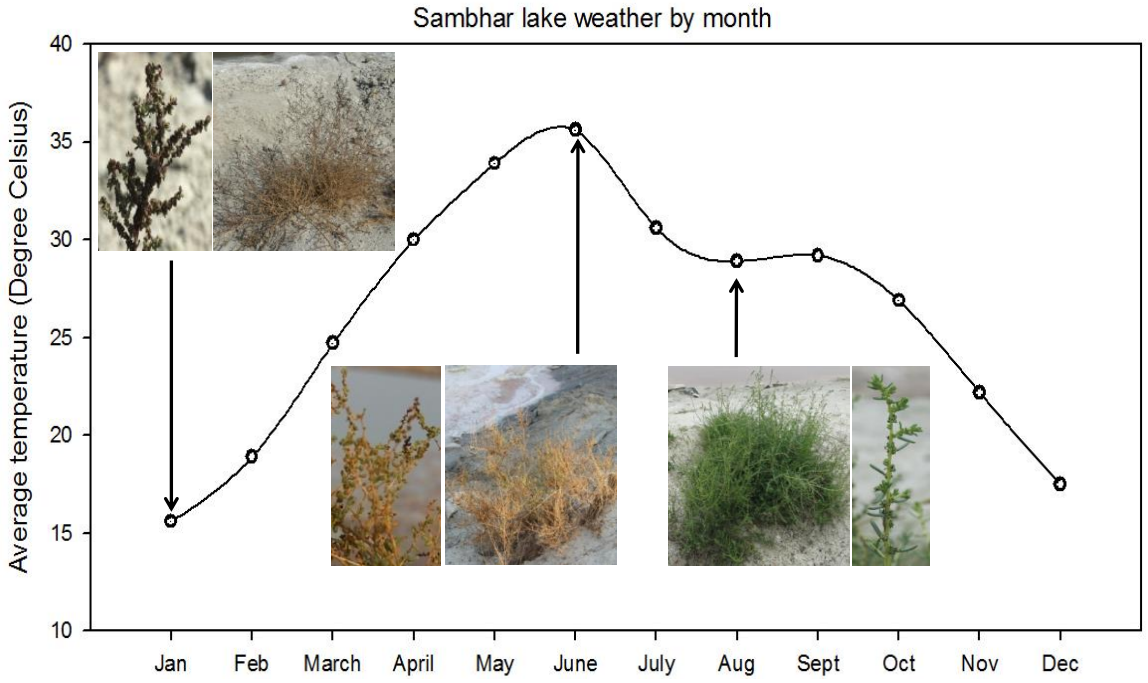

Figure 3.11. The average monthly maximum temperature at Sambhar Lake and morphology of *Suaeda fruticosa* found to be during the three different seasons. The temperature for each month was obtained from public data that is available online (http://www.meoweather.com/).

As discussed above, salinity and pH of the soil reached ~65 dSm^{-1} and 9.5, respectively while atmospheric temperature reached up to ~49^{o}C during summer. During winter, salinity and pH also were seen to remain high (~55 dSm^{-1} and 9); however, the atmospheric temperature got reduced to as low as 4^{o}C. With such a variable and harsh condition, *Suaeda fruticosa* still could complete its life cycle and continue to propagate in the area. Such a level of tolerance

could only be attained with highly adaptive features both at the physiological and molecular level. Therefore, the goal of the present work is to understand the basics of molecular adaptation in *Suaeda fruticosa* growing under natural conditions in three different seasons. In addition to the molecular adaptation, its physiological regulation was also targeted for examination.

3.4.1. The changing physical parameters have direct impact on the morphology of S. fruticosa

Plants are subjected to several combinations of both biotic and abiotic stresses which lead to molecular and physiological impairment (Fujita et al., 2006; Rejeb et al., 2014; Suzuki et al., 2014; Nongpiur et al., 2016; Wungrampha et al., 2018). Among the abiotic stresses, salinity causes ionic as well as osmotic stress which leads to physiological drought (Munns, 2002; Mahajan & Tuteja, 2005; Munns & Tester, 2008), reduction in photosynthetic efficiency (Wungrampha et al., 2018) and disruption of minerals uptake by plants (Grattan & Grieve, 1998). On the other hand, high temperature causes reduction in photosynthesis by hindering CO_2 uptake (Weis & Berry, 1998), injury to the thylakoid and impairment of electron transport chain (Wise et al., 2004), plant sterility (Satake & Yoshida, 1978) and makes plants more susceptible to biotic stress (Kassanis, 1952). Similarly, cold stress affects the normal growth and development of plants by inhibiting the full expression of its genetic makeup and also inhibit the metabolic reactions (Chinnusamy et al., 2007). However, a number of plants exists in nature which are referred to as xero-halophytes, which can tolerate high salinity as well as high temperature (Wungrampha et al., 2018).

Summer with continuous high temperature is predominant at the study site. pH and salinity of the soil were also high throughout the year. Even though salinity and pH are lowest during the post-monsoon season, it still is very high for any glycophyte to grow. Therefore, plants growing in this area face a combination of two major abiotic stresses throughout the year. During summer, *S. fruticosa* is exposed to high salinity, alkaline soil along with high temperature. On the other

hand, during winter season, these plants are exposed to cold temperature in addition to high salinity and alkaline soil. Although the temperature is high and soil is alkaline, salinity is relatively lesser during the post-monsoon season (Figure. 3.9).

The combination of the three physical factors, as mentioned above, leads to a direct impact on the floral habitat of the study area. During monsoon as the rainwater flushes away the excess salt, the seeds gets dispersed and began to germinate. During post-monsoon, the plants become mature and attain reproductive stage and began to develop seeds. During winter, most of the seeds were matured and were ready for dispersal. The plant also loses its greenery and develop more turgid and reddish leaves during winter. Most of the plants were seen to have prepared for the harsh summer by undergoing several modes of adaptations as described earlier. The dispersed seeds remained dormant until the next monsoon. The plants also develop highly succulent leaves and gradually undergo senescence and complete its life cycle. Khan et al. (2000) also observed the same phenomenon wherein *S. fruticosa* under salinity developed succulent leaves and have higher dry and fresh weight as compared to those that were grown on lesser saline soil.

As mentioned in chapter 2, we monitored the vegetation around the lake area including the changing levels of water availability, salinity, temperature, and soil pH in the three different seasons. *Suaeda fruticosa* was one of the very few halophytes growing at the site that completes its life cycle in roughly 12 months. Following germination, which occurs during monsoon, until its final life cycle at summer, the plant undergoes several changes in its morphology (Figure. 3.12.

During post-monsoon, in which salinity and soil pH are relatively lower, the plant was seen to have maximum growth. The leaves were greener, healthier, and less succulent (Figure. 3.12a & b). Some of the plants were observed to develop flowers and attract insects and ants for pollinations (Figure. 3.12.1e & f).

However, most of the plants were still developing and are yet to reach the flowering stage.

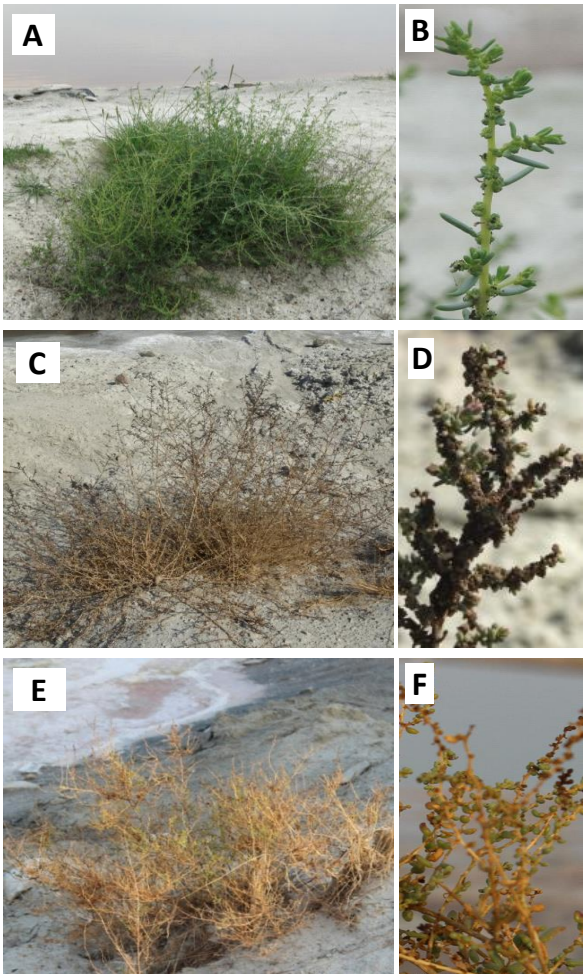

Figure 3.12: Changing morphology of *S. fruticosa* growing in three different seasons. A) Healthy and greener looking plant during post-monsoon. B) A close-up image of the leaf from the plant during post-monsoon. C) The plant becomes grey and fissured during winter. Matured seeds were seen clustering along with the leaves at the tip of the plant. D) A close-up image of the leaf from the plant during winter. E) Brown and senescence plant during summer. F) A close-up image of the leaf from the plant during summer.

As the temperature around the lake reduced, dropping up to ~5^{o}C during the night, in winter, and salinity gradually increasing with the decline in water availability, the morphology of the plant changed drastically. The healthy greener plants that were seen during post-monsoon turned grey and fissured (Figure.

3.12c & d). The leaves were found densely clustered together. The stems turn woody. Several black matured seeds clustering around the leaves at the tips of the plants contribute to its grey fissured morphology.

During summer, as salinity, temperature, and pH were maximum whereas water availability was minimum, the plant developed highly succulent leaf as one mode of adaptation to the changing environment. The number of leaves reduces in order to decrease the level of transpiration. Biomass of the plant was also minimum during this season. By the time summer sets in, all the mature seeds have been dispersed (Figure. 3.12e & f).

Plants undergo diverse morphological and anatomical changes in response to abiotic stress (Patakas, 2012). This, in turn, can reduce the plant growth. Likewise, histology and SEM images revealed dramatic changes in the morphology and anatomy of the *S. fruticosa* leaf across the three seasons. We observed that during the post-monsoon season, where conditions are more favorable, leaves are larger in size, and are made up of a multi-layered hypodermis. During summer, where both temperature and salinity are high, leaves become smaller in size and are more succulent. Remarkably, the hypodermis showed a reduction in the number of cell layers as also observed by Cramer et al. (2011).

3.4.2. Suaeda fruticosa accumulates ions for buffering pH and reducing its transpiration rate

With the changes in seasons and the level of salinity around the site, *S. fruticosa* not only changes its morphology but also adapts by sequestering as well as accumulating Na^+ ions on its leaves. Halophytes, as discussed in chapter 2, can behave as an accumulator, excluder or conductor (Yensen & Biel, 2006; Grigore et al., 2014) to survive under highly saline environment. By accumulating salts such as Na^+ ions in the leaf and its organelles, halophytes reduce the water potential in the leaf as compared to that of the soil. This helps in water absorption

from the saline soil (Hasegawa et al., 2000; Khan et al., 2000; Koyro et al., 2011). Compartmentalization of ions such as Na^+ and Cl^- between the mesophyll and epidermal layers has been reported in several plants such as sorghum (Boursier & Läuchli, 1989), wheat (Malone et al., 1991), barley and beans (Outlaw *et al.*, 1984). Most plants prefer to accumulate ions in the epidermal layers as this help in buffering the pH of the leaf under saline environment (Outlaw *et al.*, 1984). In addition, the ions that are accumulated on the epidermal layer lead to shrunken stomata that further reduces the rate of transpiration and water loss (Boursier & Läuchli, 1989; Malone et al., 1991).

In *S. fruticosa*, with the change in season, the level of salts, especially Na^+ varies. During post-monsoon, as water is abundant and salinity is minimum, Na^+ ions accumulating the in leaf epidermal, as well as the mesophyll layer, were relatively low (Figure. 3.9). However, as salinity increases during winter and summer, Na^+ ions also accumulated heavily on the epidermal as well as the mesophyll layer. During summer, Na^+ ions were found to accumulate more at the epidermal layer as compared to the mesophyll layers. This could be helping to buffer the pH of the leaf as well as to reduce the rate of water loss through transpiration.

3.5 Conclusions

Sambhar Lake in Rajasthan, which also is the largest inland salt extraction unit in India, encounters severe climatic conditions, which is not favorable for any glycophytes to grow. Salinity, pH, and temperature in and around the area are on the extreme for vegetation. However, some annual halophytes were seen to grow during monsoon, of which *Suaeda fruticosa* was seen to grow throughout the year. Germination happened during monsoon and post-monsoon, seed dispersal during winter and summer. Understanding the mode of adaption both at the physiological and molecular level of *S. fruticosa* can broaden the knowledge of stress adaptation in plants.

Chapter 4

CO_2 uptake and chlorophyll a fluorescence of *Suaeda fruticosa* grown under diurnal rhythm and after transfer to continuous dark

4.1 Introduction

Salinity stress, irrespective of plant's developmental stage, leads to severe reduction in plant growth, development, as well as yield (Joshi et al. 2016; Kumar et al. 2012; Pareek et al. 2010; Wungrampha et al. 2018). Salinity affects the whole plant architecture causing reduction in leaf area, which further limits light interception by the canopy, stomatal diffusion and photosynthetic rate (Chen et al. 2017). It is well established that high level of salinity primarily targets photosynthesis by impairing the photochemical efficiency of both PSI and PSII, by reducing their overall maximum quantum yield, the rate of electron transport and the overall performance index (Allakhverdiev et al. 2000; Kan et al. 2017; Soda et al. 2018). High salinity also causes swelling and degradation of thylakoids, impairs granal stacking, as well as chloroplast envelope development; further, it increases the number of plastoglobuli. In general, all these effects are most likely due to the production of reactive oxygen species (ROS), which lead to ultrastructural damage of the chloroplasts, as has been shown in several plants (Bastías et al. 2015; Meng et al. 2016). Although plants are sessile, they are able to deal with sublethal levels of several abiotic stresses (such as salinity, low temperatures, oxidative stress) as well as daily fluctuations in photosynthesis (due to changes in light intensity) by relying on and utilizing circadian oscillators (Bendix et al. 2015; Sharan et al. 2017; Shor and Green 2016; Webb 2003). Light intensities, as well as the duration of light and dark cycles (photoperiodic length), play a crucial role in the growth and development of plants (McClung 2006; Schaffer et al. 2001). This photoperiodic entrainment modulates the physiological

harmony of the plant such as its growth, stomatal opening, leaf movement and molecular responses by regulating the expression of certain genes at particular times (McClung 2006; Schaffer et al. 2001; Singh et al. 2015). Two parameters that modulate the photoperiod cycle of an organism are: diurnal and circadian rhythm. The endogenous cycle/rhythm that occurs within a period of 24 hrs is called circadian. However, the oscillating rhythm that is synchronized by day/night cycle is diurnal rhythm (see e.g., Soni et al. 2013; Webb 2003).There are two principal factors that govern diurnal rhythm in plants: the internal oscillating clock, the circadian clock (circadian rhythm), and light (De Caluwé et al. 2017; Schaffer et al. 2001). Endogenous circadian oscillators occur in all organisms which act as autoregulatory feedback loops driving the rhythmic behaviour of genes, proteins and metabolites (De Caluwé et al. 2017). In plants, the photoperiodic entrainment of environmental cues is 'gating' of the response to a stimulus through rhythmic synchronization of transcriptional, translational and post-translational modulations of large gene families. These genes, in turn, regulate plant growth and development by activating and accumulating stress-responsive proteins and metabolites (Greenham and McClung 2015). The fine-tuning responses are brought in by "alternative splicing", controlled protein turnover, and chromatin modifications, which allow the plants to coordinate their temporal organization of biological processes with daily and seasonal changes with light and temperature cycles (Greenham and McClung 2015; Mora-García et al. 2017). Both the internal state of the plant and the external environment influence the "pulse" of the oscillator clock by regulating the expression of its components. Successively, the clock ensures the activation of certain genes regulating multitude of metabolic and physiological aspects of plants that are suitable, during day or night, in providing fitness advantage in developmental processes during the life cycle of a plant (Cano-Ramirez and Dodd 2018; De Caluwé et al. 2017; Dodd et al. 2014).

We know that the pattern of changes in photosynthesis and respiration is influenced by diurnal rhythm in various plants including oak-grass savanna

species (Tang et al. 2005), *Quercus palustris* (Epron et al. 1992), *Glycine max* (Zhang et al. 2007), *Zea mays* (Leakey et al. 2004), *Vitis vinifera* (Downton et al. 1987), grassland species (Bahn et al. 2009), and Chinese flowering *Castanea* sp. (Cheng et al. 2016). Further, under stress, regulation of photosynthetic machinery is influenced by diurnal rhythm in plants such as *Solanum lycopersicum* (Ikkonen et al. 2015), *Hordeum vulgare* (Goldstein et al. 2017), *Oryza sativa* (Kim et al. 2017; Singh et al. 2015), *Zea mays* (Feng et al. 2017), *Glycine max* (Pan et al. 2015), *Arabidopsis* (Nitschke et al. 2016) and *Gossypium* sp. (García-Plazaola et al. 2017).

Unlike the glycophytes, halophytes have acquired certain photoprotective mechanisms since they have 'superior' alleles of the genes (involved in ion homeostasis, or production of osmoprotective compounds or anti-oxidative enzymes) for avoiding photodamage under high salinity (Sengupta et al. 2018). *Suaeda fruticosa*, used in our study, is a xero-halophyte well adapted to extreme desert environments and high saline conditions; it does it by maintaining high chlorophyll (Chl) *a*/*b* ratio and by accumulating osmoprotectants, such as proline and sugars (Flowers and Colmer 2015; Ullah and Bano 2015). However, no study has, thus far, been carried out to investigate the photoperiodic control of photosynthesis in this plant. Thus, the aim of our study was to understand the complex machinery associated with photosynthesis under diurnal rhythm conferring adaptive advantage to this plant by measuring the CO_2 gas exchange and Chl *a* fluorescence. These will provide us information on the basic photosynthetic efficiency of *S. fruticosa* surviving under xerophytic conditions (Mishra et al. 2016). To further test if eliminating light in *S. fruticosa* by keeping it under continuous dark affects CO_2 and H_2O fluxes, we maintained the plants under diurnal rhythm initially for 24 hrs, and then kept them under complete darkness for 48 hrs, under their natural habitat.

In this paper, we have systematically studied the entrainment capability of *S. fruticosa* at different photoperiods of the light-dark cycle in order to analyze the

influence of diurnal rhythm and of continuous dark on Photosystem II (PSII) efficiency. This was done by measuring changes in the maximum quantum yield of PSII photochemistry (via changes in the ratio of the variable (F_v) to maximal (F_m) chlorophyll fluorescence). Additionally, we measured the overall photosynthesis performance index at dawn and at dusk under both diurnal and continuous dark conditions. Our investigation provides a comprehensive analysis of PSII photochemistry, photoinhibition and photoprotection in *S. fruticosa* under extreme saline conditions. Furthermore, the dynamic behaviour of the photosynthetic machinery observed, in this study, under diurnal condition confirms the contribution of the photoperiodic entrainment in providing tolerance against the saline environment in xero-halophytes.

4.2 Material and Methods

4.2.1 Plant material and study conditions

We conducted our study at the Sambhar Salt Lake (India's largest inland playa within the Thar desert) located in the middle of the Aravalli schists, India (26°58' N, and 75°5' E), where *S. fruticosa* population is high (Figure 3.2 in Chapter 3). The average temperature of this area reaches up to 50°C during the summers and goes down to as low as 3ºC during the winters, with a total salinity of 45-60 dSm^{-1} and the pH range of 8.4-10.5 throughout the year (Krishna et al. 2014; Roy and Singhvi 2016; Chapter 3). Sambhar lake receives an annual rainfall of 100-500 mm, mostly during the monsoon season (Sinha and Raymahashay 2004). At the site of our research, light intensity was measured from ~ 05:00 to ~ 20:00 hrs, before and after which the light intensity was reduced to nearly zero (to provide darkness). The maximum photosynthetically active radiation (PAR) on a clear day was 1,800 µmol photons $m^{-2}s^{-1}$, as measured by LX-101A Lux Meter (HTC Instruments, India) between 10:00 hrs to 15:00 hrs (Figure. 3.5 in Chapter 3). The plants that were monitored under continuous dark had been covered with a double-layered thick dark cloth, which had only ~ 1% transmission of the day light

(Figure. 4.1), from 300 to 900 nm, as measured by a Cary 300 UV-Visible spectrophotometer (Agilent, USA).

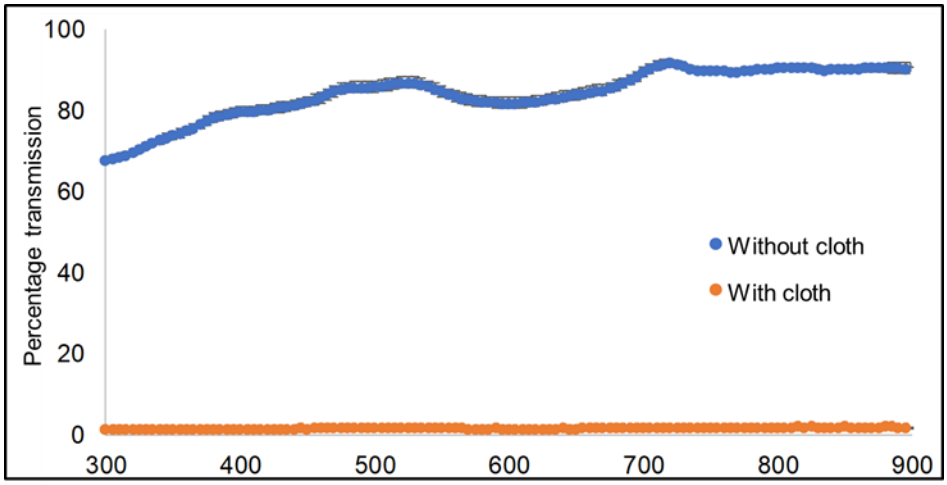

Figure 4.1: Percentage transmission from the double layered black cloth that was used for covering plants to maintain continuous dark. Transmission from the dark cloth for the wavelength range of 300-900 nm was only ~ 1%.

4.2.2 Gas exchange measurements

Leaf gas exchange parameters for *S. fruticosa*, under diurnal and continuous dark, were recorded using a Li-6400XT (Li-Cor Inc., Lincoln, USA) portable infra-red gas analyzer. Measurements were made continuously for 72 hrs at 3 hrs intervals on plants kept under both the experimental conditions (see above); in these experiments, at least 2/3 of the infrared gas analyzer chamber area was covered with leaves of *S. fruticosa*. For the case of continuous dark, the first 24 hrs of the experiment was under diurnal condition, and then, for the next 48 hrs the plant was covered with two layers of the black cloth (cf. Kolosova et al. 2001). However, all other conditions were maintained similar to those used for plants under diurnal condition. In order to measure transpiration rate (Tr), stomatal conductance (Gs), net photosynthetic rate (NPR) and intercellular CO_2 mole fraction (Ci) under *in situ* conditions, we measured them at ambient CO_2 concentration (400 µmol mol^{-1}) and at photosynthetic photon flux density (PPFD)

of 2,900 µmol photons m^{-2} s^{-1}, obtained from the blue and the red LEDs (light emitting diode) of the leaf chamber.

4.2.3 Measurement of Chlorophyll a fluorescence

The Chl *a* fluorescence kinetics was measured with Handy PEA-Plant Efficiency Analyser (Hansatech Instruments, King's Lynn, Norfolk, UK) instrument. The parameter for non-photochemical quenching (NPQ) of the excited state of Chl*a*, the coefficient for photochemical quenching (qP), the coefficient for non-photochemical quenching (qN), and the total electron transport rate through PSII (ETR) were calculated as follows (see e.g., Lazár 2015): (1) **NPQ** = (Fm − Fm′)/Fm′, where Fm is the maximum Chl fluorescence in dark adapted plants, and Fm′ is the maximum Chl fluorescence in light adapted plants, which is a measure of the excitation energy dissipation in PSII antenna; (2) **qP** = (Fm′ − F(t))/(Fm′ − Fo′), where F(t) is the Chl fluorescence measured at time t, which indicates the proportion of open PSIIs (i.e., with Q_A in the oxidized state); (3) **qN** = ((Fm − Fo) − (Fm′ − Fo′))/(Fm − Fo), which is a coefficient for non-photochemical quenching that requires measurement of the initial fluorescence of the dark-adapted and light-adapted sample (i.e., Fo and Fo′); and (4) **ETR** $\approx \Phi_{PSII} \cdot PPFD \cdot A \cdot 0.5$, where Φ_{PSII} = (Fm′–Fs)/Fm′ is the light-adapted quantum yield of PSII, Fs being the Chl fluorescence of the light adapted sample, and PPFD (photosynthetically active photon flux density) being the incident irradiance, A the leaf absorbance (estimated as 0.84), and 0.5 is for the assumed equal distribution of photons between PSI and PSII,. In addition, the variable to maximum fluorescence ratio, F_v (=Fm – Fo)/F_m, was measured on dark-adapted (10 min) leaves of *S. fruticosa,* by Handy PEA-Plant Efficiency Analyser (Hansatech Instruments Ltd, Petney, Norfolk, UK). Measurements were made for 72 hrs at every three hrs.

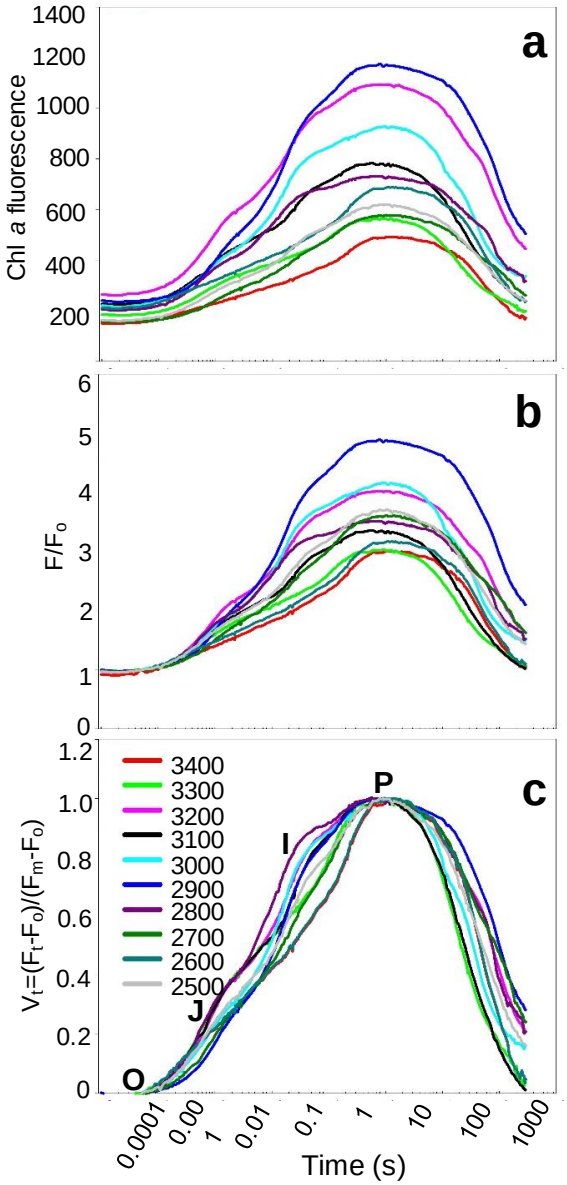

Figure 4.2: Polyphasic Chl a fluorescence transient of dark-adapted *S. fruticosa* leaves at different intensities (2500-3400 µmol photons m^{-2} s^{-1}) of 650 nm light. () Chlorophyll a fluorescence transient of the leaves of S. fruticosa plotted on a logarithmic time scale. The O, J, I and P steps are marked in the figure, where, O is for origin (the minimum fluorescence Fo), J and I are for the intermediary fluorescence levels at 2 ms and 30 ms (Fj and Fi), and P is for the peak (Fp). (b) Fluorescence transients measured at different light intensities; the O–J–I–P transients showed here were normalized at Fo. (c) Variable fluorescence measured from the leaves of *S. fruticosa* at different light intensities; the O-J-I-P fluorescence shown here were double normalization at F_o and Fp phase; $V = (F_t – F_o)/(F_m – F_o)$.

The Chl a florescence induction transient of the dark-adapted samples was measured with a 300 second 650 nm excitation light of several intensities between 2,500 and 3,400 µmol photons $m^{-2}s^{-1}$, to find the light intensity at which the "P" level reaches the maximal fluorescence (Fm); our results showed that in our samples, Fm is reached when the excitation light intensity is 2,900 µmol photons $m^{-2}s^{-1}$ (Figure. 4.2 and Figure. 4.3). For measurement of OJIP, 1-2 seconds are used; however, to include S(M)T phase, we measured Chl fluorescence up to 300 seconds (Stirbet et al. 2018). However, no maxima were detected in SMT phase region; therefore, it is not discussed in this paper. Further, the readings obtained from the Handy-PEA were double normalized at Fo and at Fm by using the PEA Plus software (version 1.12), and analyzed it using the so-called JIP-test, which is based on the general concepts of energy fluxes in bio-membranes (see Strasser 1978; Strasser et al. 2004). The following energy fluxes were defined in the JIP test:Photon absorption by PSII antenna (ABS); trapping of excitation energy flux by the PSII reaction center (TRo); dissipation of the excitation energy flux in PSII antenna (DIo) (where DIo= ABS – TRo); electron transport (ETo) from PSII to the plastoquinone (PQ) pool; and reduction of the end (electron) acceptors of PSI (REo). The Chl *a* fluorescence transient was plotted on a logarithmic time scale to be able to see clearly all the steps of the "OJIP" phase; further, Chl a fluorescence at 50 µs was taken as the minimum fluorescence (Fo). Using the measured fluorescence data sets, we have calculated several JIP parameters (see Table 4. 1 for the abbreviations, definitions and equations), as presented by Stirbet and Govindjee (2011) and Stirbet et al.(2018).

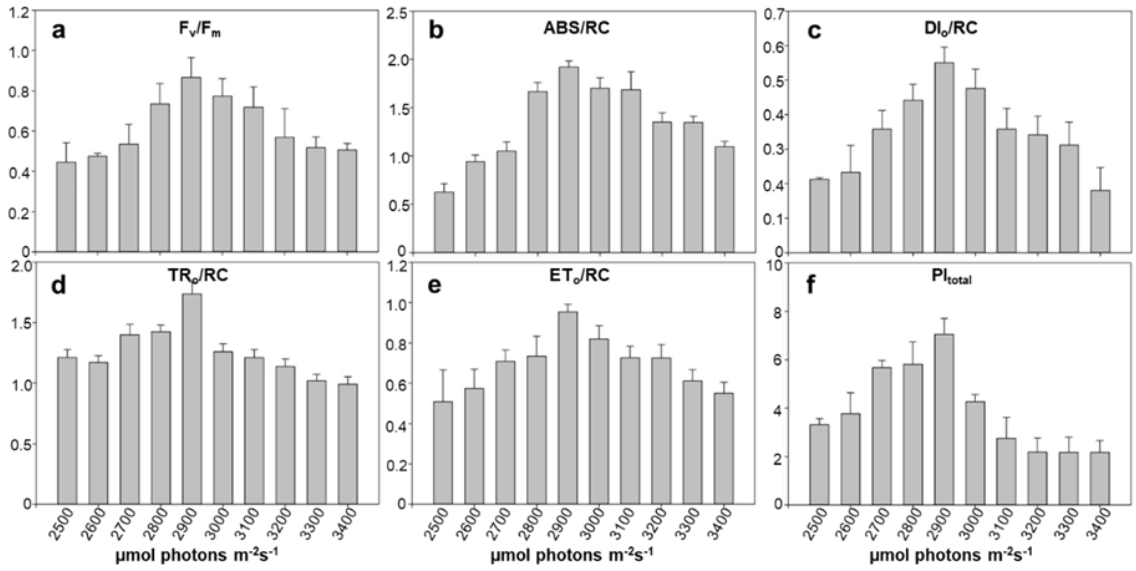

Figure 4.3: Several photosynthetic parameters of photosynthesis of *S. fruticosa*, as calculated from the data in Figure 4.2. (a) Quantum yield of the photosystem II as inferred from the Chl a fluorescence (Fv/Fm) (b) ABS/RC, absorbed photon flux by an active PSII reaction center (c) DIo/CSm, energy flux dissipated per active PSII reaction center (D) Tro/CSm, maximal trapped energy flux by a PSII reaction center (e) ETo/RC, the electron transport flux per active PSII reaction center (f) Performance index [PI_{total} = PI_{ABS}·(1-Vi)/(Vi -Vj)] showing the conservation of energy from excitation of PSII

Table 4.1: Abbreviations, formulas, and definitions of the JIP-test parameters used in the current study

Technical Fluorescence parameter		
t_{Fm}	Total time taken to attain maximum fluorescence	Time to reach F_m
Area	The area between the fluorescence curve and the line F = F_m	The total area over the O-J-I-P curve
F_o	F(50µs)	Minimum fluorescence (fluorescence at 50µs)
F_m		Maximum fluorescence
V_j	$(F_j - F_o)/(F_m - F_o)$	Relative variable fluorescence at 2 ms
V_i	$(F_i - F_o)/(F_m - F_o)$	Relative variable fluorescence at 30 ms
N	$[Area/(F_m-F_o)]·Mo·(1/V_j)$	Turnover number: Number of Q_A reduction events between time 0 to

		Fm
M_o	$4\{F_k(0.3ms) - F_o\}/(F_m - F_o)]$	Initial slope of the O-J-I-P curve (slope of the O to J rise)
M_{ji}	$\{F(3ms) - F(2ms)\}/(F_m - F_o)$	Slope of the J to I rise
M_{ip}	$0.2\{F(35ms) - F(30ms)\}/(F_m - F_o)]$	Slope of the I to P rise
Specific energy fluxes per active PSII reaction center		
ABS/RC	$(Mo/V_j)/(F_v/F_m)$	Absorbed photon flux by an active PSII reaction center (i.e., the antenna size of an active PSII reaction center)
DI_o/RC	$(ABS/RC) - (TR_o/RC)$	Energy flux dissipated per active PSII reaction center
TR_o/RC	M_o/V_j	Maximal trapped energy flux by a PSII reaction center
ET_o/RC	$M_o \cdot (1/V_j) \cdot (1 - V_j)$	The electron transport flux per active PSII reaction center
Phenomenological energy fluxes defined at F_o		
ABS/CS_o	$\approx F_o$	Absorbed photon flux per excited PSII cross section at time zero
DIo/CS_o	$(ABS/CS_o) - (TR_o/CS_o)$	Energy flux dissipated per excited PSII cross section at time zero
TRo/CS_o	$(F_v/F_m) \cdot (ABS/CS_o)$	The maximum trapped exciton flux per excited PSII cross section a time zero
ET_o/CS_o	$(F_v/F_m) \cdot (1-V_j) \cdot (ABS/CS_o)$	Electron transport flux per excited PSII cross section at time zero
Phenomenological energy fluxes, defined at F_m		
ABS/CS_m	$\approx F_m$	Absorbed photon flux per excited PSII cross section at F_m
DI_o/CS_m	$(ABS/CS_m)-(TR_o/CS_m)$	Energy flux dissipated per excited PSII cross section at F_m
TR_o/CS_m	$(F_v/F_m) \cdot (ABS/CS_m)$	Maximum trapped exciton flux per excited PSII cross section at F_m
ET_o/CS_m	$(F_v/F_m) \cdot (1-V_j) \cdot (ABS/CS_m)$	Electron transport flux per excited PSII cross section at F_m
Performance index		
PI_{total}	$PI_{total} = PI_{ABS} \cdot (1-V_i)/(V_i - V_j)$	Performance index showing the conservation of energy from excitation of PSII, until the reduction of the last acceptor molecules of PSI (the complete photochemistry)

4.3.4 *Statistical analysis*

Measurements of Chl *a* fluorescence as well as for gas exchange were statistically analyzed using ANOVA model (Fisher 2002). Only measurements having significant values ($p< 0.05$) are shown in the figures. For each time point, six replicate readings were taken for both diurnal and continuous dark experiments. From this, a heat map was developed using Multi Experiment Viewer (MeV) version 4.9 to visualize the values of the JIP parameters used in the analysis (Saeed et al. 2006). This heat map was generated by normalizing the values and bringing them all to a percentage range between 1 to 100% to provide an unbiased color code. Three color code combination of red for high (100%), yellow for medium (50%) and green for the lowest value (1%) was used to represent the heatmap.

4.3. Results

4.3.1. Leaf gas exchange measurements under diurnal rhythm and continuous dark conditions

The leaf gas exchange of *S. fruticosa* was measured under *in-situ* conditions for the plants under diurnal as well as under continuous dark condition at three-hour intervals for 72 hrs (as described in the Material and methods section). Clear rhythmic activity was observed in all the photosynthetic parameters calculated in this study, repeated every 24 hrs (Figure. 4.4 and Figure 4.5). Plants kept under continuous dark showed damping in the gas exchange values under dark conditions (right panel of Figure. 4.4 and 4.5). However, parameters such as F_v/F_m, NPR, ETR, and Tr (Figure.4.4) showed noticeable rhythm even under dark conditions (though the amplitudes were smaller than under diurnal rhythm). The parameters that noticeably changed under continuous dark condition are shown in Figure 4.4, while the parameters that did not exhibit any noticeable change under continuous dark, as compared to changes observed under diurnal condition are presented in Figure 4.5. The weak fluctuation in photosynthetic

parameters, observed in *S. fruticosa,* kept under continuous dark, is shown in Figure 4.6, after separating observations from two datasets (i.e., diurnal for the first 24 hrs, and continuous dark for the next 48 hrs).

The maximum PSII quantum yield calculated from the Chl *a* fluorescence (i.e., F_v/F_m), showed the highest value at 23:00 hrs, with its high-level maintained till dawn under diurnal rhythm. However, under continuous dark, F_v/F_m was high between 08:00 to 17:00 hrs, with its maximum value observed at 14:00 hrs (Figure. 4.4a and Figure. 4.4b), while under the diurnal rhythm it had the lowest value during the same period. In contrast to the maximum quantum yield, the net photosynthesis rate (NPR) and electron transport rate (ETR) had the highest values at 08:00 hrs and between 08:00 to 14:00 hrs under diurnal conditions (Figure. 4.4c, e and Figure 4.4d, f), as well as at 05:00 hrs under continuous dark condition (Figure. 4.4e and Figure. 4f). Similarly, the transpiration rate (Tr) showed the highest value between 08:00 to 17:00 hrs under diurnal conditions (Figure. 4.4g), and at 05:00 hrs under continuous dark condition (Figure. 4.4h). Parameters such as internal CO_2 concentration (Ci), stomatal conductance (Gs), non-photochemical quenching with values between zero to infinity (NPQ), photochemical quenching (qP) and non-photochemical quenching (qN), with values ranging from zero to one showed damping under continuous dark condition, and the fluctuations could not be noticed, as compared to those under diurnal conditions (Figure. 4.5a –j).

S. fruticosa under continuous dark showed maximum ETR, Tr, Ci and NPQ at 05:00 hrs, which gradually decreased until the next cycle, which is an opposite response observed under diurnal rhythm, where, it showed maximum activities of the same parameter during daytime i.e., between 08:00 to 17:00 hrs. However, Gs, NPR, qP and qN, under continuous dark, showed almost a similar pattern of activity as under diurnal rhythm (with some minor differences in the time of the peak). However, the amplitude for all these parameters were strikingly lower under dark than the diurnal setup (Figure. 4.4, 4.5 and 4.5).

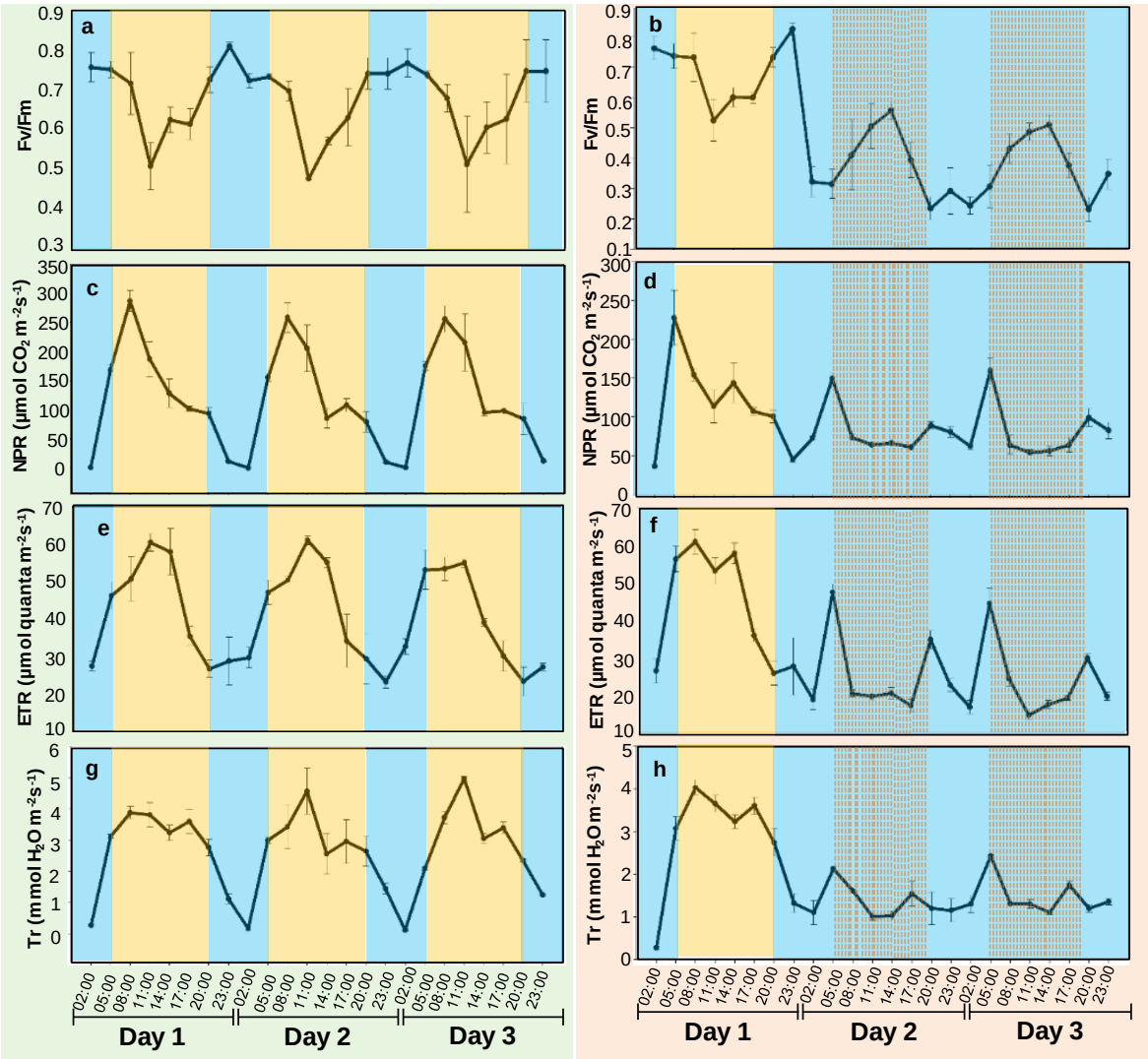

Figure 4.4: Photosynthetic parameters for *S. fruticosa* showing noticeable fluctuations in amplitude under diurnal rhythm and continuous dark. The right panel shows photosynthesis parameters under "continuous dark," where during the first 24 hours the plant was kept under diurnal condition, followed by 48 hours under dark (as described in section 4.2). All parameters, at different time points of the day, were measured on the leaves of *S. fruticosa* for 72 hours (3 days). A clear rhythmic activity that repeats after every 24 hours was seen in all the parameters. (A, B) Quantum yield of the photosystem II as inferred from the Chl a fluorescence (C, D) Net photosynthesis rate, (E, F) Electron transport rate, (G, H) Transpiration rate. The blue area indicates night, orange depicts day and the dotted portion indicates continuous dark that was maintained by covering with two layers of black cloth.

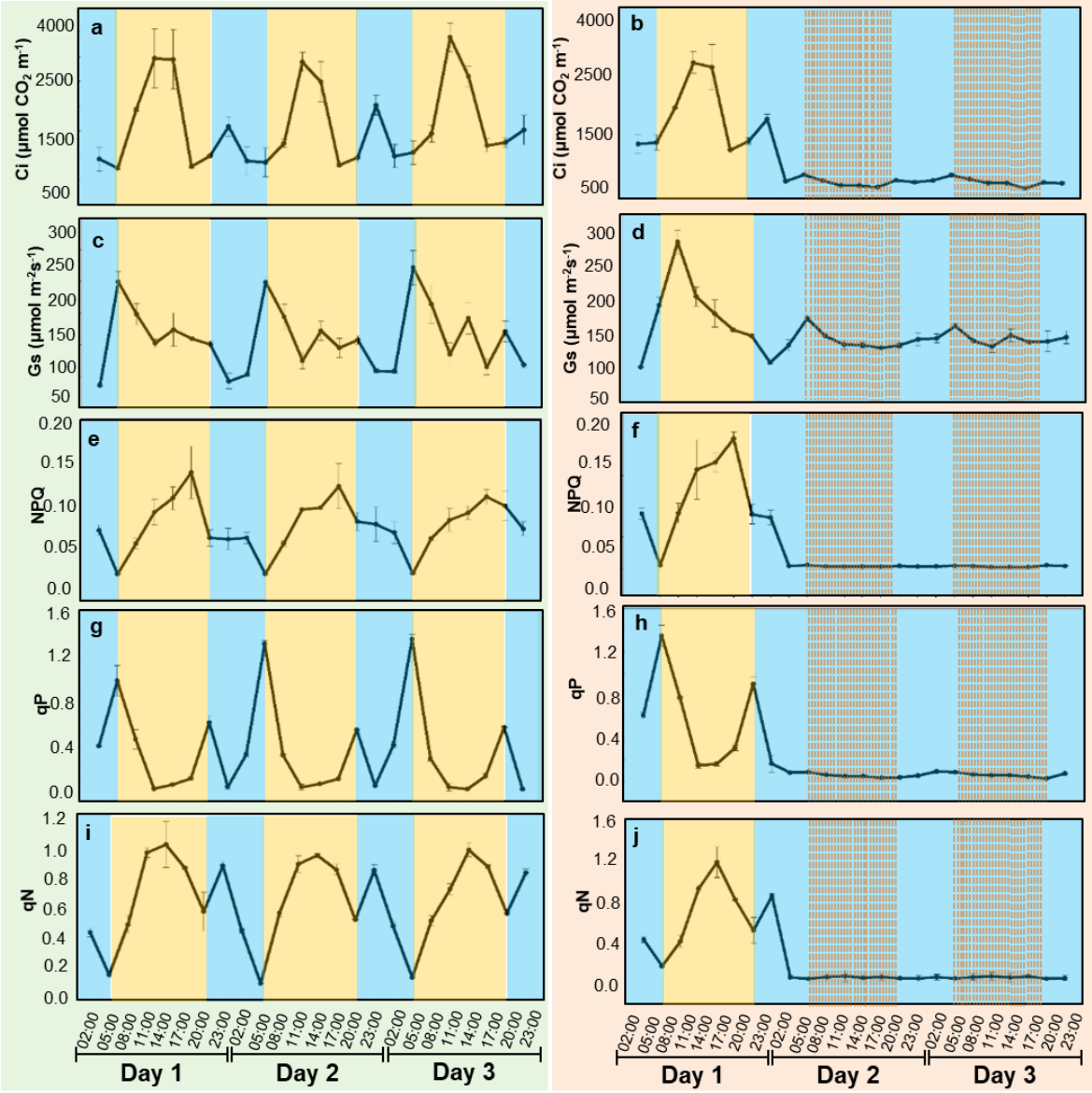

Figure 4.5: Photosynthetic parameters that do not show any noticeable amplitude of fluctuation after maintaining under continuous dark. The right panel shows the photosynthesis parameters under continuous dark where the first 24 hours the plant was maintained under diurnal condition followed by a 48-hour dark period. Photosynthetic parameters at different time points of the day were measured from the leaves of *S. fruticosa* for 72 hours (3 days). (A, B) Internal CO_2 concentration, (C, D) Stomatal conductance, (E, F) Non-photochemical quenching of the excited state of Chl, usually by heat loss (G, H) a quotient for photochemical quenching of the excited state of Chl, (I, J) a quotient for non-photochemical quenching of the excited state of Chl. The blue areas indicate night, orange depicts day and the dotted portion continuous dark (maintained by covering with a double layer of black cloth).

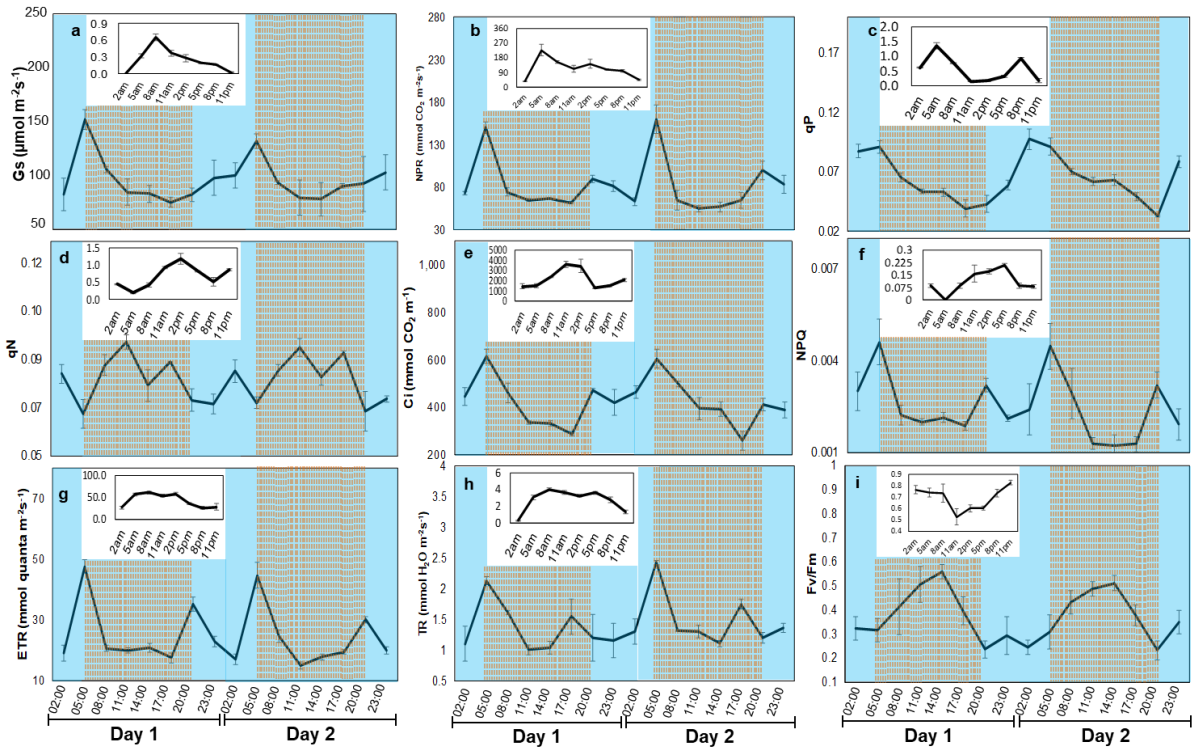

Figure 4.6: Parameters of photosynthesis in *Suaeda fruticosa* under diurnal condition for the first 24 hrs followed by continuous dark for 48 hrs. Using IRGA, parameters during different time points of the day were measured in the leaves of S. fruticosa for 72 hrs (3 days). The shaded portion of the graph represents night. To maintain continuous dark, the plant was completely covered with a dark cloth. A clear rhythmic activity that repeats every 24 hrs was seen in all the parameters. a) Stomatal conductivity, b) Net photosynthesis rate, c) a quotient for photochemical quenching of the excited state of Chl, d) a quotient for non-photochemical quenching of the excited state of Chl, e) Internal carbon dioxide concentration, f) Non-photochemical quenching of the excited state of Chl, usually by heat loss, g) Electron transport rate, h) Transpiration rate and i) Quantum yield of photosystem II as inferred from Chl a fluorescence. The values of corresponding parameter as observed under the diurnal setup during the first 24 hrs are shown in the inset

4.3.2. Polyphasic chlorophyll a fluorescent rise in S. fruticosa under diurnal rhythm and continuous dark conditions

To further determine the influence of the diurnal rhythm and the elimination of light on the function and qualitative parameters of PSII, we analyzed the OJIP

phase of Chl *a* fluorescence transient (Figure. 4.7). The average fluorescence of *S. fruticosa* from zero to 300 seconds for each time point for 72 hrs under diurnal rhythm is shown in Figure. 4.7a, on a logarithmic time scale. The distinct rise (from O to P) in the O-J-I-P fluorescence curve was observed at all the time points measured in both diurnal and continuous dark conditions. However, the O level (Fo) varied throughout the day, wherein the minimum value was observed at 14:00 hrs and 11:00 hrs under diurnal, and at 11:00 hrs and 05:00 hrs under continuous dark. The OJIP curve was plotted as F/Fo (i.e., normalized to the "O" level; see calculation in Table 1) to focus on the changes in the OJIP curve. The highest OJIP polyphasic rise was observed at 23:00 hrs, whilst the minimum fluorescence rise was observed between 14:00 to 17:00 hrs (Figure. 4.7b). Throughout the day, each time point showed variability in photosynthetic activity as well as in the functional and qualitative parameters of PSII. To further analyze the differences in various photosynthetic parameters, such as the area of the OJIP fluorescence rise, the time to attain Fm, and other parameters represented in Table 1, the measured fluorescence curve was double normalized, i.e., at both Fo and Fm levels, and represented by V(t) = (F(t)-Fo)/(Fm-Fo) (Figure. 4.7c). This allowed us to focus on observing the rates of changes during the entire OJIP curves, across all the time points. Distinct changes in the OJIP rise and in the parameters, such as the initial slope, the time to reach J, I and P levels, and the area over the curve, were observed for all the time points under both continuous dark and diurnal conditions. With respect to the J level, two distinct sets of OJIP transient rise were observed under diurnal condition. The time taken to reach J at 11:00, 14:00, 17:00 and 23:00 hrs was shorter than that at 02:00, 05:00, 08:00 and 20:00 hrs. However, under continuous dark, such a distinction was not observed.

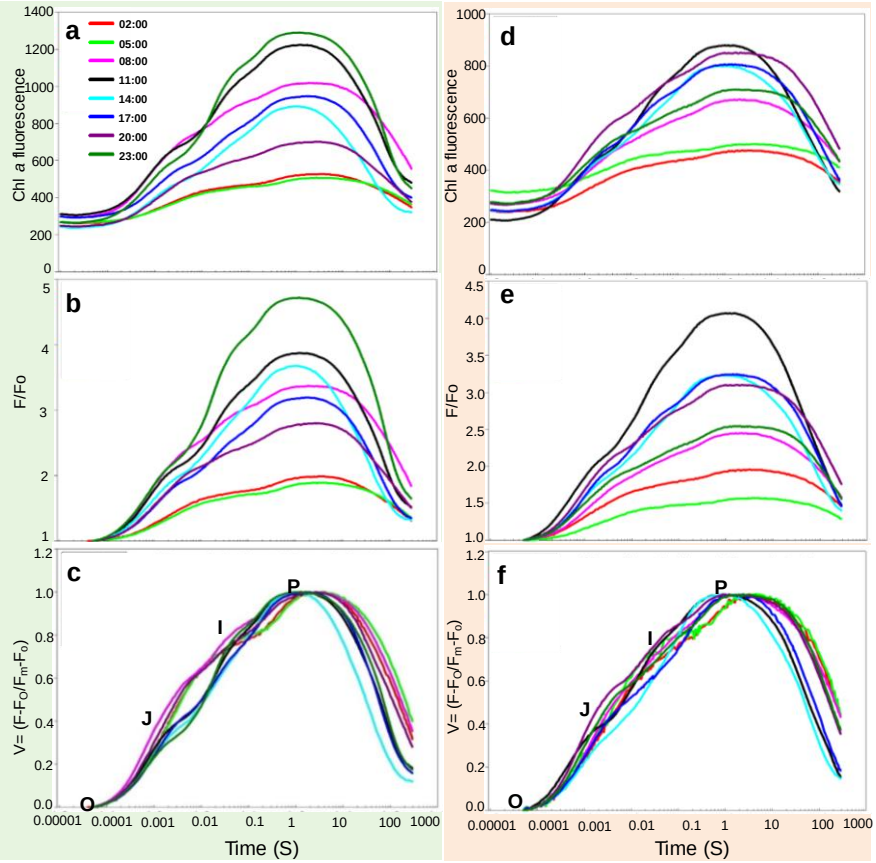

Figure 4.7: Polyphasic OJIP transient rise for *S. fruticosa* under diurnal or continuous dark. For each time point, the relative variable fluorescence was measured for 300 seconds, and the data obtained was plotted on a log scale. The right panel shows the OJIP curve obtained from the plant that is under diurnal condition. The left panel is for the plant that is under continuous dark condition. (a, d) the raw Chl a fluorescence obtained at different time points (b, e) fluorescence curve obtained after normalizing at O level (Fo), and (c, f) variable fluorescence (V) at time t obtained after normalizing at O and P (Fo and Fm) levels.

Similarly, the time-resolved fluorescence induction kinetics of *S. fruticosa* from zero to 300 seconds for each time point for 48 hrs (excluding the first 24 hrs) under continuous dark, plotted on a logarithmic scale, is shown in Figure. 4.7d. Further, Figure. 4.7e shows the curves normalized to Fo (i.e., F/Fo). In contrast to the diurnal rhythm, the typical OJIP polyphasic fluorescence rise under continuous dark was maximum at 11:00 hrs, while the minimum fluorescence rise was observed at 02:00 hrs. The relative variable fluorescence

V(t) = (F(t)-Fo)/(Fm-Fo) was calculated and represented at different time points throughout the day at three-hour intervals under dark conditions. Unlike the plant under diurnal condition, which showed two distinct kinetics of the OJIP fluorescence rise, no such distinct sets were observed under continuous dark condition, but the OJIP kinetics was different at each time point (Figure. 4.7f).

Quantitative estimation of the PSII activity by analyzing the transient fluorescence rise of *S. fruticosa* under diurnal as well as continuous dark conditions showed comparable significant changes unlike the parameters obtained from the gas exchange data, using IRGA, wherein, the measured parameters showed lower amplitude during continuous dark (Figure. 4.6).

4.3.3. Relative variable fluorescence under the diurnal rhythm and continuous dark conditions

To compare the fluorescence-rise between plants under diurnal and continuous dark (Figure.**3**), single normalized (at F_o or "O" level) fluorescence (F/F_o) was calculated for both the conditions at each time point (Figure. 4.8). To observe the difference in the O-J-I-P rise, fluorescence rise was plotted on a log scale from zero to 300 second at the same scale. Differences were observed in the pattern of the polyphasic O-J-I-P transient rise between the plant that was under diurnal and those that are under continuous dark at each time point. At 02:00 and 05:00 hours, plants under both conditions showed slow fluorescence rise (Figure. 4.8a and Figure 4.8b). From 08:00 hours until 23:00 hours, the OJIP rise under both the condition increases (Figure. 4.8c-h). The OJIP rise at 08:00, 14:00 and 23:00 hours under diurnal condition was higher than that under continuous dark. However, at 11:00 and 20:00 hours, the OJIP rise was higher under continuous dark condition. Under both the conditions maximum fluorescence rise was observed at 11:00 hours (Figure. 4.8h). Under continuous dark, maximum fluorescence was observed at 11:00 hours (Figure. 4.8d). The increase in the OJIP rise corresponded to the increased in F_v/F_m as described in section 5.1 under both diurnal and continuous dark conditions.

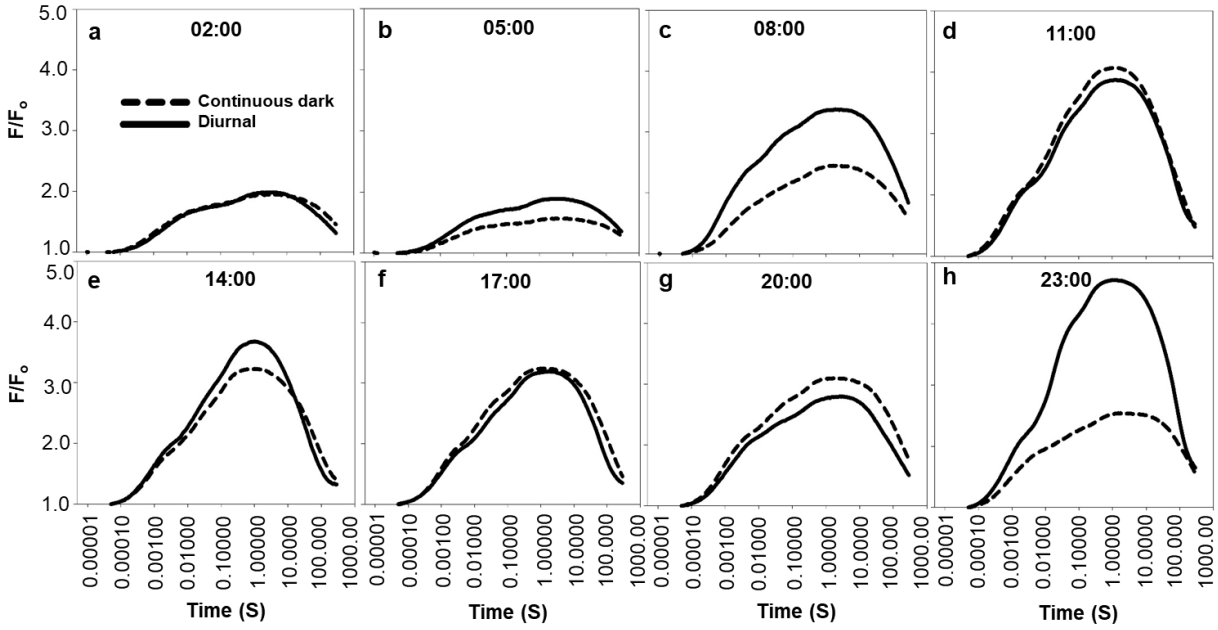

Figure 4.8: Comparison of the OJIP fluorescence curve (normalized at F_o level) between *S. fruticosa* leaves under diurnal (full line) and continuous dark (broken line) at different time points.

To further compare the variable fluorescence between the plants under diurnal and continuous dark, the transient fluorescence (V_t) was calculated for both the conditions at each time point (Figure. 4.8). Differences were observed in the pattern of the polyphasic O-J-I-P transient rise between the plant that was under diurnal and those that are under continuous dark at each time point. However, under both conditions, distinct 'J' peak (OJ rise is the photochemical phase) was not observed during 02:00 and 05:00 hours (Figure. 4.8a and b). A slower O-J fluorescence rise was observed during 08:00 and 20:00 hours (Figure. 4.8c and Figure 4.8g) under both the conditions. In addition, under diurnal condition, distinct 'J' and 'I' (thermal phase) "peaks" were observed during 23:00 hours; however, the I peak was not observed in the plant that was under continuous dark (Figure. 4.9h).

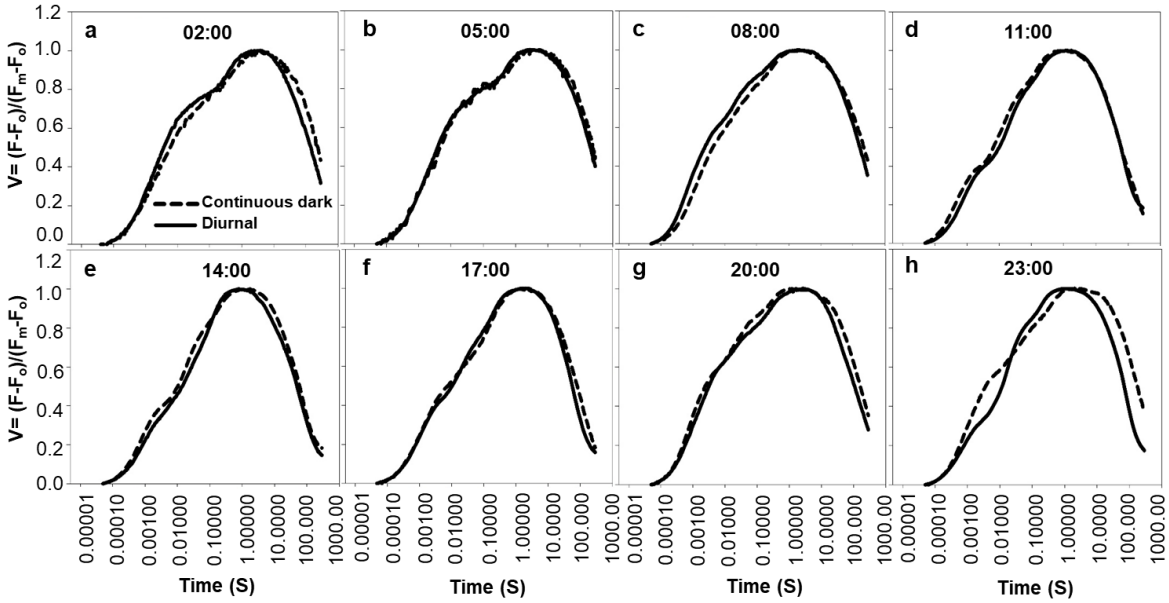

4.9: Comparison of the OJIP transient curve between *S. fruticosa* leaves under diurnal (full line) and continuous dark (broken line) at different time points. At all the time points, the observed parameters showed that the continuous dark and the diurnal clock of *S. fruticosa* differ from each other.

4.3.4. Photosynthetic parameters obtained from the OJIP transient by using the JIP test

The result of the JIP-test (Strasser et al., 2000, 2004), obtained after double normalizing the raw fluorescence of *S. fruticosa*, was categorized as follows: technical fluorescence parameters, specific fluxes, phenomenological fluxes, and performance index, as described earlier (Bussotti et al., 2010; Stirbet and Govindjee, 2011; Gururani et al., 2015; Marcińska et al., 2017). The parameters thus calculated were then represented in a heat-map by scaling them to lie between 1-100 with the color code green signifying low and red as high (Figure. 4.10); their respective values are given in the Table 4.2 and 4.3.

Table 4.2: Photochemistry parameters obtained from JIP calculated from the plants under diurnal rhythm

	Time of the day							
Parameters	**2am**	**5am**	**8am**	**11am**	**2pm**	**5pm**	**8pm**	**11pm**
Technical Fluorescence parameter								
t for Fm	2388.89	2457.1	1857.1	1411.1	991.66	1944.4	1575	1372.7
Area	36161.4	32055	38036	47821.	37889	48368	40902.75	52293
Fo	272.44	261.35	216.14	267.55	228.58	322.33	295.875	258.277
Fm	689.11	533.35	872.85	1057.6	905.33	900	874.375	1170.54
Fv	416.667	272	656.71	790.11	676.75	577.66	578.5	912.272
Vj	0.39785	0.4019	0.4635	0.3719	0.3767	0.3303	0.416063	0.3276
Vi	0.70908	0.7292	0.7603	0.6886	0.6752	0.6137	0.7164	0.69121
N	87.0853	120.78	64.990	64.86	62.221	92.029	68.7929	71.6141
M_o = (F0.3ms - F0.05ms)/Fv	0.3526	0.3676	0.517	0.3967	0.3694	0.3383	0.424454	0.36129
M_{ji} = (F3ms-F2ms)/Fv	0.07139	0.0667	0.0576	0.0325	0.0354	0.0487	0.070003	0.02810
M_{ip} = (F35ms-F30ms)/Fv	0.00162	0.0022	0.002	0.0043	0.004	0.003	0.00228	0.0046
Specific flux or specific activities per Q_a^- reducing PSII reaction centre								
ABS/RC	1.4699	2.10	1.4739	1.4054	1.4659	1.688	1.471013	1.5491
DIo/RC	0.5915	1.087	0.368	0.383	0.3738	0.688	0.523788	0.3634
TRo/RC	0.878	1.015	1.105	1.0221	1.092	0.999	0.947213	1.1844
ETo/RC	0.5304	0.6054	0.5945	0.6439	0.6751	0.6705	0.5527	0.79514
Phenomenological fluxes or phenomenological activities								
ABS/CSo	272.44	261.3	216.1	267.5	228.58	322.33	295.875	258.272
DIo/CSo	109.54	134.82	53.999	70.845	58.88	124.44	106.3155	59.996
TRo/CSo	162.894	126.53	162.1	196.71	169.6	197.88	189.5596	198.2
ETo/CSo	98.0341	76.084	86.775	123.4	103.73	132.55	110.9881	132.633
Chlorophyll a fluorescence kinetics								
ABS/CSm	689.111	533.35	872.8	1057.7	905.3	900	874.375	1170.54
DIo/CSm	272.44	261.35	216.14	267.55	228.58	322.33	295.875	258.272
TRo/CSm	416.6	272	656.7	790.11	676.75	577.66	578.5	912.27
ETo/CSm	250	163.7	352.1	497.6	417.58	383.77	334.625	613.63
Performance index								
PI abs	1.8812	0.803	2.4747	8.9723	8.0946	3.4154	2.62225	6.9252

Table 4.3: Photochemistry parameters obtained from JIP curves (calculated from the plants under continuous dark)

	Time of the day							
Parameters	**2am**	**5am**	**8am**	**11am**	**2pm**	**5pm**	**8pm**	**11pm**
Technical Fluorescence parameter								
t for Fm	4157	2483	1916	1271.4	1100	1685.7	2128.5	2183.3
Area	2123	1996	2569	2990	3006	3017	4128	3100
Fo	233.43	313	249	216.43	236.50	239.29	272.86	301.17
Fm	496	533	637	857.57	767.00	587.86	758.29	827.17
Fv	262.57	169	354	684.00	630.50	420.00	714.00	426.00
Vj	0.48	0.41	0.42	0.36	0.39	0.37	0.49	0.45
Vi	0.79	0.78	0.73	0.70	0.68	0.59	0.75	0.72
N	129.29	117.90	80.77	66.33	62.88	78.12	58.23	92.66
Mo = (F0.3ms - F0.05ms)/Fv	0.42	0.36	0.21	0.32	0.34	0.28	0.64	0.21
M_{ji} = (F3ms-F2ms)/Fv	0.06	0.06	0.04	0.02	0.03	0.04	0.07	0.03
M_{ip} = (F35ms-F30ms)/Fv	0.002	0.001	0.002	0.001	0.001	0.001	0.004	0.001
Specific flux or specific activities per Q_a^- reducing PSII reaction centre								
ABS/RC	2.27	2.40	1.84	1.68	1.65	1.66	1.42	1.72
DIo/RC	0.82	1.74	1.03	0.39	0.74	0.74	0.45	0.67
TRo/RC	1.09	0.94	0.97	1.33	1.11	0.96	1.05	1.05
ETo/RC	0.54	0.61	0.49	0.81	0.66	0.60	0.50	0.57
Phenomenological fluxes or phenomenological activities								
ABS/CSo	233.43	313	283	202.14	236.50	239.29	272.86	267.83
DIo/CSo	117.75	197	113	47.53	72.58	99.25	89.88	117.85
TRo/CSo	115.68	116	153	154.61	163.92	155.75	175.84	148.31
ETo/CSo	61.34	70.4	90.2	99.20	103.58	97.35	88.05	80.50
Chlorophyll a fluorescence kinetics								
ABS/CSm	481.71	499	604	914.71	833.67	559.29	901.14	660.50
DIo/CSm	233.43	313	283	202.14	236.50	239.29	272.86	301.17
TRo/CSm	262.57	153	321	698.29	663.83	348.57	642.57	359.33
ETo/CSm	128.86	107	159	466.57	311.00	230.14	292.14	208.00
Performance index								
PI abs	0.50	0.28	0.72	3.37	3.53	2.07	2.39	1.38

Under diurnal rhythm (Figure. 4.10a), the time to attain maximum fluorescence (t_{Fm}) was at 14:00 hours; however, the minimum time to attain F_m was observed between 02:00 to 05:00 hours. Similarly, under continuous dark (Figure. 4.10b), the lowest time to attain F_m was observed between 11:00 and 17:00 hours, and the maximum time at 02:00 hours The maximum complementary area of the O-J-I-P transient rise was found to be at 23 :00 hours under the diurnal, but at 20:00 hours under continuous dark, while the minimum was obtained around 05:00 hours in both cases. The slopes of the O-J rise (M_o), J-I phase (M_{JI}) and I-P phase (M_{IP}) were maximum around 08:00 hours, 02:00 hours, and 23:00 hours, under diurnal condition (Figure. 4.10a). However, these three slopes were maximum around 20:00 hours under continuous dark (Figure. 4.10b).

Our results on four photosynthetic parameters, included in the specific flux category, are described below. The maximum absorbed excitonic flux per active PSII (ABS/RC) and the dissipated excitonic energy flux per PSII reaction center (DI_o/RC) were observed at 05:00 and in between 08:00 to 14:00 hrs, under the diurnal condition. However, under continuous dark condition, both these parameters were maximum at 05:00 hours. On the other hand, the minimum values for ABS/RC and DI_o/RC were observed around 11:00 and 23:00 hours, under the diurnal condition, but at 20:00 and 11:00 hours, under the continuous dark. Furthermore, the maximum PSII trapping rate (TR_o/RC) and electron transport rate through PSII (ET_o/RC) were observed at 23:00 hours, under diurnal, and at 11:00 hours, under continuous dark.

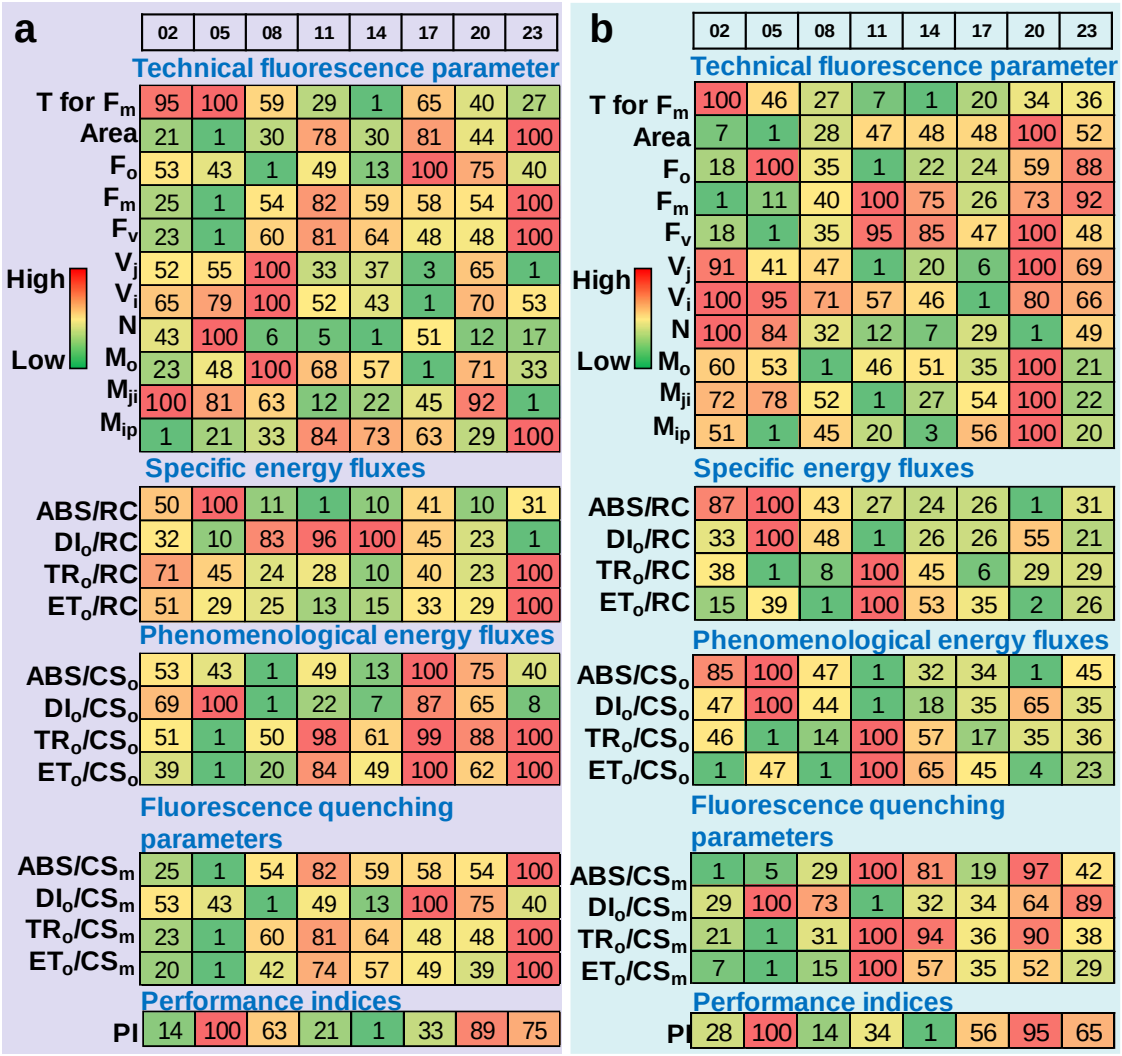

Figure 4.10: Heat map representation of several photosynthesis-related parameters, obtained after using the JIP test for *Suaeda* under (a) diurnal and (b) continuous dark. Data are for different time points (02:00 to 23:00hrs), obtained during 3 days (72 hrs). The plant under continuous dark was kept under diurnal condition for the first 24 hrs, followed by dark for 48 hrs where darkness was ensured by completely covering the plant with a dark cloth. Heat map of the parameters are shown in the figure: red is for high (100%), yellow for medium (50%) and green for the lowest values (1%). All the data obtained were first normalized to bring the value of the parameters in the range of 1-100 to provide an unbiased color code. Abbreviation and terminology of the parameters are given in table 4.1.

Our data on the four parameters of phenomenological fluxes defined at the level of F_o, i.e., absorbed photon flux per cross section at time zero (ABS/CS_o), dissipation of excitonic energy flux in the form of heat per cross section at time zero (DI_o/CS_o), trapped energy flux per cross section at time zero (TR_o/CS_o) and electron transport flux at time zero (ET_o/CS_o) (Figure. 4.10) gave the following result. They were highest around 17:00 hours under the diurnal condition. However, under continuous dark condition, the maximum flux for both ABS/CS_o and DI_o/CS_o was at 05:00 hours, while for both TR_o/CS_o and ET_o/CS_o, it was at 11:00 hours. In addition, the absorbed photon flux per cross section at F_m (ABS/CS_m), excitation energy trapped per cross section at F_m (TR_o/CS_m) and electron transport rate per cross section at F_m (ET_o/CS_m) were found to be maximum at 23:00 hours under diurnal and 11:00 hours, under continuous dark. In contrast, the energy dissipated at F_m (DI_o/CS_m) was found to be maximum around 17:00 hours, under diurnal and at 05:00 hours, under continuous dark. Further, the overall performance index (PI_{total}) of *S. fruticosa* was found to be maximum at around 05:00 and at 20:00 hours, while the minimum was at 14:00 hours, under both conditions.

4.4. Discussion

4.4.1. The photoperiodic entrainment tightly regulates gas exchange and photosynthetic machinery in Suaeda fruticosa

In the hyper-saline inland playa located in the middle of the Aravalli schists within the Thar desert of western India, roots of *S. fruticosa* are continuously exposed to highly saline soil (EC ranging from 45-50 dSm^{-1}), while their shoots are exposed to extremely hot (~50^oC during summer) and dry atmosphere (Sinha and Raymahashay, 2004; Krishna et al., 2014; Roy and Singhvi, 2016). Photosynthesis is the primary physiological process leading to growth and life of plants, and xerohalophytic *S. fruticosa* possess a wide range of specialized adaptation mechanisms to protect their photosynthetic apparatus under these extreme saline conditions (Wungrampha et al., 2018). The daily fluctuation in the

temperature (from ~30^{o}C to 50^{o}C during the summer) and the high light intensity (1,800 µmol photons $m^{-2}s^{-1}$) make it imperative for the plants to adjust its photosynthesis machinery with the changes in these environmental conditions. Studies have been done in the past showing the existence of diurnal rhythm in the physiology of many plant species with respect to their photosynthesis (Singh et al., 2015; de Dios, 2017; Matthews et al., 2017; Vialet-Chabrand et al., 2017).

Endogenous circadian oscillators occur in all organisms which autoregulate the feedback loops driving the rhythmic behavior of genes, proteins, and metabolites (De Caluwé et al., 2017). In plants, the circadian entrainment of environmental cues is 'gating' of the response to a stimulus through rhythmic synchronization of transcriptional, translational and post-translational modulations. This further regulates alternative splicing, controls protein turnover, and chromatin modifications which allow plants to coordinate the temporal organization of biological processes with daily and seasonal changes in light and temperature cycles (Greenham and McClung, 2015; Mora-García et al., 2017). The internal state of the plant and external environment impinge on the pulse of the oscillator clock by regulating the expression of its components. Successively, the clock ensures the activation of certain gene(s) regulating multitude of metabolic and physiological aspects that is/are suitable during day or night, thereby providing fitness advantage in developmental processes during plant life cycle (Dodd et al., 2005; De Caluwé et al*., 20*17; Cano-Ramirez and Dodd, 2018). Bendix and colleague (2015) reported that in plants, the key circadian clock genes are found abundant throughout the day. However, the transcriptional phase representing multi-core circadian clock proteins activities were observed distinctly during morning, mid-day, and evening (Bendix *et al.*, 2015). Previous studies also have reported that, under stress, the photosynthetic machinery regulation is influenced either by diurnal rhythms such as in tomato (Ikkonen *et al.*, 2015), barley (Goldstein et al., 2017), rice (Singh et al., 2015; Kim et al., 2017), and maize (Feng et al., 2017), or by circadian rhythms such as in soybean (Pan et al., 2015), Arabidopsis (Nitschke et al., 2016), tomato (Müller et al., 2016)

and cotton (García-Plazaola et al., 2017). However, the present study is a unique attempt to study detailed photosynthesis parameters in a xero-halophyte as affected by diurnal rhythm and under the absence of light growing in Salt Lake. Attempts were also made in this study to identify and to examine the photosynthesis components associated with the two complex adaptive processes in *S. fruticosa* under diurnal rhythm and under continuous dark conditions. Results, obtained in this study, support our hypothesis that the photosynthetic activity of *S. fruticosa* is tightly regulated which not only helps in its growth and development but also in providing adaptation under extreme environmental conditions.

Photoperiodism in plants is a critical machinery that regulates the physiological behavior and its responsiveness under changing environmental conditions (Bendix et al., 2015; Moraes et al., 2019). In the present study, we measured *in-situ* gaseous exchange and the photosynthesis parameters of *S. fruticosa* under diurnal as well as continuous dark conditions. Under both the conditions, the gaseous exchange and the photosynthetic parameters of *S. fruticosa* followed a rhythmic cycle repeating after every 24 hours. However, under continuous dark condition, the amplitudes of the measured parameters (such as Gs, NPQ, qP, qN and Ci) were observed to be lower as compared to that under diurnal (Figure. 4.4 and Figure. 4.5). Some of the parameters such as Gs, NPR, qP and qN showed similar rhythmic pattern under both diurnal and continuous dark conditions. On the other hand, other parameters such as Ci, NPQ, ETR, Tr and F_v/F_m showed reverse rhythmic pattern under continuous dark (Figure. 4.6). Vialet-Chabrand et al. (2017) showed that the leaf of Arabidopsis grown under fluctuating light and low light are thinner yet the photosynthesis rate per unit area remains the same like that under diurnal conditions. However, we observed that the rate of photosynthesis decreased in *S. fruticosa* under dark conditions.

Under diurnal conditions, parameters (arbitrarily called set 'A') such as the maximum quantum yield of PSII (F_v/F_m), stomatal conductance (Gs) and photochemical quenching (qP) were found to be maximum at dawn, i.e. 05:00 hours, and remained low during the rest of the day. This could be an adaptive feature by avoiding irreversible photodamage during high PAR and atmospheric temperature. In contrast, with the increase in PAR and temperature (from 08:00 to 17:00 hours), parameters (arbitrarily called set 'B'), such as non-photochemical quenching (NPQ), intercellular CO_2 concentration (Ci), net-photosynthetic rate (NPR), non-photochemical quenching coefficient (qN), electron transport rate through PSII (ETR), and transpiration rate (Tr) (Figure. 4.4 and Figure. 4.5) increased and showed a reverse pattern with the set 'A' parameters. However, within the set 'B' parameters, Ci and qN showed another peak during 23:00 hours but the amplitude of this peak was roughly half of that observed during light (around 14:00 hours) (Figure. 4.5a and Figure. 4.5i). Interestingly, qP stands out unique among all the parameters as it was found to have one peak each at dawn and at dusk i.e., at 05:00 and 20:00 hours (Figure. 4.5g).

Biomass and yields of a plant are directly proportional to the rate of photosynthesis (Zhu et al., 2008). Abiotic stress, such as salinity, directly affects the photosynthesis machinery of the plants by degrading the photosynthesis pigments such as chlorophyll leading to several reduction in the photosynthesis (Wungrampha *et al.,* 2018). In *S. fruticosa*, NPR and ETR was observed to be tightly regulated even under highly saline environment wherein, maximum NPR was observed at 08:00 hours under diurnal and 05:00 hours during continuous dark (Figure. 4.4). As the light intensity and temperature increases during the day, NPR gradually decline which could be due to protection of the photosynthetic pigments under high light and temperature (Taylor and Rowley, 1971).

Plants such as *Arabidopsis thaliana*, *Phaseolus vulgaris*, *Vicia faba*, *Triticum aestivum*, and *Nicotiana tabacum,* under stable environment, balance the gain in carbon and water loss by tightly regulating NPR and Gs. However, the correlation between them varies depending on the availability of water since Gs also regulates net transpiration (Tr) in plants (Matthews et al., 2017). For instance, under long periods of drought leading to carbon starvation, plants choose to reduce the rate of Tr by suppressing Gs rather than increasing the NPR to prevent water loss (Hills et al., 2012). Apart from this environmental factor, the role photoperiodic regulation affecting the synchronic response of Gs and NPR is now emerging as a supplementary mechanism in plants to regulate carbon flux and water loss (de Dios, 2017). However, the photoperiodic regulation for both Gs and NPR are different and are mutually independent of each other (Dodd *et al.*, 2014). In *Suaeda fruticosa*, Gs and NPR were found to be corelated under both diurnal rhythm (Figure. 4.4b and Figure. 4.4f) and under continuous dark (Figure. 4.5a and Figure. 4.5f); however, the net Tr and Ci varied under both the conditions.

de Dios (2017) showed that 30% and 70% of the gas exchange in *Gossypium* sp. and members of the family *Fabaceae* are controlled by photoperiodic cycle. Additionally, in cotton and beans, the photoperiodic memory of the previous day regulates the gas exchange parameter irrespective of the environmental conditions (de Dios et al., 2016). However, in *S. fruticosa*, a similar effect of the 'previous day memory' was not observed in parameters such as Ci, NPQ, ETR, Tr and F_v/F_m, which showed a reverse pattern under continuous dark (Figure. 4.4 and Figure. 4.5). This could be due to its plasticity to adapt quickly under a changing environment.

Glycophytes such as Arabidopsis (Stepien and Johnson, 2009), rice (Soda et al., 2018), barley, sorghum (Sharma and Hall, 1991), and maize (Guo et al., 2017) respond to salinity by closing their stomata followed by a reduction in Ci, Gs, F_v/F_m, NPR and ETR (Huang et al., 2016; Hwang and Choo, 2016; Schuback

et al., 2016). However, halophytes such as *Cakile* (Megdiche et al., 2008), *Artimisia anethifolia* (Wen et al., 2005), *Suaeda salsa* (Wang et al., 2004), *Odyssea paucinervis* (Naidoo et al., 2008), and *Paspalum vaginatum* (Lee et al., 2004) do not show significant changes in these parameters even though growth and biomass are compromised to a certain extent (Megdiche et al., 2008; Stepien and Johnson, 2009). Likewise, *S. fruticosa* also showed routine cyclic pattern in these parameters representing acute adaptation under salinity stress.

4.4.2. Non-photochemical and photochemical quenching are regulated by the intensity of light

Under natural conditions, excess light intensity during mid-day leads to the production of reactive oxygen species (ROS) such as superoxide ($O_2^{\cdot -}$) and hydrogen peroxide (H_2O_2), resulting in photo-oxidative damage (Roach *et al.*, 2015). It is interesting to know how certain organisms such as *Chlamydomonas*, *Chlorella* (Roach et al., 2015), *Erythrophleum*, *Khaya* (Huang et al., 2016), Ginkgo (Yang and Chen, 2015), *Zea mays* (Leakey et al., 2004), *Vitis vinifera* (Downton et al., 1987) and phytoplankton (Schuback et al., 2016) protect their photosynthetic machinery by regulating the electron transport chain of their photosynthesis. One possible approach to do so is by operating reversible NPQ reaction coupled with qP reaction or under the extreme case, through irreversible NPQ reaction (photoinhibition) (Stepien and Johnson, 2009). The two parameters, i.e. NPQ and qP, occur in reverse order wherein, an increase of NPQ is followed by a decrease in qP and vice versa (Huang *et al.*, 2016). Increase in NPQ can broadly be due to two reasons: high-energy state quenching with the release of heat or due to photoinhibition (irreversible photosystem damage) (Stepien and Johnson, 2009). In our study, we observed an increase in NPQ level in *S. fruticosa* at midday (Figure. 4.4e) followed by reduction in qP. This could be due to the increase in PAR, after 11:00 hours until 16:00 hours (above 1500 µmol photons $m^{-2}s^{-1}$). This tight regulation of the NPQ and qP to protect the photosynthesis machinery against high PAR might

contribute to its adaptation under the combination of high temperature and salinity stress during the noon.

Furthermore, in *S. fruticosa,* we observed an increase in F_v/F_m during dawn and dusk. This could be due to its ability for effective processing of light during low light intensities. Decrease in F_v/F_m during midday (after 08:00 hours) until 17:00 hours suggest photoprotection of the photosystem by reversible inactivation or down regulation of PSII during high light intensity, rather than photodamage. It is known that plants maintain higher photosynthesis rate and photochemical quenching during early morning hours when there is low radiation and high enzymatic activity of CO_2 reduction cycle (Stepien and Johnson, 2009). This observation further correlates with higher electron transport rate, gas exchange and transpiration rate during early morning hours. Since the midday depression in qP was accompanied by enhanced C_i, it could be attributed to decreased photosynthetic activity of mesophyll cells, rather than the stomatal closure (Yang and Chen, 2015). These mechanisms protect the photosystems of the plant from photooxidation by dissipating the excess energy in the form of heat and also by maintaining low steady-state fluorescence yield of the photosystem (Hajiboland, 2014).

However, within a span of 24 hours, under diurnal condition, maximum F_v/F_m and NPR were observed between 20:00 to 05:00 hours (in the absence of light) and at 08:00 hours (Figure. 4.4a and Figure. 4.4c). However, under continuous dark, the quantum yield of PSII (as reflected by F_v/F_m) was seen to increase gradually after dusk, attaining its maximum 2 hours after noon (14:00 hours) (Figure. 4.6i), which is a reverse pattern to that under diurnal condition. This result gives us an alternative perspective in addition to the photoprotective mechanism of PSII and that is, *S. fruticosa* has a quick and systemic repair mechanism of the photosystem II that operates as PAR reduces (in the night, there is no light). This might further help in reviving the PSIIs that were damaged during high light. Repair of the PSII by D1 protein during the night/low light has

been reported in several photosynthetic organisms such as diatoms (Li *et al.*, 2016), Arabidopsis (Järvi et al., 2015) and spinach (Suorsa et al., 2014). Further, the increase in quantum yield during noon day under the absence of light brings a new perspective of the inner clock (circadian) regulating the photosynthesis machinery in *S. fruticosa*. However, this further need to be validated by analyzing the circadian regulations in this plant.

4.4.3. The alternate channel of electron transport chain regulates the carbon sink in S. fruticosa during exposure to high light intensity

When *Thellungiella*, a halophyte, is subjected to salinity above 500 mM, there is a marginal inhibition in gas exchange with a significant increase in electron flow involving PSII (Stepien et al., 2009). This was found to be due to increased activity of terminal oxidase in the plastids that acts as an alternative electron sink. This additional electron flow accounts to ~ 30% of the total ETR observed in plants under stress (Joët et al., 2002; Stepien and Johnson, 2009). In *S. fruticosa*, Gs was seen to be lowest at the time when ETR was highest, i.e., between 05:00 to 14:00 hours (Figure. 4.5c and Figure. 4.5e). The increase in total electron transport rate (ETR) when stomatal conductivity (Gs) is lower could be due to the activity of plastid terminal oxidase under the combination of both high temperature and salinity stress. Additionally, the observed increase in ETR at 05:00 hours (even though the area of O-J-I-P is the lowest) could be due to chlororespiration involving both non-photochemical reduction as well as oxidation of plastoquinone during the induction of dark to the light phase of the photosynthesis (Joët et al., 2002). The midday depression in qP which was accompanied by enhanced C_i could be correlated with the decrease in photosynthetic activity of mesophyll cells, rather than the stomatal closure like that of *Ginkgo biloba* (Yang and Chen, 2015). These mechanisms further protect photosystems from photooxidation by dissipating the excess energy in the form of heat and also by maintaining low steady-state fluorescence yield of the photosystem (Hajiboland, 2014).

4.4.4 Chlorophyll a fluorescence follows rhythmic cycle under both diurnal and constant dark conditions in Suaeda fruticosa

In general, Chl *a* fluorescence induction begins with a steep rise followed by a slow decline, when dark-adapted plants are exposed to light (cf. Stirbet and Govindjee, 2011). Strasser et al. (2004) classified it as a polyphasic rise and labelled it as OJIP. The OJIP transient rise directly reflects the influence of environment along with the state of the plant (Luo et al., 2016), as PSII reaction center is the primary target under stress (Gururani *et al.*, 2015; Soda *et al.*, 2018). Under salinity (Lee *et al.*, 2004; Soda et al., 2018), high temperature (Mathur et al., 2011), drought (Luo *et al.*, 2016) and change in light intensity during diurnal condition (Bacarin et al., 2016), changes in the value of F_o, time to reach F_m (t_{Fm}), complementary area of the OJIP curve, and other JIP parameters, have been reported in several photosynthetic organisms over the years. Analyzing the OJIP transient rise has broadened the understanding of the structure, function and behaviour of PSII under many conditions (cf. Strasser *et al.*, 2000; Strasser *et al.*, 2004; Stirbet *et al*., 2018). The JIP-test, used here, has been the main explanatory model to quantify the energy flow through PSII through translation of fluorescence transient measurements to biophysical parameters (Zhu et al., 2005; Stirbet and Govindjee, 2011; Luo et al., 2016).

Our aim to study the OJIP-transient as well as the parameters that the JIP-test provides was to investigate the effect of photoperiod (under diurnal and continuous dark) on PSII chemistry of *S. fruticosa* that thrives under a high saline environment. By calculating the parameters (as tabulated in Table 4.1), we observed a decline in the I-P phase and the complementary area of the OJIP curve during the day (Fig. **5**). This might be due to the acclimation response of *S. fruticosa* to tolerate high PAR under prevailing salinity to maintain the redox poise of the PQ pool. It has been reported that the hindrance of the electron flow, either due to stress or any other factors, lead to drastic reduction in the complementary area of the OJIP curve (see e.g., Gautam et al., 2014).

Furthermore, the rapid recovery of photodamaged PSII is dependent on PSI activity as the stabilization of PSI activity during the daytime has been shown to contribute towards photoprotection and recovery of PSII activity (Huang et al., 2016). Thus, our study suggests that *S. fruticosa* stabilizes PSII complex proteins and prevents the disruption of electron transport to the plastoquinone pool under high saline conditions.

Under circadian rhythm (by maintaining constant light), *Gonyaulax polyedra* display faster OJIP rise as compared to that under diurnal rhythm (Govindjee et al*.,* 1979). The same phenomenon was also observed here in *S. fruticosa* under constant dark wherein, at all the time points, the time taken to attain F_m was faster under continuous dark condition (Figure. 4.10). Changes in energy fluxes per PSII reaction center are specific functional parameters, while the energy fluxes per excited cross section correspond to phenomenological energy fluxes (Gururani et al., 2015). Thus, by analyzing Chl *a* fluorescence transient, the energy flow cascade through electron transport chain can be determined (see e.g., Bacarin *et al.*, 2016). In this work, we observed high amount of energy dissipated in the form or heat from a PSII reaction center (DI_o/RC) during the daytime; this was further followed by decreased energy trapping at the reaction center (TR_o/RC). In contrast, and as expected, under low light intensities, most of the light absorbed by the chlorophyll is utilized in photochemical reactions.

PSII is known to be much more susceptible to high temperature as compared to PSI, since high temperature inhibits the water oxidation complex (see e.g. Nash et al., 1985; Bacarin et al., 2016). Thus, a decrease in electron transport to the PQ pool (ET_o/RC) and in antenna size of an active PSII reaction center (ABS/RC) was observed in this study (Figure. 4.10) during noon. These suggest that under high light intensity (i.e., during daytime) *S. fruticosa* regulates the total electron flux by decreasing the size of the antenna in PSII. The increase in DI_o/RC further confirms that excess absorbed light is dissipated primarily

through reaction centers as well as antenna during the daytime leading to a decrease in photochemical reactions. Changes in PI_{total} followed the pattern of F_v/F_m with similar amplitude, indicating a similar sensitivity of PI_{total} to changes in light and temperature in this plant. Previous studies on different halophytes such as *Artimisia anethifolia* (Lu et al., 2003; Wen et al., 2005), *Suaeda salsa* (Wang et al., 2004), *Paspalum vaginatum* (Lee et al., 2004), *Cakile maritima* (Megdiche et al., 2008), *Porteresia coarctata* (Sengupta and Majumder, 2009), *Aster tripolium* (Duarte et al., 2017), *Odyssea paucinervis* (Naidoo et al., 2008), and *Thellungiella salsuginea* (Goussi et al., 2018) also demonstrated that these plants maintain their phenomenological energy flux even under salinity. Similarly, it had been shown earlier that circadian oscillations contribute towards the regulation of light harvesting from the photosynthetic apparatus at both transcriptional and post-translational level (Dodd et al., 2014). It is highly likely that this may be due to the accumulation of osmolytes and soluble compounds such as sugars and proteins that helps in stabilizing the oxygen-evolving complex and PSII core from salinity stress. In our previous study (Singh et al., 2015), we have shown that expression of genes such as *Prr*, *HK*s, *Hpt*s and *RR* of the 'two-component system' gene family regulates the circadian clock in rice seedlings under different abiotic stress conditions, thus unraveling an alternate transcriptional control mechanism in higher plants.

4.5 Conclusions

The present study integrates *in-situ* chlorophyll fluorescence kinetics of *S. fruticosa* with diurnal and constant dark conditions under extreme saline conditions. In our previous studies (Soda et al., 2018) on glycophytes, we had reported that salinity stress severely influences PSI and PSII activities as well as Chl *a* fluorescence. The work presented here is the first study demonstrating that the prime strategy enabling the halophyte *S. fruticosa* to grow in extremely saline environment is to maintain structural integrity and electron flow through PSI and

PSII along with the protection of photosynthesis machinery from photoinhibition during high irradiance at midday. Moreover, Chl *a* fluorescent parameter revealed that midday depression in photosynthesis and photochemical activity of PSII in *S. fruticosa* enables the maintenance of the equilibrium of electron flow from the antenna complex to PSII reaction center and CO_2 gas exchange in the fluctuating microclimate.

Chapter 5

Diurnal and seasonal variations in metabolome of the leaves of *Suaeda fruticosa*

5.1 Introduction

Salinity is one of the most severely affecting abiotic stresses in plants. It not only causes salt/ionic stress but also the osmotic stress which further alters the physiology and metabolism of plants (Purty et al., 2009, Kumari et al., 2009, Joshi et al., 2016). Plants sense an immediate osmotic shock when subjected to salinity stress primarily due to changes in their water potential. Prolong exposure to salinity leads to ionic imbalances as Na^+ and Cl^- ions enter the plant and hinder the uptake of essential minerals such as K^+, Mn^{2+}, and Ca^{2+} (Das et al., 2015, Nongpiur et al., 2016, Wungrampha et al., 2018, Munns & Tester, 2008). Excess Na^+, in turn, causes sodium toxicity which results in yellowing of leaf margins and progressive necrosis. Similarly, excess Cl^- ions cause premature yellowing of the leaf tip margins, ultimately leading to necrosis (Cassaniti et al., 2009). Overall, salinity disturbs almost all process of the plants including germination, development, respiration, and photosynthesis and ultimately reduces the crop yield (Wungrampha et al., 2018, Munns, 2002, Khan et al., 2000, Koyro et al., 2011).

Saline water, having abundance of Na^+ and Cl^- ions cover 72% of the Earth surface (Flowers & Colmer, 2015). This contributes majorly to the salinization of the Earth crust as the rate of evapotranspiration exceed the rate of precipitation leading to elevation of ground saline water to the soil surface (Endo et al., 2011). At the same time, arable lands accounting for millions of hectares worldwide are lost due to salinity. United Nation University's Canada-based Institute for Water, Environment and Health (UNU-INWEH) reported in 2014 that roughly 20% of the irrigated land (size equivalent to the total area of France) and

2.1% of the total dry land are already affected by salinity (Qadir et al., 2014). Over the past three decades, it is roughly estimated that soil salinity has increased from 45 to 62 million hectares resulting in an economic loss of 27 billion USD per annum (Qadir et al., 2014, Munns & Tester, 2008). Thus, there is a growing need to find ways of mitigating the effects of salinity on plants, especially crop plants.

Depending on their habitat, plants can broadly be classified into two categories: extremophiles- plants that can grow and complete their life cycle in extreme conditions such as high saline, drought, cold and heat; and glycophytes - those that can grow under favorable conditions only (Flowers & Colmer, 2015). Halophytes fall under the category of extremophiles. These plants can grow in areas of high saline soil or water that comes in direct contact with their roots. Halophytes represent ~2% of the terrestrial plant kingdom and are widely distributed in the coastal regions, marsh soils, mangroves swamps, saline semi-deserts, etc. They can complete their normal life cycle even at a salt concentration higher than 200 mM (Kosova et al., 2013, Sharma et al., 2016; Flowers & Colmer, 2015). These plants have unique anatomical, physiological, and morphological adaptations that help them strive well under saline condition (Mishra & Tanna, 2017). With the fresh water depleting and saline soil elevating, halophytes can help in understanding the mechanism of salt tolerance for crop improvement. These plants hold the future as genetic resources to develop new niche plants/crops that can potentially be used for saline agriculture (Flowers & Colmer, 2015).

In recent years, several attempts have been made to understand the adaptation of *S. fruticosa* towards harsh environmental conditions such as high temperature, heavy metal, and salinity. Hameed et al. (2012) showed that *S. fruticosa* could optimally grow at 300 mM salt by adjusting the leaf osmolarity and by accumulating H_2O_2 and Malondialdehyde (MDA). Ca^{2+} ions were also seen to increase under salinity, which helps in its normal growth (Hameed et al., 2012).

Under heavy metal stress, the level of phytochelatins was seen to increase in *S. fruticosa* that protect it against reactive oxygen species (ROS) (Bankaji et al., 2015). Salt tolerance genes such as zeaxanthin epoxidase (ZEP), aquaporin TIP2, dehydration responsive protein (DRE) and glutathione S-transferase (GST) were also seen to accumulate abundantly in *S. fruticosa* under salinity stress (Diray-Arce et al., 2015). In our previous chapter (Chapter 4), we also have measured the CO_2 assimilation in *S. fruticosa* under diurnal as well as continuous dark condition. But so far, the metabolic changes associated with the tolerance of *S. fruticosa* to high temperature and salinity have not been studied.

In the present study, we have analyzed the metabolic profiles of *S. fruticosa* harvested from its natural habitat during three different seasons, i.e. post-monsoon, winter, and summer. We also check for the changes in metabolic profiles diurnally in each season. This is the first seasonal comparative metabolic profiling work done on *S. fruticosa* harvested from its natural habitat to analyze the diurnal pattern of accumulation and to study the changes in seasonal metabolic profile. We found significant changes in the levels of sugars, amino acids, and fatty acids in each season, and these changes may play a vital role in the adaptation of the plant towards abiotic stresses.

5.2. Material and methods

5.2.1. Plant material and study conditions

Leaves of *S. fruticosa* growing naturally on the bank of the salt mining site in Sambhar Lake, Rajasthan were harvested during three seasons, i.e. post-monsoon, winter and summer (Chapter 3 Figure. 3.7). Three months, i.e. August, January, and June to represent post-monsoon, winter and summer seasons respectively were decided based on the data presented in Chapter 3. For every season, leaf samples were harvested at the time interval of 3 hours viz. 2 am, 5 am, 8 am, 11 am, 2 pm, 5 pm, 8 pm, and 11 pm to check for the metabolic

changes influenced by diurnal rhythm. Harvested samples were frozen immediately into liquid nitrogen and stored at -80°C until further use.

5.2.2. Sample preparation for GCMS

Maintaining the temperate as cold as possible by constantly pouring liquid Nitrogen, 100mg of *S. fruticosa* leaf tissues were crushed into fine powder. For every sample, nine replicates (three biological and three technical) were taken. Extraction of metabolites was essentially carved out as described by Bagri at al. (2017). To each sample, 5ml pre-chilled extraction solvent [acetonitrile:isopropanol:water with 3:3:2 ratio] and internal standard ribitol (2mg/ml) was added, thawed in an ice bucket and centrifuged at 15,000g at 4^{o}C for 10 minutes. The supernatant was transferred into fresh tube and dried in a speed vacuum. The extracted metabolites were derivatized by two chemical steps. Firstly, 50µl of freshly prepared methoxyamine hydrochloride dissolved in pyridine was added to each sample. Samples were then incubated at 32^{o}C for 90 minutes with continuous shaking. Secondly, trimethylsilylate of the polar functional groups was performed by adding 100µl of N-methyl-N-trimethyl silyl triflouro acetamide (MSTFA) (Sigma Aldrich) and incubating the sample at 37 °C for 30 minutes.

5.2.3. GCMS analysis

The metabolites of freshly derivatized samples were analyzed using Shimadzu QP2010 series Gas Chromatography coupled with a mass selective detector. Aliquoted samples of 1µl were injected into Rtx® - 5MS (60 m × 0.25 mm × 0.25 µm) column (Restek Corporation, US) at 1:25 split ratio mode. The GC system was programmed at initial isothermal heating of 80°C for 2 minutes, which was then followed by 5^{o}C min^{-1} ramp rate till it reached 250^{o}C and further withheld for 2 minutes. Further, the system was raised to 280^{o}C with 10^{o}Cmin^{-1} ramp rate for the next 35 minutes of detection. Helium gas was used as a sample carrier at rate flow of 1mlmin^{-1}. The chromatogram and mass spectra obtained was

analyzed with GCMS-solution software (Shimadzu). Spectral libraries from NIST08, NIST11 and Wiley08 were used for identifying the peaks.

5.2.4. Data filtering and statistical analysis

The peaks identified were aligned according to their retention time with a window period of 20 seconds. The data was normalized by dividing the area obtained for each peak with the area obtained from the internal standard, i.e. ribitol. Common names of the metabolites were identified using NIST chemistry WebBook (http://webbook.nist.gov), ChemSpider (www.chemspider.com) and PubChem (https://pubchem.ncbi.nlm.nih.gov/). The data are grouped into four sets; three sets for the individual seasons (summer, post-monsoon, and winter) and one set by combining all the three seasons. Statistical analysis of the data was done using MetaboAnalyst 3.0 (Xia & Wishart, 2016). To compare the peaks, the whole set was grouped and matched across all samples. The grouping was done by keeping mass tolerance 0.02 (m/z) and retention time of 5 seconds. To further remove the data variables, the data were filtered by Interquartile range (IQR) followed by log transformation and Pareto scaling to normalize the data. One-way ANOVA and post-hoc Tests were performed by keeping the cut-off adjusted p-value and false discovery rate (FDR) to 0.05.

5.3. Results

5.3.1. Overview of the metabolites identified from the leaves of S. fruticosa under the influence of diurnal rhythm during different seasons

Each season affects the metabolic profile of *S. fruticosa* uniquely. As the physical parameters such as temperature, pH, salinity, availability of water as well as the biological state of the plant vary, it is expected to see variations of metabolite profiles in our study. Hierarchical clustering of the metabolites identified in our study and also during each season viz. post-monsoon, winter and summer are given in figure 5.1, 5.2., 5.3 and 5.4.

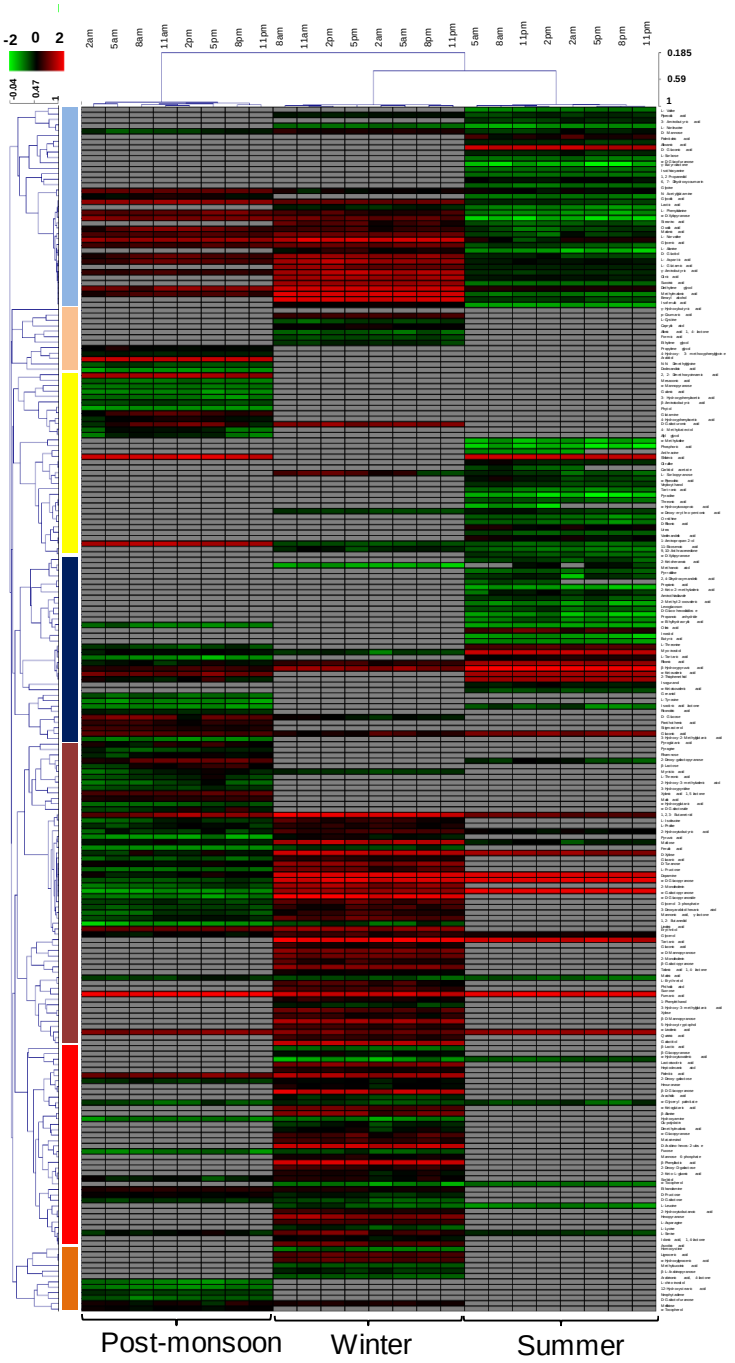

Figure 5.1: Hierarchical clustering of 222 metabolites identified in leaves of *S. fruticosa* during the three seasons. A heat map is drawn by taking Log10 of the normalized value for each metabolite. Red indicates maximum accumulation; green depicts minimum accumulation and black show median accumulation of the metabolite identified. Metabolites that were not detected at a particular season and during particular time point are denoted in grey.

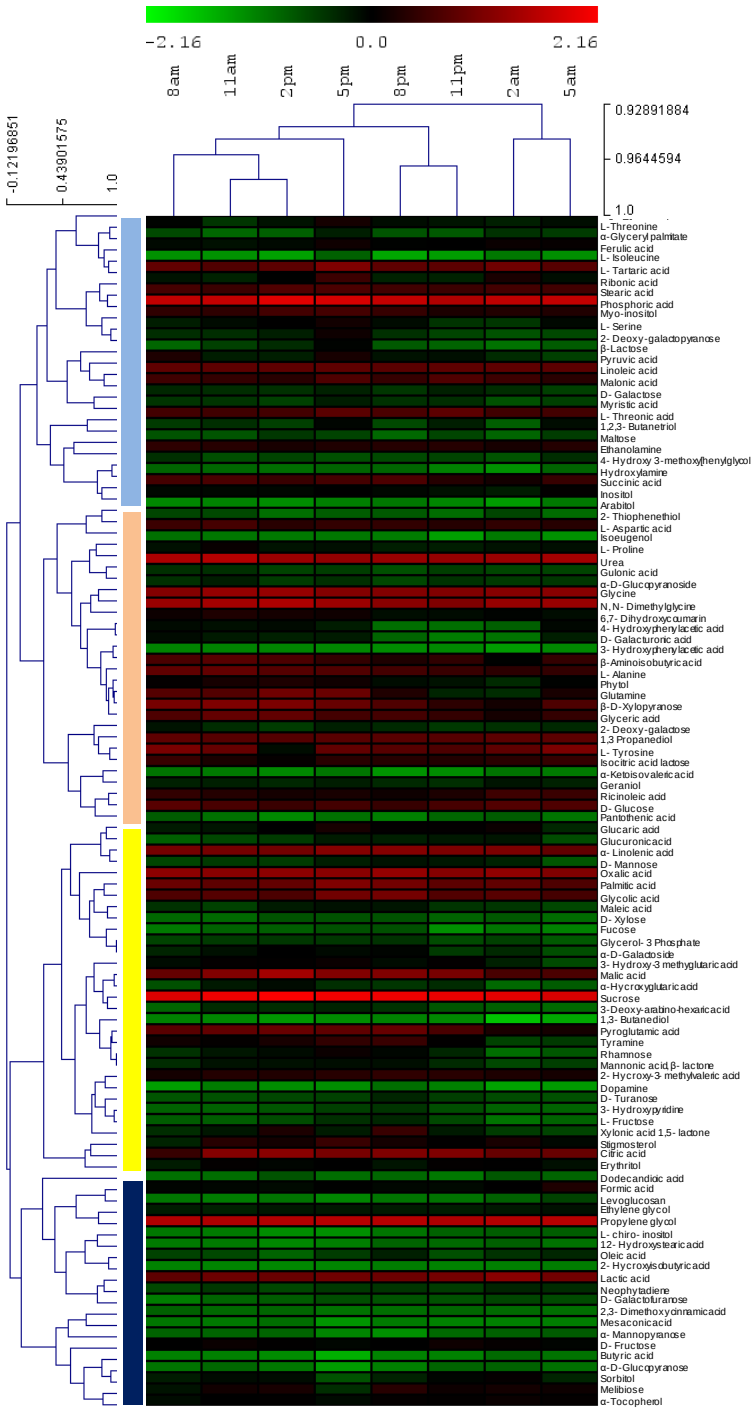

Figure 5.2: Hierarchical clustering of 106 metabolites identified leaves of *S. fruticosa* during post-monsoon season. The heat map is drawn by taking Log10 of the normalized value for each metabolite. Red indicates maximum accumulation; green depicts minimum accumulation and black show median accumulation of the metabolite identified.

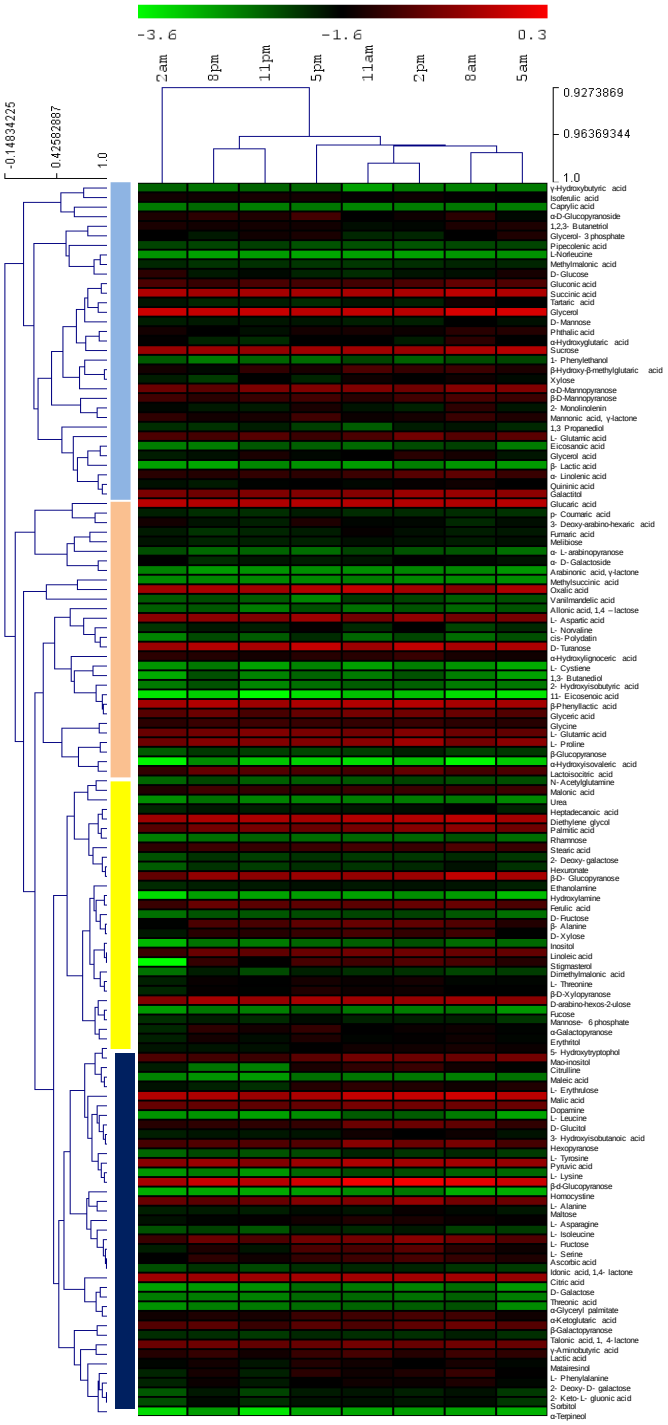

Figure 5.3: Hierarchical clustering of 129 metabolites identified leaves of *S. fruticosa* during winter season. The heat map is drawn by taking Log10 of the normalized value for each metabolite. Red indicates maximum accumulation; green depicts minimum accumulation and black show median accumulation of the metabolite identified.

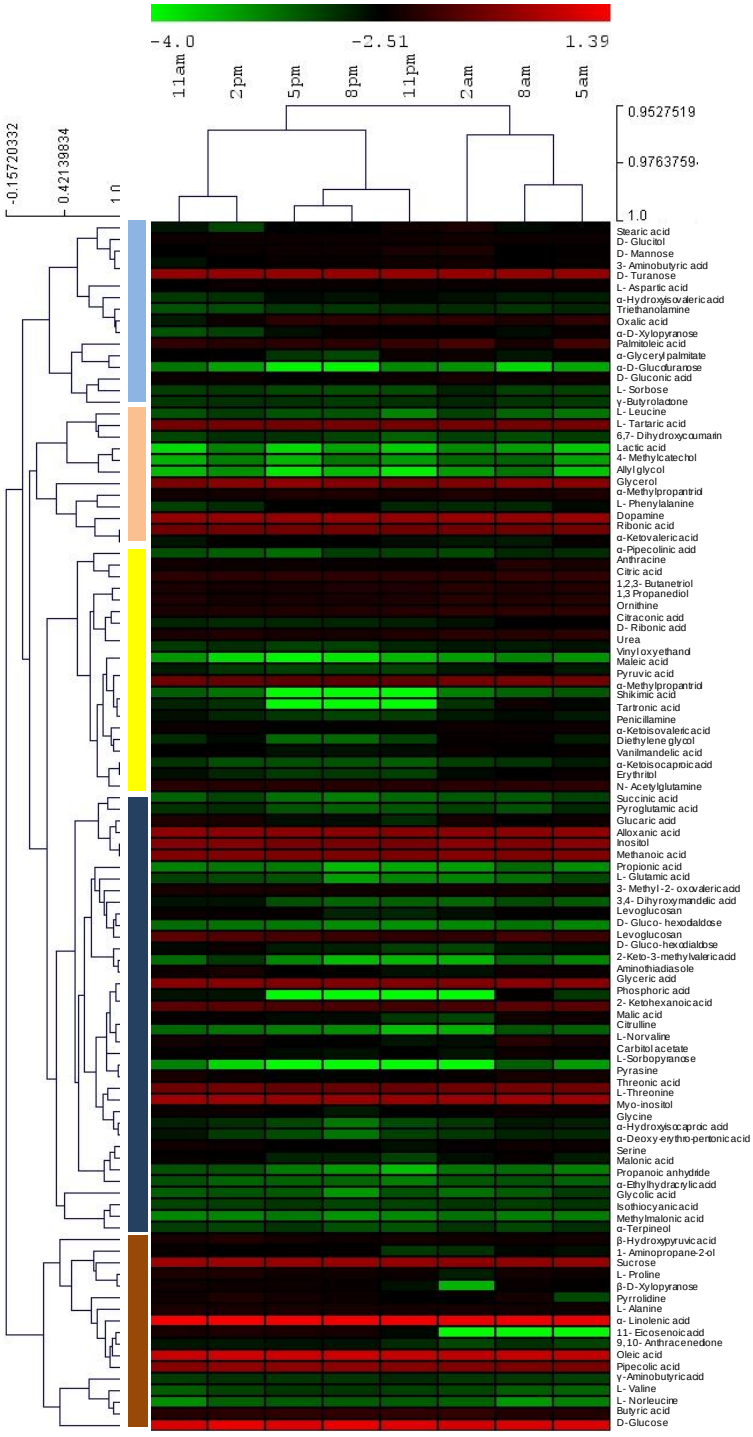

Figure 5.4: Hierarchical clustering of the 104 metabolites identified leaves of *S. fruticosa* during summer season. The heat map is drawn by taking Log10of the normalized value for each metabolite. Red indicates maximum accumulation; green depicts minimum accumulation and black show median accumulation of the metabolite identified.

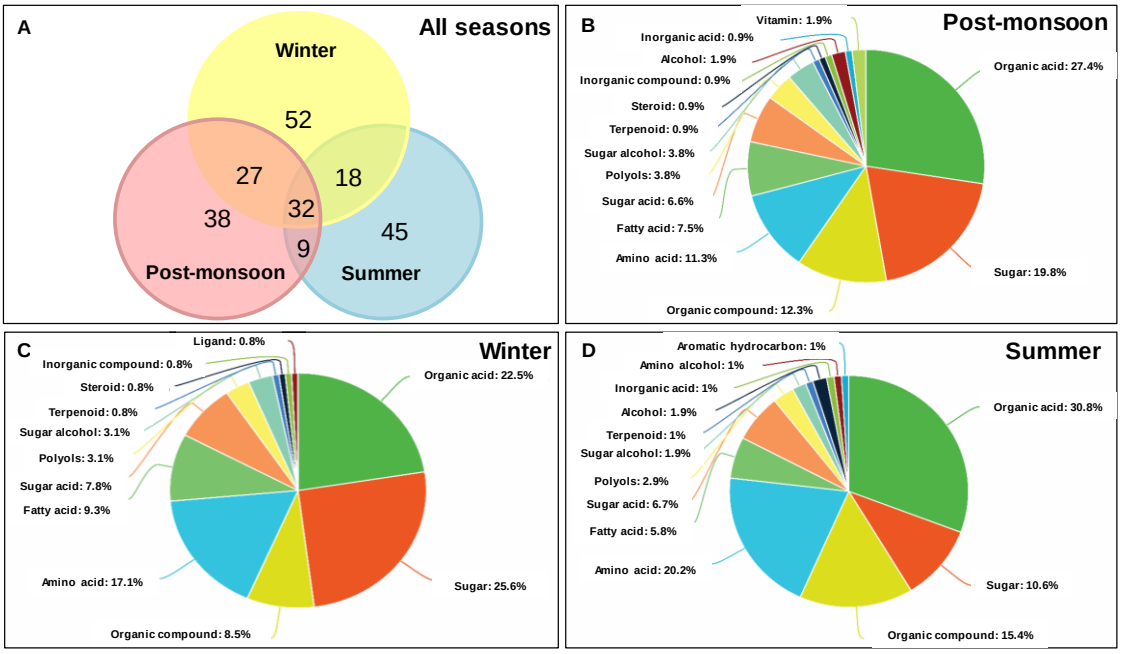

Figure 5.5: Venn diagram and pie charts showing the distribution and categorization of the metabolites detected. Metabolites were annotated based on their chemical identity A) Venn diagram of the 222 metabolites indicating the number of metabolites that are common as well as unique in each season. B) Pie chart depicting the diversity of metabolites detected from the leaves of *S. fruticosa* during post-monsoon season C) Pie chart depicting the diversity of metabolites detected from the leaves of *S. fruticosa* during winter season. D) Pie chart depicting the diversity of metabolites detected from the leaves of *S. fruticosa* during summer season. according to its chemical properties.

In total, 222 metabolites belonging to different types of metabolic category which includes alcohol, amino acid, amino-alcohol, aromatic hydrocarbon, fatty acid, inorganic compound, steroid, polyols, sugar, sugar acid, sugar alcohol, organic compound, terpenoid and vitamins were identified (Table 5.1-5.3). Although common metabolites were identified in all three seasons and between the seasons, their seasonal and diurnal distribution vary evidently (Figure. 5.2).

The number of metabolites detected during the post-monsoon, winter, and summer seasons were 106, 129, and 104, respectively (Figure 5.2-5.4). Of these, 32 metabolites were found common in all the seasons, 27 between post-monsoon and winter, 9 between post-monsoon and summer, and 18 between

summer and winter (Figure. 5.5a). Further, 38, 52 and 45 metabolites were were unique to post-monsoon, winter and summer respectively.

Of the total metabolites detected during the post-monsoon season, amino acids constitute ~12%, which is much lesser as compared to summer (~20%) and winter (~17%) seasons (Figure. 5.5b). Of the total metabolites detected during winter, 9% belonged to fatty acids (Figure. 5.5c), which is higher than during post-monsoon (~7%) and summer (~6%). Total sugar and its derivatives (sugar and sugar acids) were detected lowest during summer with just ~11% of the total metabolites. Whereas, these were found to be high during post-monsoon (~20%) and winter (~27%) (Figure. 5.5d). The relative abundance of metabolites during summer and winter season as compared to post-monsoon for the 32 common metabolites is shown in Figure 5.6.

Most of the fatty acids, both saturated and unsaturated, could be detected in leaf sample analyzed during winter. Apart from stearic acid, α-glyceryl palmitate and α-linolenic acid that were detected in all the seasons, fatty acids such as 2-monolinolenin, arachidic acid, caprylic acid, heptadecanoic acid, lignoceric acid, and α-hydroxylignoceric acid were detected only during winter. Myristic acid and ricinoleic acid were detected only during post-monsoon, whereas palmitoleic acid was detected only during summer. Oleic acid was detected in both summer, and post-monsoon, 11-eicosenoic acid was detected during summer and winter, while linoleic acid and palmitic acid were detected during post-monsoon and winter. Some metabolites such as stigmasterol, a steroid metabolite was detected only during post-monsoon. Similarly, matairesinol, plant lignin, was also detected only during winter. Aminoalcohol such as 1-Aminopropan-2-ol and aromatic hydrocarbon such as anthracene were detected only during summer. Vitamins like pantothenic acid and α-tocopherol were detected during post-monsoon, whereas, ascorbic acid was detected only during winter (Table 5.1-5.3).

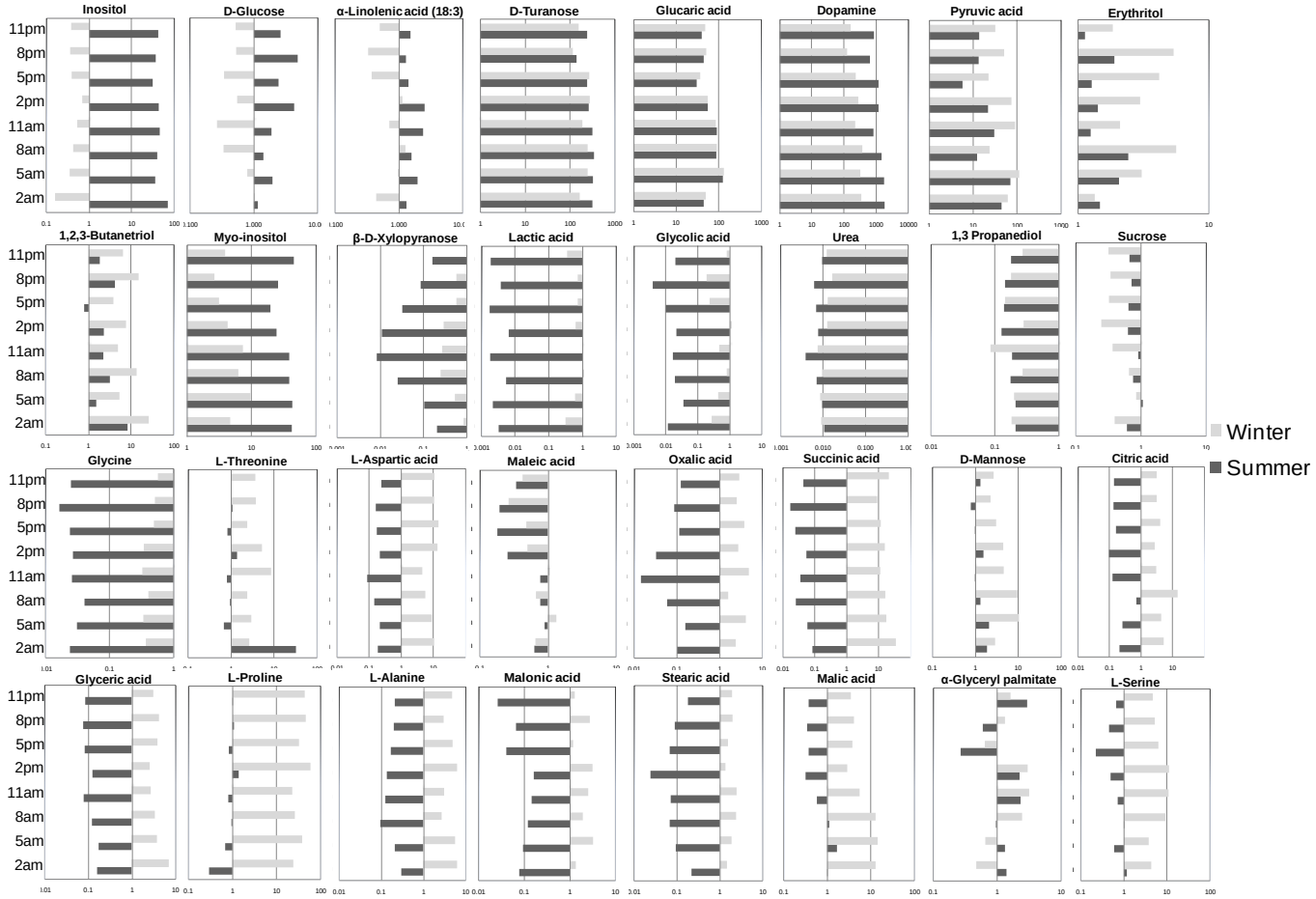

Figure 5.6: Relative abundance of metabolites detected during summer and winter with respect to their abundance during post-monsoon season. Each normalized value for the respective metabolites from summer and winter were divided by the normalized value of the metabolites from post-monsoon season. The results obtained were then plotted in log10 scale.

Table 5.1: List of the metabolites and its average value of abundance detected during post-monsoon seasons from the leaves of *S. fruticosa*

Compound	Time of the day							
	2am	5am	8am	11am	2pm	5pm	8pm	11pm
Alcohol								
2-Thiophenethiol	0.26	0.12	0.26	0.24	0.12	0.17	0.17	0.12
Phytol	0.43	0.96	1.12	1.59	1.81	1.39	0.78	0.70
Amino acid								
Glutamine	0.42	1.65	5.28	5.05	9.16	7.79	1.91	0.49
Glycine	14.4	14.9	13.4	18.9	19.5	13.4	13.3	12.8
L-Alanine	2.38	2.75	6.76	7.15	5.43	5.00	3.87	3.09
L-Aspartic acid	2.65	2.18	3.23	3.92	2.26	2.73	2.70	2.10
L-Isoleucine	0.10	0.06	0.06	0.06	0.04	0.15	0.04	0.05
L-Proline	0.70	0.75	0.73	1.21	0.68	0.73	0.56	0.56
L-Serine	0.34	0.85	0.56	0.81	1.06	1.46	0.81	0.37
L-Threonine	0.54	0.77	0.94	0.35	0.70	1.54	0.78	0.67
L-Tyrosine	6.38	11.2	10.9	7.35	0.78	6.96	5.56	4.57
N,N-Dimethylglycine	20.0	20.6	20.5	25.1	31.0	22.1	15.2	12.2
Pyroglutamic acid	1.70	1.54	5.86	6.97	7.76	6.51	7.68	4.31
Tyramine	0.27	0.32	1.42	1.10	1.66	2.67	3.11	1.07
Fatty acid								
Linoleic acid (18:2)	6.51	6.11	6.59	6.35	6.51	6.61	6.01	6.56
Myristic acid (14:0)	0.20	0.28	0.35	0.35	0.28	0.56	0.38	0.41
Oleic acid (18:1)	0.37	0.47	0.27	0.24	0.14	0.31	0.54	0.21

Palmitic acid (16:0)	6.72	4.60	7.97	6.37	7.13	12.6	9.79	6.20
Ricinoleic acid (18:1)	3.48	3.15	2.70	2.09	1.56	1.64	1.36	1.77
Stearic acid (18:0)	3.82	3.67	3.99	3.22	4.86	4.43	3.68	3.28
α-Glyceryl palmitate	0.38	0.31	0.24	0.13	0.16	0.55	0.19	0.17
α-Linolenic acid (18:3)	11.5	6.95	10.3	10.0	9.80	14.4	14.1	11.7
Inorganic acid								
Phosphoric acid	43.4	47.1	46.4	47.6	85.7	67.6	47.5	32.3
Inorganic compound								
Hydroxylamine	0.06	0.14	0.14	0.13	0.12	0.14	0.14	0.08
Polyol								
Glycerol-3-phosphate	0.28	0.17	0.27	0.32	0.34	0.34	0.37	0.23
Inositol	0.57	1.09	0.87	0.86	0.86	1.01	0.86	0.73
L-chiro-inositol	0.16	0.16	0.10	0.09	0.06	0.06	0.10	0.15
Myo-inositol	2.02	1.93	2.57	2.52	3.78	3.85	2.94	1.78
Steroid								
Stigmasterol	1.65	0.86	0.50	2.17	1.50	3.08	1.52	1.09
Organic acid								
12-Hydroxystearic acid	0.15	0.11	0.09	0.09	0.07	0.08	0.14	0.13
2,3-Dimethoxycinnamic acid	0.12	0.11	0.15	0.13	0.14	0.11	0.11	0.14
2-Hydroxy-3-methylvaleric acid	1.81	1.55	1.53	2.05	1.91	2.20	2.57	2.25
2-Hydroxyisobutyric acid	0.08	0.09	0.08	0.08	0.07	0.07	0.09	0.08
3-Hydroxy-3-methylglutaric acid	0.53	0.24	0.80	1.11	1.10	1.26	0.80	1.11
3-Hydroxyphenylacetic acid	0.05	0.07	0.08	0.08	0.07	0.07	0.07	0.07
4-Hydroxyphenylacetic acid	0.16	0.86	0.81	0.75	0.81	0.58	0.12	0.12
Butyric acid	0.12	0.10	0.08	0.08	0.06	0.03	0.08	0.08
Citric acid	7.59	7.65	2.93	13.7	15.6	10.4	12.3	12.2

Dodecandioic acid	0.18	0.14	0.11	0.12	0.19	0.12	0.13	0.10
Ferulic acid	1.24	1.15	0.84	0.72	0.83	1.38	0.96	0.99
Formic acid	1.00	1.86	0.92	0.88	0.82	0.96	0.87	0.83
Glucaric acid	1.27	0.47	0.59	0.67	1.00	1.61	1.10	1.09
Glucuronic acid	0.65	0.22	0.15	0.25	0.31	0.59	0.54	0.62
Glycolic acid	5.65	3.93	4.70	5.25	4.46	9.29	9.97	4.97
Gulonic acid	0.25	0.26	0.40	0.40	0.27	0.30	0.21	0.30
Lactic acid	14.9	9.52	6.50	8.57	7.91	9.13	8.70	9.97
L-Tartaric acid	8.92	5.54	6.78	4.92	6.08	12.0	6.46	6.11
Maleic acid	0.35	0.25	0.38	0.28	0.58	0.71	0.66	0.36
Malic acid	4.22	4.49	7.21	13.0	25.3	13.3	12.6	10.5
Malonic acid	3.36	2.28	3.52	2.77	2.23	4.75	2.87	4.80
Mesaconic acid	0.08	0.08	0.10	0.09	0.11	0.05	0.09	0.08
Oxalic acid	17.3	12.6	16.1	15.3	16.0	15.0	19.2	14.2
Pyruvic acid	0.43	0.29	1.80	0.56	0.55	1.62	0.70	0.74
Ribonic acid	1.68	0.77	0.68	0.51	0.97	3.23	0.51	0.51
Succinic acid	1.50	2.99	3.96	4.36	3.14	3.98	4.65	2.13
α-Hydroxyglutaric acid	0.13	0.17	0.21	0.61	0.79	0.40	0.35	0.43
α-Ketoisovaleric acid	0.10	0.09	0.11	0.09	0.07	0.10	0.06	0.06
β-Aminoisobutyric acid	0.96	2.85	4.37	5.75	4.52	2.78	1.87	2.61
Organic compound								
1,2,3-Butanetriol	0.16	0.79	0.32	0.40	0.29	0.90	0.24	0.55
1,3 Propanediol	6.07	6.05	6.42	5.53	5.30	5.72	5.69	5.43
1,3-Butanediol	0.02	0.04	0.08	0.07	0.05	0.06	0.08	0.07
3-Hydroxypyridine	0.15	0.14	0.15	0.15	0.19	0.29	0.36	0.22
6,7-Dihydroxycoumarin	0.93	0.78	1.31	1.86	1.56	1.38	0.77	0.81

Dopamine	0.04	0.05	0.04	0.09	0.06	0.06	0.11	0.08
Ethanolamine	1.61	2.06	2.50	2.17	1.65	1.90	2.11	2.10
Ethylene glycol	0.62	0.72	0.58	0.52	0.64	0.62	0.60	0.56
Isoeugenol	0.09	0.06	0.11	0.10	0.09	0.10	0.09	0.04
Levoglucosan	0.15	0.27	0.10	0.09	0.10	0.07	0.10	0.10
Neophytadiene	0.49	0.43	0.24	0.34	0.25	0.33	0.35	0.31
Propylene glycol	35.2	37.0	33.7	31.2	34.6	36.8	36.6	31.2
Urea	20.6	25.0	29.8	34.9	21.6	18.0	20.2	19.0
Sugar								
2-Deoxy-galactopyranose	0.20	0.24	0.41	0.41	0.56	1.35	0.39	0.26
2-Deoxy-galactose	0.39	0.46	0.69	0.42	0.31	0.55	0.45	0.33
4-Hydroxy-3-methoxyphenylglycol	0.19	0.41	0.39	0.22	0.26	0.21	0.23	0.26
D-Fructose	1.14	0.92	0.98	1.25	1.07	0.88	0.99	1.36
D-Galactofuranose	0.26	0.23	0.09	0.14	0.16	0.22	0.20	0.20
D-Galactose	0.41	0.28	0.47	0.41	0.39	0.52	0.35	0.53
D-Mannose	0.51	0.18	0.26	0.32	0.31	0.56	0.69	0.63
D-Turanose	0.23	0.21	0.19	0.20	0.25	0.28	0.48	0.30
D-Xylose	0.18	0.12	0.13	0.13	0.20	0.20	0.20	0.14
Fucose	0.10	0.08	0.09	0.15	0.16	0.20	0.21	0.06
L-Fructose	0.10	0.14	0.17	0.16	0.22	0.40	0.47	0.24
Maltose	0.14	0.31	0.20	0.19	0.34	0.27	0.13	0.26
Melibiose	1.48	1.34	0.69	1.42	1.61	0.41	2.20	1.32
Rhamnose	0.12	0.18	0.38	0.65	0.80	1.28	0.89	0.47
Sucrose	90.3	69.6	76.4	111.1	144.8	120.5	109.1	102.7
α-D-Galactoside	0.45	0.22	0.49	0.72	0.99	0.82	0.91	0.32
α-D-Glucopyranose	0.15	0.11	0.10	0.13	0.09	0.05	0.08	0.14

α-D-Glucopyranoside	0.32	0.34	0.39	0.56	0.31	0.39	0.25	0.38
α-Mannopyranose	0.15	0.17	0.14	0.14	0.14	0.07	0.06	0.13
β-D-Xylopyranose	1.50	4.61	10.2	11.9	11.4	7.63	4.83	2.44
β-Lactose	0.11	0.17	0.13	0.28	0.42	0.93	0.17	0.14
Sugar acid								
3-Deoxy-arabino-hexaric acid	0.15	0.13	0.14	0.43	0.41	0.50	0.37	0.19
D-Galacturonic acid	0.11	0.56	0.79	0.60	0.53	0.58	0.14	0.09
Glyceric acid	1.55	2.79	4.61	7.01	6.77	3.77	3.89	2.79
Isocitric acid lactone	2.34	2.90	3.09	1.71	1.13	2.30	2.18	2.00
L-Threonic acid	3.58	3.81	3.74	3.61	3.82	5.83	4.38	6.18
Mannonic acid, γ-lactone	0.24	0.30	0.42	0.70	0.72	0.78	0.76	0.43
Xylonic acid, 1,5-lactone	0.31	0.26	0.41	0.65	1.78	0.59	3.11	0.59
Sugar alcohol								
Arabitol	0.05	0.09	0.07	0.07	0.06	0.08	0.09	0.07
D-Glucose	5.13	4.75	5.63	4.23	3.15	3.83	2.96	4.06
Erythritol	1.04	0.74	0.58	1.10	0.90	1.01	0.68	1.09
Sorbitol	1.14	0.49	0.58	0.82	0.80	0.20	0.51	0.90
Terpenoid								
Geraniol	0.66	0.52	0.53	0.54	0.46	0.56	0.45	0.40
Vitamin								
Pantothenic acid	0.17	0.10	0.17	0.11	0.07	0.11	0.08	0.14
α-Tocopherol	1.26	1.11	0.79	0.99	1.08	0.81	1.12	1.09

Table 5.2: List of the metabolites and its average value of abundance detected during winter seasons from the leaves of *S. fruticosa*

Compound	Time of the day							
	2am	5am	8am	11am	2pm	5pm	8pm	11pm
Amino acid								
Citrulline	1.47	2.36	3.46	5.80	6.70	4.01	0.32	0.26
Glutamine	9.50	11.91	10.71	9.24	17.82	6.91	8.15	11.0
Glycine	5.32	5.05	5.40	6.21	6.67	6.64	6.81	7.31
Homocystine	0.11	0.11	0.11	0.20	0.29	0.15	0.12	0.12
L-Alanine	15.0	15.53	18.37	22.30	34.53	24.3	11.8	14.7
L-Asparagine	1.86	2.69	3.05	4.53	3.94	3.52	2.31	2.76
L-Aspartic acid	28.07	19.98	18.16	17.95	30.89	39.4	28.4	23.0
L-Cysteine	0.17	0.11	0.17	0.14	0.26	0.23	0.28	0.13
L-Glutamic acid	15.2	13.57	16.27	17.97	24.52	20.5	18.2	23.9
L-Isoleucine	0.58	0.86	0.80	1.21	1.63	1.34	0.79	0.54
L-Leucine	0.17	0.13	0.27	0.50	0.48	0.19	0.17	0.14
L-Lysine	0.16	0.38	0.43	0.67	0.63	0.40	0.26	0.16
L-Norleucine	0.18	0.19	0.16	0.14	0.14	0.12	0.13	0.15
L-Norvaline	0.95	1.18	0.75	1.18	2.46	2.81	1.61	1.44
L-Phenylalanine	1.30	2.66	6.68	3.34	4.35	5.33	3.76	1.40
L-Proline	17.0	29.05	18.81	27.37	40.20	24.1	26.0	24.5
L-Serine	1.48	3.20	5.21	8.81	11.84	9.35	4.27	1.74
L-Threonine	1.42	2.29	2.23	2.99	3.64	3.70	2.96	2.45
L-Tyrosine	0.39	0.87	1.24	1.33	0.97	0.66	0.67	0.56
N-Acetylglutamine	0.39	0.61	0.61	0.52	0.74	0.46	0.70	0.45

β-Alanine	2.39	4.61	10.19	14.88	13.27	12.8	9.21	8.73
γ-Aminobutyric acid	15.77	15.14	17.59	18.40	15.11	15.2	17.0	13.9
Fatty acid								
11-Eicosenoic acid	0.04	0.04	0.04	0.08	0.08	0.04	0.06	0.02
2-Monolinolenin (18:3)	2.22	1.66	5.54	1.77	1.37	3.95	1.58	1.55
Arachidic acid (20:0)	0.25	0.27	0.80	0.37	0.65	0.45	0.27	0.52
Caprylic acid (8:0)	0.28	0.26	0.29	0.22	0.27	0.30	0.38	0.26
Heptadecanoic acid (17:0)	1.25	1.36	2.42	1.68	1.96	1.57	1.65	1.47
Lignoceric acid (24:0)	5.41	3.42	3.90	5.05	6.59	4.98	4.65	3.65
Linoleic acid (18:2)	7.01	14.01	15.13	18.26	16.94	15.5	15.5	13.1
Palmitic acid (16:0)	11.0	17.16	29.06	19.22	26.04	15.7	18.1	19.7
Stearic acid (18:0)	5.62	6.88	9.65	8.11	6.68	6.98	7.38	6.42
α-Glyceryl palmitate	0.18	0.20	0.59	0.42	0.47	0.35	0.26	0.28
α-Hydroxylignoceric acid (25:0)	5.41	3.42	3.90	5.05	6.59	4.98	4.65	3.65
α-Linolenic acid (18:3)	5.09	6.76	12.95	7.11	11.21	5.43	4.71	5.94
Inorganic compound								
Hydroxylamine	0.05	0.08	0.15	0.13	0.19	0.15	0.14	0.13
Lignan								
Matairesinol	2.29	2.22	3.73	3.41	2.56	4.44	3.50	1.71
Polyol								
Glycerol	86.3	102	105.0	75.00	60.85	63.2	72.6	79.0
Glycerol-3-phosphate	2.55	4.30	2.55	1.25	1.27	3.99	1.59	3.42
Inositol	0.09	0.38	0.37	0.45	0.59	0.39	0.31	0.27
Myo-inositol	9.47	18.5	15.99	18.47	16.20	12.1	7.87	6.87
Organic acid								
2-Hydroxyisobutyric acid	0.28	0.29	0.27	0.47	0.44	0.34	0.57	0.22

3-Hydroxyisobutanoic acid	1.45	1.80	3.22	3.40	2.58	1.74	1.69	1.65
Citric acid	40.0	33.8	43.25	42.06	41.99	42.6	38.8	38.4
Dimethylmalonic acid	0.32	0.85	0.72	1.05	1.03	1.39	1.47	0.66
Ferulic acid	6.71	9.21	15.31	12.18	14.92	12.6	15.0	12.0
Fumaric acid	1.55	1.62	1.47	2.85	1.89	1.50	1.00	1.28
Glucaric acid	63.6	61.7	54.11	58.32	55.13	59.6	55.6	52.8
Gluconic acid	9.13	10.0	14.01	7.95	9.41	8.11	6.56	9.15
Glycolic acid	1.51	1.69	3.75	2.48	5.16	2.18	1.88	4.00
Isoferulic acid	3.48	2.53	2.73	2.79	3.23	3.60	3.39	3.83
Lactic acid	4.76	5.69	7.33	8.60	4.89	6.59	6.28	3.50
Maleic acid	0.23	0.33	0.25	0.30	0.29	0.34	0.17	0.15
Malic acid	54.4	64.1	91.94	73.05	73.03	49.9	51.3	36.6
Malonic acid	4.55	7.44	6.84	7.04	7.11	5.72	7.99	6.28
Methylsuccinic acid	0.21	0.19	0.20	0.27	0.21	0.21	0.22	0.21
Oxalic acid	42.4	52.1	25.95	75.93	44.09	58.2	49.6	41.6
Phthalic acid	3.56	4.75	5.15	3.76	3.18	3.64	2.57	1.91
Pipecolic acid	0.74	0.73	0.68	0.59	0.55	0.56	0.73	0.82
Pyruvic acid	26.7	32.6	42.24	50.82	41.63	36.0	36.2	23.9
Quininic acid	1.87	2.59	3.33	2.21	2.88	2.52	1.55	2.36
Succinic acid	51.7	51.7	65.58	48.81	49.25	46.6	42.1	44.5
Tartaric acid	1.72	2.45	3.40	1.69	1.43	1.15	1.25	1.51
Vanilmandelic acid	0.49	0.60	0.46	0.92	0.73	0.22	0.64	0.48
α-Hydroxyglutaric acid	2.71	2.60	5.38	2.57	1.51	2.52	1.33	1.15
α-Hydroxyisovaleric acid	0.03	0.07	0.03	0.05	0.08	0.06	0.20	0.07
β-Hydroxy-β-methylglutaric acid	3.55	4.19	7.17	9.49	6.25	3.96	2.13	5.86
β-Lactic acid	0.14	0.16	0.17	0.15	0.26	0.18	0.12	0.22

β-Phenyllactic acid	43.2	43.0	46.69	55.22	58.31	51.3	54.9	38.5
γ-Hydroxybutyric acid	0.42	0.27	0.24	0.14	0.27	0.40	0.31	0.42
Organic compound								
1,2,3-Butanetriol	4.05	4.22	4.19	1.97	2.22	3.45	3.53	3.55
1,3 Propanediol	1.11	1.20	1.74	0.47	1.49	0.81	1.02	1.48
1,3-Butanediol	0.12	0.13	0.26	0.27	0.58	0.42	0.60	0.24
1-Phenylethanol	0.50	0.72	0.64	0.73	0.44	0.36	0.27	0.41
5-Hydroxytryptophol	1.74	3.13	3.76	3.45	3.40	2.63	1.73	1.88
cis-Polydatin	0.23	0.60	0.35	0.39	0.71	1.14	0.67	0.48
Diethylene glycol	39.2	42.8	66.09	54.36	53.38	44.7	49.8	50.0
Dopamine	14.5	15.3	16.46	19.38	17.24	14.3	14.0	12.9
Ethanolamine	1.16	1.41	1.74	1.63	1.79	1.87	1.43	1.56
p-Coumaric acid	1.43	1.01	1.13	1.14	1.16	1.51	1.09	1.08
Urea	0.19	0.22	0.29	0.26	0.27	0.23	0.33	0.23
Sugar								
2-Deoxy-D-galactose	1.33	2.18	4.21	3.39	3.06	2.61	3.11	1.58
2-Deoxy-galactose	0.57	0.93	1.17	0.89	0.92	1.01	1.02	0.80
2-Keto-L-gulonic acid	0.51	0.89	1.82	1.70	1.41	1.57	1.61	0.73
Allonic acid, 1,4-lactone	0.45	0.56	0.39	0.32	0.57	0.61	0.53	0.27
D-arabino-hexos-2-ulose	24.9	28.0	39.14	39.56	34.58	46.0	45.1	33.5
D-Fructose	0.33	0.34	0.51	0.72	0.78	0.63	0.56	0.52
D-Galactose	0.13	0.16	0.36	0.27	0.24	0.37	0.15	0.19
D-Glucitol	4.96	5.91	13.37	15.91	15.79	6.22	5.69	5.58
D-Mannose	1.50	1.90	2.45	1.46	1.42	1.72	1.58	1.69
D-Turanose	38.3	50.9	47.44	37.76	69.31	75.8	56.3	47.3
D-Xylose	1.63	2.42	7.66	8.59	6.03	6.65	5.08	4.88

Fucose	0.15	0.16	0.31	0.28	0.26	0.52	0.29	0.25
Hexopyranose	8.39	8.45	20.12	27.03	15.62	10.2	10.1	9.94
Hexuronate	0.47	1.03	1.84	0.98	1.20	1.06	1.01	0.82
L-Erythrulose	1.82	4.49	3.42	5.50	4.45	4.81	1.38	1.07
L-Fructose	6.87	9.94	18.90	18.54	26.67	17.6	16.1	9.62
Maltose	1.46	1.66	2.17	1.74	2.94	2.01	1.52	1.48
Mannose-6-phosphate	1.08	0.94	1.43	1.37	1.43	2.04	1.47	1.17
Melibiose	1.78	1.85	1.49	1.90	1.82	1.37	1.31	1.40
Rhamnose	0.25	0.35	0.59	0.38	0.41	0.36	0.34	0.43
Sucrose	35.8	58.8	50.51	41.10	36.03	39.2	37.6	32.5
Xylose	1.49	2.10	3.22	3.27	2.61	1.29	0.86	2.46
α-D-Galactoside	2.57	1.80	2.24	1.74	2.47	1.51	1.13	1.70
α-D-Glucopyranose	46.2	82.28	130.8	160.1	167.9	90.8	79.2	58.8
α-D-Glucopyranoside	4.15	2.18	5.31	2.64	3.27	8.17	5.37	4.38
α-D-Mannopyranose	7.72	7.13	9.10	5.04	7.87	7.94	5.22	6.65
α-Galactopyranose	10.4	10.8	15.9	9.27	12.98	11.4	11.8	6.54
β-d-Glucopyranose	13.8	45.6	70.6	32.1	37.18	36.4	31.5	28.9
β-D-Mannopyranose	15.9	23.5	26.1	22.6	16.96	23.4	12.3	21.2
β-D-Xylopyranose	1.25	2.45	2.54	3.24	3.30	4.38	2.80	2.42
β-Galactopyranose	1.22	2.34	3.23	2.52	3.05	6.20	5.53	3.61
β-Glucopyranose	0.48	0.91	0.77	0.80	1.41	0.70	0.90	0.80
β-L-Arabinopyranose	0.62	0.33	0.54	0.75	0.55	0.34	0.37	0.42
Sugar acid								
3-Deoxy-arabino-hexaric acid	3.54	1.92	1.21	2.28	2.18	4.29	1.77	1.41
Arabinonic acid, γ-lactone	0.24	0.17	0.22	0.19	0.22	0.19	0.15	0.17
Glyceric acid	10.8	10.3	15.3	19.1	17.19	14.4	16.1	8.65

Idonic acid, 1,4-lactone	0.60	0.87	0.97	1.24	1.30	1.07	0.98	0.69
Lactoisocitric acid	5.96	9.33	8.01	8.01	13.55	9.25	14.22	10.66
Mannonic acid, γ-lactone	5.76	4.36	6.91	3.09	3.69	7.74	3.51	3.85
Methylmalonic acid	1.25	1.28	1.30	0.92	1.08	0.95	0.99	1.05
Talonic acid, 1,4-lactone	1.13	1.08	1.46	1.11	1.08	1.23	1.12	0.89
Threonic acid	0.26	0.26	0.44	0.38	0.33	0.38	0.27	0.24
α-Ketoglutaric acid	3.38	3.42	7.74	7.63	8.65	7.10	4.35	3.82
Sugar alcohol								
D-Glucose	5.28	3.77	1.89	1.12	1.73	1.32	1.58	2.13
Erythritol	1.40	2.27	3.29	2.30	2.71	4.23	3.66	2.02
Galactitol	20.89	28.96	35.11	25.38	37.07	23.9	17.09	23.21
Sorbitol	0.63	0.93	1.98	1.85	1.68	1.78	2.06	1.08
Terpenoid								
α-Terpineol	0.05	0.10	0.13	0.12	0.14	0.12	0.15	0.04
Vitamin								
Ascorbic acid	2.49	4.35	6.30	7.31	8.65	6.18	5.60	3.35

Table 5.3: List of the metabolites and its average value of abundance detected during summer seasons from the leaves of *S. fruticosa*

Compound	Time of the day							
	2am	**5am**	**8am**	**11am**	**2pm**	**5pm**	**8pm**	**11pm**
Alcohol								
Vinyloxyethanol	0.04	0.04	0.05	0.04	0.02	0.01	0.01	0.03
α-Methylpropantriol	0.95	0.98	0.71	0.69	0.63	0.92	0.92	0.69

Amino acid								
Citrulline	0.12	0.55	0.58	0.39	0.41	0.26	0.26	0.14
Glycine	0.34	0.46	0.54	0.49	0.53	0.32	0.22	0.32
L-Alanine	0.71	0.57	0.64	0.90	0.75	0.86	0.77	0.65
L-Aspartic acid	0.48	0.47	0.46	0.33	0.48	0.46	0.44	0.50
L-Glutamic acid	0.69	0.65	0.69	0.80	0.83	0.75	0.56	0.62
L-Leucine	0.13	0.06	0.08	0.10	0.13	0.10	0.10	0.05
L-Norleucine	0.08	0.05	0.04	0.04	0.08	0.09	0.09	0.09
L-Norvaline	0.03	0.08	0.10	0.07	0.06	0.05	0.04	0.02
L-Phenylalanine	0.18	0.27	0.18	0.13	0.17	0.30	0.30	0.18
L-Proline	0.20	0.51	0.68	0.96	0.93	0.61	0.59	0.55
L-Serine	0.41	0.50	0.58	0.57	0.52	0.32	0.37	0.24
L-Threonine	17.69	18.15	20.20	17.51	20.40	13.02	13.70	14.11
L-Valine	0.12	0.08	0.08	0.08	0.12	0.15	0.15	0.12
N-Acetylglutamine	0.09	0.13	0.09	0.08	0.12	0.07	0.05	0.07
Ornithine	1.67	1.66	1.73	0.89	0.99	1.05	1.05	1.24
Penicillamine	0.58	0.53	0.50	0.52	0.46	0.30	0.30	0.42
Pyroglutamic acid	0.73	0.53	0.34	1.02	0.86	0.25	0.26	0.17
α-Hydroxyisocaproic acid	0.14	0.20	0.22	0.20	0.16	0.12	0.06	0.11
α-Methylvaline	0.05	0.09	0.08	0.08	0.06			
α-Pipecolinic acid	0.11	0.17	0.18	0.10	0.09	0.07	0.13	0.12
γ-Aminobutyric acid	0.14	0.13	0.14	0.13	0.15	0.15	0.15	0.17
Amino alcohol								
1-Aminopropan-2-ol	0.16	0.25	0.29	0.44	0.34	0.39	0.37	0.14
Aromatic hydrocarbon								
Anthracene	0.46	0.86	1.21	0.62	0.50	0.50	0.46	0.45

Fatty acid								
11-Eicosenoic acid				0.78	0.96	0.83	0.77	0.27
Oleic acid (18:1)	2.96	3.15	3.83	4.23	5.63	5.13	4.75	4.06
Palmitoleic acid (16:1)	4.33	3.72	0.79	1.89	1.30	1.42	1.46	2.38
Stearic acid (18:0)	0.83	0.35	0.27	0.23	0.12	0.30	0.33	0.60
α-Glyceryl palmitate	0.53	0.41	0.23	0.31	0.35	0.15	0.12	0.51
α-Linolenic acid (18:3)	15.2	13.5	16.2	23.97	24.5	20.5	18.2	17.9
Inorganic acid								
Phosphoric acid	32.8	43.6	43.6	48.84	42.7	35.6	35.6	34.1
Polyol								
Glycerol	31.5	43.6	50.9	26.94	44.8	59.2	36.2	23.1
Inositol	40.4	39.1	34.4	39.25	36.3	31.6	31.6	30.6
Myo-inositol	84.8	81.7	97.8	97.22	91.8	74.9	74.9	79.6
Organic acid								
2-Keto-3-methylvaleric acid	0.12	0.25	0.22	0.27	0.47	0.21	0.20	0.13
2-Ketohexanoic acid		0.14	0.34	0.24	0.23			
3,4-Dihydroxymandelic acid	0.25	0.36	0.39	0.48	0.44	0.42	0.19	0.18
3-Aminobutyric acid	0.62	0.41	0.31	0.24	0.31	0.44	0.44	0.58
3-Methyl-2-oxovaleric acid	0.07	0.09	0.11	0.24	0.24	0.10	0.08	0.08
Alloxanic acid	43.7	45.2	30.1	36.68	36.4	22.0	22.0	23.3
Butyric acid	2.13	1.16	1.00	1.24	1.54	1.72	1.79	1.82
Citraconic acid	0.24	0.35	0.35	0.19	0.17	0.18	0.18	0.20
Citric acid	1.56	1.98	2.04	1.69	1.47	1.67	1.67	1.69
D-Gluconic acid	0.80	0.54	0.46	0.47	0.49	0.33	0.42	0.53
D-Ribonic acid	1.43	1.68	1.28	0.91	1.06	0.76	0.72	1.03
Glucaric acid	56.1	58.9	51.5	61.53	55.2	48.4	48.4	42.7

Glycolic acid	0.07	0.14	0.09	0.09	0.10	0.09	0.04	0.10
Isothiocyanic acid	0.15	0.15	0.13	0.12	0.13	0.15	0.12	0.13
Lactic acid	0.05	0.02	0.04	0.02	0.05	0.02	0.03	0.02
L-Tartaric acid	19.9	19.6	19.7	19.44	20.0	19.6	19.6	19.2
Maleic acid	0.22	0.22	0.29	0.21	0.15	0.13	0.13	0.12
Malic acid	4.18	7.43	7.88	7.41	8.04	4.95	4.37	3.93
Malonic acid	0.26	0.21	0.43	0.41	0.36	0.19	0.19	0.12
Methanoic acid	0.04	0.04	0.07	0.05	0.06	0.06	0.02	0.03
Oxalic acid	1.78	2.00	0.97	0.22	0.52	1.69	1.69	1.74
Pipecolic acid	0.33	0.23	0.26	0.44	0.59	0.53	0.53	0.41
Propionic acid	0.05	0.11	0.07	0.12	0.11	0.10	0.03	0.05
Pyruvic acid	19.3	20.2	22.4	16.78	12.1	9.35	9.35	10.0
Ribonic acid	18.1	19.7	17.6	17.77	19.3	19.2	19.2	18.1
Shikimic acid	0.16	0.28	0.58	0.19	0.16			
Succinic acid	0.13	0.18	0.10	0.15	0.17	0.10	0.08	0.09
Tartronic acid	0.22	0.22	0.26	0.25	0.18	0.14	0.12	0.13
Vanilmandelic acid	0.13	0.21	0.15	0.15	0.10	0.10	0.10	0.09
α-Hydroxyisovaleric acid	0.24	0.20	0.20	0.14	0.16	0.27	0.24	0.29
α-Ketoisovaleric acid	0.45	0.21	0.45	0.17	0.27	0.07	0.07	0.13
β-Hydroxypyruvic acid	0.61	0.63	0.53	0.78	1.08	0.63	0.56	0.68
Organic compound								
1,2,3-Butanetriol	1.30	1.19	1.01	0.90	0.67	0.71	1.00	1.02
1,3 Propanediol	1.27	1.28	1.13	1.03	0.67	0.79	0.82	0.98
4-Methylcatechol	0.07	0.03	0.08	0.03	0.06	0.03	0.06	0.04
6,7-Dihydroxycoumarin	0.13	0.13	0.11	0.12	0.16	0.15	0.12	0.08
9,10-Anthracenedione	0.12	0.13	0.16	0.23	0.23	0.24	0.24	0.17

Allyl glycol	0.04	0.02	0.06	0.02	0.04	0.01	0.02	0.01
Aminothiadiazole	0.03	0.05	0.08	0.07	0.14	0.05	0.02	0.03
Carbitol acetate	0.25	0.76	1.46	0.67	0.59	0.37	0.32	0.23
Diethylene glycol	0.49	0.40	0.37	0.32	0.34	0.24	0.24	0.26
Dopamine	77.4	84.7	66.1	71.69	75.0	74.1	74.1	68.1
Levoglucosan	0.05	0.05	0.06	0.07	0.06	0.06	0.04	0.04
Propanoic anhydride	0.06	0.05	0.07	0.10	0.10	0.06	0.04	0.02
Pyrazine		0.04	0.09	0.05	0.02			
Pyrrolidine	0.36	0.11	0.71	0.62	0.93	0.68	0.52	0.32
Triethanolamine	0.17	0.18	0.15	0.10	0.11	0.15	0.14	0.16
Urea	0.22	0.24	0.21	0.14	0.17	0.12	0.12	0.18
Sugar								
D-Glucitol	0.57	0.54	0.54	0.53	0.54	0.54	0.55	0.55
D-Gluco-hexodialdose	1.98	3.10	4.04	8.52	5.78	4.37	2.66	1.76
D-Mannose	0.97	0.39	0.34	0.31	0.49	0.54	0.54	0.83
D-Turanose	72.4	67.7	64.5	63.04	65.3	68.2	68.2	72.9
L-Sorbopyranose	0.23	0.43	0.55	0.39	0.40	0.26	0.24	0.33
L-Sorbose	0.19	0.13	0.13	0.13	0.15	0.11	0.10	0.11
Sucrose	55.7	74.9	58.0	100.82	91.2	78.1	78.1	69.1
α-D-Glucofuranose	0.04	0.03	0.02	0.06	0.03	0.01	0.01	0.05
α-D-Xylopyranose	0.03	0.34	0.43	0.64	0.56	0.55	0.43	0.24
β-D-Xylopyranose	0.31	0.48	0.26	0.10	0.13	0.25	0.42	0.39
γ-Butyrolactone	0.18	0.14	0.15	0.15	0.16	0.16	0.13	0.16
Sugar acid								
Glyceric acid	0.24	0.49	0.56	0.56	0.84	0.31	0.30	0.24
Methylmalonic acid	0.07	0.06	0.05	0.05	0.05	0.06	0.04	0.05

Threonic acid	0.41	0.66	0.78	0.78	0.45	0.29	0.29	0.33
α-Deoxy-erythro-pentonic acid	0.14	0.18	0.19	0.23	0.14	0.11	0.06	0.13
α-Ethylhydracrylic acid	0.09	0.08	0.10	0.10	0.08	0.08	0.08	0.05
α-Ketoisocaproic acid	0.27	0.44	0.33	0.25	0.18	0.14	0.14	0.13
α-Ketovaleric acid	0.22	0.41	0.21	0.23	0.36	0.31	0.31	0.26
Sugar alcohol								
D-Glucose	5.96	9.33	8.01	8.01	13.5	9.25	14.2	10.6
Erythritol	1.54	1.53	1.41	1.38	1.28	1.29	1.29	1.24
Terpenoid								
α-Terpineol	0.15	0.16	0.12	0.13	0.12	0.15	0.10	0.10

5.3.2. Pathway enrichment analysis of the common as well as unique metabolites detected in leaves of S. fruticosa during different seasons

MetaboAnalyst 3.0 was used to identify the pathways that the metabolites detected were involved. This software predicts the pathways of the metabolites using the KEGG database. The predicted pathways were then correlated with the enriched pathway and topology of the metabolite map, which helps to identify the significant pathway under a set experiment. In the present study, metabolic pathway analysis for all the common metabolites that were detected in all the seasons and for those metabolites that were explicitly detected at particular season only, as represented in Figure. 5.5, was conducted (Figure. 5.7).

The 32 common metabolites identified from all the seasons were found to be involved in; glyoxylate and dicarboxylate metabolism, TCA cycle, alanine aspartate and glutamate metabolism, carbon fixation in photosynthetic organisms, glycine-serine and threonine metabolism, pyruvate metabolism, galactose metabolism, arginine and proline metabolism, tyrosine metabolism, starch and sucrose metabolism, glutathione metabolism and isoquinoline alkaloid biosynthesis. Almost all the identified pathways were primary pathways involved in sugar and amino acid metabolism, which are crucial for plants' growth, development, and survival irrespective of any physical condition the plants are in. Pathway analysis showed glyoxylate and dicarboxylate metabolism known to be a stress-responsive pathway, especially drought responsive (Dong et al., 2014) as the most significant pathway among the identified pathways (Figure. 5.7a).

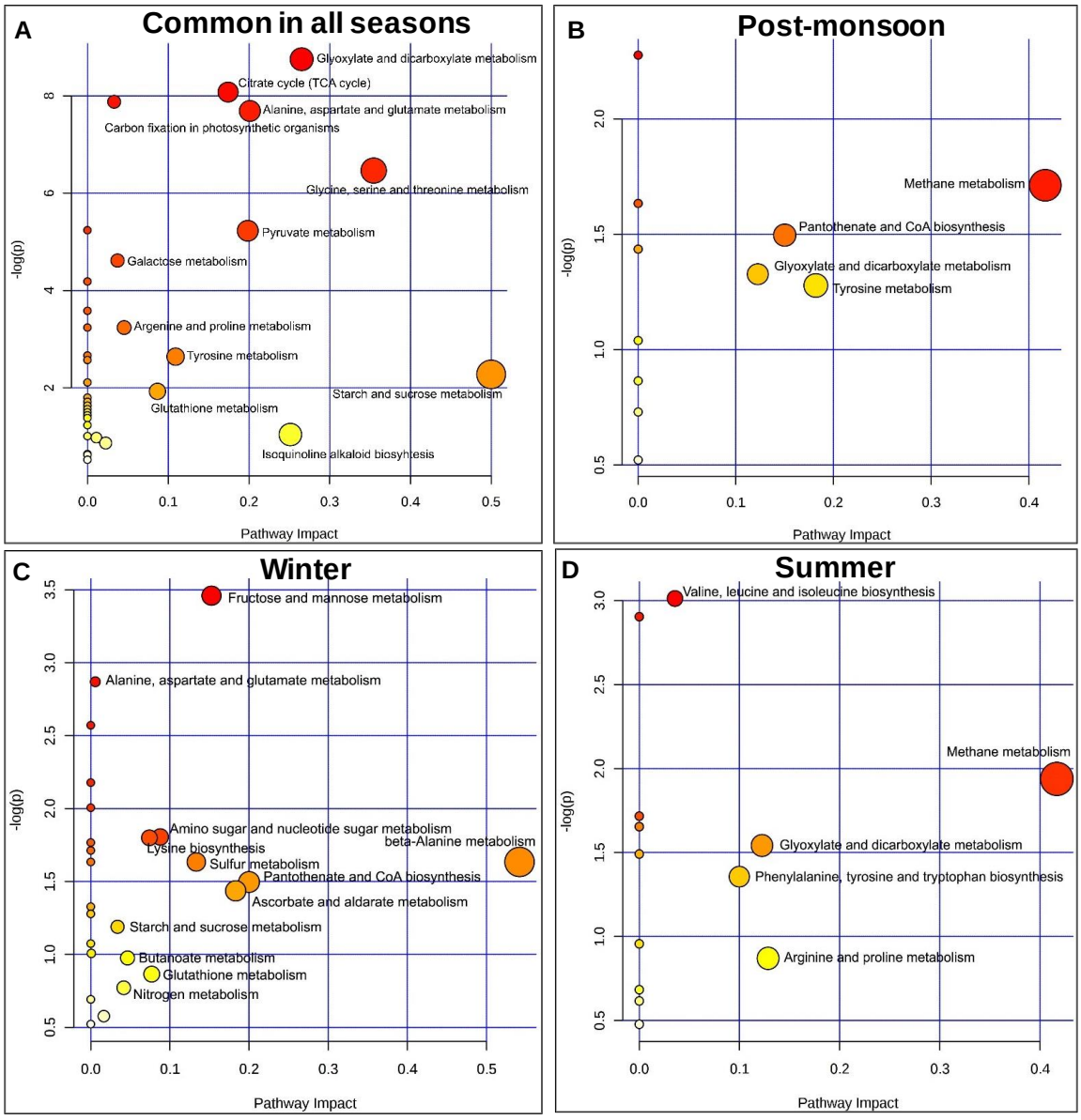

Figure 5.7: Metabolite pathway analysis. Pathway enrichment analysis is represented by plotting -log(p) of the matching pathways values against the pathway impact values. Colors and radii of the nodes are based on their p-values and their pathway impact values, respectively. Smaller the p-values and larger the radii indicate higher influence on the pathway. A) Metabolic pathways distribution associated with the common metabolites identified from leaves during the three seasons. B) Metabolic pathways distribution associated with the metabolites that were identified only in leaf during post-monsoon. C) Metabolic pathways distribution associated with the metabolites that were identified in leaves only during winter. D) Metabolic pathways distribution associated with the metabolites that were identified in leaves only during summer.

During post-monsoon, 38 metabolites uniquely identified in this season were seen to be involved in methane metabolism, panthothenate and CoA biosynthesis, glyoxylate, and dicarboxylate metabolism and tyrosine metabolism (Figure. 5.7b). Methane metabolism appearing as the most significant pathway could be due to the release of methane under UV and high-temperature stress (Nisbet et al., 2009). The 52 metabolites detected only during winter were seen to be involved in fructose and mannose metabolism, alanine, aspartate and glutamate metabolism, amino acid sugar and nucleotide sugar metabolism, beta-alanine metabolism, lysine biosynthesis, sulfur metabolism, pantothenate and CoA biosynthesis, ascorbate and aldarate metabolism, starch and sucrose metabolism, butanoate metabolism, glutathione metabolism and nitrogen metabolism. Important KEGG pathways that are regulated during cold stress, i.e. starch and sucrose metabolism (An et al., 2012) were found to be among the significant pathways (Figure. 5.7c). Similar to the profile obtained under post-monsoon season, the 45 metabolites specific to the summer season showed methane metabolism as the most significant pathway. Apart from this pathway, glyoxylate and dicarboxylate metabolism, phenylene, tyrosine, and tryptophan biosynthesis and arginine and proline metabolism were also detected (Figure. 5.7d).

5.3.3. Principal component analyses (PCA) of the metabolites

Two-dimension PCA is a powerful statistical tool to identify maximum variance and also to find the correlation of the variance from any large data (Wold et al., 1987). PCA of the metabolites identified in each season at different time point to compare the pattern of variation of the metabolites across the seasons and also to provide an overview of the unsupervised GCMS metabolite fingerprinting was done using MetaboAnalyst 3.0. The total metabolites detected at a specific time point is taken as one variance, which is then correlated with those metabolite variances detected at different time points. Metabolites, from every season, identified from eight-time points i.e. 02:00, 05:00, 08:00, 11:00, 14:00, 17:00,

20:00 and 23:00 hours were clustered into eight variances. These were then statistically analyzed with the first two PCA, i.e., PC1 and PC2, to represent the total variance and to find its correlation. Both these components separated the variance into two vectors, with each having a positive and a negative axis. Clear diurnal rhythmic variation of the metabolite profile was seen in tissue sample analyzed during the three seasons (Figure. 5.8).

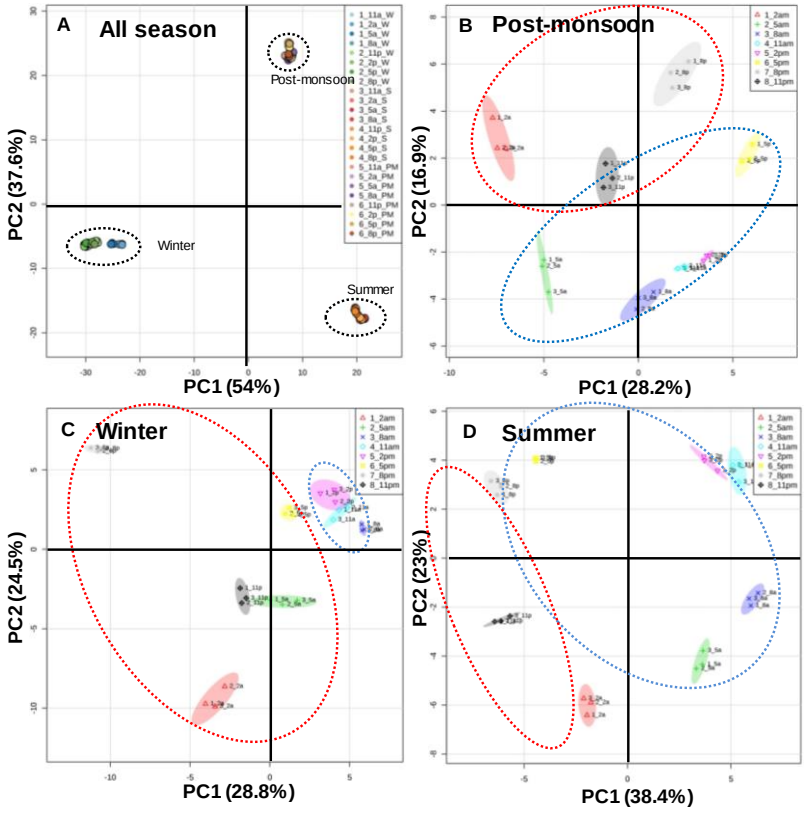

Figure 5.8: PCA of the metabolites extracted from leaves of *S. fruticosa* during the three different seasons. All the 222 metabolites identified from the three seasons showed diurnal as well as seasonal rhythmic pattern. The blue and the red area represents the metabolites clustered during the day (light) and night (dark) respectively. All the PCA shown here are represented by the first two principal component, i.e. PC1 and PC2 of the variables. A) The PCA of the complete 222 metabolites identified in all the three seasons is also represented by PC1 of 54% and PC2 of 37.6%. B) PCA of the metabolites identified during post-monsoon is represented by PC1 with 28.2% and PC2 with 16.9% variance. C) PCA of the metabolites identified during winter is represented by PC1 with 28.8% and PC2 of 24.5%. D) PCA of the metabolites identified during summer is represented by PC1 with 38.4% and PC2 of 23%.

Seasonal variations were seen to have a direct impact on the pattern of metabolite accumulations, which is visible through PCA (Figure. 5.8a). PC1 and PC2 represent 91.6% of the seasonal variants wherein, PC1 separated the seasonal variations according to the atmospheric temperature wherein, the two hotter seasons, i.e. post-monsoon and summer occupied the positive axis and winter occupied the negative axis. PC2 separated the three seasons according to salinity, wherein, complete metabolites identified during post-monsoon, when the salinity is the least, occupied the positive axis whereas the remaining two seasons, wherein salinity is at its peak, i.e. summer and winter were seen to occupy the negative axis.

During the post-monsoon season, of the 106 metabolites identified, 45.1% variants were represented by PC1 and PC2 (Figure. 5.8b). PC1 separates the variants according to the atmospheric temperature wherein, the positive axis is occupied by the metabolites accumulated during the hottest time of the day, i.e. between 08:00 and 20:00 hours PC2 separates the variants according to the day and night cycle, wherein, metabolites from 20:00 to 02:00 hours (night) occupied the positive axis and the rest, i.e. during day time occupy the negative axis. Likewise, 53.3% of the variants from 129 metabolites identified during winter were represented by PC1 and PC2 (Figure. 5.8c). However, in this case, PC1 separates the variants according to day and night cycle, wherein, metabolites accumulated during the short-day time from 08:00 to 02:00 hours occupied the positive axis. On the other hand, PC2 separated the variants according to the atmospheric temperature, wherein, the negative axis is occupied by the metabolites accumulating at the time point when its coldest, i.e. during 11:00 to 05:00 hours. Similarly, 61.4% of the 104 metabolite variants during summer are represented by PC1 and PC2 (Figure. 5.8d). PC1 separated the variants in day and night cycle wherein, metabolites accumulating during 05:00 to 17:00 hours occupied the positive axis. PC2 separated the variants according to the atmospheric temperature wherein; the positive axis is occupied by the

metabolites accumulated at the time point when its hottest, i.e. between 11:00 to 20:00 hours.

5.3.4. Sugar, TCA, fatty acid and amino acid pathway mapping of the detected metabolites in leaves of S. fruticosa

To identify the change in the pattern of accumulation of the metabolites detected as well as to find the possible pathways that each metabolite affects diurnally and seasonally in *S. fruticosa*, map for tricarboxylic acid (TCA) cycle, glycolysis/gluconeogenesis, amino acids, and fatty acid metabolism were analyzed (Figure. 5.9). The mentioned pathways are specifically considered with reference to figure 5.5b, c and d wherein, majority of the metabolites detected in all the seasons were of sugar, organic compound, and amino acids. The maps were drawn mostly by referring pathways from KEGG pathway database (http://www.genome.jp/kegg/pathway.html) along with some targeted and simplified maps given by Broun and Somerville (1997) for lipids metabolism, Hildebrandt et al. (2015) for amino acids metabolism, Stoop et al. (1996), Gupta and Kaur (2005) for glucose metabolism. To represent the differential pattern of accumulation diurnally as well as seasonally, color gradient codes ranging from green (lowest) to red (highest) was used.

Five metabolites that are directly involved in the TCA cycle were identified, of which, pyruvate, citrate, succinate, and malate were detected all through-out the seasons whereas fumarate was detected only during winter. All the five metabolites were most abundant during winter, of which, fumarate is found to be the highest at 11:00 hours and lowest at 23:00 hours, however, the rest four were seen highly accumulated throughout the day. Citrate, succinate, and malate were seen to be minimum during summer towards the late hour and early morning, i.e. 20:00 to 02:00 hours. However, pyruvate was seen lowest during the early hour of the day, i.e. 2 am to 5 am during post-monsoon.

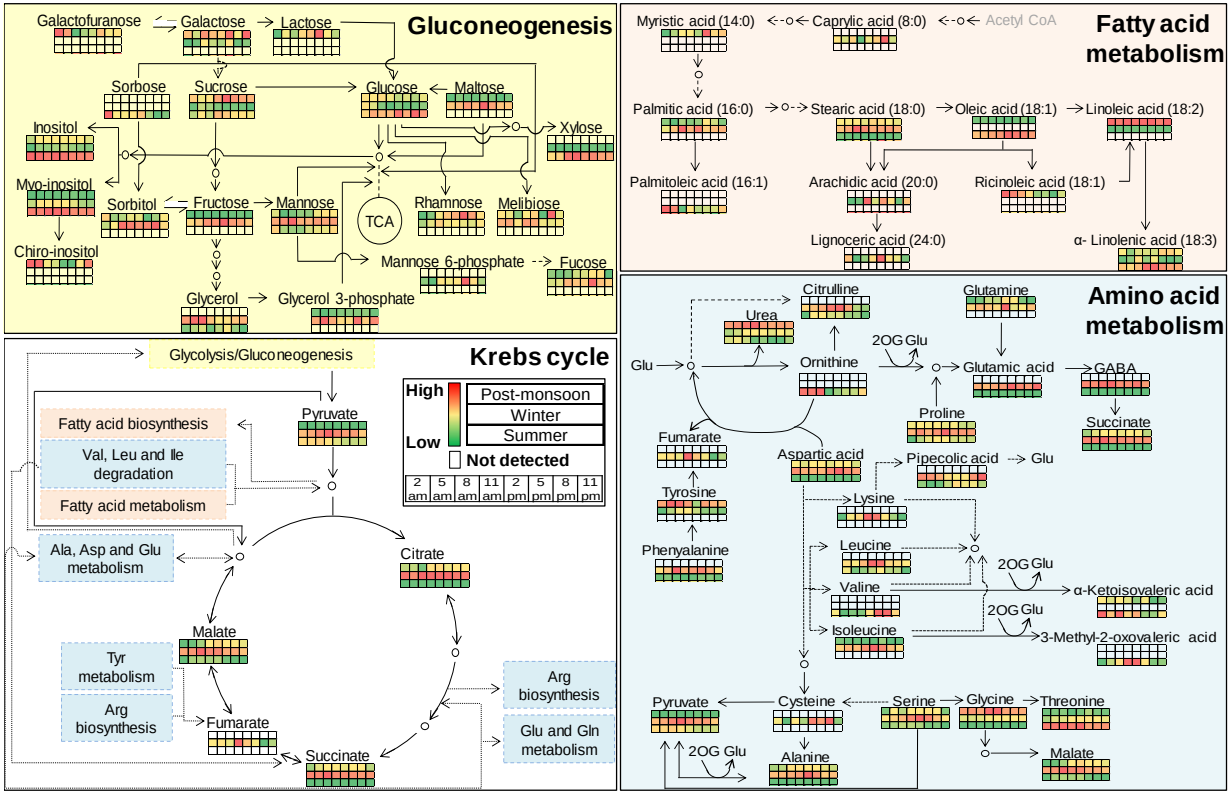

Figure 5.9: Pathway mapping for the leaves of *S. fruticosa*. Each of the pathways are mapped separately in a color box wherein; the yellow box shows the pathway for gluconeogenesis, pink for fatty acid and blue for amino acid. Accumulation of the metabolites for each time point as well as seasons is represented in heatmap. The color code for each metabolite shown in the heat map represents: red is for high (100%), yellow for medium (50%) and green for the lowest values (1%). The relative abundance of each metabolite was first normalized (individually for each metabolite) to bring the value of the parameters in the range of 1-100 to provide an unbiased color code. To know the exact amount of each metabolite accumulated, please refer to Table 5.1-5.3. The blank box, without any color code, represents non-detected metabolites for the particular time point and/or season

Of the 67 sugar compounds and its derivatives that were identified in all the seasons of our study, 20 metabolites that are involved in sugar metabolisms were considered in the map. Metabolites such as lactose (abundant during post-monsoon at 17:00 hours), sorbose (abundant during winter at 02:00 hours), chiro-inositol (abundant during post-monsoon between 23:00 to 05:00 hours) and mannose 6-phosphate (abundant during winter at 17:00 hours) were detected only during one of the seasons. Whereas, sucrose, glucose, myo-inositol, inositol, mannose, and melibiose were detected in all the seasons.

Similarly, pathway map for the 11 saturated and unsaturated fatty acids out of the 16 detected were analyzed. Of which, myristic acid (abundant during post-monsoon at 20:00 hours), caprylic acid (abundant during winter at 20:00 hours), palmitoleic acid (abundant during summer at 02:00 hours), eicosanoic acid (abundant during winter at 08:00 hours), ricinoleic acid (abundant during post-monsoon at 02:00 hours) and lignoceric acid (abundant during winter at 23:00 hours) were detected only in one of the seasons. Whereas stearic acid and α-linolenic acid were detected in all the seasons. Likewise, of the 32 amino acids and its derivatives detected, metabolic pathway map for the 18 metabolites wasanalyzed. Along with amino acids, some other compounds such as urea, pyruvate, fumarate, pipecolic acid, succinate, α-ketoisovaleric acid, malate and 3-methyl-2-oxovaleric acid, which were detected during our study and are directly involved in the pathway, were also included in this map. Amino acid such as ornithine (abundant during summer between 02:00 to 08:00 hours), lysine (abundant during winter between 11:00 to 14:00 hours), valine (abundant during summer between 17:00 to 20:00 hours) and cysteine (abundant during winter between 17:00 to 20:00 hours) were detected only during one of the seasons. However, aspartic acid, proline, serine, glycine, threonine, and alanine were detected in tissues harvested during all the seasons.

5.4. Discussion

5.4.1. The changing physical parameters have a direct impact on the morphology of S. fruticosa

Plants are subjected to several combinations of both biotic and abiotic stresses which lead to molecular and physiological impairment (Rejeb et al., 2014, Nongpiur et al., 2016, Wungrampha et al., 2018, Fujita et al., 2006, Suzuki et al., 2014). Among the abiotic stresses, salinity causes ionic as well as osmotic stress which leads to physiological drought (Munns, 2002, Munns & Tester, 2008, Mahajan & Tuteja, 2005), reduction in photosynthetic efficiency (Wungrampha et al., 2018) and disruption of minerals uptake by plants (Grattan & Grieve, 1998). On the other hand, high temperature causes reduction in photosynthesis by hindering CO_2 uptake (Weis & Berry, 1998), injury to the thylakoid and impairment of electron transport chain (Wise et al., 2004), plant sterility (Satake & Yoshida, 1978) and makes plants more susceptible to biotic stress (Kassanis, 1952). Similarly, cold stress affects the normal growth and development of plants by inhibiting the full expression of its genetic makeup and also inhibit the metabolic reactions (Chinnusamy et al., 2007). However, a number of plants exist, referred to as xero-halophytes, that can tolerate high salinity as well as temperature (Wungrampha et al., 2018). To shed light on the underlying mechanism of how these plants adapt themselves to such harsh conditions, we carried out an unsupervised metaboprofiling analysis of a xero-halophyte species *S. fruticosa* growing naturally on the bank of the salt extraction site in Sambhar Salt Lake, Rajasthan, India.

Summer, with high temperature (reaching up to ~50^{o}C), is predominant at the study site. pH and salinity (~10 and 65dS/m) respectively of the soil are also high throughout the year (as mentioned in Chapter 3). Even though salinity and pH are lowest during the post-monsoon season, it still is very high for any glycophytes to grow. Therefore, plants growing in this area faced a combination of two significant abiotic stresses throughout the year. During summer, *S.*

fruticosa is exposed to high salinity, alkaline soil, and high temperature. During winter, these plants are exposed to cold temperature in addition to high salinity and alkaline soil. Although the temperature is high and soil is alkaline, salinity is relatively lesser during the post-monsoon season.

The combination of the three physical factors, as mentioned above, leads to a direct impact on the floral habitat of the study area. Krishna et al. (2014) listed six halophytes species *Sporobolus virginicus, Eleusine compressa, Cressa cretica, Aeluropus lagopoides* and *Suaeda fruticosa* inhabiting the saline grassland of Sambhar Lake. During our study, we found that not all the halophytes could last to survive all the seasons apart from *S. fruticosa*. The representative life cycle of *S. fruticosa* is given in Chapter 3 Figure. 3.9. The rainwater dilutes the excess salt during the monsoon which allows the dispersed seeds to germinate. By the month of July and September, the plants became mature and began to flower. As winter sets in, the water level declines and salinity increases, by then, the seeds are mature and are ready for dispersal. The plants also lose its greenery and develop succulent reddish leaves. Seeds dispersed during this season remain dormant until monsoon. By summer, almost all the seeds gets dispersed and the plant also undergo several modes of adaptation as described in the earlier chapters. The plants also develop highly succulent leaves and gradually undergo senescence and completes its life cycle. Khan et al. (2000) also observed the same phenomenon wherein *S. fruticosa* under salinity developed succulent leaves and have higher dry and fresh weight.

Plants undergo morphological and anatomical changes in response to abiotic stress (Patakas, 2012). This, in turn, can reduce plant growth. Likewise, histology and SEM images revealed dramatic changes in the morphology and anatomy of the *S. fruticosa* leaf across the three seasons. We observed that during the post-monsoon season, where conditions are more favorable, leaves are larger, and are made up of a multi-layered hypodermis. During summer, where both temperature and salinity are high, leaves become smaller in size and

are more succulent. Remarkably, the hypodermis showed a reduction in the number of cell layers. In a number of plant species such as tobacco, rapeseed, and grapes, growth inhibition as a result of abiotic stress was shown to be associated with a lower accumulation of sugars and fatty acids (Cramer at al., (2011) and references therein). This appears to be the case with *S. fruticosa* also, as discussed below. But unlike these plants, amino acid accumulation in the leaves of *S. fruticosa* is not affected by high temperature and salinity. Thus, tolerance to abiotic stress in *S. fruticosa* manifested as significant changes in the structure and anatomy of the leaves is associated with a reduced accumulation of sugars and fatty acids.

5.4.2. Metabolic profile of S. fruticosa is regulated diurnally as well as seasonally

In recent years, several work related to the understanding of changes in seasonal metabolite fingerprinting of plants growing naturally as well as in control environment have been reported (Rivas-Ubach et al., 2012, Kutyshenko et al., 2015, Falasca et al., 2013, Scognamiglio et al., 2014, Liu et al., 2016, Freitas et al., 2018, Kim et al., 2011, Ahuja et al., 2010, Bundy et al., 2008). In *S. fruticosa*, we identified 222 metabolites from the three seasons accumulating during various time points regulated diurnally during three seasons. However, most of the metabolites detected were exclusive to either one of the seasons.

Pie charts of the identified metabolites arranged according to their chemical properties show a majority of them belonging to organic acid, organic compound, sugar, fatty acid, and amino acids. However, some unique compounds such as geraniol, stigmasterol, matairesinol, and anthracene belonging to terpenoid, steroid, lignan and aromatic hydrocarbon, respectively, were found to be present only in one of the seasons (Table - 5.1-5.3). Sorting out the metabolites according to their chemical properties, provides an insightful relation with the metabolic pathway map. Total organic compounds and acids detected in all the seasons did not alter significantly. However, significant changes in total amino acids, fatty acids, and sugars were observed across the

seasons. Overall levels of sugars decreased drastically during winter and summer; however, some sugars like sucrose were seen to increase during winter and summer. This could be due to the severe decline in photosynthetic activity of the plant under such harsh environmental stress conditions (Bose et al., 2017, Wungrampha et al., 2018, Becker et al., 2017, Bose et al., 2014, Lakra et al., 2017, Munns & Tester, 2008). However, amino acids were seen to increase significantly. This may be due to nutrient recycling of the proteins and other cell organelles degradation to provide a substrate for amino acids catabolism as an adaptive mechanism (Hirota et al., 2018). It is known that under severe stress, especially drought, plants undergo senescence either due to dis-functioning of water transport (hydraulic failure) or carbon starvation (Saiki et al., 2017). During such stressful conditions, plants recycle the available nutrient by degrading the long-lived proteins, lipids, chlorophyll, and other organelles through autophagy (Díaz-Troya et al., 2008, Xiong et al., 2005), proteasomal degradation(Wang et al., 2009, Moon et al., 2004) and Target of Rapamycin (TOR) nutrient sensing pathway (Loewith & Hall, 2011, Levine & Klionsky, 2004, Araujo et al., 2011). The degraded cellular components such as protein, lipids, and other organelles are then released in the form of metabolites that are further transported for use in other parts of the plant (Araujo et al., 2011, Hirota et al., 2018). Cuin and Shabala (2007) also found that, under salinity, plants maintain a high concentration of amino acids, which not only help as an osmoprotectant but also in maintaining optimum K^+/Na^+ ratio inside the plasma membrane.

5.4.3. Metabolites accumulating at the specific time points of the day as well as during particular seasons contribute to the adaptation in S. fruticosa

Healthier and younger plants growing during the post-monsoon season show an overall accumulation of every type of metabolites. However, unlike the other two seasons, specific metabolites that are richly and exclusively accumulating during this season were not observed (Table 5.1-5.3). During this season, among the fatty acids identified, palmitic acid and α-linolenic acid were seen to accumulate

most abundantly, of which palmitic acid was seen to accumulate sufficiently between 17:00 to 20:00 hours. Diurnal variations of the other fatty acids identified were not observed. Larkindale and Huang (2004) found that the level of saturated lipids such as palmitic acid and linolenic acid decreases but linoleic acid accumulates abundantly in bentgrass (*Agrostis stolonifera*) under high temperature stress. However, in *S. fruticosa*, palmitic acid and α-linolenic acid was found to accumulate abundantly during post-monsoon even though the atmospheric temperature was high. In addition, high level of linoleic acid was also seen to accumulate during this season. Likewise, of the 12 amino acids identified in this season, L-tyrosine, L-alanine and N, N-dimethylglycine were seen to show diurnal variation. L-tyrosine was seen to accumulate highest during the early hours of the day, i.e. between 05:00 to 08:00 hours. L-alanine was seen highest during 08:00 and 11:00 hours. N, N-dimethylglycine, an intermediate product for the synthesis of glycine betaine served as an excellent reliever for *Bacillus subtilis* under heat stress (Bashir et al., 2014). In *S. fruticosa*, during post-monsoon as the temperature is high, among the amino acids, N, N-dimethylglycine was observed to accumulate most abundantly. In addition, N, N-dimethylglycine was seen highest during 11:00 and 14:00 hours when the temperature was maximum.

Apart from L-chiro-inositol, which shows maximum accumulation during 05:00 hours, the rest of the three polyols, namely glycerol-3-phosphate, inositol, and myo-inositol were seen to accumulate mostly between 08:00 to 20:00 hours. Likewise, among the organic acids and organic compounds, propylene glycol, urea, lactic acid, oxalic acid, citric acid, succinic acid, and L-tartaric acid were found to be most abundant. Almost all the 42 metabolites of organic acids and compounds detected show the diurnal rhythm. However, no significant variations were seen in ferulic acid, formic acid, gluconic acid, mesaconic acid, oxalic acid, α-ketoisovaleric acid, 1,3 propanediol, ethylene glycol, and neophytadiene. Dopamine, which helps plants by alleviating photosynthetic activity and nutrient uptake under salinity and nutrient stress (Liang et al., 2017, Li et al., 2015), were

seen to be accumulated abundantly. However, not much of the diurnal variation was observed. Sucrose, the most abundantly accumulated metabolite for the season is found highest during day time, specifically at 14:00 hours. As night sets in, the level decreases gradually. By 17:00 hours in the morning, the level has reduced to roughly 50% from that during 14:00 hours (Table 5.1-5.3).

During winter, amino acids and fatty acids account for 22%, and 12% of the total metabolites identified, respectively. The relative amount of most of the amino acids accumulated in this season is much higher than that from the two seasons. Amino acids such as L-proline, L-threonine, L-aspartic acid, L-alanine, and L-serine that were found common in all the seasons show maximum accumulation during winter. Almost all the amino acids identified in this season show diurnal rhythm; however, no significant variation was seen for homocysteine, L-cysteine, L-norleucine, L-threonine, and N-acetylglutamine. Citrulline, an amino acid that contributes to plant tolerance for salinity and drought (Kusvuran et al., 2013) was found most abundant in this season at the time point between 05:00 to 17:00 hours. Amino acids related to cold acclimatization for plants such as L-proline, L-serine, glutamine, and L- glutamic acid (Draper, 1972) were also seen highly accumulating throughout the day.

In both prokaryotes as well as eukaryotes, cold stress induce the accumulation of both saturated and unsaturated fatty acids for cold shock tolerance (Thieringer et al., 1998; Phadtare et al., 1999; Ozheredova et al., 2015). Similarly, in *Suaeda fruticosa*, both saturated and unsaturated fatty acids were found to accumulate abundantly during winter. Transgenic lines of wheat carrying BADH gene shows an increase accumulation of linoleic and α-linolenic acid which gives membrane stability during cold stress (Zhang et al., 2010). Similarly, of all the fatty acids identified, three of the unsaturated fatty acids 2-monolinolenin, linoleic acid, and α-linolenic acid and three long chain saturated fatty acids such as palmitic acid, α-hydroxylignoceric acid, and lignoceric acid were found abundant in this season. However, significant diurnal variations of all

the 12 fatty acids identified in this season were not observed. Increase in accumulation of organic acid and organic compounds (solutes) under hypersaline (Edwards et al., 1987), cold stress (Hennion and Bouchereau, 1998) has been reported in both prokaryotes and eukaryotes. Organic acid and organic compound correspond to 39% of the total metabolites identified during winter. Compounds such as citric acid, ferulic acid, glucaric acid, malic acid, oxalic acid, pyruvic acid, succinic acid, β-phenyllactic acid, diethylene glycol, and dopamine were found highly accumulated during this season. Apart from fumaric acid, isoferulic acid, lactic acid, malonic acid, tartaric acid, α-hydroxyglutaric acid, β-lactic acid, 1,3 propanediol, ethanolamine, p-coumaric acid and urea, all other organic metabolites identified in this season show significant diurnal rhythm. Some organic compounds such as citric acid, pyruvic acid, malic acid, and diethylene glycol were seen to accumulate mostly between 08:00 to 17:00 hours whereas, α-hydroxyglutaric acid, succinic acid, isoferulic acid, and glucaric acid were found to accumulate more between 20:00 hours to 05:00 hours.

In *Pringlea antiscorbutica*, under salinity and permanent cold stress, high amount of soluble carbohydrates and sugar molecules were seen to accumulate along with proline for its tolerance (Hennion and Bouchereau 1998). In S. fruticosa, sugar molecules such as sucrose, D-turanose, hexopyranose, L-fructose, α-D-glucopyranose, glyceric acid, galactitol, and D-glucose were found abundantly accumulated during winter. Almost all the sugars and its molecules show diurnal rhythmic change, of which α-D-glucopyranose, L-fructose, D-glucitol, hexopyranose, α-ketoglutaric acid, glyceric acid, L-erythrulose, and few others show significant accumulation between 08:00 to 17:00 hours. However soluble sugars such as D-glucose, α-D-glucopyranoside, β-L-arabinopyranose, and methylmalonic acid were found mostly between 20:00 to 05:00 hours as the temperature is minimum. The accumulation for which are also known for cold tolerance in plants such as *Curly kale* (Steindal et al., 2015), tomato (Hu et al., 2015) and Litopenaeus vannamei (Fan et al., 2016). Sugars such as rhamnose, melibiose, and mannose-6-phosphate did not show diurnal rhythmic change.

Like those of the susceptible chickpea (Pusa256 and Pusa 261) under high temperature leading to the reduction of total sugars (Arunkumar et al., 2012), during summer, total sugars and fatty acids detected reduces in *S. fruticosa* as compared to post-monsoon and winter, respectively. On the contrary, total amino acids increase during the combination of salinity and high temperature (summer) in *S. fruticosa* like that of OsMYB55 gene overexpressed rice transgenic plants which shows higher amino acid biosynthesis during high temperature (El-Kereamy et al., 2012). Among the amino acids identified during summer, L-threonine was found to be most abundant. Kaplan and Guy (2004) reported that, Arabidopsis under heat shock leads to the increase in the pool size of amino acids such as threonine, alanine and valine. Apart from N-acetyl glutamine, L-aspartic acid, penicillamine, pyroglutamic acid, and γ-aminobutyric acid, all the amino acids identified showed the significant diurnal rhythm. Two of the amino acids, L-valine, and ornithine that was detected exclusively during summer were found to accumulate mostly between 05:00 to 17:00 hours. Others like citrulline, L-alanine, glycine, L-glutamic acid, L-proline, L-leucine and L-serine were found to accumulate abundantly between 08:00 to 17:00 hours when the average atmospheric temperature reaches to nearly 45° C. Significant roles of glycine amino acid (Ashraf and Foolad, 2007; Bita and Gerats, 2013) which accumulation in plants leading to stress tolerance has been reported in several plants.

Fatty acids composition during summer is relatively the least in our study. Hugly and Somerville (1992) showed that plants acclimatized to warmer environments by decreasing the membrane lipid unsaturation level. Likewise, in our present study, only six fatty acids were detected in this season. Of the six fatty acids identified, three were poly-unsaturated fatty acids (PUFA), which are abundantly accumulated. α-Linolenic acid, the most abundant among the PUFA's identified, that is known to have a significant role in both biotic and abiotic stress tolerance (Upchurch, 2008, Wasternack, 2007) was found to be most abundant between 11:00 to 17:00 hours. Similarly, oleic acid was also found abundant

between 11:00 to 17:00 hours. However, a reverse pattern was seen with palmitoleic acid, which showed maximum accumulation between 23:00 to 05:00 hours. 11-Eicosenoic acid, a saturated fatty acid was detected only after 11:00 hours and attained its maximum at 14:00 hours, after which its accumulation declined gradually till 11 pm. No 11-eicosenoic acid was detected between 02:00 to 08:00 hours. However, α-glyceryl palmitate and stearic acids were seen to accumulate more between 23:00 to 05:00 hours. Almost all the organic acids and compounds detected in this season show diurnal rhythm. However, compounds such as butyric acid, citric acid, glycolic acid, β-hydroxypyruvic acid, succinic acid, D-gluconic acid, D-ribonic acid, isothiocyanic acid, dopamine, and triethanolamine did not show significant diurnal change. Among the organic compounds and acids detected, dopamine, alloxanic acid, glucaric acid, L-tartaric acid, malic acid, and pyruvic acid were found to accumulate abundantly. Some of the compounds such as 3-Methyl-2-oxovaleric acid, 3,4-Dihydroxymandelic acid, malonic acid, malic acid, maleic acid, allyl glycol, aminothiadiazole, carbitol acetate, levoglucosan, pyrazine, and pyrrolidine were seen to accumulate abundantly between 08:00 to 17:00 hours when the temperature is maximum. However, compounds like pyruvic acid, oxalic acid, d-gluconic acid, and 3-Aminobutyric acid were seen to accumulate more between 23:00 to 05:00 hours when the temperature falls in the night. 2-Ketohexanoic acid is detected only between 05:00 to 14:00 hours. Similarly, shikimic acid and pyrazine are detected only between 02:00 to 14:00 hours and 05:00 to 14:00 hours, respectively.

RFO (raffinose family oligosaccharides) which helps in conferring to abiotic stress such as salinity and high temperature in Arabidopsis are synthesized from sucrose and myo-inositol (El-Sayed et al., 2014). Accumulation of sucrose and myo-inositol independently also help plants in conferring to high temperature and salinity stress (Nuccio et al., 1999; Majee et al., 2004; Joshi et al., 2013). In *S. fruticosa*, polyols such as myo-inositol, inositol, and glycerol were detected abundantly during summer. The significant diurnal rhythm was not observed in inositol and glycerol, whereas, myo-inositol showed a substantial

increase during the day time between 08:00 to 14:00 hours. Almost all the sugars and its derivatives were seen to decline during summer. Among the sugar, D-turanose, D-glucose, and sucrose were observed to accumulate most abundantly. Sucrose, like the two seasons, accumulate mostly between 11:00 to 20:00 hours; however, D-turanose accumulate more during the night between 23:00 to 02:00 hours. D-glucose was seen to accumulate mostly afternoon till late evening, i.e. between 14:00 to 23:00 hours.

5.4.4. Seasonal and diurnal metabolite distribution helps S. fruticosa to combat diverse stresses

Several metabolites detected in the present study that showed diurnal, as well as seasonal variations, point to a significant correlation to the adaptation of *S. fruticosa* under different environmental stresses. As mentioned earlier, plants growing in this area faced a severe combination of abiotic stresses throughout the year. Several metabolites such as myo-inositol (Borges et al., 2006), inositol, valine (Qi et al., 2017), proline (Bates et al., 1973), sucrose (Suzuki et al., 2014), glycerol 3-phosphate (Zandalinas et al., 2016), glycine (Ashraf & Foolad, 2007), ornithine (Kalamaki et al., 2009) and polyols (Bohnert et al., 1995) that confer stress tolerance to plants have been characterised earlier. Similarly, in the present study, all the metabolites mentioned above were detected significantly.

However, unlike most plants, *S. fruticosa* was found to accumulate proline as one of the osmolytes during winter, but, under the combination of heat and salinity (physiological drought), i.e. during summer and post-monsoon, sucrose is accumulated more than proline. In both the seasons, the maximum level of sucrose was seen during the noontime (between 11:00 to 14:00 hours) when the temperature is highest. Accumulation of osmolytes such as sucrose, rather than proline, is known to help the plant from hyper reaction and mitochondrial susceptible due to proline toxicity and accumulation of pyrroline-5-carboxylate under the combination of high temperature and salinity (Rizhsky et al., 2004, Suzuki et al., 2014). Similarly, glucose, α-ketoisovaleric acid, oleic acid, and

inositol were also seen to accumulate abundantly during the combination of salinity and heat as compared to salinity alone (winter).

However, metabolites such as myo-inositol, xylose, glycerol, leucine, pyruvate, threonine, pipecolic acid, glutamic acid, GABA (γ-aminobutyric acid), citrulline and glutamine were seen to accumulate more under the influence of salinity and drought (winter and summer). Citrulline is known to accumulate under salinity and severe drought in plants such as watermelon, which in turn confers tolerance to both stresses (Kusvuran et al., 2013). Accumulation of this amino acid in *S. fruticosa* during winter and summer when drought and salinity are maximum might also contribute to its tolerance. Obata et al. (2015) also found that in maize, myo-inositol and threonine showed maximum accumulation under drought and combination of heat and drought stress as compared to heat stress alone. The same pattern of accumulation was also seen in *S. fruticosa*.

GABA, a non-protein amino acid, is known to accumulate abundantly under severe biotic as well as abiotic stresses, which confer to its tolerance (Ramesh et al., 2015). It is also known to regulate osmotic as well as pH of the plants under long and short salinity stress (Akçay et al., 2012). Additionally, it is known to stimulate the growth of the pollen tube and guide the pollen to the ovary for fertilization (Palanivelu et al., 2003). In the present study, GABA is seen to accumulate abundantly during winter and summer when salinity is highest. Between the two seasons, it is found to accumulate more during winter. This could be due to the flowering stage of *S. fruticosa* that falls between early and late winter, i.e. October to February (http://flora.org.il/en/plants/SUAFRU/) and during which salinity is also high.

Some sugar metabolites and their derivative such as galactofuranose, lactose and chiro-inositol were seen to accumulate only under the influence of high temperature (post-monsoon) but not during severe salinity stress (winter) or its combination (summer). These metabolites were also seen abundant towards evening or early morning, i.e. between 17:00 to 05:00 hours. Metabolites such as

cysteine, lysine, fumarate, and mannose 6- phosphate were seen to be induced only during cold and salinity stress. Whereas, sorbose, valine, ornithine, and 3-methyl 2-oxovaleric acid were seen to be induced only during the combination of high temperature and salinity stress.

Accumulation of valine and ornithine was found to be detrimental in barley as these metabolites disturb K+/Na+ ratio (Cuin & Shabala, 2007). However, *S. fruticosa* is a halophyte which sequesters Na+ and Cl-ions (a typical includer) in its leaf tissues (Labidi et al., 2010) which helps in maintaining lower water potential as to the soil for water absorption (Koyro et al., 2011). Secondly, the accumulation of valine and ornithine helps in leaf turgidity during stress, which helps in tolerance (Zandalinas et al., 2018). Therefore, the accumulation of these two metabolites was not seen to be detrimental, but beneficial to *S. fruticosa*.

5.4.5. Unique diurnal distribution pattern of metabolites during winter reveals the minimum threshold temperature for cold acclimatization in S. fruticosa

Unlike other seasons, i.e., summer and post-monsoon, cold, salinity, and high soil pH are the significant factors that the plants faced during winter (Chapter 3). Even though, winter in this region might be very short (mid-November to mid-February, during this season the temperature can drop to as low as 5°C during the night and have an average temperature of 12.96°C during the day (Chapter 3). During summer and post-monsoon seasons, the average temperature recorded during the day was around 37^{o}C and 31^{o}C respectively, which is about 20 to 25 degrees above that during winter. This temperature variation reflects a significant change in the pattern of metabolites accumulated during this season.

PCA clustering of the metabolites obtained from different time points of this season showed maximum grouping as well as scattering unlike those in summer and post-monsoon which follow a particular cyclic pattern. Three distinct groups obtained from the variants were seen in the PCA during this season. Metabolites from; i) 20:00 hours are grouped uniquely at positive X and negative

Y-axis, ii) 23:00 to 05:00 hours were grouped in the negative X and Y-axis, and iii) 08:00 to 17:00 hours were grouped in positive X and Y axis. The three groups directly correlate with the change in atmospheric temperature. As discussed in the earlier section, between 11:00 to 20:00 hours the temperature is above 20^{o}C, after which, from 20:00 hours, the temperature quickly dropped to below average. This transition point from above 20 to below 20^{o}C happens at 20:00 hours. And it is during this transition that the metabolites detected occupy the first cluster in the PCA. After 20:00 till 05:00 hours when the temperature is below 20^{o}C, the metabolite cluster grouped showing a common response for cold stress, this is the second cluster. After 05:00 hours, i.e., from 08:00 hours as the temperature rise to above 20^{o}C, the cluster re-grouped to form the third cluster. This shows that 20^{o} Celsius is the minimum threshold temperature after which the accumulation of cold-responsive metabolites in *S. fruticosa* began. Additionally, this also shows that cold stress plays an essential limiting factor in the molecular adaptation of *S. fruticosa*.

Apart from amino acids, as discussed in the earlier section, saturated and unsaturated fatty acids were seen to accumulate mostly during winter (Figure. 5.5). Strong association of lipids and fatty acids in the plasma membrane for cold acclimatization in plants have been studied in details by several scientist (Hugly & Somerville, 1992, Vega et al., 2004, Lynch & Steponkus, 1987, Nishida & Murata, 1996, Novitskaya et al., 2000, Cruz et al., 2010). In the present study; out of the total 16 fatty acids identified, 12 of them were present during winter. Of the 12 metabolites, 2-monolinolenin, arachidic acid, caprylic acid, heptadecanoic acid, lignoceric acid, and α-hydroxylignoceric acid were detected only during this season. Caprylic acid (8:0), a short chain saturated fatty acid with 8 carbon chain is an early intermediate product in the biosynthesis of fatty acid (Mikolajczyk & Brody, 1990). In *Pseudoalteromonas haloplanktis*, under cold shock, the supply of caprylic acid shows a higher flux of reaction for the biosynthesis of fatty acid (Mocali et al., 2017). In the present study, caprylic acid was detected most abundantly at 20:00 hours during winter (Figure. 8). This further adds to the cold

threshold point for *S. fruticosa* to be 20°C and the preparedness for the cold acclimatization.

5.5. Conclusions

In the present work, we studied the morphological as well as molecular changes through unsupervised metabo-profiling to decipher the adaptations in *S. fruticosa* under harsh environmental conditions. *S. fruticosa* growing naturally at Sambhar Salt Lake wherein, the salinity reaches up to 60 dSm^{-1}, pH up to 9.8, temperature up to 49^{o}C during summer and as cold as 5^{o}C during winter was studied.

The amino acid, sugar, and fatty acids are three groups of metabolites that are found to vary mostly due to season. The sugar level is seen highest during post-monsoon and winter, however, during summer, the concentration decreased drastically. This could be due to a reduction in the photosynthesis of the plant to reduce water loss during high temperature and highly saline condition. Amino acid during winter and summer were seen highest. This could be one of the ways in which *S. fruticosa* adapts the harsh climate through nutrient recycle of the long-lived proteins, lipids, chlorophyll and other organelles (Díaz-Troya et al., 2008, Xiong et al., 2005, Wang et al., 2009, Moon et al., 2004, Loewith & Hall, 2011). Plants maintaining a high concentration of amino acids not only help as osmoprotectant but also in maintaining optimum K+/Na+ ratio inside the plasma membrane (Cuin & Shabala, 2007). Maximum of the fatty acids were identified during winter which helps in membrane stability and tolerance against cold stress (Hugly & Somerville, 1992, Vega et al., 2004, Lynch & Steponkus, 1987, Nishida & Murata, 1996, Novitskaya et al., 2000, Cruz et al., 2010).Some metabolites such as; sucrose, proline, GABA, myo-inositol, inositol, valine, ornithine, caprylic acid and citrulline were seen to accumulate differentially thought-out the seasons as well as diurnally that confers to tolerance.

From our study, we found that *S. fruticosa* can tolerate temperature up to 49°C and salinity up to 60 dSm-1 and still follow the normal diurnal rhythm.

However, under cold and salinity, the cyclic pattern of the diurnal rhythm is disturbed. We further found that the minimum threshold for cold acclimatization is 20^{o}C below which, cold responsive metabolites began to accumulate and change the pattern of the metabolome.

Chapter 6

Diurnal regulation of proteome in leaves of *S. fruticosa* as influenced by seasonal variations

6.1 Introduction

Being sessile, plants are often exposed to multiple stresses (combined as well as sequential) as they grow in their natural habitat (Shaar-Moshe et al., 2017; Wungrampha et al., 2019). Among the stresses, salinity is one of the major abiotic stress that has led to the significant degradation of arable land (Munn and Gilliham, 2015). Losses due to salinity both in terms of economic and agriculture sectors, has been reported by organizations such as FAO (Vargas et al., 2018), UN (Qadir et al., 2014) and other government agencies such as Agriculture Victoria, Australia (Muller and Hocking, 2002; http://vro.agriculture.vic.gov.au) and ICAR, India (Sharma and Anshuman 2015; https://krishi.icar.gov.in). Salinity affects the plant in two ways; first, the sudden osmotic stress followed by ionic stress which leads to severe physiological and molecular imbalances that further disturb the process of germination, photosynthesis, respiration and ultimately causes senescence (Purty et al., 2008; Kumari et al., 2009; Das et al., 2015; Joshi et al., 2016; Nongpiur et al., 2016). Several reports on salinity leading to crop loest and reduction of yields has been reported over the years (Khan et al., 2000; Munns, 2002; Koyro et al., 2011). Amidst all the cause and effect of salinity on plants being known, one need to venture on plants/crops that can tolerate saline environment as saline soil are considered potentially irreversible (Mounzer et al., 2013; Peterson and Murphy, 2015).

Based on their ability to adapt and tolerate stress, plants can broadly be classified as extremophiles and glycophytes (Flowers and Colmer, 2015). Halophytes are a group of plant species that comes under the category of extremophiles as they can complete their normal life cycle even at salinity

equivalent to sea water (Kosova et al., 2013, Sharma et al., 2016; Flowers and Colmer, 2015). Flower and Colmer (2015) highlighted the importance of halophytes in the coming generation as these group of plant species hold the future of genetic resources to develop new niche plants/crops that can potentially be used for saline agriculture. Several works on trying to understand the mode of adaptations that halophyte undergo in order to combat the harsh environment are richly available in literature (Flowers and Colmer, 2008; Amtmann, 2009; Abideen et al., 2011; Bita and Gerats, 2013). To further strengthen the knowledge of stress adaptation that halophytes undergo, several omics studies ranging from metabolomics (Scognamiglio et al., 2014: Freitas et al., 2018), transcriptomics (Zhang et al., 2014a; Diray-Arce et al., 2015; Yuan et al., 2016), genomics (Oh et al., 2010; Oh et al., 2012), ionomics (Singh et al., 2016) and proteomics (Yu et al., 2011; Yi et al., 2014) for halophytes have been done.

Proteomics is the study of large-scale proteins present in an organism which not only gives the information of the gene functions but also provides knowledge on post translational modifications (Burley et al., 1999; Tyers and Mann 2003; Tsiatsiani and Heck 2015). Factors such as stress (Kasova et al., 2018; Lakra et al., 2018; Lakra et al., 2019), heavy metals (Singh et al., 2016; Georgiadou et al., 2018), cellular and organelles development (Francoz et al., 2015; Wang et al., 2017), early and late stages of plants (Li et al., 2015) and seasons (Jespersen et al., 2015; Masi et al., 2015; Uarrota et al., 2019) can alter the proteome of an organism. Abiotic stresses such as salinity and drought impact the proteome of the plant by altering the relative abundance of stress-related proteins, remodeling the cellular localization of proteins, altering the regulations of pre and post-translational modifications, and also by hindering the protein-protein interactions as well as other protein interacting partners (Kosová et al., 2018; Lakra et al., 2018; Lakra et al., 2019). Over the years, several techniques have been developed to perform proteomics such as thin-layer chromatography (Boyle et al., 1991), 2D gel electrophoresis (Shevchenko et al., 1996; Gibson et al., 2008), two-dimensional difference gel electrophoresis

(DIGE) (Ünlü et al., 1997), iTRAQ (Shadforth et al., 2005; Aggarwal et al., 2006), LCMS (Ishihama, 2005) and SILAC (Ong et al., 2002).

Although tedious and time consuming (Shevchenko et al., 1996; Celis and Gromov, 1999), 2D-DIGE is one technique that has been used extensively by biologists as compared to that of simple 2D gel electrophoresis as, gel-gel variations that are observed in 2D gels are taken care by the addition of internal standards in 2D-DIGE. Further, addition of internal standard also improves the quantification of proteins besides helping in detection of the small proteins that are differentially expressed under stress with respect to their controls (Graves and Haystead, 2002; Diez et al., 2010). Over the years, the development of algorithm has led to significant improvement in carrying out 2D-DIGE experiments (Diez et al., 2010). 2D-DIGE is also used mostly for protein expression profiling of an organism by labeling them with fluorescent or radiolabeled isotopes (Dunn, 2000). Using 2D-DIGE, proteomics-based studies for halophytes such as *Sesuvium portulacastrum* (Yi et al., 2014), *Mesembryanthemum crystallinum* (Barkla et al., 2016), *Thellungiella salsuginea* (Vera-Estrella et al., 2014) and *Dunaliella salina* (Jia et al., 2016) have been done in recent years. These studies have broadened our understanding of stress physiology in halophytes through their proteome homeostasis. However, no work on proteomics of *S. fruticosa* has been reported till date. In the present study, we have analyzed the proteome of the leaves of *S. fruticosa* under different time points and seasons to investigate the relative expression of proteins that are regulated by diurnal and seasonal changes.

The present study is also the first seasonal comparative proteome profiling work done on *S. fruticosa* harvested from its natural habitat to analyze the diurnal pattern of protein accumulation and also study the impact of seasonal changes on the proteome. Using 2D-DIGE, we have identified 177 proteins that were differentially expressed and also showed 1.5-fold change in their abundance with respect to protein profile in tissue harvested at 8 am. Using BLAST2GO and

MAPMAN, the proteins identified were further filtered out, and the enriched peptide sequences thus obtained were subjected to gene ontology and functional enrichment analyses. Several stress-related proteins such as SNAP-25, 14-3-3 like protein, and HSP18.1 were identified to which might be contributing to the high tolerance to stresses observed in *S. fruticosa.*

6.2. Material and methods

6.2.1. Plant material and study conditions

Leaf samples of *S. fruticosa* growing naturally on the bank of the salt mining site in Sambhar Lake, Rajasthan were harvested during three seasons, i.e. post-monsoon, winter and summer with the conditions as described in chapter 2 (Figure. 2.7).

6.2.2. Protein extraction from the leaf of S. fruticosa

Protocol as described by Wu et al., (2014) was followed for extracting protein from the leaf of *S. fruticosa*. About 500 mg of leaf tissues were crushed into fine powder using mortar and pestle by continuously pouring liquid nitrogen. The crushed samples were washed with 1 ml of pre-chilled 10% (wt/vol) trichloro acidic acid (TCA) dissolved in 100% acetone for five minutes. The supernatant containing the phenols, salts and other pigments were discarded after centrifuging at 10,000 rpm for five minutes. Washing was done thrice until all the pigments were removed from the pellet. The pellet was further washed twice with 70% acetone to remove the TCA from the pellet. All washings were done in the cold room.

Following washing, 2 ml of SDS- extraction buffer containing 1% SDS, 0.15M Tris-HCl of pH 8.8, 1mM EDTA, 0.1 M DTT and 2mM PMSF- a protease inhibitor, was added to the pellet. The mixtures were kept in the shaker at room temperature for one hour. The supernatant containing the protein were further collected in an Eppendorf tube after centrifuging at 12,000 rpm for 10 minutes.

To the supernatant, an equal volume of Tris-equilibrated phenol of pH 7 was added for further washing. The two mixtures were incubated at room temperature by continuous shaking in a rocker. The upper phenolic phase obtained after centrifuging at 12,000 rpm for 15 minutes was collected in a clean Eppendorf tube and further mixed with an equal volume of wash buffer-1 which is made up of 10 mM Tris-HCL with pH 8.0, 1mM EDTA and 0.7M sucrose. After shaking the mixture for 5 minutes, the phenolic phase was collected in a clean Eppendorf tube after centrifuging at 12,000 rpm for 5 minutes. The phenolic phase obtained was further washed with wash buffer-2 containing 1% (W/V) CTAB, 10mM Tris-HCL of pH 8.0 and 0.7M of sucrose for 5 minutes and centrifuged at 12,000 rpm for five minutes. The phenolic phase containing dissolved crude protein was finally mixed with 5x volume of 0.1 M ammonium acetate dissolved in methanol and kept at -20^{o}C overnight to precipitate the protein.

6.2.3. Sample preparation for 2D gel electrophoresis and DIGE

After overnight incubation, the samples were centrifugated at 10,000 rpm for 15 minutes at 4^{o}C. The supernatant was discarded, and the protein pellet was left to dry in the laminar air flow hood. The pellet was dissolved in 200-300 µl of rehydration buffer containing 7M urea, 2M thiourea, 4% CHAPS (wt/vol),2% IPTG buffer (wt/vol), 20 mM DTT and 0.001% bromophenol blue (wt/vol) as described in Lakra et al., (2018). The suspension was further centrifuged at 12,000 rpm for 15 minutes, and the supernatant was collected in a clean Eppendorf tube for further analysis. Extracted protein was also quantified using Bradford reagent (Zor and Selinger 1996). Following quantification, about 250 µg of proteins were further subjected to 2-dimension separation wherein, the first separation happens through IEF that separates proteins according to its isoelectric point and the second through SDS-PAGE.

6.2.4. Isoelectrical focusing of the proteins

To separate the extracted protein, two-dimensional (2D) gel electrophoresis was performed as mentioned in Gyri et al., (2000). Protein of about 500 µg dissolved in rehydration buffer was loaded on the Iso-electrical focusing (IEF) strips of pH 4-7 overnight. The first-dimension separation of the protein was done according to its isoelectric point (steps for the IEF are tabulated in Table 6.1) followed by second dimension separation in 10% SDS-PAGE. The gel was further stained with Coomassie Brilliant Blue (R-250).

Table 6.1: Steps and voltage gradient for isoelectric focusing of protein in IEF strips

Steps/Gradient	Voltage	Time (V/H)	Total
24 cm strips			
Steps	100	3-6 hrs	600
Steps	500	2 hrs	1000
Steps	1000	2 hrs	2000
Gradient	5000	2 hrs	10000
Gradient	10000	5 hrs	50000
Steps	10000	2.5 hrs	25000
		Total	88600
18 cm strips			
Steps	100	3-6 hrs	600
Steps	500	2 hrs	1000
Steps	1000	2 hrs	2000
Gradient	5000	2 hrs	10000
Gradient	10000	4 hrs	40000
Steps	10000	2 hrs	20000
		Total	73600
13 cm strips			
Steps	100	3-6 hrs	600
Steps	500	2 hrs	1000
Steps	1000	2 hrs	2000
Gradient	8000	2.5 hrs	20000
Steps	8000	1 hrs	8000
		Total	31600

11 cm strips			
Steps	100	3-6 hrs	600
Steps	500	1 hr	500
Steps	1000	2 hrs	2000
Gradient	8000	2.5 hrs	20000
Steps	8000	30 min	4000
		Total	22600
7 cm strips			
Steps	100	3-6 hrs	600
Steps	500	1 hr	500
Steps	1000	2 hrs	2000
Gradient	5000	2.5 hrs	8000
Steps	5000	30 min	2500
		Total	13600

6.2.5. Labelling of protein labeling with Cy-dye for DIGE analysis

For DIGE analysis, protocols as described in Lakra et al., (2018) and Lilley and Friedman (2004) were followed. Protein samples extracted from the leaf of *S. fruticosa* harvested at 8 am of each season was taken as control, and the relative expression for each protein extracted at different time points was measured. Three Cy-dye fluorescence was used to label the protein of which, Cy3 was used to label the control sample (protein from 8 am), Cy5 the protein extracted at different time points and Cy2 to the internal control that was prepared by mixing all aliquot of all the proteins extracted at different time point i.e. 2am, 5am, 8am, 11am, 2pm, 5pm, 8pm and 11pm. For each labeling, 50µg protein were labeled with 250 pmol of Cy-dye separately for 30 minutes in a dark room. The substrate was further quenched by adding 1ml of 10mL lysine for five minutes. After quenching, Cy-labelled proteins were mixed and rehydrated on the IEF strip of pH 4-7 overnight.

Similar to 2D gel electrophoresis, the rehydrated protein sample was further separated using IEF (by following the steps given in Table 6.1) followed by SDS-PAGE separation as described earlier. All the separations were done by

maintaining minimum light (dark room) exposure. The fractionated protein on the gel was further viewed using Typhoon^{TM} 9500 gel imager (GE Healthcare) using an appropriate filter for each fluorescent labeled. The images obtained from the scanner were further analyzed using DeCyder V.7.0. Software (GE Healthcare) (Cecconi 2016).

6.2.6. Enzymatic digestion of the protein spots

Protein spots of interest were identified from the CBB labeled 2D gel electrophoresis and further digested (in-gel) using trypsinusing Matrix-assisted laser desorption/Ionization-Time of Flight (MALDI-TOF-MS) as described in Shevchenko et al., (2006). The spectrum thus obtained from the mass spectrometer were further analyzed using MASCOT (MatrixScience, www.matrixscience.com, London, UK), which is linked to the NCBI database for protein identification.

6.2.7. Statistical analysis

Statistical analysis for the identified proteins from the DIGE analysis was done using DeCyder software. For each time point, two replicates were considered. To detect the relative expression of the protein of interest, batch processing to compare and match every protein spot from all the gels (inter gel) was performed. A total of 1500 spots was programmed for co-detection from each gel by keeping a threshold variance of 1.5 folds spot volume ratio, out of which, all the artifact spots were manually discarded. After filtering, the spots were further confirmed using differential in-gel analysis (DIA) program from DeCyder software, following which, biological variance analysis (BVA) of the multiple gels were performed to identify spots that were differentially expressed at different time points. One-way ANOVA for all the protein spots identified was performed, and those protein spots that gave the statistically significant value ($P<0.05$ with 1.5-fold) change were considered for further analysis.

6.2.8. Hierarchical clustering, gene ontology search and functional enrichment analysis of proteins

Hierarchical clustering of the proteins identified at different time points from different seasons viz. post-monsoon, winter and summer was done using MeV 4.6.2. (http://mev.tm4.org/). Gene ontology and functional enrichment to cluster the protein according to its biological, cellular and molecular functions were done using BLAST2GO PRO (https://www.blast2go.com/) and MapMan (https://mapman.gabipd.org/) as described in Lakra et., (2019).

6.3. Results

As mentioned earlier, the plants of *S. fruticosa* growing in Sambhar Lake are continuously exposed to multiple stresses. During the post-monsoon season, the plants are under high-temperature stress; cold and high salinity stress during winter and high temperature and salinity stress during summer. These environmental factors have been found to affect the metabolic profile (chapter 5) as well as the physiology (chapter 4) of the plant. To further check for the changes in proteomic profile of the plant under as influenced by the above-mentioned stresses, proteomics using DIGE was performed.

Total proteins isolated from the leaves of *S. fruticosa* harvested at different points time viz. 2 am, 5 am, 8 am, 11 am, 2 pm, 5 pm, 8 pm, and 11 pm during post-monsoon, winter and summer was extracted using SDS extraction buffer (as described in material and method sections) to analyze the seasonal and diurnal regulation of proteins expression. To check the quality of protein samples 1D gel electrophoresis were analyzed before 2D gel electrophoresis (Figure. 6.1).

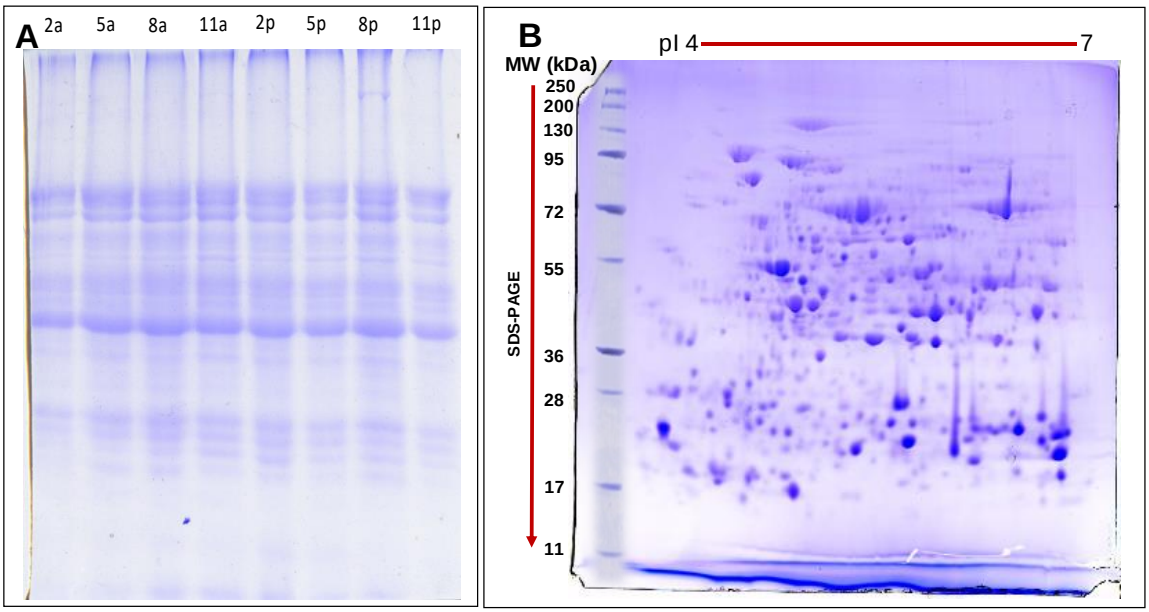

Figure 6.1: Analysis of total soluble proteins from the leaves of *S. fruticosa*. A) To check the integrity of the proteins that were extracted, 10 µg of protein samples were analyzed on 1D gel electrophoresis and stained with CBB (R-250). B) To further check the quality of protein sample about 250 µg of protein was analyzed through 2D gel electrophoresis.

As the extracted protein sample were found to be of suitably good quality, the proteins were further labeled with fluorescent dye for the DIGE analysis, keeping protein obtained for the leaves harvested at 8 am as the control sample (to calculate the relative expression). Proteins harvested at 8 am were considered as control sample because in all the seasons viz. post-monsoon, winter and summer, the temperature rise for the day began from 8 am onwards. In addition, as inferred from the detail study on photosynthesis of the plant (chapter 4), maximum photosynthesis (net photosynthesis rate) was recorded during dawn after which, the rate declined gradually until noon. With these observation in mind, we hypothesize that the plant would also be at its active state during the morning hours (8 am in our study).

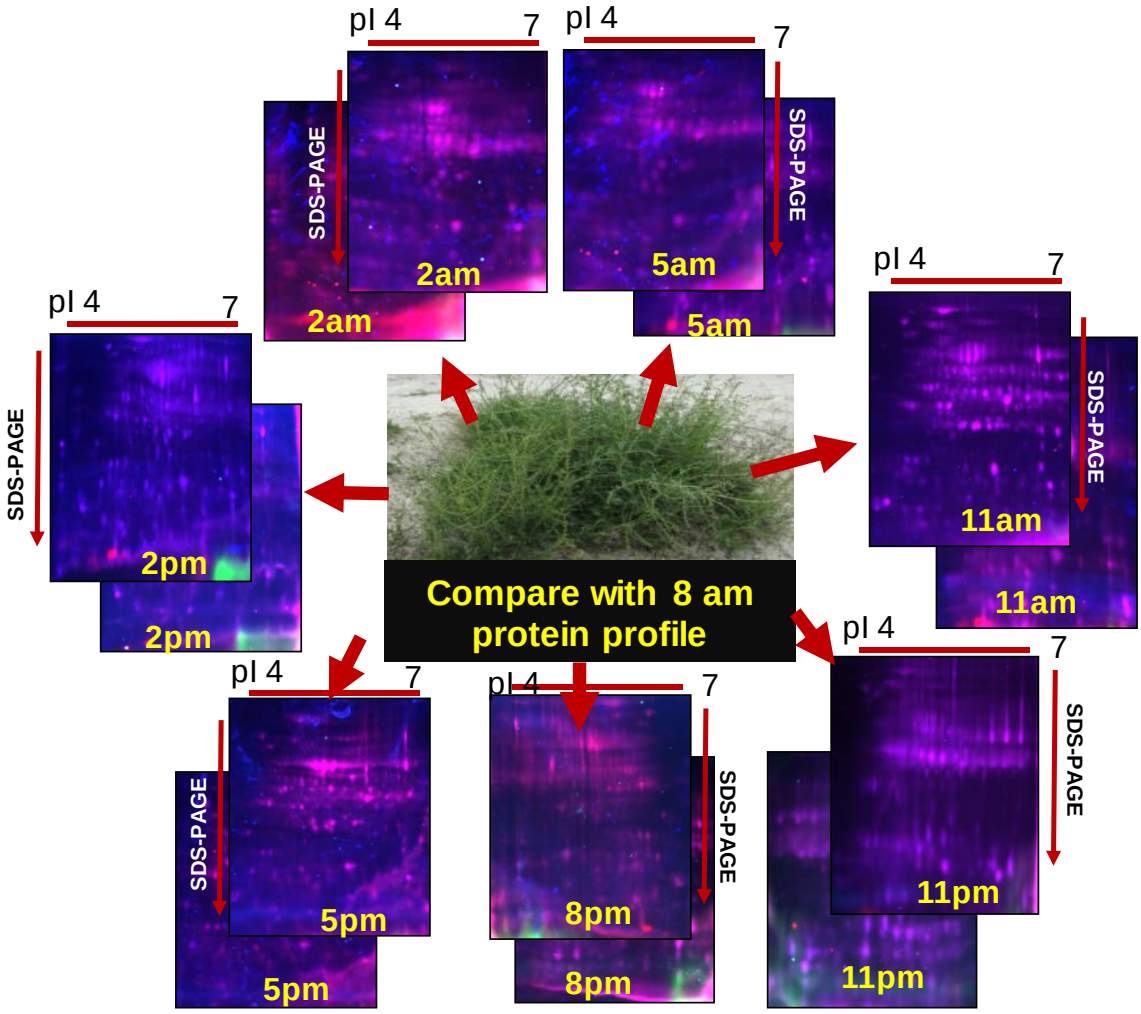

Figure 6.2: DIGE of the proteins extracted from the leaves of *S. fruticosa* harvested at different time points of day during the post-monsoon season. For each time point, two replicates each were considered for further analysis.

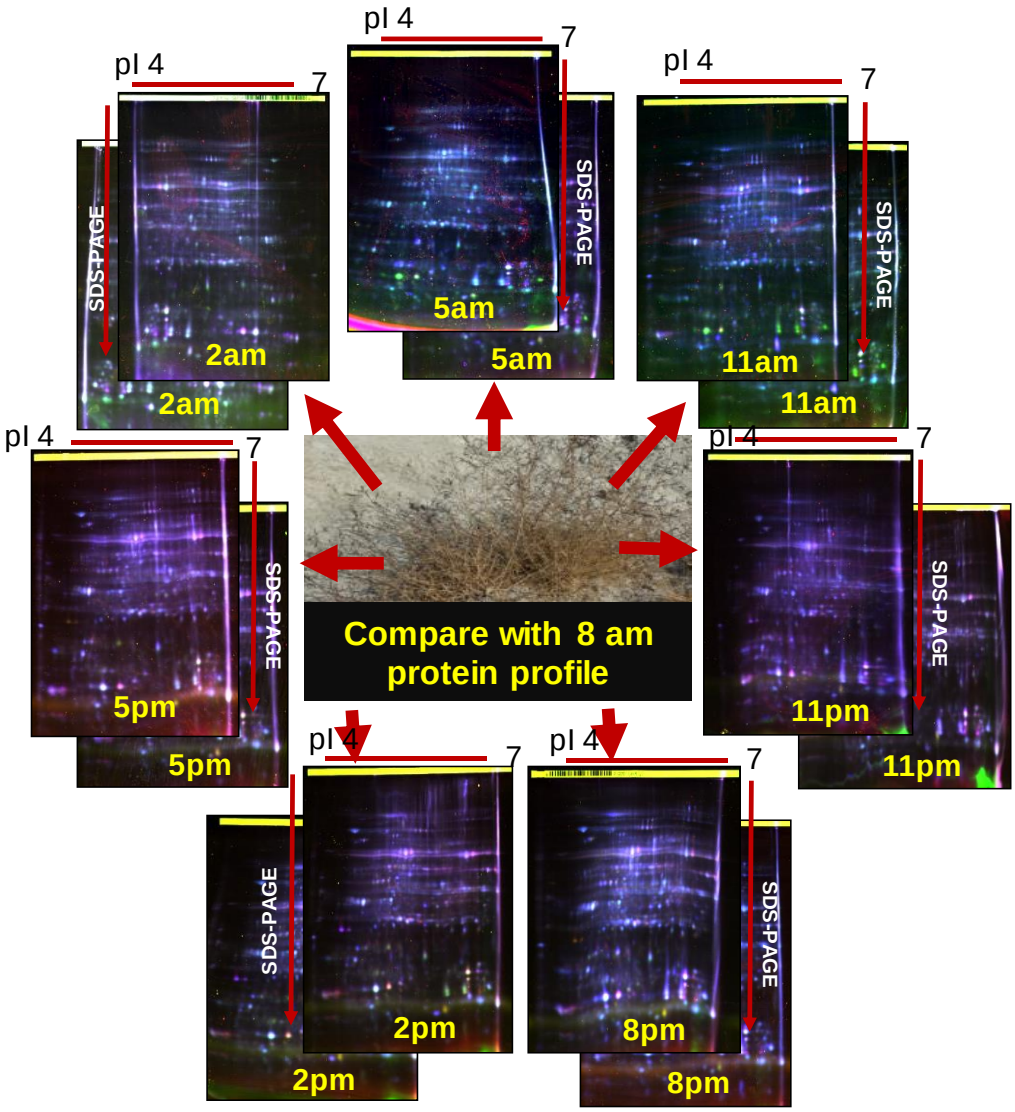

Figure 6.3: DIGE of the proteins extracted from the leaves of *S. fruticosa* harvested at different time points of day during the winter season. For each time point, two replicates each were considered for further analysis.

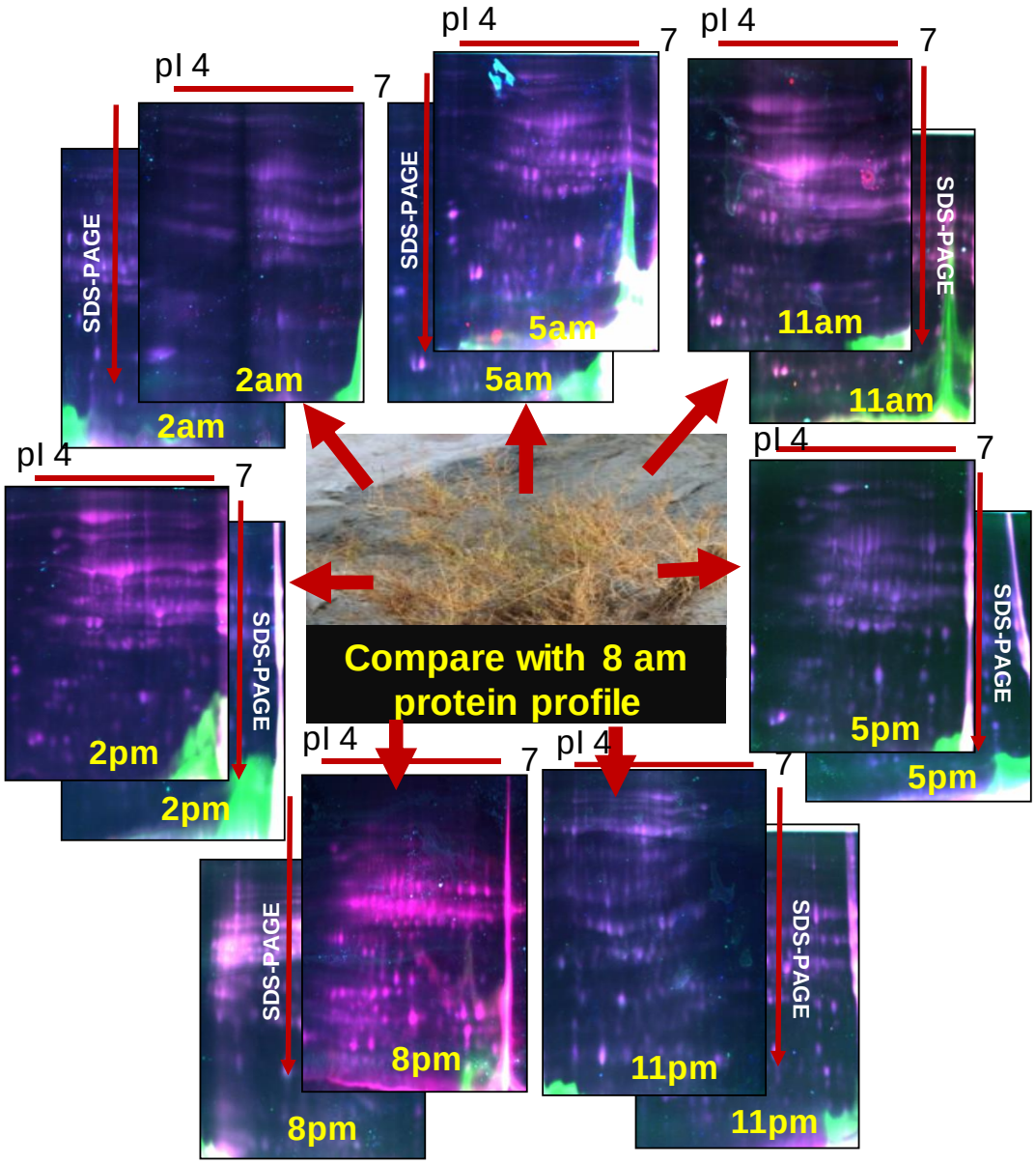

Figure 6.4: DIGE of the proteins extracted from the leaves of *S. fruticosa* harvested at different time points of day during the summer season. For each time point, two replicates each were considered for further analysis.

As described in the material and method section, proteins exacted from *S. fruticosa* harvested at a different time points during different seasons were labeled with fluorescent dye and analyzed using DIGE (Figure. 6.2-6.4). Images for the gel was taken using Typhoon™ 9500 (GE Healthcare). Two replicates/gels were analyzed for each of the time points. The gel images, as

obtained from the scanner, were further analyzed using Decyder 7.0 software (GE Healthcare).

6.3.1. Differential expression of global proteins identified from leaves of S. fruticosa at different time points and seasons

In a time-span of 24 hours, salinity, pH and water availability at the site where *S. fruticosa* grows does not alter drastically, however, the atmospheric temperature (chapter 4) and the light intensity (chapter 4) fluctuated throughout the day. Changes in these parameters lead to alteration in the photosynthetic activity as well as the metabolome of *S. fruticosa* (Chapter 4 and 5). To further elucidate the global changes in protein expression and abundance, differential in-gel analysis (DIA) with respect to the protein profile obtained 8 am was performed using DeCyder 7.0 software for each time point. To gather all the proteins expressed, the co-detector was monitored to detect 1500 spots from each gel. By manual filtering, all artifacts were discarded such as, the peak observed due to dust and gel. Following which, the relative expression of the global proteins was represented using the volcano plots (Figure. 6.5-6.7).

During the post-monsoon season; most of the proteins were found to be similarly expressed like that at 8 am. However, during 11 am and 8 pm, the number of proteins showing similar expression like that of 8 am were found to be lowest (60.2% and 62.1% respectively). During these times, 34% and 36.9% of the total proteins showed lower expression (down expression) w.r.t. that of 8 am. The percentage of the total proteins that showed higher expresion w.r.t. that of 8 am throughout the time points were found to range between 11.1% (at 2 pm) to as low as 0.8% (at 8 pm and 11 pm). (Figure. 6.5).

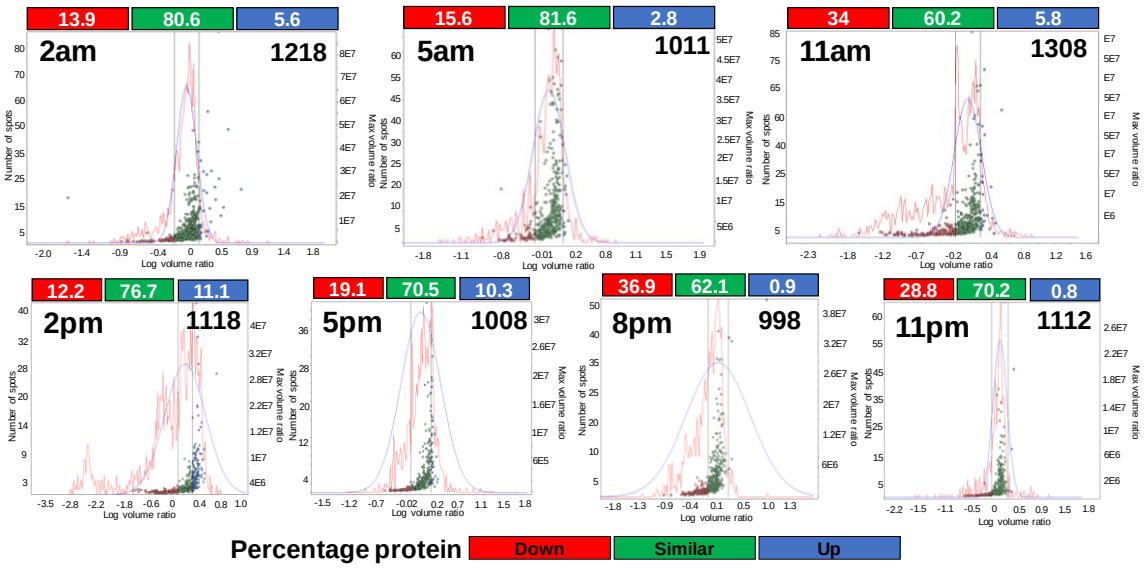

Figure 6.5: Volcano plot representing differentially expressed global protein spots identified from the leaves of S. *fruticosa* harvested at different time points of day during the post-monsoon season. Protein spots that showed a decrease in relative expression with respect to that of 8 am are shown in red. Protein spots that showed similar expression with respect to that of 8 am are shown in green. Protein spots that showed higher relative expression with respect to that of 8 am are shown in blue. Total percentage of the proteins that are lower, similar, or higher in expression for each time points are indicated in the box. Total protein spots taken into consideration for plotting the volcano plot is mentioned on the right side of the box.

Similarly, during winter season, most of the proteins also were found to be similarly expressed like that of 8 am. However, during 5 am and 8 pm, only 49.4% and 40.9% of the proteins showed similar expression like that of 8 am. Also, the percentage of proteins that showed lower expression during 2 am, 5 am, 11 am, 2 pm and 8 pm w.r.t. that of 8 am were found to be 28.6%, 30.6%, 20.1%, 20.7%, and 24.9% respectively which is relatively higher than that observed during the post-monsoon season. Further, most of the total proteins that showed higher expression than that of 8 am were also observed to be more than that during post-monsoon season except during 2 am, which showed only 0.6% of the total proteins (Figure. 6.6).

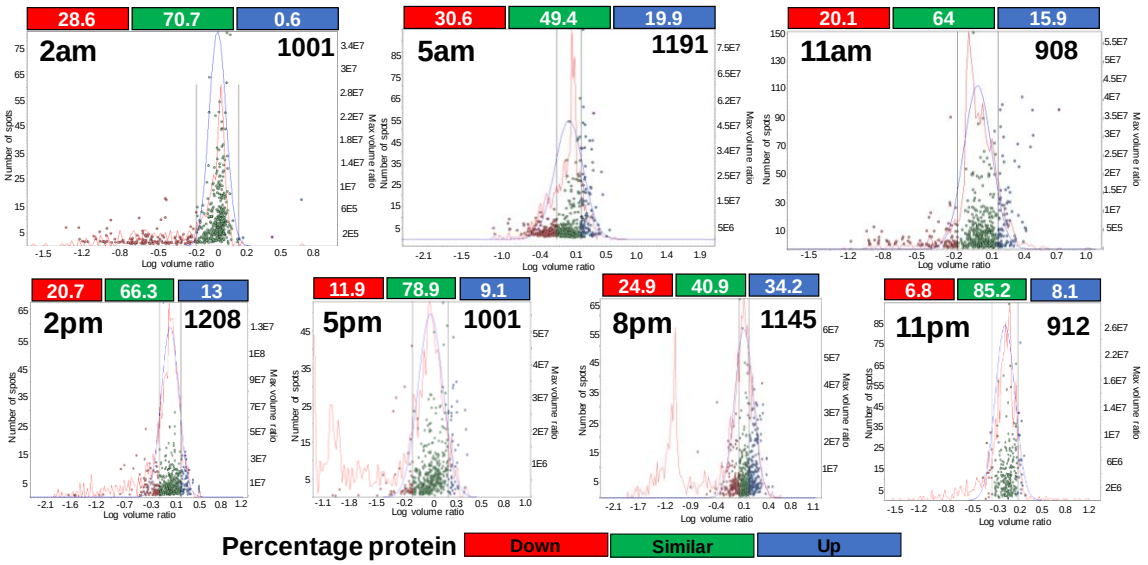

Figure 6.6: Volcano plot representing differentially expressed global protein spots identified from the leaves of S. *fruticosa* harvested at different time points of day during the winter season. Protein spots that showed a decrease in relative expression with respect to that of 8 am are shown in red. Protein spots that showed similar expression with respect to that of 8 am are shown in green. Protein spots that showed higher relative expression with respect to that of 8 am are shown in blue. Total percentage of the proteins that are lower, similar, or higher in expression for each time points are indicated in the box. Total protein spots taken into consideration for plotting the volcano plot is mentioned on the right side of the box.

During the summer season also, almost all the proteins (>70%) for each time points were found to be similarly expressed like that of 8 am. The total protein showing lower expression w.r.t. that of 8 am ranges between 12 to 26% and those showing higher expression ranges between 1.6% to 3.6%, except during 2 pm which showed 0.5% of the protein showing higher expression (Figure 6.7).

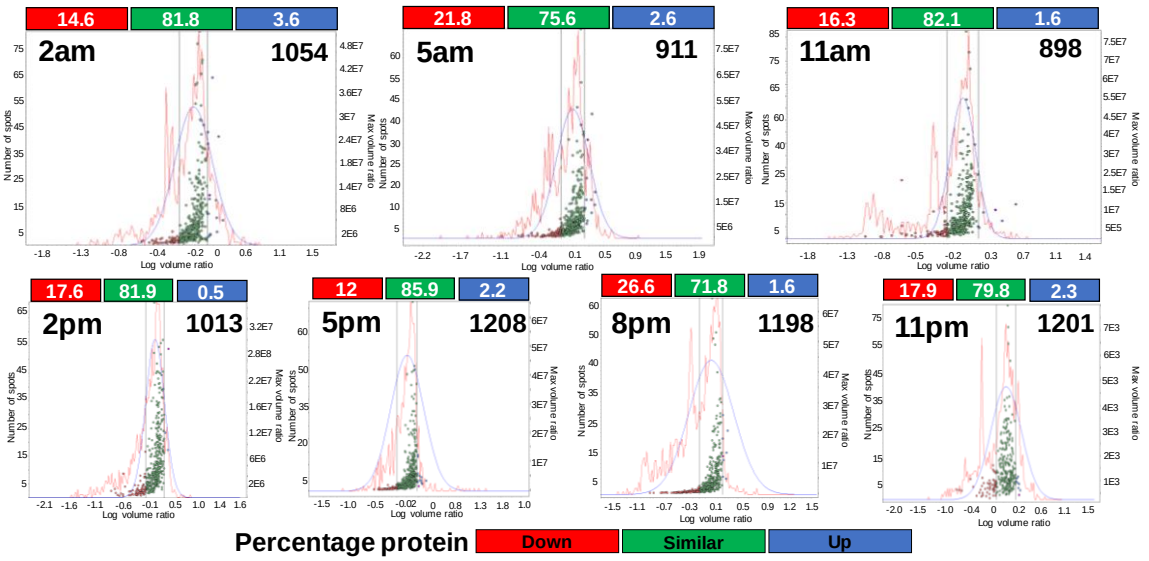

Figure 6.7: Volcano plot representing differentially expressed global protein spots identified from the leaves of S. *fruticosa* harvested at different time points of day during the summer season. Protein spots that showed a decrease in relative expression with respect to that of 8 am are shown in red. Protein spots that showed similar expression with respect to that of 8 am are shown in green. Protein spots that showed higher relative expression with respect to that of 8 am are shown in blue. Total percentage of the proteins that are lower, similar, or higher in expression for each time points are indicated in the box. Total protein spots taken into consideration for plotting the volcano plot is mentioned on the right side of the box.

6.3.2. Identifying the protein spots of interest

Using DeCyder 7.0 software, and performing Differential In-gel Analysis (DIA), several protein spots were detected which showed a change in expression level as compared to that at 8 am (Figure 6.6-6.8). To filter out the proteins of interest, the spots which showed a minimum of 1.5-fold change in abundance, at least during the one-time point of the day or season, and have *P-value*< 0.05 were chosen for further analysis. Based on this criterion, a total of 177 protein spots were identified, which were excised from the CBB stained 2D gel for sequencing and identification using MALDI-TOF-MS (Figure 6.9). Out of the 177 protein spots of interest, four predicted proteins, four probable protein, six hypothetical proteins, six protein that were not-assigned (NA) and eleven putative proteins

were identified. Eliminating these redundant and non-assigned proteins, a total of 147 protein spots were further taken into account for analysis.

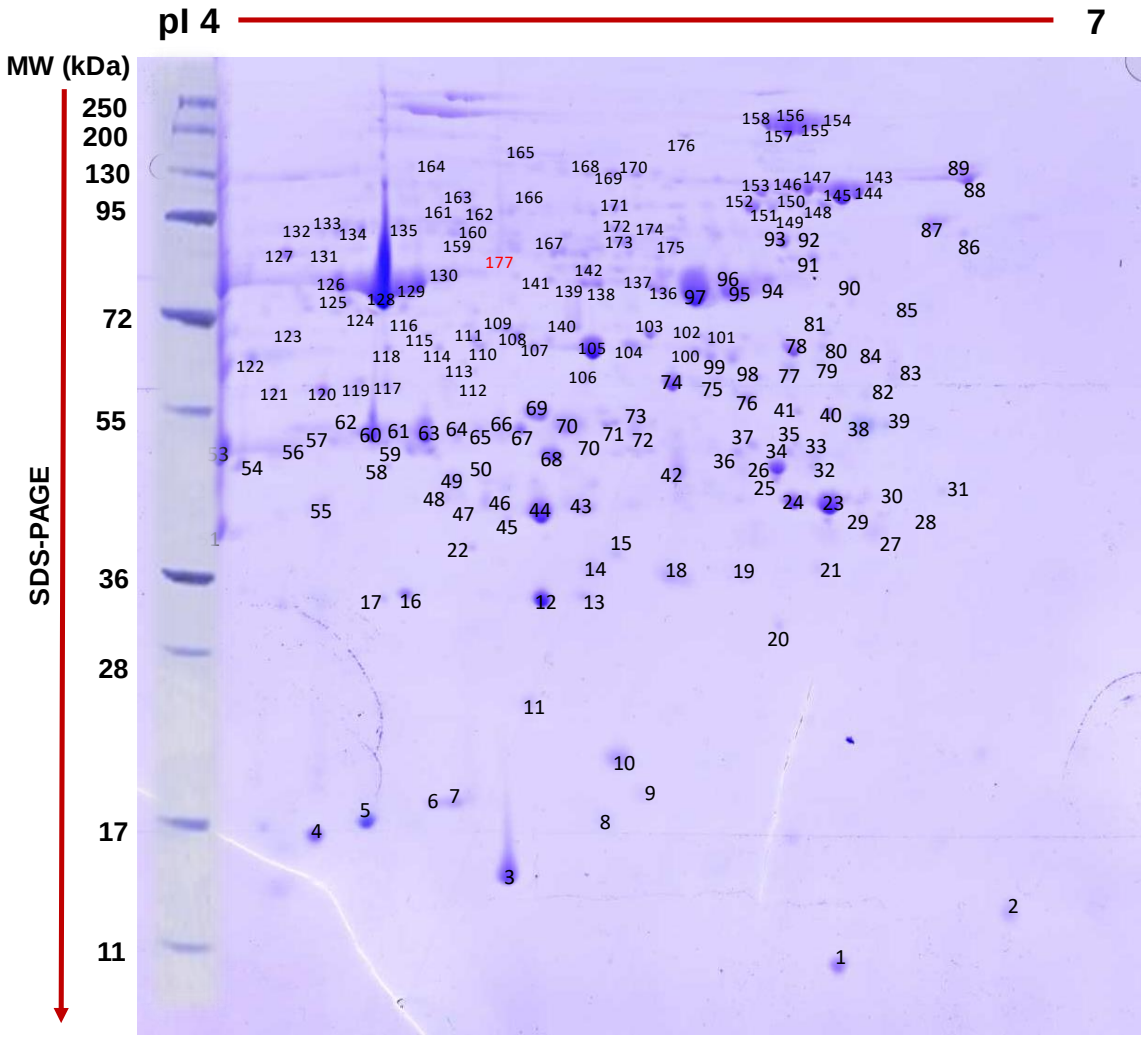

Figure 6.8: A Coomassie stained 2D gel showing the major protein of interest taken into consideration in this study. CBB stained gel showing abundant protein spots. Of which, 177 spots which showed a minimum of 1.5-fold change in abundance and have p-value < 0.05 were picked up for further analysis. The spots were further sequenced for the identification of proteins using MALDI-TOF-MS.

Heatmap showing the hierarchal clustering of the total protein spots (177) identified from each season is shown in Figure 6.9.

Figure 6.9: Heatmap showing the hierarchically clustering of the 177protein of interest identified from the leaves tissue of *S. fruticosa* under various seasons. A heat map is drawn by taking Log_{10} of the normalized value for each protein. Color gradient code with red indicating maximum, green for minimum and black for median are used for representing the pattern of accumulation.

6.3.3. Differential expression of the proteins of interest identified from S. fruticosa abundant at different time points and seasons

To further elucidate the changes in abundance of the proteins of interest (177 protein spots), the level of accumulation of each protein was compared with that of the proteins identified at 8 am. Keeping a 1.5-fold change of abundance as the minimum threshold, the level of expression was categorized as lower expression, similar expression, and higher expression (Figure 6.10). Throughout the seasons, the maximum of proteins identified were found to be expressed similarly with that of those identified at 8 am. During the post-monsoon season, at 2 am, and 5 pm, maximum number of the proteins (76% and 69%) were found to be similarly expressed w.r.t. that of 8 am. During this time, 16% and 20% of the proteins were found to be down-regulated. At 5 am, similarly expressed proteins were found to be lowest with only 23% value. During this time, 46% of the proteins were down-regulated. At 2 am, 11 am, 8 pm and 11 pm the percentage of protein showing higher expression w.r.t. that of 8 am were found to be lowest with 8%, 7%, 1%, and 7% respectively (Figure 6.10a).

During the winter season, the percentage of proteins showing similar expression w.r.t. that of 8 am ranged mostly between ~60% to ~70%, except during 5 am and 11 pm wherein, the total similarly expressed proteins w.r.t. 8 am were observed to be 53% and 88%. However, the percentage of proteins showing lower expression and higher expression w.r.t. that of 8 am were seen to vary at different time points. Time point at which maximum proteins showing lower expression w.r.t. that of 8 am were observed at 2 pm, 5 pm and 11 pm with 8%, 8%, and 11% respectively. On the other hand, time point at which maximum proteins showing higher expression w.r.t. that of 8 am were observed at 11 am, and 2 pm with 22% and 23% respectively. Similarly, time point at which minimum proteins showing lower expression w.r.t. that of 8 am were observed at 2 pm, 5 pm and 11 pm with 8%, 8% and 11%. And, time point at which minimum proteins showing higher expression w.r.t. that of 8 am were observed at 2 am and 11 pm

with just 2% and 1% (Figure 6.10b). Likewise, during summer similarly expressed protein w.r.t. that of 8 am were observed to be between the range of 70% to 80% except during 2 pm and 8 pm wherein, the total similarly expressed proteins w.r.t. 8 am were observed to be 56% and 91%. In addition, during this season, the percentage of proteins showing higher expression w.r.t. that of 8 am also ranged between 1% to 4% expect during 5 pm which have 10% of the proteins showing higher expression w.r.t. that of 8 am. Maximum of the proteins showing lower expression w.r.t. that of 8 am were observed at 2 pm with 35% of the total protein. And the minimum number of proteins showing lower expression w.r.t. that of 8 am were observed at 8 pm with 8% of the total protein (Figure 6.10c).

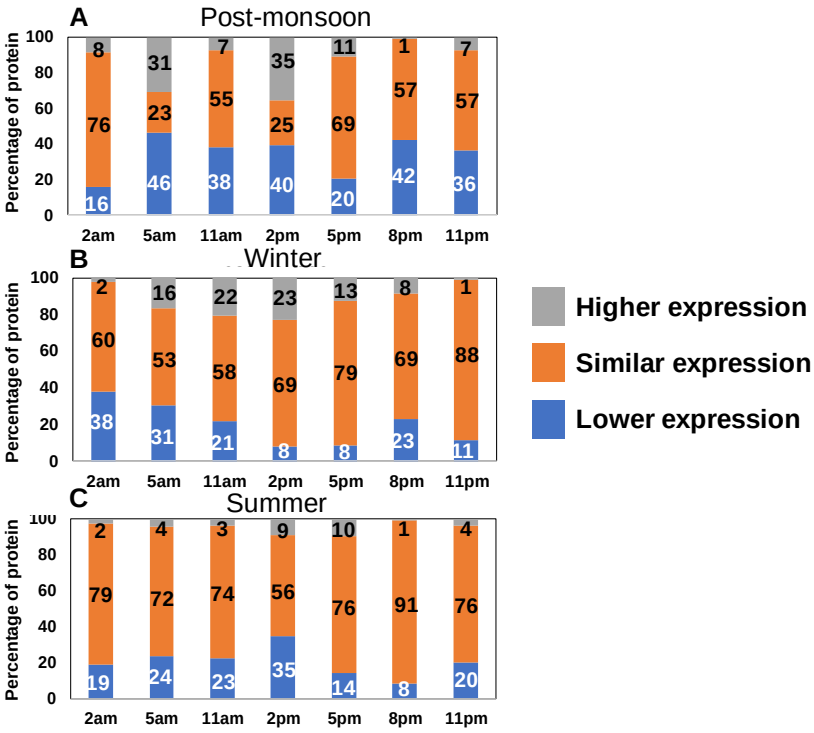

Figure 6.10: Comparison of differentially expressed protein spots of interest identified from the leaf of S. *fruticosa* harvested at different time points of the day during different seasons viz. post-monsoon, winter and summer. Total percentage of the protein spots, which showed a decrease in expression with respect to that of 8 am is shown in the blue bar. Total percentage of the protein spots, which showed similar expression with respect to that of 8 am is shown in the orange bar. Total percentage of the protein spots, which showed higher expression with respect to that of 8 am is shown in the grey bar. Number in each bar represents the percentage of protein showing change in abundance.

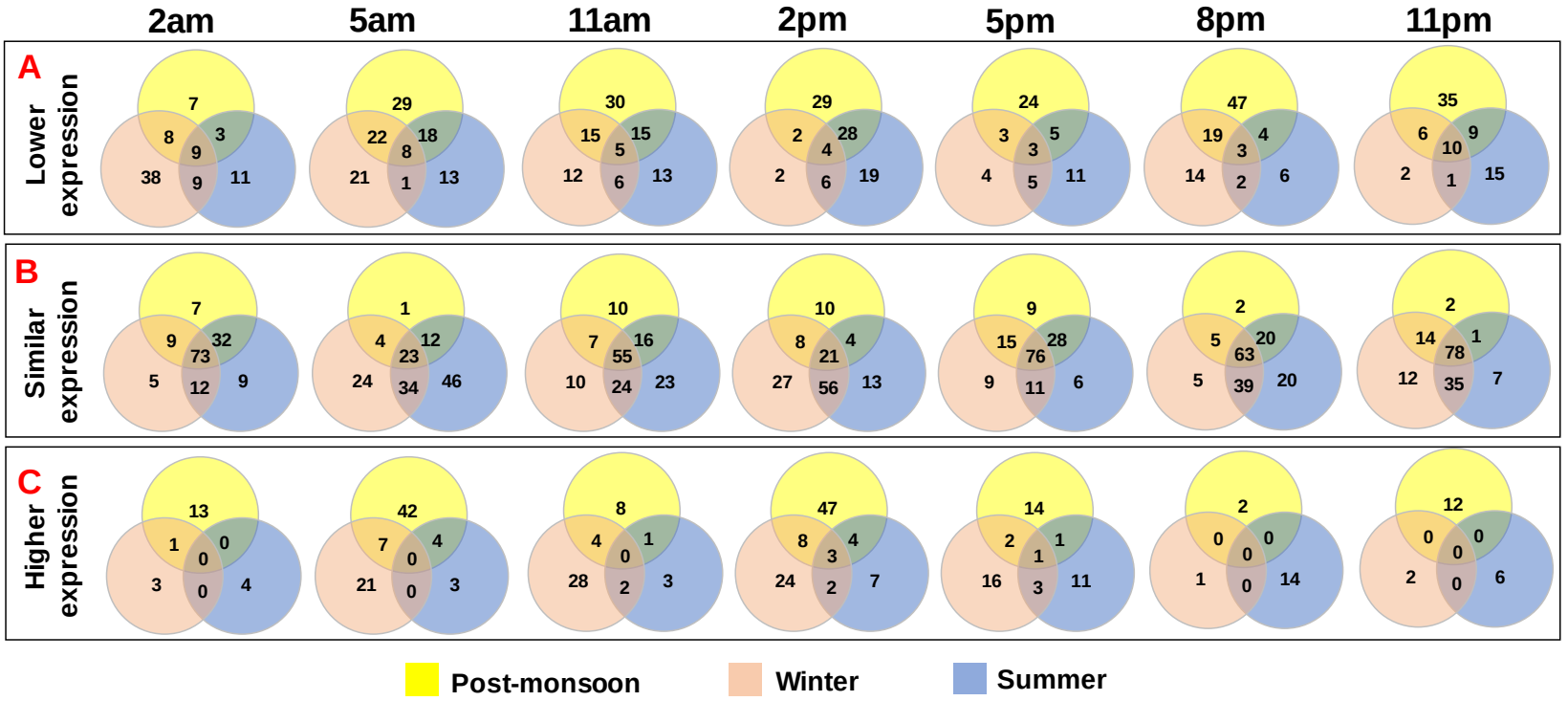

Figure 6.11: Venn diagrams representing the number of proteins that were similarly and uniquely expressed at different time points in leaves of *S. fruticosa* across the seasons. A) The number of proteins that were found to show lower expression during all the seasons was categorized to check for the number of similar and unique proteins expressed at a specific time point. B) The number of proteins that were found to show similar expression during all the seasons was categorized to check for the number of similar and unique proteins expressed at a specific time point. C) The number of proteins that were found to show higher expression during all the seasons was categorized to check for the number of similar and unique proteins expressed at a specific time point.

To further identify the number of global proteins, as identified in section 5.3.1., whose; abundance does not change significantly, which showed lower expression and, which showed higher expression w.r.t. that of 8 am, at a particular time point, a Venn diagram was generated (Figure 6.11). During different seasons, at a given time point, several unique proteins were seen to be expressed apart from those that are similarly expressed either in two seasons or during the three seasons

6.3.4. Principle component analysis of proteins

Two-dimensional principle component analysis (PCA) is a powerful statistical tool to identify maximum variance and also to find the correlation of the variance from any large data (Zhao et al., 2004). PCA of the proteins identified from each season at different time points was carried out to compare the pattern of variation of the proteins across the seasons and also to provide an overview of proteomics profile using MetaboAnalyst 3.0. (https://www.metaboanalyst.ca/). For each of the seasons, the total proteins detected at a specific time point was taken as one variance, which was then correlated with those protein variances detected at other time points. Proteins, from every season, identified from samples harvested at seven-time points, i.e. 2am, 5 am, 8 am, 11 am, 2 pm, 5 pm, 8 pm, and 11 pm were clustered into eight variances. These were then statistically analyzed with the first two PCA, i.e., PC1 and PC2, to represent the complete variance and find its correlation. Both of these components separated the variance into two vectors, with each having a positive and a negative axis. Clear diurnal and seasonal variation of the proteomic profile was seen in all the samples representing the three seasons (Figure 6.12).

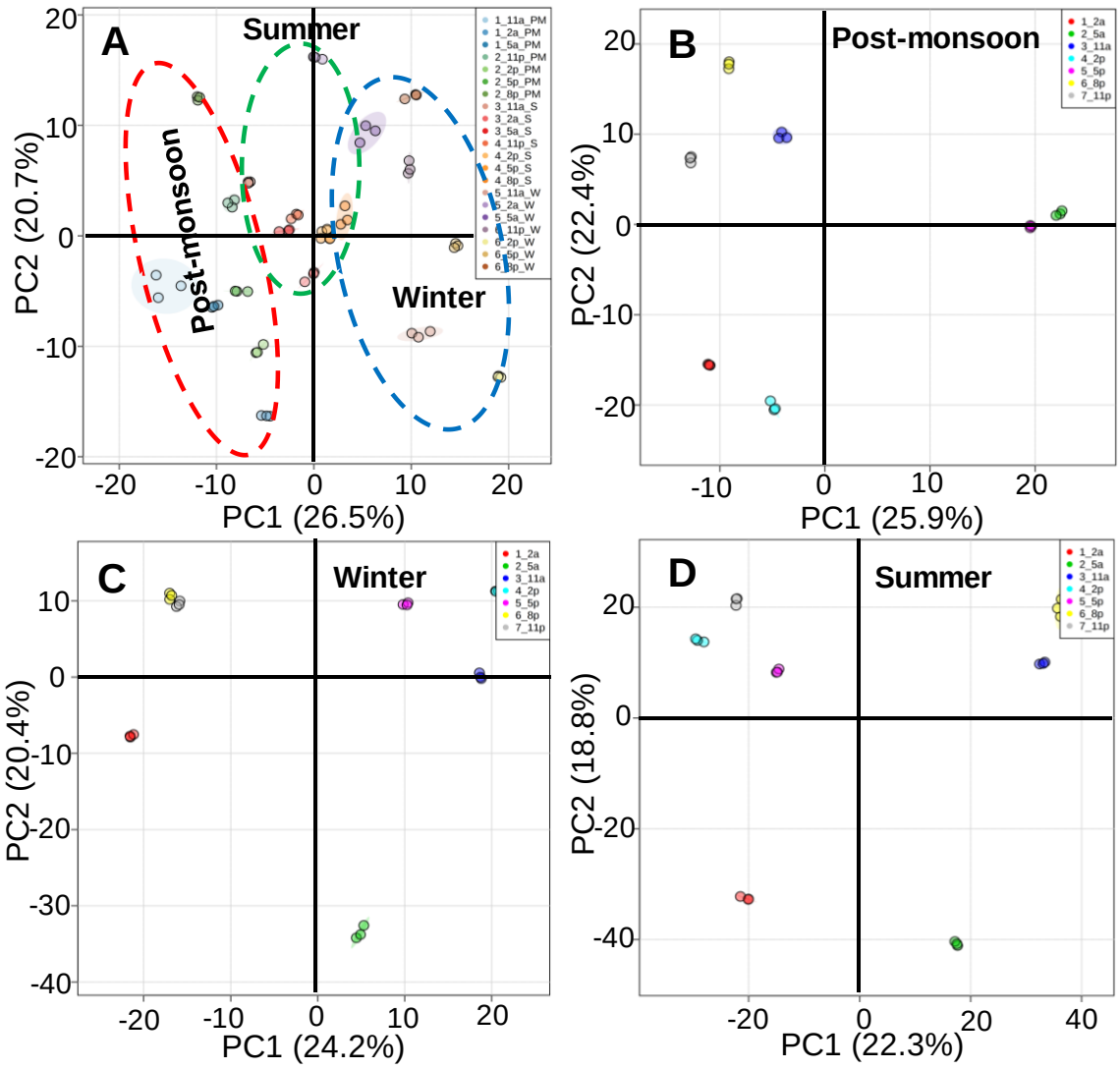

Figure 6.12: PCA of the proteins extracted from the leaves of *S. fruticosa* during the three different seasons: The177proteins identified from the three seasons showed diurnal as well as seasonal rhythmic pattern. All the PCA shown are represented by the first two principle component, i.e. PC1 and PC2 of the variables. A) The PCA of the complete 177 proteins identified in all the three seasons is also represented by PC1 of 26.5% and PC2 of 20.7%. B) PCA of the proteins identified during the post-monsoon season is represented by PC1 with 25.9% and PC2 of 22.4% variance. C) PCA of the proteins identified during the winter season was represented by PC1 with 24.2% and PC2 of 20.4%. D) PC1 and PC2 describe the PCA of the proteins identified during the summer season with 22.3% and 18.8% variance.

Seasonal variations were seen to have a direct impact on the pattern of protein expression, which is visible through PCA (Figure 6.12a). PC1 and PC2 represent 48.2% of the seasonal variants wherein, PC1 separated the seasonal variations according to the atmospheric temperature wherein, the two hot seasons, i.e. post-monsoon and summer occupied the negative axis and winter occupied the positive axis.

During the post-monsoon season, of the 177proteins identified, 48.3% variants were represented by PC1 and PC2 (Figure 6.12b). Clear separation of the variance with the change in day-night as well as high-low temperature was not observed. However, clustering of the proteins identified during 2 am, and 2 pm, 5 pm and 5 am, 11 am, and 11 pm were observed which were scattered across the axis. Likewise, 44.6% of the variants from 177proteins identified during winter were represented by PC1 and PC2 (Figure 6.12c). However, in this case, PC1 separates the variants according to the day and night cycle, wherein, proteins accumulating during the short-day time from 8 am to 5 pm occupied the positive axis. Those proteins accumulating during the night time, i.e. from 8 pm to 5 am occupied the negative axis.

Similarly, 41.4% of the 177 protein variants during summer were represented by PC1 and PC2 (Figure 6.12d). In this case, no distinct clustering of the variance according to time as well as day-night and the high-low temperature was observed. However, proteins identified from each time point were seen to cluster together, showing its variance with respect to other time points.

6.3.5. Gene ontology search and functional characterization of the differentially expressed proteins

The goal of gene ontology search/consortium is to provide knowledge of the role of genes/proteins in a cell by producing a dynamic vocabulary that can be applied to all types of eukaryotic system. For which, three independent ontological searches have been made accessible and widely accepted: biological

process, cellular component, and molecular function (Ashburner et al., 2000). To find the ontologies of the protein identified from *S. fruticosa*, the protein sequences were blast searched using its accession-id through BLAST2GO. A total of 177 protein accessions were analyzed (Table 6.2-6.4) of which, GO for 139 proteins were obtained. No blast hit was obtained for 3 proteins sequences. GO for 9 of the protein sequences could not be obtained even though they were mapped using BLAST2GO (Figure 6.13).

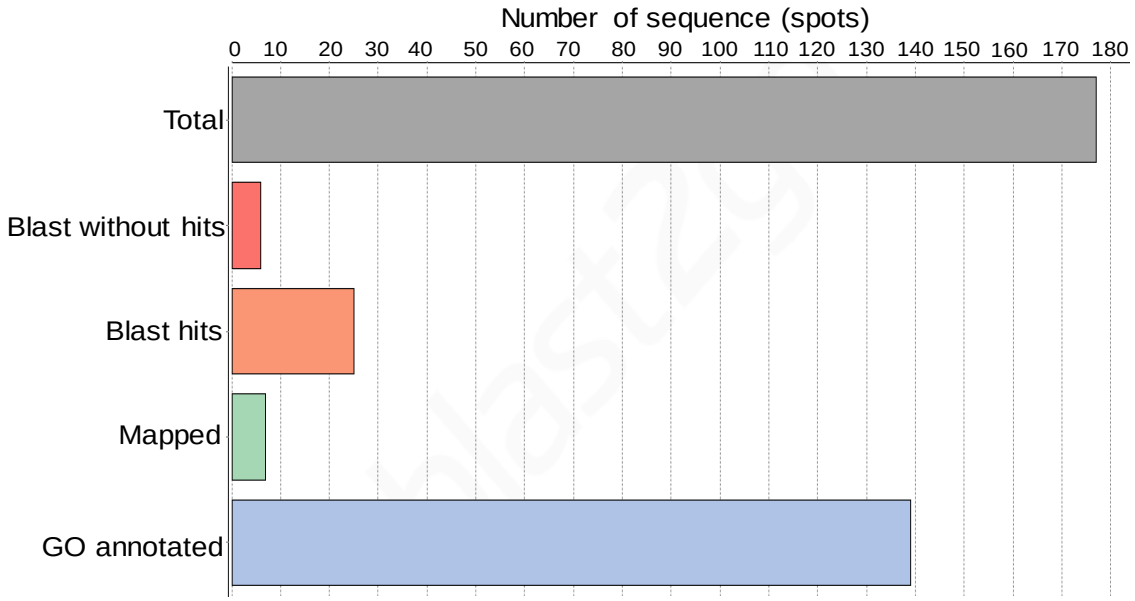

Figure 6.13: Data distribution of the protein sequences. Out of 177 sequences, inquiry loaded for GO search annotation for 139 sequences was successful.

Following the blast search, GO for the 139 sequences was categorized into three groups: Gene Ontology Biological Process (GOBP), Gene Ontology Cellular Component (GOCC) and Gene Ontology Molecular Function (GOMF) (Figure 6.14-6.16). Based on the blast annotation search and GOBP classification, the biological properties of the peptides identified are shown in Figure 6.14. Of the 139 sequences that were annotated for GO search, 109 peptide sequences (61.9%) were found to be involved in 69 biological processing (GOBP). Group of peptides involved in biological regulations, biosynthetic

process, cellular metabolic process, organic compound metabolism, and response stimuliwere found to be the significant component of the GOBP (Figure 6.14). Several of the identified peptides were found to regulate the biological process in cellular processing and regulations (50.28%), metabolic process (50.27%), nitrogen metabolism (35.02%), primary metabolic process (36.15%), cellular metabolic process (41.24%) and organic substrate metabolic process (40.67%).

Similarly, blast search for the peptides to find the annotation and their role in GOCC are shown in Figure 6.15. Of the 139 sequences that were annotated for GO search, 96 peptide sequences (54.23%) were found to be involved in 28 cellular components (GOBP). Group of peptides found associated with cell organelles (40.67%), intracellular organelles (37.38%), cell part (40.13%), membrane-bound (30.5%), Intracellular membrane-bounded organelle (27.2%) and membrane-bounded organelle (28.25%) were annotated (Figure 6.15). Likewise, gene ontology search for finding the peptides associated with molecular functions (GOMF) are represented in Figure 6.16. Of the 139 peptides sequences that were annotated for GO search, 112 peptides sequences (63.3%) were found associated with molecular functions. Several peptides were found to be involved in binding and catalytic activity of the cells and nucleus. Peptides found associated with the organic cyclic compound binding (30.5%), ion binding (23.7%), catalytic activity (42.9%) and nucleic acid binding (18.1%) were annotated (Figure 6.16).

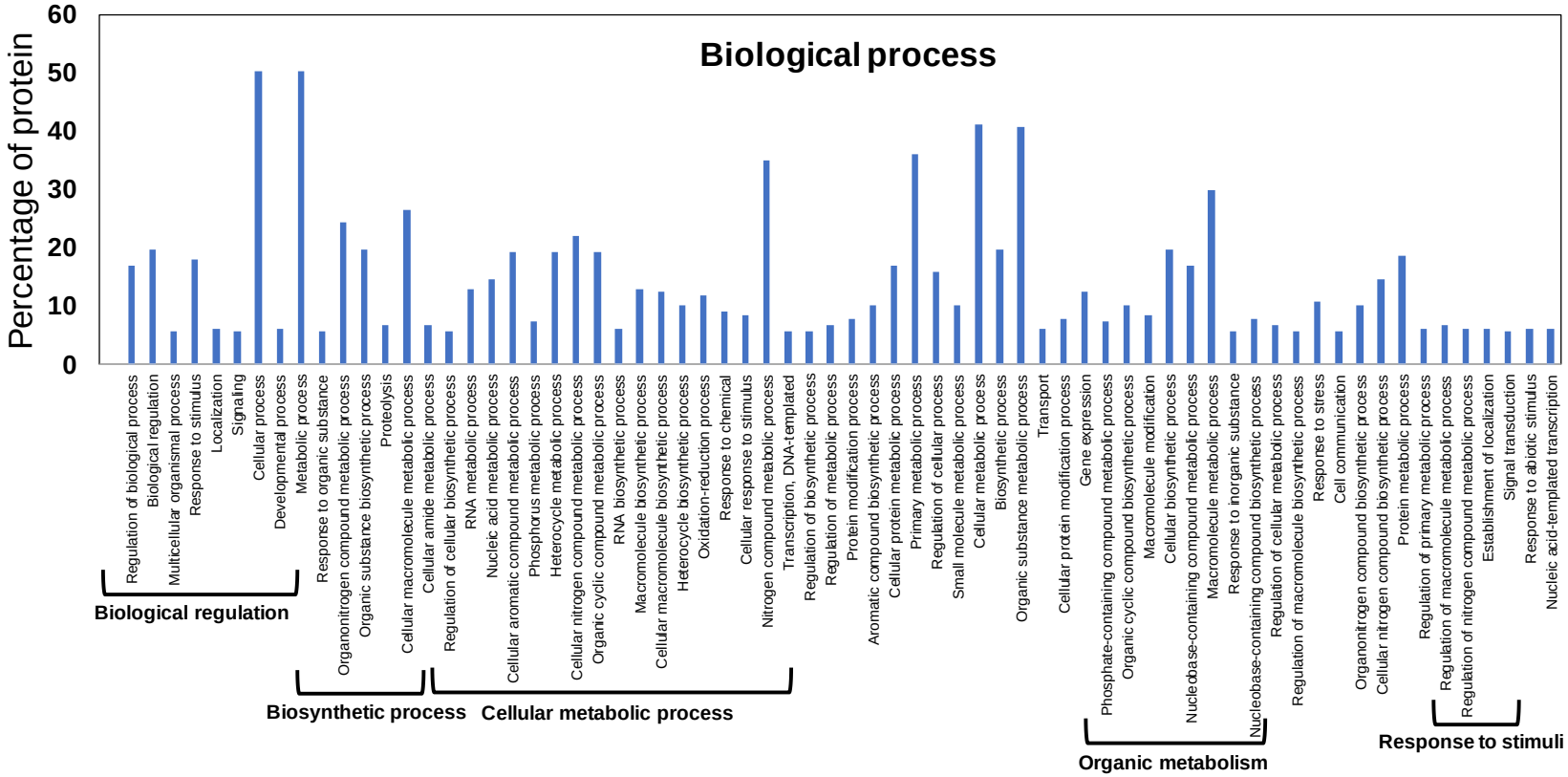

Figure 6.14: Gene ontology search showing the peptides involved in the biological process in *S. fruticosa*. The functions of the identified peptides that are differentially accumulating in *S. fruticosa* at different time points of the day during three different seasons viz. post-monsoon, winter and summer**.**

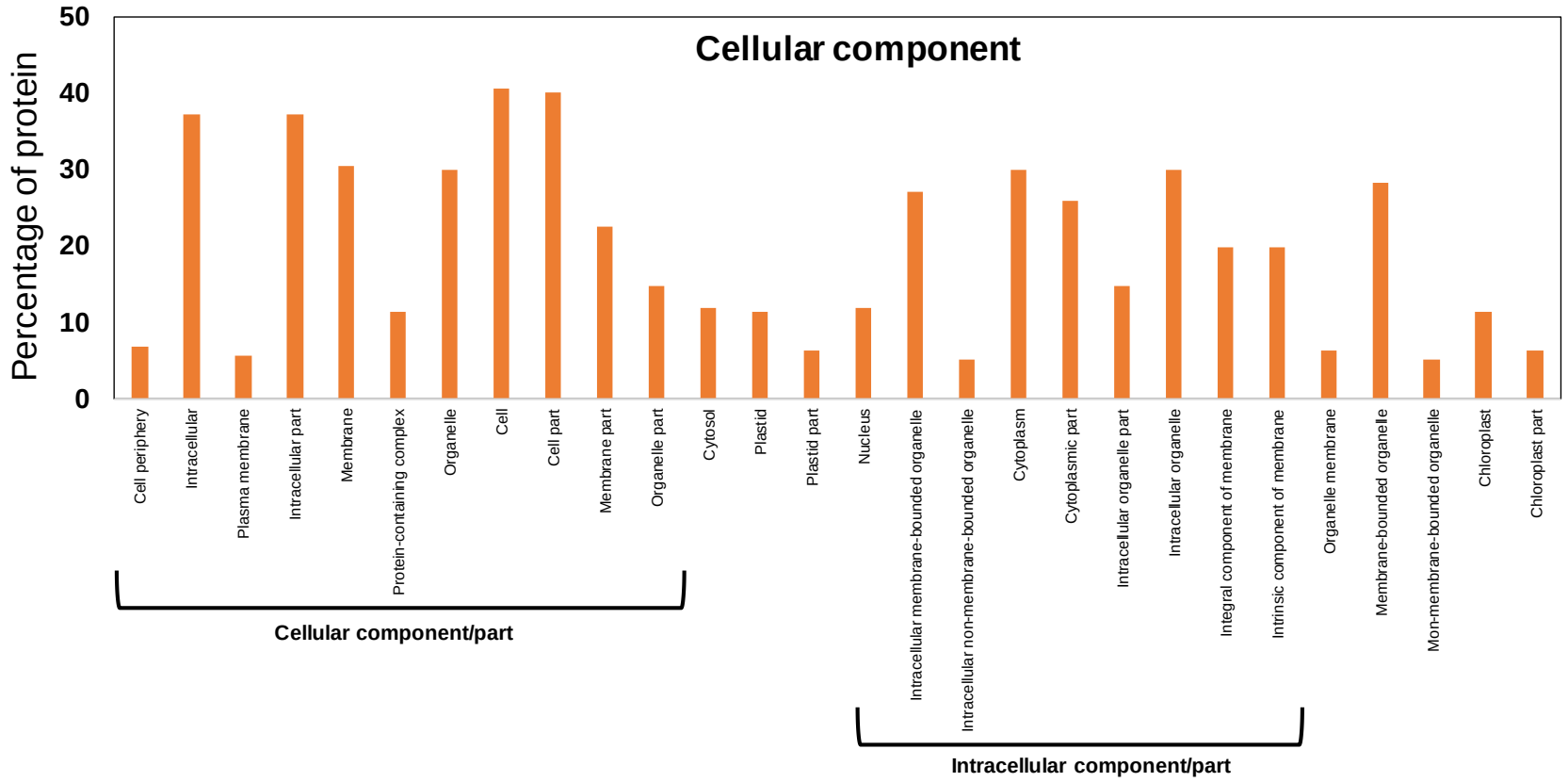

Figure 6.15: Gene ontology search showing the peptides involved inthe cellular component in *S. fruticosa*. The functions of the identified peptides that are differentially accumulating in *S. fruticosa* at different time points of the day during three different seasons viz. post-monsoon, winter and summer.

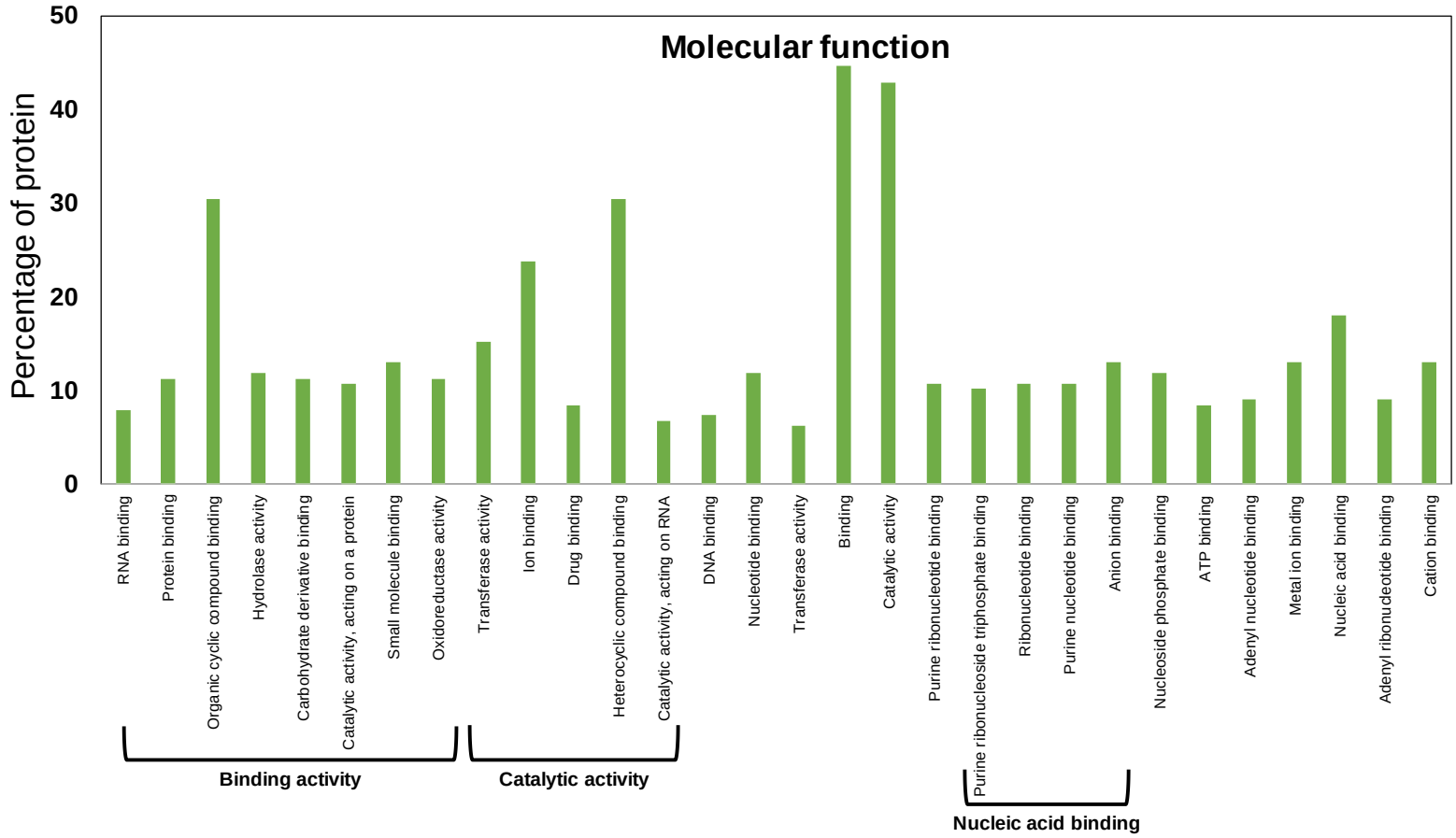

Figure 6.16: Gene ontology search showing the peptides involved in molecular function in *S. fruticosa*. The functions of the identified peptides that are differentially accumulating in *S. fruticosa* at different time points of the day during three different seasons viz. post-monsoon, winter and summer are shown.

Table 6.2: Proteins detected during the post-monsoon season from the leaves of *S. fruticosa*

Protein ID	>FASTA name	Protein description	Time of the day						
			2am	5am	11am	2pm	5pm	8pm	11pm
gi|147765954	CAN59951.1	11S globulin seed storage protein 2	-1.84	-3.26	-1.57	-1.45	-1.57	0.005	-1.33
gi|2492488	sp|Q41418.1	14-3-3-like protein	-1.32	2.125	1.63	-1.19	1.56	-3.09	-1.62
gi|316937092	ADU60530.1	14-3-3-like protein C	1.045	1.915	-1.82	1.46	1.285	-1.71	-1.16
gi|11138322	BAB17822.1	14-3-3-like protein C	1.5	-3.46	1.145	-1.52	1.38	1.2	1.39
gi|255558874	XP_002520460.1	18.1 kDa class I heat shock protein	-1.09	2.705	1.17	-3.14	1.505	1.165	-1.15
gi|110816068	YP_684400.1	30S ribosomal protein S11	1.11	-1.98	-0.06	1.605	-1.4	-2.15	-1.12
gi|157849590	ABV89582.1	4-hydroxy-3-methylbut-2-enyl diphosphate reductase, chloroplastic-like	1.095	-1.15	-1.3	-1.34	-1.24	-1.21	1.075
gi|14575543	CAA55659.2	4-hydroxy-tetrahydrodipicolinate synthase, chloroplastic	1.265	-2.07	-3.35	1.4	-1.23	-2.44	1.19
gi|42572781	NP_974486.1	50S ribosomal protein L1, chloroplastic	1.035	-1.54	-1.79	1.795	1.24	-2.35	-1.26
gi|115438116	NP_001043461.1	50S ribosomal protein L25	1.265	-1.27	1.35	1.45	-1.04	-1.51	-1.14
gi|327493145	AEA86279.1	ABC transporter family protein	1.37	-1.42	-1.27	1.57	-1.75	1.065	1.21
gi|15221890	NP_175874.1	Agamous-like MADS-box protein AGL29	1.495	1.25	-1.4	1.76	1.32	-1.76	-1.86
gi|15229233	NP_187064.1	Ankyrin repeat family protein	1.45	-1.38	-2.99	2.21	-1.43	1.31	1.07
gi|298569868	ADI87449.1	Jasmonic acid carboxyl methyltransferase	1.7	-2.2	-1.3	1.69	-1.83	-1.24	-1.46
gi|2632103	CAB11467.1	Arginyl-tRNA synthetase, class Ic	-1.14	-1.41	-1.22	-1.75	-1.31	-1.47	-1.81
gi|224038410	ACN38309.1	ARGOS-like protein	1.25	-1.12	-2.73	1.625	-1.41	-1.27	-1.04
gi|624672	AAA82741.1	ASR	-1.66	1.7	-1.75	-1.37	1.675	-1.41	-2.59
gi|20563267	AAM27953.1	At5g03840	1.4	2.485	-1.62	1.52	1.36	-1.27	-1.29

gi|228017304	ACP52122.1	ATP synthase CF0 B subunit (chloroplast)	-1.53	1.79	-1.53	-1.11	1.72	1.375	-1.03
gi|29565571	NP_817148.1	ATP synthase cf0 b subunit (chloroplast)	-1.58	-1.56	1.705	1.615	-1.33	-1.64	-3.1
gi|38567798	CAE76084.1	B1340F09.22	-1.23	-2.08	-0.02	-1.76	-1.46	1.185	-1.53
gi|168007657	XP_001756524.1	BTB/POZ domain-containing protein At3g56230 isoform X1	1.075	1.475	-1.82	1.635	1.25	-1.1	1.345
gi|297846056	XP_002890909.1	Cell growth defect protein	-1.17	1.72	1.3	-2.35	1.195	1.02	1.135
gi|224088202	XP_002308368.1	Centromere-associated protein E isoform X1	1.34	-1.38	0.035	1.575	-1.4	-1.22	1.13
gi|7258408	CAB77451.1	Chitinase, partial	1.045	-3.5	-1.43	1.415	1.125	-1.08	-1.26
gi|226490526	BAH56544.1	CLAVATA3/endosperm surrounding region 13	-1.33	1.555	-1.31	-1.42	1.265	-1.06	-1.76
gi|296006082	BAJ07539.1	Cold-responsive protein WCOR15-2A	1.27	-1.97	-2.75	1.585	-1.32	-1.15	-1.36
gi|255560737	XP_002521382.1	Conserved hypothetical protein	-1.52	1.255	-2.06	-1.06	2.005	-1.55	-1.05
gi|3929325	AAC79873.1	Cyclic dof factor 3-like	-1.11	-2.27	-1.47	1.36	-1.06	-1.44	-1.59
gi|18424030	NP_568867.1	Cytochrome c oxidase subunit 6b-3	1.085	-2.04	-2.41	-1.69	-1.75	-1.35	-1.14
gi|57546342	AAW52039.1	Cytochrome P450	-1.41	-2.43	-1.58	-2.29	-1.45	-1.25	-1.76
gi|226694227	sp|P0C8Y5.1	DEF1_HEUSARecName: Full=Defensin-like protein 1; AltName: Full=Cysteine-rich antifungal protein 1; AltName: Full=Defensin AFP1; Short=HsAFP1	-1.45	-2.2	-2.26	-1.6	-1.1	-1.35	-2.23
gi|139005020	BAF52544.1	Defensin-like protein	1.14	-2.32	-2.22	1.24	-1.16	1.14	1.18
gi|115466620	NP_001056909.1	Dehydration-responsive element-binding protein 1A	-0.35	-1.4	1.085	2.115	-1.53	-1.48	-1.53
gi|301139697	ADK66263.1	Dehydrin ERD10-like	1.39	-1.53	-1.5	-1.78	0.105	-1.3	-1.66
gi|50299542	AAT73629.1	Diacylglycerol O-acyltransferase 1C	-1.07	1.72	1.5	1.795	-1.1	-1.64	-0.06

gi|12248378	BAB20075.1	Dihydroflavonol 4-reductase	1.08	-1.83	-1.42	1.05	1.26	-1.24	-1.21
gi|51558023	AAU06584.1	Dihydroflavonol 4-reductase	1.36	-1.31	-1.25	1.125	-1.2	-1.24	1.2
gi|328796759	AEB40418.1	DNAJ heat shock N-terminal domain-containing protein	1.12	-1.76	-1.53	-1.26	-1.5	-1.52	1.04
gi|262212637	ACY35971.1	Dof-type zinc finger protein	-1.41	-1.7	1.095	1.265	1.675	-1.1	-1.31
gi|108711833	ABF99628.1	Dolichol-phosphate mannosyltransferase subunit 1	-1.21	-2.73	-1.14	-1.33	-1.61	-2.51	-1.3
gi|323282157	ADX35881.1	Dolichyl-diphosphooligosaccharide protein glycosyltransferase subunit STT3A	1.19	-1.51	-1.68	-1.65	-1.25	-1.37	-2.67
gi|255582119	XP_002531854.1	E3 ubiquitin-protein ligase RING1-like	1.22	-1.72	-0.08	-1.63	-1.29	-1.59	-1.24
gi|255602381	XP_002537843.1	Elongation factor G	-1.59	1.405	-2.77	1.655	1.365	-1.98	-2.02
gi|15225842	NP_180273.1	ETHYLENE INSENSITIVE 3-like 1 protein	-1.13	-2.73	-1.62	2.585	-1.07	-1.51	-1.61
gi|147801420	CAN68056.1	F-box/FBD/LRR-repeat protein At1g13570-like	-1.19	1.875	1.31	1.3	-1.1	-3	-1.11
gi|47824945	AAT38719.1	F-box/kelch-repeat protein At3g23880-like	-1.49	1.8	0.245	-2.05	1.13	-1.22	-1.55
gi|323444150	ADX68824.1	Flavanone 3-hydroxylase	-1.25	-1.72	-3.07	1.73	-1.24	1.15	1.08
gi|108708342	ABF96137.1	Flavonoid 3',5'-hydroxylase 1	1.2	1.825	-1.44	-2.82	-1.33	-1.19	-1.17
gi|22135898	AAM91531.1	Floral homeotic protein APETALA 2	-1.23	-2.23	1.125	-1.85	-1.27	-1.1	1.475
gi|226496826	NP_001152602.1	Gibberellin-regulated protein 1	1.125	1.41	-1.77	1.23	1.505	-1.42	-1.88
gi|195650967	ACG44951.1	Gibberellin-regulated protein 2 precursor	-1.43	1.485	1.14	-2.15	1.175	-1.19	-1.2
gi|3868853	BAA34247.1	GPI-anchored protein LLG1	-1.15	1.73	1.41	-1.63	1.225	1.205	1.445
gi|162463546	NP_001105546.1	GTP-binding protein YPTM1	1.44	-1.49	-1.18	-4.57	-1.38	-1.18	-1.31
gi|227603	prf||1707300A	GTP-binding protein YPTM1	1.24	-1.3	-1.33	1.24	-1.23	-1.35	-1.68
gi|51104295	AAT96693.1	G-type lectin S-receptor-like serine/threonine-protein kinase	-1.14	1.165	1.32	-2.96	-1.28	-2.35	-1.28

		LECRK3							
gi|47971184	BAD22534.1	Harpin inducing protein	-1.22	1.43	-2.36	1.4	-1.12	-1.1	-1.19
gi|302121697	ADK92863.1	Histidine kinase 2	-1.19	-1.32	-2.15	-1.78	-1.5	-1.55	1.285
gi|56784402	BAD82441.1	Hypothetical protein	-1.05	-1.41	1.145	-1.39	-1.22	-1.31	1.435
gi|40538962	AAR87219.1	Hypothetical protein	1.18	2.67	-1.31	1.625	1.165	-1.52	-1.29
gi|125589199	EAZ29549.1	Hypothetical protein OsJ_13623	-1.2	1.52	-0.08	-2.7	1.24	-1.22	1.225
gi|147800133	CAN73206.1	Hypothetical protein VITISV_009746	-1.32	1.41	-2.02	1.44	1.265	-1.14	1.28
gi|147859750	CAN78710.1	Hypothetical protein VITISV_043136	-1.3	-2.62	1.26	-1.32	-1.34	1.08	-1.2
gi|302853022	XP_002958028.1	Hypothetical protein VOLCADRAFT_99231	-1.46	0.11	1.965	-1.43	-1.13	-2.16	-1.53
gi|224082806	XP_002306846.1	Inorganic phosphate transporter 1-4	-1.16	-1.53	-1.23	1.88	-1.13	-1.72	-1.14
gi|125003	sp|P09407.1	ITI3_MOMCHRecName: Full=Trypsin inhibitor MCI-3	1.205	-2.07	-1.07	-2.85	1.085	-1.22	-1.13
gi|224179497	YP_002601027.1	L protein of photosystem II (chloroplast)	-1.41	1.325	-1.33	2.105	1.32	-1.8	-1.67
gi|297831316	XP_002883540.1	Late embryogenesis abundant protein (LEA) family protein	-1.54	-2.29	-2.54	-2.47	-1.06	1.11	-1.64
gi|297611560	NP_001067600.2	Leucine-rich repeat protein kinase family protein	1.28	-1.31	1.745	-1.08	-1.24	-1.46	-1.29
gi|225425967	XP_002269216.1	Lignin-forming anionic peroxidase	1.23	-2.1	-1.51	-2.21	1.415	-1.17	1.07
gi|242040459	XP_002467624.1	LysM domain containing protein	-1.01	1.65	1.1	-2.22	1.125	-1.17	1.1
gi|2281237	AAB64056.1	Maturase (chloroplast)	1.105	1.265	-2.2	1.13	1.18	-2.4	-1.66
gi|296171301	CBI71372.1	Maturase K (chloroplast)	-1.3	-1.58	1.925	1.615	-1.5	-1.14	1.13
gi|28804507	BAC57959.1	Metallothionein-like protein 1	1.145	-1.92	-1.74	-2.54	-1.45	-3.84	-2.32
gi|18652285	AAL77049.1	Metallothionein-like protein 1	1.28	1.63	-1.33	-2	1.175	-3.2	-1.44
gi|303276647	XP_003057617.1	Methionine-tRNA ligase	1.24	1.52	-1.19	1.855	1.105	1.25	1.285
gi|18414298	NP_568125.1	Monodehydroascorbate reductase 2	1.355	-1.65	1.09	1.335	-1.55	-1.63	-1.23

gi|119434027	ABL75109.1	---NA---	-1.43	-2.66	-1.38	-2.02	-1.34	-1.86	-2.04
gi|330318652	AEC10986.1	---NA---	-1.41	-1.17	-2.17	-2.76	-1.34	-1.41	-2.23
gi|168033184	XP_001769096.1	---NA---	1.285	-3.19	1.23	-1.49	-1.43	1.125	1.485
gi|30315163	AAP30805.1	---NA---	1.1	2.425	-1.71	1.875	-1.7	1.145	-1.36
gi|154269004	ABS72216.1	---NA---	1.215	-2.33	1.425	1.325	1.085	-1.11	1.865
gi|302143158	CBI20453.3	---NA---	1.32	-3.26	-0.3	-1.61	-1.34	1.11	-1.19
gi|242074306	XP_002447089.1	NAD(P)-binding Rossmann-fold superfamily protein	1.115	-1.22	-2.01	1.865	-1.16	-1.13	1.48
gi|42569711	NP_181313.3	NAD(P)-linked oxidoreductase superfamily protein	-1.04	-2.43	-1.17	-1.13	1.135	-1.53	1.025
gi|308809874	XP_003082246.1	NAD-dependent epimerase/dehydratase family protein	-1.14	-1.42	-1.31	1.51	-1.34	-1.4	-1.25
gi|307108859	EFN57098.1	NADH dehydrogenase [ubiquinone] iron-sulfur protein 4, mitochondrial	1.2	-1.28	1.34	1.99	-1.12	1.21	1.14
gi|118140538	CAL69657.1	NBS-LRR resistance protein	-1.12	-1.97	-1.53	1.615	1.075	-2.63	-1.08
gi|729135	sp|Q06509.1	O-methyltransferase	1.405	2.515	0.28	-1.5	1.15	-1.12	-1.47
gi|33641720	AAQ24345.1	O-methyltransferase	-1.4	-3.51	1.325	1.25	-1.53	1.22	-1.62
gi|195636260	ACG37598.1	O-methyltransferase	1.665	-3.45	-1.3	-1.72	-1.37	1.435	1.185
gi|224077820	XP_002305422.1	Organ-specific protein P4-like	-1.38	-2.66	-1.37	1.52	-1.37	-1.52	-2.34
gi|297721633	NP_001173179.1	Os02g0793150	-1.32	1.49	-1.35	-1.6	1.17	-1.44	-2.6
gi|11934654	AAG41763.1	P23A_BRANARecName: Full=Co-chaperone protein p23-1; AltName: Full=Bnp23-1	-1.72	1.285	-1.74	1.495	1.495	1.345	-1.11
gi|297830098	XP_002882931.1	P53/DNA damage-regulated protein	-1.07	-1.96	-1.93	-1.76	-1.27	1.29	-1.48
gi|224105841	XP_002313951.1	Peptide methionine sulfoxide reductase B5-like	1.17	1.3	1.31	2.245	1.105	-1.4	1.145
gi|302819856	XP_002991597.1	Peptidyl-prolyl cis-trans isomerase FKBP20-2, chloroplastic	1.435	1.28	0.74	-1.59	1.47	-3.47	-1.25

gi|159470805	XP_001693547.1	Peptidyl-prolyl cis-trans isomerase FKBP20-2, chloroplastic	1.03	2.16	1.355	-2.62	1.475	-1.03	-1.51
gi|15240486	NP_200335.1	PEROXYGENASE 2	1.19	1.135	-1.31	-1.09	1.135	-1.25	-1.59
gi|307105956	EFN54203.1	Phosphatidylinositol N-acetylglucosaminyltransferase subunit P	1.105	-2.18	-1.78	-1.95	1.225	-1.27	-1.17
gi|10303403	CAA65117.1	Phosphoenolpyruvate carboxylase	-1.38	1.425	-1.37	-1.2	1.205	-1.31	1.125
gi|145346793	XP_001417867.1	Photosystem II PsbR protein, chloroplast precursor	1.16	-1.49	1.17	2.125	-1.32	-1.37	1.37
gi|87241065	ABD32923.1	Polynucleotidyl transferase, Ribonuclease H fold	1.235	-3.61	-1.29	-1.77	-1.29	-1.57	1.155
gi|53749467	AAU90321.1	Polyprotein, related	1.095	-1.16	1.335	-2.56	-1.13	-1.18	1.46
gi|307104521	EFN52774.1	Predicted protein	1.525	1.83	-1.14	1.785	1.41	-1.07	1.185
gi|303282497	XP_003060540.1	Predicted protein	-1.38	-2.05	-1.84	-1.9	-2.11	-1.16	-1.48
gi|308802616	XP_003078621.1	Predicted protein	-1.14	1.83	-1.31	1.565	1.19	-2.07	-1.29
gi|104294980	ABF71996.1	2-oxoglutarate-dependent dioxygenase	-1.29	1.295	1.305	1.415	1.36	1.14	-1.56
gi|11385435	AAG34800.1	Probable glutathione S-transferase	-1.31	1.58	-1.13	1.285	1.355	-1.13	1.195
gi|108863932	ABA91188.2	Probable serine/threonine-protein kinase WNK5	1.315	1.48	-1.25	1.96	1.235	-1.36	1.685
gi|255613348	XP_002539501.1	Probable WRKY transcription factor 40	-1.32	2.12	-1.28	1.64	-1.63	-1.26	-1.14
gi|225166539	ACN81327.1	Prolycopene isomerase, chloroplastic	-1.18	1.4	1.3	-1.34	1.115	-1.1	-1.08
gi|41352687	AAS01050.1	Proteasome subunit beta type-5-B	-1.73	1.225	-1.33	-1.92	1.13	-1.66	1.325
gi|21592365	AAM64316.1	Proteasome subunit beta type-6	1.185	-1.48	-1.15	1.975	-1.3	-2.12	1.69
gi|15235889	NP_194858.1	Proteasome subunit beta type-6	-1.21	-1.36	-1.65	1.62	-1.02	-1.23	1.035
gi|41352683	AAS01048.1	Proteasome subunit beta type-6	-1.09	-1.26	1.28	1.95	-1.08	-1.33	1.04
gi|255553675	XP_002517878	Protein ARABIDOPSIS THALIANA ANTHER 7	1.26	1.37	-3.32	1.735	1.08	-1.42	-1.1
gi|29367477	AAO72594.1	Protein DA1-related 1-like	-1.06	-2.51	-1.27	-1.34	1.35	-1.37	1.425

gi|125548557	EAY94379.1	Protein EPIDERMAL PATTERNING FACTOR 2-like	1.72	-2.77	-1.47	-2.59	-1.3	-1.46	-1.69
gi|270306970	ACZ71729.1	Protein FLUORESCENT IN BLUE LIGHT, chloroplastic isoform X1	1.09	1.355	-2.19	1.87	1.385	-1.35	1.43
gi|1141784	AAB07225.1	Protein SLE2	-1.55	-2.28	-1.27	-1.68	-1.09	-2.04	-2.12
gi|212275286	NP_001130992.1	Protein WVD2-like 5	1.35	-2.4	-1.46	-1.96	1.27	1.155	-2.2
gi|195652255	ACG45595.1	Protein WVD2-like 5	1.175	1.425	-1.53	1.375	1.215	-1.89	1.32
gi|255564613	XP_002523301.1	Protein yippee-like At4g27745	1.21	-3.1	1.05	-2.48	1.2	-1.49	-1.22
gi|45533925	AAS67334.1	Protein YLS9-like	-1.42	-1.85	-1.2	1.605	-1.59	-1.33	-1.67
gi|222630446	EEE62578.1	Pseudo histidine-containing phosphotransfer protein 2	1.51	1.87	0.11	-1.5	1.23	1.215	-1.58
gi|168809271	ACA29392.1	Pseudo-response receiver	-1.25	1.59	1.415	1.16	1.325	-1.21	1.435
gi|53791569	BAD52691.1	Putative Bowman Birk trypsin inhibitor	1.05	1.46	-1.53	1.44	1.275	-1.5	-1.86
gi|108796756	YP_636482.1	Putative chloroplast RF66 (chloroplast)	-1.09	-2.14	-1.4	-2.73	1.085	-2.24	-1.08
gi|224132552	XP_002321348.1	Putative F-box/FBD/LRR-repeat protein At1g78840	-1.74	-1.91	-0.29	-1.65	-1.35	-1.12	-1.57
gi|213958295	ACJ54654.1	Putative methionyl-tRNA synthetase	1.58	1.64	1.8	-0.08	1.205	-1.07	-1.47
gi|18423398	NP_568773.1	Putative rRNA 2'-O-methyltransferase fibrillarin 3	-1.24	-1.3	1.24	1.45	-1.25	1.37	-1.56
gi|255542090	XP_002512109.1	Putative SNAP25 homologous protein SNAP30	-1.38	2.445	1.315	-0.29	1.47	1.025	1.655
gi|15228199	ABA97802.2	Putative, Retrotransposon protein, Ty3-gypsy subclass	1.13	-2.53	-1.44	1.215	1.36	1.36	-1.75
gi|157086556	AAX96116.1	Putative, Retrotransposon, centromere-specific	-1.23	-1.39	-1.37	-2.57	-1.75	-1.52	1.05
gi|51536238	ACU15849.1	Putative, Transmembrane protein	-1.19	1.54	1.275	1.125	1.51	-1.41	-1.73
gi|149390755	AAX96588.1	Putative, Transposable element protein, Retrotrans_gag	1.185	1.78	-1.49	-2.31	1.14	-1.45	-1.42
gi|108862524	ABA98441.1	Putative, Transposon protein,	-1.1	1.61	1.38	1.65	1.2	-1.65	1.15

		CACTA, En/Spm sub-class							
gi|62734007	NP_188264.1	Pyk10-binding protein 1	1.15	1.52	1.37	1.9	1.355	-2.47	1.09
gi|294864350	ABV21224.1	Pyrophosphate--fructose 6-phosphate 1-phosphotransferase subunit beta	-1.61	-2.26	-1.59	-1.42	1.15	1.28	1.27
gi|313183891	BAD38408.1	Receptor-like protein 2	-1.55	-2.05	-1.9	1.5	1.41	-1.79	-2.05
gi|56180897	ABR25395.1	Remorin	1.085	-1.75	1.58	1.455	-1.27	-1.03	-1.4
gi|148907015	ADF46049.1	Reverse transcriptase	-1.02	1.32	1.14	-3.16	-1.36	-1.95	1.16
gi|79325265	YP_004021745.1	Ribosomal protein L22 (chloroplast)	1.155	-2.31	1.13	2.105	-1.33	-2.02	1.345
gi|255567135	AAV83543.1	Ribosomal protein S19 (chloroplast)	1.23	-2.72	-1.21	-1.65	-1.47	-1.1	-2.31
gi|256567906	ABR16651.1	Ribosomal RNA small subunit methyltransferase	1.24	1.645	-1.42	1.465	-1.21	-1.27	-1.19
gi|154705504	NP_001031718.1	RNA binding Plectin/S10 domain-containing protein	1.435	-1.28	-1.13	-1.51	-1.23	1.255	1.285
gi|7209504	XP_002524549.1	RNA polymerase C (plastid)	1.22	-1.44	1.305	1.21	-1.07	-1.49	-1.4
gi|148356707	ACU87438.1	RNA polymerase subunit (plastid)	1.07	-1.31	1.15	1.465	-1.13	-1.32	-1.19
gi|257209021	ABS84178.1	RNase S6	1.19	-1.34	-0.13	-1.55	-1.59	-2.2	-1.5
gi|50251378	BAA92247.1	S locus protein 11	1.275	-3.09	-0.75	-1.07	-1.17	1.16	-1.37
gi|115474139	BAF63026.1	Serine racemase	-1.11	-1.57	-1.34	-3.68	-1.19	-1.25	1.105
gi|4160416	CBB36498.1	Sorghum bicolor protein targeted either to mitochondria or chloroplast proteins T50848	1.305	-1.42	1.13	1.85	-1.69	-2.36	1.215
gi|255565226	BAD28405.1	Splicing coactivator subunit-like protein	1.315	-2.45	1.09	-1.35	-1.54	-1.47	-1.2
gi|218199733	NP_001060668.1	Stress responsive protein	-1.52	-3.75	-1.51	-1.16	-0.14	-1.99	-1.89
gi|226531284	AAD05231.1	Stylar self-incompatibility protein	1.095	1.215	-2.81	-1.16	-1.06	-1.3	-1.4
gi|159480794	XP_002523605.1	Subtilisin-like protease SBT1.9	1.21	1.525	1.64	1.345	1.325	-1.23	-1.36
gi|297852252	EEC82160.1	Succinate dehydrogenase subunit 3	-2.02	-2.43	-1.95	-2.65	-2.74	-1.34	-2.67

gi|15222488	NP_001147086.1	Thiol protease SEN102 precursor	1.06	-2.45	-1.65	-1.17	-1.87	-1.71	1.305
gi|255074655	XP_001698467.1	Thioredoxin	1.11	-1.18	1.05	1.83	-1.34	-1.41	1.195
gi|5230656	XP_002894007.1	Thioredoxin H5	-1.39	-1.28	-2.51	-2.79	-1.39	-1.6	-1.84
gi|195643542	NP_177146.1	Thioredoxin H8	1.415	1.455	-1.03	-2.3	1.36	-1.17	-1.36
gi|302761140	XP_002501002.1	Thioredoxin-like 3-3	-1.17	1.565	1.055	1.36	1.925	-1.33	-1.35
gi|145346800	AAD40953.1	Transcription factor AS1	-1.31	-3.16	-1.25	1.485	-2.26	-2.52	1.04
gi|255630970	ACG41239.1	Transmembrane protein	1.12	-2.63	-1.79	-2.12	-1.28	1.435	-1.83
gi|62734479	XP_002963992.1	Transmembrane protein	0.235	-1.22	-1.23	1.165	-1.73	-1.4	1.11
gi|77555645	XP_001417870.1	Transmembrane protein 120 homolog	-1.75	1.6	1.27	1.65	1.315	-1.12	-2.56
gi|224142047	XP_002324370.1	Transposon Tf2-12 polyprotein	-1.58	1.64	-2.09	-1.47	1.225	-2.07	-2.73
gi|147782013	CAN76654.1	Transposon Ty3-G Gag-Pol polyprotein	-1.33	-3.57	-2	-3.11	-1.57	-2.27	-1.47
gi|162459877	NP_001105107.1	Ubiquitin-conjugating enzyme E2 7	-1.14	-3.5	-0.8	2.69	-1.14	-1.15	-1.59
gi|31088843	sp|Q42540.1	Ubiquitin-conjugating enzyme E2 7	1.18	-1.77	1.945	-1.83	-1.59	1.205	-1.26
gi|18408206	NP_566884.1	Ubiquitin-conjugating enzyme E2 7	1.19	1.865	-1.69	-1.81	1.415	1.295	-2.03
gi|302804260	XP_002983882.1	UBP1-associated protein 2C-like	1.21	1.51	1.38	2.16	1.79	-1.95	-1.91
gi|302784754	XP_002974149.1	Uncharacterized protein LOC9655997	1.295	1.55	-1.43	-1.09	1.875	-2.93	-1.14
gi|302148438	BAJ14098.1	V-type proton ATPase catalytic subunit A	1.19	-1.13	-1.34	-1.42	-1.79	1.365	1.06
gi|222822683	ACM68454.1	Zinc finger A20 and AN1 domain-containing stress-associated protein 8-like	1.08	1.375	-1.38	-2.53	-1.25	-1.42	-1.28
gi|12322419	AAG51230.1	Zinc finger CCCH domain-containing protein 4-like	-1.08	-1.91	-1.77	-2.23	-1.8	-1.33	-1.3

Table 6.3: Proteins detected during the winter season from the leaves of *S. fruticosa*

Protein ID	>FASTA name	Protein description	Time of the day						
			2am	5am	11am	2pm	5pm	8pm	11pm
gi|147765954	CAN59951.1	11S globulin seed storage protein 2	-2.76	1.44	-1.22	1.81	-1.27	-1.49	-1.49
gi|2492488	sp|Q41418.1	14-3-3-like protein	-2.55	-1.67	-1.23	1.605	1.17	1.515	-1.08
gi|316937092	ADU60530.1	14-3-3-like protein C	1.26	-1.74	1.305	1.4	1.445	1.35	1.025
gi|11138322	BAB17822.1	14-3-3-like protein C	-1.56	-1.99	-1.36	1.31	-1.11	1.145	-1.28
gi|255558874	XP_002520460.1	18.1 kDa class I heat shock protein	-1.13	1.195	-1.55	1.19	1.215	-1.21	-1.16
gi|110816068	YP_684400.1	30S ribosomal protein S11	-1.08	1.075	1.065	1.37	-1.29	1.33	1.05
gi|157849590	ABV89582.1	4-hydroxy-3-methylbut-2-enyl diphosphate reductase, chloroplastic-like	1.11	-1.12	-1.17	1.125	-1.01	-1.13	-1.13
gi|14575543	CAA55659.2	4-hydroxy-tetrahydrodipicolinate synthase, chloroplastic	1.125	-1.05	-1.28	1.15	-1.11	1.14	1.24
gi|42572781	NP_974486.1	50S ribosomal protein L1, chloroplastic	1.1	1.575	1.305	2.015	1.1	-1.69	-1.12
gi|115438116	NP_001043461.1	50S ribosomal protein L25	-1.3	1.295	-2.45	1.43	1.62	-1.57	-1.26
gi|327493145	AEA86279.1	ABC transporter family protein	1.095	-1.69	-1.15	-1.1	1.055	1.275	1.25
gi|15221890	NP_175874.1	Agamous-like MADS-box protein AGL29	1.095	-1.43	-1.16	-1.13	-1.15	1.06	-1.25
gi|15229233	NP_187064.1	Ankyrin repeat family protein	1.155	-1.48	1.27	1.06	-1.58	1.165	-1.06
gi|298569868	ADI87449.1	Jasmonic acid carboxyl methyltransferase	-1.28	-1.28	-1.83	1.65	1.42	1.38	1.25
gi|2632103	CAB11467.1	Arginyl-tRNA synthetase, class Ic	1.07	-1.39	-1.05	1.155	-1.24	1.365	1.305

gi|224038410	ACN38309.1	ARGOS-like protein	-1.76	1.55	-1.18	-1.26	-1.22	-1.23	-1.13
gi|624672	AAA82741.1	ASR	-2.29	-2.19	-1.64	1.72	1.18	1.37	-1.14
gi|20563267	AAM27953.1	At5g03840	1.2	1.485	-1.53	-1.37	1.15	-1.08	1.135
gi|228017304	ACP52122.1	ATP synthase CF0 B subunit (chloroplast)	-1.46	-1.36	1.435	1.41	1.265	1.325	-1.27
gi|29565571	NP_817148.1	ATP synthase cf0 b subunit (chloroplast)	-1.04	1.465	1.385	1.21	-1.44	-1.59	-1.43
gi|38567798	CAE76084.1	B1340F09.22	1.37	-1.22	-1.22	-1.35	1.22	-1.31	-1.08
gi|168007657	XP_001756524.1	BTB/POZ domain-containing protein At3g56230 isoform X1	-1.71	1.385	-1.17	1.215	1.12	1.68	1.115
gi|297846056	XP_002890909.1	Cell growth defect protein	1.17	1.62	1.505	-1.42	-1.14	1.21	1.135
gi|224088202	XP_002308368.1	Centromere-associated protein E isoform X1	1.165	-1.7	-1.1	1.115	1.215	1.14	1.285
gi|7258408	CAB77451.1	Chitinase, partial	1.225	1.12	-2.52	1.27	1.08	1.27	-1.2
gi|226490526	BAH56544.1	CLAVATA3/endosperm surrounding region 13	-1.45	1.085	1.14	1.335	-1.29	1.29	-2.07
gi|296006082	BAJ07539.1	Cold-responsive protein WCOR15-2A	1.14	-1.06	-1.72	-1.22	1.295	-1.12	-1.68
gi|255560737	XP_002521382.1	Conserved hypothetical protein	-1.23	-1.09	1.585	1.33	1.095	-1.4	1.19
gi|3929325	AAC79873.1	Cyclic dof factor 3-like	-1.16	-1.66	1.39	-1.24	-1.11	-1.17	1.145
gi|18424030	NP_568867.1	Cytochrome c oxidase subunit 6b-3	-1.14	-1.3	1.095	1.21	-1.1	-1.2	-1.22
gi|57546342	AAW52039.1	Cytochrome P450	-1.81	1.475	1.565	-1.35	-1.22	-1.02	-1.48
gi|226694227	sp|P0C8Y5.1	DEF1_HEUSARecName: Full=Defensin-like protein 1; AltName: Full=Cysteine-rich antifungal protein 1; AltName: Full=Defensin AFP1; Short=HsAFP1	-1.25	1.36	-1.11	1.505	1.495	1.38	-2.25
gi|139005020	BAF52544.1	Defensin-like protein	1.04	1.09	1.5	1.04	-1.14	1.455	-1.24

gi|115466620	NP_001056909.1	Dehydration-responsive element-binding protein 1A	1.035	-1.54	1.175	1.25	1.27	1.135	1.145
gi|301139697	ADK66263.1	Dehydrin ERD10-like	-1.64	1.265	-2.73	-1.28	1.265	-1.35	-1.28
gi|50299542	AAT73629.1	Diacylglycerol O-acyltransferase 1C	-1.13	1.395	1.455	1.1	1.045	1.12	1.175
gi|12248378	BAB20075.1	Dihydroflavonol 4-reductase	-1.33	-1.51	1.97	-1.12	1.285	1.185	-1.33
gi|51558023	AAU06584.1	Dihydroflavonol 4-reductase	-1.08	-1.39	-3.06	-1.52	1.245	-1.33	1.275
gi|328796759	AEB40418.1	DNAJ heat shock N-terminal domain-containing protein	-1.02	-1.27	-2.11	1.255	1.445	-1.48	-1.09
gi|262212637	ACY35971.1	Dof-type zinc finger protein	-1.35	-1.14	1.555	1.49	-1.34	-1.42	1.22
gi|108711833	ABF99628.1	Dolichol-phosphate mannosyltransferase subunit 1	-1.15	-1.39	-1.25	-1.32	1.345	-1.29	-1.16
gi|323282157	ADX35881.1	Dolichyl-diphosphooligosaccharide protein glycosyltransferase subunit STT3A	-1.73	1.37	1.415	1.555	1.395	-1.48	-1.67
gi|255582119	XP_002531854.1	E3 ubiquitin-protein ligase RING1-like	-1.13	-1.51	1.13	1.46	1.015	-1.41	1.095
gi|255602381	XP_002537843.1	Elongation factor G	-1.48	1.6	-1.49	1.205	1.38	-1.15	1.26
gi|15225842	NP_180273.1	ETHYLENE INSENSITIVE 3-like 1 protein	-3.41	1.465	1.475	-1.39	-1.5	-1.41	-1.39
gi|147801420	CAN68056.1	F-box/FBD/LRR-repeat protein At1g13570-like	-2.19	1.22	-1.41	-1.11	1.1	1.24	1.16
gi|47824945	AAT38719.1	F-box/kelch-repeat protein At3g23880-like	-1.23	-1.42	-3.67	1.555	-1.68	-1.69	-1.29
gi|323444150	ADX68824.1	Flavanone 3-hydroxylase	1.07	-1.36	-3.12	-1.23	1.27	1.215	1.07
gi|108708342	ABF96137.1	Flavonoid 3',5'-hydroxylase 1	1.16	1.175	-2.78	-1.34	-1.14	1.38	-1.25
gi|22135898	AAM91531.1	Floral homeotic protein APETALA 2	1.09	-2.06	1.135	1.55	-1.18	1.425	-1.18
gi|226496826	NP_001152602.1	Gibberellin-regulated protein 1	-1.56	-1.14	-1.79	-2.09	-1.27	1.54	1.135

gi|195650967	ACG44951.1	Gibberellin-regulated protein 2 precursor	1.085	-2.3	-1.07	1.12	-1.17	-1.03	1.215
gi|3868853	BAA34247.1	GPI-anchored protein LLG1	1.115	-1.73	1.395	-1.42	1.11	-1.14	1.14
gi|162463546	NP_001105546.1	GTP-binding protein YPTM1	-1.24	1.305	-0.02	1.38	-1.47	1.51	1.365
gi|227603	prf||1707300A	GTP-binding protein YPTM1	-1.25	1.525	-2.52	1.355	1.215	1.4	1.32
gi|51104295	AAT96693.1	G-type lectin S-receptor-like serine/threonine-protein kinase LECRK3	-1.24	-1.29	1.22	1.12	1.245	1.22	-1.16
gi|47971184	BAD22534.1	Harpin inducing protein	-1.52	-1.5	1.46	1.05	-1.18	-1.16	-1.2
gi|302121697	ADK92863.1	Histidine kinase 2	1.125	-1.17	1.135	1.23	-1.29	1.255	1.05
gi|56784402	BAD82441.1	Hypothetical protein	-1.43	1.75	1.13	1.155	1.24	1.345	-1.4
gi|40538962	AAR87219.1	Hypothetical protein	1.025	1.455	2.25	1.41	1.16	-1.11	1.325
gi|125589199	EAZ29549.1	Hypothetical protein OsJ_13623	1.02	-1.44	-1.03	1.27	1.36	1.83	-1.19
gi|147800133	CAN73206.1	Hypothetical protein VITISV_009746	-1.58	-1.22	1.1	1.38	1.085	1.13	1.085
gi|147859750	CAN78710.1	Hypothetical protein VITISV_043136	-2.19	68.07	-1.52	1.385	1.15	-1.59	-1.35
gi|302853022	XP_002958028.1	Hypothetical protein VOLCADRAFT_99231	-1.44	1.355	-1.57	1.31	1.535	-1.2	-1.66
gi|224082806	XP_002306846.1	Inorganic phosphate transporter 1-4	-1.39	-1.16	1.265	1.19	1.14	1.115	1.12
gi|125003	sp|P09407.1	ITI3_MOMCHRecName: Full=Trypsin inhibitor MCI-3	1.28	-1.38	-2.34	1.11	-1.17	1.14	1.21
gi|224179497	YP_002601027.1	L protein of photosystem II (chloroplast)	-2.31	-1.16	1.605	1.43	-1.33	-1.69	-0.28
gi|297831316	XP_002883540.1	Late embryogenesis abundant protein (LEA) family protein	-1.41	-1.26	1.25	1.44	1.45	-1.8	1.435
gi|297611560	NP_001067600.2	Leucine-rich repeat protein kinase family protein	-1.47	1.365	-1.9	1.23	1.21	-1.06	1.215
gi|225425967	XP_002269216.	Lignin-forming anionic	-1.04	-3.69	1.37	-1.09	-1.18	1.32	-1.21

	1	peroxidase							
gi|242040459	XP_002467624.1	LysM domain containing protein	-1.04	-0.25	1.105	1.47	-1.39	-1.44	-1.25
gi|2281237	AAB64056.1	Maturase (chloroplast)	-1.2	-1.22	-1.98	1.505	-1.47	1.335	-1.17
gi|296171301	CBI71372.1	Maturase K (chloroplast)	-1.12	-1.35	-1.46	1.32	-1.18	1.375	1.115
gi|28804507	BAC57959.1	Metallothionein-like protein 1	1.37	-2.51	-1.48	-1.47	1.32	-1.53	-0.2
gi|18652285	AAL77049.1	Metallothionein-like protein 1	-1.47	-1.58	1.435	1.41	1.37	1.31	-1.07
gi|303276647	XP_003057617.1	Methionine-tRNA ligase	-1.6	-1.44	1.1	1.16	1.31	-1.34	-1.32
gi|18414298	NP_568125.1	Monodehydroascorbate reductase 2	-1.65	-1.45	2.245	1.305	1.195	1.25	1.075
gi|119434027	ABL75109.1	---NA---	1.485	-1.13	1.445	1.555	1.57	-1.77	-1.3
gi|330318652	AEC10986.1	---NA---	-3.47	-1.27	1.495	1.725	1.2	-1.36	-1.6
gi|168033184	XP_001769096.1	---NA---	1.07	-1.79	0.08	1.58	1.265	1.375	1.13
gi|30315163	AAP30805.1	---NA---	-1.24	-1.18	1.505	1.22	-1.4	-1.7	-1.23
gi|154269004	ABS72216.1	---NA---	-1.49	1.365	1.49	-1.25	-1.2	-1.43	-1.15
gi|302143158	CBI20453.3	---NA---	1.1	0.33	-1.19	-1.24	-1.04	1.215	1.125
gi|242074306	XP_002447089.1	NAD(P)-binding Rossmann-fold superfamily protein	1.225	-1.7	-1.16	1.23	-1.11	-1.55	-1.12
gi|42569711	NP_181313.3	NAD(P)-linked oxidoreductase superfamily protein	-1.45	1.525	1.585	1.13	-1.07	1.485	1.13
gi|308809874	XP_003082246.1	NAD-dependent epimerase/dehydratase family protein	1.48	-1.55	-1.09	-1.08	1.065	1.16	1.3
gi|307108859	EFN57098.1	NADH dehydrogenase [ubiquinone] iron-sulfur protein 4, mitochondrial	1.12	-1.32	-1.37	1.535	1.085	-1.47	1.28
gi|118140538	CAL69657.1	NBS-LRR resistance protein	1.09	-2.5	1.425	1.145	-1.22	1.435	1.205
gi|729135	sp|Q06509.1	O-methyltransferase	-1.15	-1.85	1.22	1.545	1.14	-1.11	-1.15
gi|33641720	AAQ24345.1	O-methyltransferase	-1.57	1.33	1.21	-1.51	1.105	-1.31	-1.05

gi|195636260	ACG37598.1	O-methyltransferase	-1.28	-1.09	-1.48	1.165	0.045	-1.52	1.065
gi|224077820	XP_002305422.1	Organ-specific protein P4-like	-1.88	1.315	-1.08	-1.49	-1.53	-1.61	-1.51
gi|297721633	NP_001173179.1	Os02g0793150	-1.17	-1.34	1.04	1.46	1.435	-1.27	-1.63
gi|11934654	AAG41763.1	P23A_BRANARecName: Full=Co-chaperone protein p23-1; AltName: Full=Bnp23-1	-1.7	1.21	1.11	1.27	1.405	1.21	-1.23
gi|297830098	XP_002882931.1	P53/DNA damage-regulated protein	-1.29	-2.74	-2.36	1.075	1.235	-1.6	-1.24
gi|224105841	XP_002313951.1	Peptide methionine sulfoxide reductase B5-like	1.12	1.275	-1.28	1.25	1.125	1.24	1.05
gi|302819856	XP_002991597.1	Peptidyl-prolyl cis-trans isomerase FKBP20-2, chloroplastic	1.085	-1.73	2.295	1.33	1.29	1.285	1.33
gi|159470805	XP_001693547.1	Peptidyl-prolyl cis-trans isomerase FKBP20-2, chloroplastic	-1.58	-1.05	-1.23	1.41	1.185	-1.44	-1.08
gi|15240486	NP_200335.1	PEROXYGENASE 2	-1.36	1.475	1.41	1.455	1.42	1.335	1.225
gi|307105956	EFN54203.1	Phosphatidylinositol N-acetylglucosaminyltransferase subunit P	-1.2	1.455	1.24	-1.14	-1.14	-1.24	-1.15
gi|10303403	CAA65117.1	Phosphoenolpyruvate carboxylase	1.085	1.515	-1.22	-1.09	0.26	1.33	1.07
gi|145346793	XP_001417867.1	Photosystem II PsbR protein, chloroplast precursor	1.1	-1.54	-1.13	1.205	-1.06	1.285	1.12
gi|87241065	ABD32923.1	Polynucleotidyl transferase, Ribonuclease H fold	-1.41	-1.29	-2.39	-1.27	-1.04	-1.06	1.335
gi|53749467	AAU90321.1	Polyprotein, related	-1.91	-1.24	-1.25	-1.01	1.09	1.255	1.365
gi|307104521	EFN52774.1	Predicted protein	-1.54	-1.7	-1.21	1.385	-1.12	1.26	1.19
gi|303282497	XP_003060540.1	Predicted protein	0.35	-1.18	1.03	1.56	-1.49	-1.46	-1.44
gi|308802616	XP_003078621.	Predicted protein	-1.27	1.115	1.465	1.27	1.545	-1.21	-1.09

	1								
gi|104294980	ABF71996.1	2-oxoglutarate-dependent dioxygenase	-1.26	-0.63	1.23	1.065	-1.05	-1.33	-1.09
gi|11385435	AAG34800.1	Probable glutathione S-transferase	1.14	-1.37	1.125	1.3	-1.09	1.365	1.33
gi|108863932	ABA91188.2	Probable serine/threonine-protein kinase WNK5	1.14	-1.37	1.125	1.65	1.35	1.275	1.24
gi|255613348	XP_002539501.1	Probable WRKY transcription factor 40	-1.2	1.375	-1.14	-1.26	1.53	-1.25	-0.05
gi|225166539	ACN81327.1	Prolycopene isomerase, chloroplastic	-2.89	-1.43	-1.51	-1.4	-1.37	-1.39	1.14
gi|41352687	AAS01050.1	Proteasome subunit beta type-5-B	-1.04	-1.37	1.175	1.26	1.4	-1.29	1.07
gi|21592365	AAM64316.1	Proteasome subunit beta type-6	-1.32	1.515	1.095	-1.07	1.25	1.155	1.085
gi|15235889	NP_194858.1	Proteasome subunit beta type-6	-1.53	-1.33	-1.06	1.14	-1.07	1.44	-1.1
gi|41352683	AAS01048.1	Proteasome subunit beta type-6	-1.49	-1.5	3.545	1.285	1.35	1.25	1.12
gi|255553675	XP_002517878	Protein ARABIDOPSIS THALIANA ANTHER 7	-1.52	1.725	1.27	1.11	-1.2	1.21	1.155
gi|29367477	AAO72594.1	Protein DA1-related 1-like	1.085	1.415	1.125	1.26	-1.11	1.35	-1.19
gi|125548557	EAY94379.1	Protein EPIDERMAL PATTERNING FACTOR 2-like	-1.1	-1.96	-2.27	-1.3	1.38	-1.38	1.475
gi|270306970	ACZ71729.1	Protein FLUORESCENT IN BLUE LIGHT, chloroplastic isoform X1	1.06	1.22	1.12	1.17	1.215	1.23	1.11
gi|1141784	AAB07225.1	Protein SLE2	-1.24	1.46	1.705	1.31	-1.52	-1.34	1.32
gi|212275286	NP_001130992.1	Protein WVD2-like 5	-1.05	-2.09	-3.34	1.17	-1.32	0.07	1.065
gi|195652255	ACG45595.1	Protein WVD2-like 5	1.005	1.56	1.27	1.22	-1.31	1.33	-1.48
gi|255564613	XP_002523301.1	Protein yippee-like At4g27745	1.055	-1.48	1.105	1.51	1.29	-1.07	-1.09

gi|45533925	AAS67334.1	Protein YLS9-like	-2.97	1.52	1.36	1.17	1.045	-1.53	1.145
gi|222630446	EEE62578.1	Pseudo histidine-containing phosphotransfer protein 2	1.105	1.135	1.3	1.15	1.315	-1.18	1.275
gi|168809271	ACA29392.1	Pseudo-response receiver	-1.23	1.05	-1.36	-1.44	1.3	-1.38	-1.22
gi|53791569	BAD52691.1	Putative Bowman Birk trypsin inhibitor	-1.5	-1.3	-1.62	1.47	-1.24	1.315	1.39
gi|108796756	YP_636482.1	Putative chloroplast RF66 (chloroplast)	-1.68	1.355	1.43	1.305	-1.14	-1.39	1.04
gi|224132552	XP_002321348.1	Putative F-box/FBD/LRR-repeat protein At1g78840	-2.51	1.16	1.325	1.83	1.33	-1.52	-1.39
gi|213958295	ACJ54654.1	Putative methionyl-tRNA synthetase	-1.53	1.535	-1.17	-1.26	-1.28	-1.77	-1.42
gi|18423398	NP_568773.1	Putative rRNA 2'-O-methyltransferase fibrillarin 3	-1.16	-3.08	-1.17	-1.55	-1.34	-1.28	-1.21
gi|255542090	XP_002512109.1	Putative SNAP25 homologous protein SNAP30	-1.41	1.345	-1.45	-1.61	-1.13	1.49	-1.04
gi|15228199	ABA97802.2	Putative, Retrotransposon protein, Ty3-gypsy subclass	1.155	-1.62	1.195	1.21	1.065	1.11	-1.26
gi|157086556	AAX96116.1	Putative, Retrotransposon, centromere-specific	1.2	1.43	1.18	1.075	1.045	-3.17	1.165
gi|51536238	ACU15849.1	Putative, Transmembrane protein	-1.09	-1.15	-1.03	1.405	1.3	-2.35	-1.23
gi|149390755	AAX96588.1	Putative, Transposable element protein, Retrotrans_gag	1.355	1.135	-2.18	1.595	-1.31	-1.46	-1.39
gi|108862524	ABA98441.1	Putative, Transposon protein, CACTA, En/Spm sub-class	1.395	-1.25	1.175	-1.09	-1.05	1.3	1.1
gi|62734007	NP_188264.1	Pyk10-binding protein 1	-1.09	-1.61	1.2	1.18	-1.11	1.265	1.29
gi|294864350	ABV21224.1	Pyrophosphate--fructose 6-phosphate 1-phosphotransferase subunit beta	-1.16	-3.36	1.195	-1.1	-1.21	1.15	1.11
gi|313183891	BAD38408.1	Receptor-like protein 2	-1.34	-1.55	-2.73	-1.38	-1.19	1.12	1.12

gi|56180897	ABR25395.1	Remorin	-1.51	1.355	1.25	1.11	-1.31	-1.37	-1.11
gi|148907015	ADF46049.1	Reverse transcriptase	-1.31	-2.29	1.51	1.345	1.195	1.07	-1.14
gi|79325265	YP_004021745.1	Ribosomal protein L22 (chloroplast)	-1.1	-1.48	1.33	1.265	1.185	-1.64	1.24
gi|255567135	AAV83543.1	Ribosomal protein S19 (chloroplast)	-1.56	1.46	1.375	1.38	-1.29	-1.53	-1.8
gi|256567906	ABR16651.1	Ribosomal RNA small subunit methyltransferase	1.135	-2.24	1.345	1.235	1.195	1.115	1.22
gi|154705504	NP_001031718.1	RNA binding Plectin/S10 domain-containing protein	-1.41	-1.29	1.075	-1.23	1.235	1.37	1.105
gi|7209504	XP_002524549.1	RNA polymerase C (plastid)	-1.64	-1.19	1.15	1.535	-1.53	-1.75	-1.25
gi|148356707	ACU87438.1	RNA polymerase subunit (plastid)	-1.55	-1.63	1.83	-1.2	1.52	-1.11	1.185
gi|257209021	ABS84178.1	RNase S6	1.175	-0.25	-1.56	-1.49	1.58	-1.62	-1.25
gi|50251378	BAA92247.1	S locus protein 11	-1.94	-1.41	-1.49	-1.61	1.4	1.47	-1.28
gi|115474139	BAF63026.1	Serine racemase	-3.22	-1.16	1.12	-1.01	1.185	1.175	-1.13
gi|4160416	CBB36498.1	Sorghum bicolor protein targeted either to mitochondria or chloroplast proteins T50848	1.315	1.445	1.145	-1.3	-1.15	1.295	1.27
gi|255565226	BAD28405.1	Splicing coactivator subunit-like protein	1.05	-2.23	-1.09	-1.07	1.155	-1.09	-1.22
gi|218199733	NP_001060668.1	Stress responsive protein	-3.35	-2.01	-1.25	1.7	1.44	-1.37	-1.76
gi|226531284	AAD05231.1	Stylar self-incompatibility protein	-1.89	-0.17	1.435	-1.38	1.075	1.245	-1.34
gi|159480794	XP_002523605.1	Subtilisin-like protease SBT1.9	-1.42	1.27	1.46	1.175	1.305	-1.12	1.145
gi|297852252	EEC82160.1	Succinate dehydrogenase subunit 3	-2.37	-1.32	-1.24	1.925	1.45	-0.15	1.345
gi|15222488	NP_001147086.1	Thiol protease SEN102 precursor	-1.57	-1.32	0.07	1.36	-1.26	1.61	-1.46

gi|255074655	XP_001698467.1	Thioredoxin	-1.31	-1.36	-1.52	-1.23	1.25	-1.5	1.23
gi|5230656	XP_002894007.1	Thioredoxin H5	-2.85	1.47	1.2	1.945	1.435	-1.54	-1.3
gi|195643542	NP_177146.1	Thioredoxin H8	1.48	1.285	1.405	1.495	1.1	-1.7	-1.07
gi|302761140	XP_002501002.1	Thioredoxin-like 3-3	-1.28	-1.11	-1.25	-1.12	1.23	1.28	-1.1
gi|145346800	AAD40953.1	Transcription factor AS1	-1.44	-1.74	1.435	-1.01	1.15	1.175	1.135
gi|255630970	ACG41239.1	Transmembrane protein	-1.67	-1.15	1.495	-1.1	1.48	-1.36	-1.27
gi|62734479	XP_002963992.1	Transmembrane protein	1.03	1.37	1.26	-1.34	-1.47	-1.67	1.215
gi|77555645	XP_001417870.1	Transmembrane protein 120 homolog	-2.12	-1.62	-1.37	1.265	1.21	1.375	1.245
gi|224142047	XP_002324370.1	Transposon Tf2-12 polyprotein	-3.18	-1.56	-1.65	-1.41	-1.63	-1.76	-2.53
gi|147782013	CAN76654.1	Transposon Ty3-G Gag-Pol polyprotein	-1.25	-2.67	1.705	1.13	-1.4	-1.31	-1.22
gi|162459877	NP_001105107.1	Ubiquitin-conjugating enzyme E2 7	-2.56	1.175	-1.35	1.285	1.27	1.4	-1.52
gi|31088843	sp|Q42540.1	Ubiquitin-conjugating enzyme E2 7	-1.07	1.185	1.415	-1.27	-1.41	-1.31	1.355
gi|18408206	NP_566884.1	Ubiquitin-conjugating enzyme E2 7	-1.81	1.11	1.25	1.15	1.43	-1.32	-1.4
gi|302804260	XP_002983882.1	UBP1-associated protein 2C-like	-1.13	-1.67	1.225	1.33	1.27	-1.1	1.16
gi|302784754	XP_002974149.1	Uncharacterized protein LOC9655997	-1.48	-1.29	1.4	1.19	1.12	1.335	-1.25
gi|302148438	BAJ14098.1	V-type proton ATPase catalytic subunit A	-1.42	1.46	-1.22	-1.18	-1.08	1.235	1.22
gi|222822683	ACM68454.1	Zinc finger A20 and AN1 domain-containing stress-associated protein 8-like	-1.1	1.345	1.065	1.21	1.08	-1.12	-1.19
gi|12322419	AAG51230.1	Zinc finger CCCH domain-containing protein 4-like	1.415	1.095	-1.2	1.49	-1.35	-1.1	-1.11

Table 6.4: Proteins detected during the summer season from the leaves of *S. fruticosa*

Protein ID	>FASTA name	Protein description	Time of the day						
			2am	5am	11am	2pm	5pm	8pm	11pm
gi|147765954	CAN59951.1	11S globulin seed storage protein 2	-1.5	-1.92	-1.24	-1.4	-1.53	-1.21	-2.24
gi|2492488	sp|Q41418.1	14-3-3-like protein	-1.4	1.145	-2.47	1.34	-1.25	-1.05	-1.18
gi|316937092	ADU60530.1	14-3-3-like protein C	-1.21	-1.23	-1.47	1.775	1.245	-1.27	-1.17
gi|11138322	BAB17822.1	14-3-3-like protein C	1.08	1.19	1.08	-3.13	-1.1	-1.37	1.395
gi|255558874	XP_002520460.1	18.1 kDa class I heat shock protein	1.21	1.19	-1.22	-1.91	1.085	1.135	-1.1
gi|110816068	YP_684400.1	30S ribosomal protein S11	1.2	-1.19	1.095	1.235	1.27	1.1	-1.37
gi|157849590	ABV89582.1	4-hydroxy-3-methylbut-2-enyl diphosphate reductase, chloroplastic-like	1.23	1.18	-1.05	1.09	1.105	-1.51	-1.45
gi|14575543	CAA55659.2	4-hydroxy-tetrahydrodipicolinate synthase, chloroplastic	-1.15	-1.16	1.23	-1.44	1.25	1.12	1.21
gi|42572781	NP_974486.1	50S ribosomal protein L1, chloroplastic	-1.08	-1.14	1.065	1.28	1.125	1.1	-1.22
gi|115438116	NP_001043461.1	50S ribosomal protein L25	-1.38	-1.72	-1.4	1.665	-2.33	-1.06	-0.27
gi|327493145	AEA86279.1	ABC transporter family protein	-1.27	1.19	-1.24	-1.05	-1.65	1.34	1.265
gi|15221890	NP_175874.1	Agamous-like MADS-box protein AGL29	-1.01	1.31	1.105	1.135	1.155	-1.07	1.145
gi|15229233	NP_187064.1	Ankyrin repeat family protein	1.26	-1.25	1.115	1.315	1.275	-1.37	1.205
gi|298569868	ADI87449.1	Jasmonic acid carboxyl methyltransferase	-2.31	-1.89	-1.77	-1.38	-1.24	-1.04	-1.54
gi|2632103	CAB11467.1	Arginyl-tRNA synthetase, class Ic	1.15	-1.07	-1.19	1.105	-1.07	1.18	1.125
gi|224038410	ACN38309.1	ARGOS-like protein	1.01	1.215	-1.25	1.185	1.32	1.35	1.14
gi|624672	AAA82741.1	ASR	-1.16	1.4	1.035	-1.47	1.29	-1.38	-1.13
gi|20563267	AAM27953.1	At5g03840	1.165	1.135	-1.2	1.34	1.22	-1.25	1.095

gi|228017304	ACP52122.1	ATP synthase CF0 B subunit (chloroplast)	1.295	1.175	1.13	-1.96	1.18	1.16	1.315
gi|29565571	NP_817148.1	ATP synthase cf0 b subunit (chloroplast)	1.22	1.325	1.61	1.485	-1.36	-1.06	1.27
gi|38567798	CAE76084.1	B1340F09.22	-1.04	-1.67	1.39	-1.4	1.585	1.06	-1.5
gi|168007657	XP_001756524.1	BTB/POZ domain-containing protein At3g56230 isoform X1	1.16	-1.32	-1.14	1.265	1.165	-1.32	1.205
gi|297846056	XP_002890909.1	Cell growth defect protein	-1.2	1.085	1.19	1.19	1.285	1.175	-1.09
gi|224088202	XP_002308368.1	Centromere-associated protein E isoform X1	1.18	1.235	-1.08	-1.59	1.14	1.19	-1.13
gi|7258408	CAB77451.1	Chitinase, partial	-1.35	1.14	-1.31	-1.46	-1.21	1.055	-1.72
gi|226490526	BAH56544.1	CLAVATA3/endosperm surrounding region 13	1.34	-1.46	-1.3	1.335	1.64	1.05	1.37
gi|296006082	BAJ07539.1	Cold-responsive protein WCOR15-2A	1.15	-1.53	1.04	-1.41	-1.29	1.15	1.34
gi|255560737	XP_002521382.1	Conserved hypothetical protein	-1.48	1.635	-1.54	1.32	1.285	1.105	-0.33
gi|3929325	AAC79873.1	Cyclic dof factor 3-like	-1.18	1.325	-1.19	-1.43	1.26	-2.32	1.06
gi|18424030	NP_568867.1	Cytochrome c oxidase subunit 6b-3	1.355	1.305	1.195	-1.51	1.405	1.345	-1.53
gi|57546342	AAW52039.1	Cytochrome P450	-2.52	-1.31	-1.53	-1.95	-1.67	1.25	-1.78
gi|226694227	sp|P0C8Y5.1	DEF1_HEUSARecName: Full=Defensin-like protein 1; AltName: Full=Cysteine-rich antifungal protein 1; AltName: Full=Defensin AFP1; Short=HsAFP1	-1.75	-1.89	-1.4	-1.32	-1.31	-1.73	-2.05
gi|139005020	BAF52544.1	Defensin-like protein	1.085	-1.51	-1.45	1.39	-1.42	1.105	1.22
gi|115466620	NP_001056909.1	Dehydration-responsive element-binding protein 1A	1.07	1.135	-1.13	1.055	1.15	1.4	1.12
gi|301139697	ADK66263.1	Dehydrin ERD10-like	-2.59	-2.03	-1.66	1.14	-1.15	1.19	1.41
gi|50299542	AAT73629.1	Diacylglycerol O-acyltransferase 1C	-1.08	-1.04	1.04	-1.22	1.155	1.245	-1.23

gi|12248378	BAB20075.1	Dihydroflavonol 4-reductase	1.145	-1.27	-1.12	-1.55	-1.17	-1.42	1.25
gi|51558023	AAU06584.1	Dihydroflavonol 4-reductase	-1.72	-1.25	-1.37	1.3	1.1	-1.22	1.175
gi|328796759	AEB40418.1	DNAJ heat shock N-terminal domain-containing protein	1.37	-1.55	-1.88	1.23	1.25	1.19	-1.29
gi|262212637	ACY35971.1	Dof-type zinc finger protein	-1.22	-1.35	1.335	-1.46	1.31	-1.16	1.13
gi|108711833	ABF99628.1	Dolichol-phosphate mannosyltransferase subunit 1	-1.22	-1.08	-1.16	-1.47	-1.23	1.19	1.29
gi|323282157	ADX35881.1	Dolichyl-diphosphooligosaccharide protein glycosyltransferase subunit STT3A	-1.66	-1.1	-1.36	-1.57	-1.35	-1.11	1.27
gi|255582119	XP_002531854.1	E3 ubiquitin-protein ligase RING1-like	1.24	1.2	-1.36	-1.21	-1.76	-1.64	1.21
gi|255602381	XP_002537843.1	Elongation factor G	1.285	1.19	-1.08	1.06	1.115	-1.35	1.125
gi|15225842	NP_180273.1	ETHYLENE INSENSITIVE 3-like 1 protein	1.115	-1.35	-1.5	-1.78	-2.24	-1.11	-1.15
gi|147801420	CAN68056.1	F-box/FBD/LRR-repeat protein At1g13570-like	1.29	-1.27	1.095	1.325	-1.23	-1.22	1.26
gi|47824945	AAT38719.1	F-box/kelch-repeat protein At3g23880-like	-1.31	-1.3	1.13	1.435	1.13	1.32	1.275
gi|323444150	ADX68824.1	Flavanone 3-hydroxylase	-1.18	1.465	1.04	-1.34	-1.08	-1.26	-1.04
gi|108708342	ABF96137.1	Flavonoid 3',5'-hydroxylase 1	1.08	-1.63	1.085	1.445	1.2	1.08	1.205
gi|22135898	AAM91531.1	Floral homeotic protein APETALA 2	1.435	1.215	-1.27	-1.44	1.215	-1.21	1.255
gi|226496826	NP_001152602.1	Gibberellin-regulated protein 1	-1.2	-1.49	-1.32	-1.36	1.03	1.08	1.275
gi|195650967	ACG44951.1	Gibberellin-regulated protein 2 precursor	1.095	-1.36	-1.14	1.37	-1.14	1.155	-1.31
gi|3868853	BAA34247.1	GPI-anchored protein LLG1	1.29	-1.03	-1.09	-1.55	1.075	1.145	1.155
gi|162463546	NP_001105546.1	GTP-binding protein YPTM1	-2.49	-1.14	-1.35	1.215	1.54	-0.05	1.615
gi|227603	prf||1707300A	GTP-binding protein YPTM1	-1.5	-1.45	-1.57	-1.54	-1.17	-1.31	1.12
gi|51104295	AAT96693.1	G-type lectin S-receptor-like	1.235	1.125	1.22	1.27	-1.16	1.14	-1.29

		serine/threonine-protein kinase LECRK3							
gi|47971184	BAD22534.1	Harpin inducing protein	-1.32	1.175	1.06	1.31	1.415	1.175	1.1
gi|302121697	ADK92863.1	Histidine kinase 2	-1.53	1.12	1.265	1.21	-1.38	1.23	-1.17
gi|56784402	BAD82441.1	Hypothetical protein	1.215	1.14	1.045	-1.37	1.255	-1.19	-1.69
gi|40538962	AAR87219.1	Hypothetical protein	1.27	1.28	-1.22	-1.79	1.25	1.14	1.175
gi|125589199	EAZ29549.1	Hypothetical protein OsJ_13623	1.27	1.345	-1.18	-2.42	1.22	-1.35	-1.58
gi|147800133	CAN73206.1	Hypothetical protein VITISV_009746	1.165	1.305	-1.07	-1.55	1.31	-1.32	1.095
gi|147859750	CAN78710.1	Hypothetical protein VITISV_043136	1.575	-1.23	1.325	1.6	1.53	1.065	1.31
gi|302853022	XP_002958028.1	Hypothetical protein VOLCADRAFT_99231	-1.61	-1.77	-1.43	-1.51	1.36	-1.19	-1.5
gi|224082806	XP_002306846.1	Inorganic phosphate transporter 1-4	1.14	1.22	1.155	1.32	1.275	-1.12	1.16
gi|125003	sp|P09407.1	ITI3_MOMCHRecName: Full=Trypsin inhibitor MCI-3	1.055	-1.05	-1.36	1.3	1.105	1.155	1.145
gi|224179497	YP_002601027.1	L protein of photosystem II (chloroplast)	1.535	-1.15	-1.5	-1.62	-1.58	-1.2	1.305
gi|297831316	XP_002883540.1	Late embryogenesis abundant protein (LEA) family protein	-2.21	-1.39	-1.75	-2.01	-1.33	-1.04	-1.78
gi|297611560	NP_001067600.2	Leucine-rich repeat protein kinase family protein	1.11	1.175	-1.26	-1.21	1.36	-1.26	-3.2
gi|225425967	XP_002269216.1	Lignin-forming anionic peroxidase	-1.35	1.265	1.21	-2.47	-1.17	1.195	1.11
gi|242040459	XP_002467624.1	LysM domain containing protein	-1.68	-1.4	1.77	-1.88	1.395	1.27	-2.02
gi|2281237	AAB64056.1	Maturase (chloroplast)	-1.12	1.275	1.585	1.455	1.66	1.125	1.475
gi|296171301	CBI71372.1	Maturase K (chloroplast)	1.215	1.125	-1.07	1.195	-1.19	-1.41	-1.36
gi|28804507	BAC57959.1	Metallothionein-like protein 1	1.355	-1.39	1.32	-1.74	1.545	-1.22	0.015
gi|18652285	AAL77049.1	Metallothionein-like protein 1	-2.31	-2.54	1.625	-1.47	1.455	1.21	1.345
gi|303276647	XP_003057617.1	Methionine-tRNA ligase	1.09	1.095	1.095	-1.4	1.28	1.215	-1.27
gi|18414298	NP_568125.1	Monodehydroascorbate reductase	1.225	1.32	1.23	-1.26	1.325	-0.09	-0.02

		2							
gi|119434027	ABL75109.1	---NA---	-2.69	-1.31	-1.81	-1.92	-1.54	-3.04	-2.36
gi|330318652	AEC10986.1	---NA---	-2.8	-1.53	-2.47	-1.75	-1.22	-1.2	-1.55
gi|168033184	XP_001769096.1	---NA---	1.08	1.15	-1.14	-1.32	-1.03	1.11	1.195
gi|30315163	AAP30805.1	---NA---	-1.17	1.16	-1.1	1.515	1.335	-1.03	1.145
gi|154269004	ABS72216.1	---NA---	-1.26	-2.45	-1.39	1.35	1.115	-1.16	1.12
gi|302143158	CBI20453.3	---NA---	1.175	1.27	-1.27	-1.8	-1.21	1.13	1.125
gi|242074306	XP_002447089.1	NAD(P)-binding Rossmann-fold superfamily protein	1.25	-1.24	-1.23	-1.26	-1.31	1.2	-1.09
gi|42569711	NP_181313.3	NAD(P)-linked oxidoreductase superfamily protein	1.14	1.145	-1.6	1.36	1.58	-1.12	-1.05
gi|308809874	XP_003082246.1	NAD-dependent epimerase/dehydratase family protein	-1.18	-1.45	1.24	1.215	-2.23	-1.32	-1.95
gi|307108859	EFN57098.1	NADH dehydrogenase [ubiquinone] iron-sulfur protein 4, mitochondrial	1.09	-1.17	1.04	1.135	1.195	1.14	-1.12
gi|118140538	CAL69657.1	NBS-LRR resistance protein	1.26	-3.24	-1.13	1.145	-1.17	1.04	-1.04
gi|729135	sp|Q06509.1	O-methyltransferase	1.08	1.13	-1.21	-2.23	-1.09	1.05	1.265
gi|33641720	AAQ24345.1	O-methyltransferase	-1.19	-1.16	-1.1	1.625	1.165	-1.05	1.15
gi|195636260	ACG37598.1	O-methyltransferase	1.34	1.27	1.025	-1.91	-1.15	-1.08	1.275
gi|224077820	XP_002305422.1	Organ-specific protein P4-like	1.215	-1.54	-1.8	-1.58	-1.56	-1.15	1.37
gi|297721633	NP_001173179.1	Os02g0793150	-1.38	-1.55	-1.58	-1.7	-1.28	-1.21	1.395
gi|11934654	AAG41763.1	P23A_BRANARecName: Full=Co-chaperone protein p23-1; AltName: Full=Bnp23-1	1.14	-1.35	-1.23	1.15	1.295	-1.18	1.19
gi|297830098	XP_002882931.1	P53/DNA damage-regulated protein	1.19	-1.39	-1.22	-1.4	-1.11	1.11	-1.32
gi|224105841	XP_002313951.1	Peptide methionine sulfoxide reductase B5-like	-1.25	-1.13	-1.2	-1.22	1.26	1.14	1.225
gi|302819856	XP_002991597.1	Peptidyl-prolyl cis-trans	1.35	1.325	1.06	-1.37	-1.15	1.14	-1.06

		isomerase FKBP20-2, chloroplastic							
gi|159470805	XP_001693547.1	Peptidyl-prolyl cis-trans isomerase FKBP20-2, chloroplastic	-1.06	1.2	2.375	-1.47	1.12	-1.24	1.125
gi|15240486	NP_200335.1	PEROXYGENASE 2	-1.78	-1.43	-1.55	-1.74	-1.12	1.32	-1.6
gi|307105956	EFN54203.1	Phosphatidylinositol N-acetylglucosaminyltransferase subunit P	1.29	1.06	-1.1	1.5	-1.27	1.2	1.255
gi|10303403	CAA65117.1	Phosphoenolpyruvate carboxylase	1.105	1.22	1.18	-1.32	1.335	1.14	-2.53
gi|145346793	XP_001417867.1	Photosystem II PsbR protein, chloroplast precursor	-1.2	-1.37	-1.23	1.25	-1.07	1.095	1.055
gi|87241065	ABD32923.1	Polynucleotidyl transferase, Ribonuclease H fold	1.125	1.175	-1.12	-1.42	-1.15	-1.05	-1.02
gi|53749467	AAU90321.1	Polyprotein, related	1.37	-1.21	1.375	1.255	1.205	-1.11	-1.17
gi|307104521	EFN52774.1	Predicted protein	-1.1	1.18	-1.37	1.135	1.185	1.285	-1.13
gi|303282497	XP_003060540.1	Predicted protein	-1.96	-1.8	-2.29	-1.87	-1.68	-1.25	-1.54
gi|308802616	XP_003078621.1	Predicted protein	1.035	-1.37	-1.04	-1.57	-1.24	1.15	1.26
gi|104294980	ABF71996.1	2-oxoglutarate-dependent dioxygenase	1.18	1.315	1.33	-1.44	-1.76	1.125	-1.46
gi|11385435	AAG34800.1	Probable glutathione S-transferase	-1.37	-1.3	-1.11	1.2	-1.4	-1.46	-1.11
gi|108863932	ABA91188.2	Probable serine/threonine-protein kinase WNK5	-1.08	1.05	-1.5	-1.57	-1.15	1.305	-1.83
gi|255613348	XP_002539501.1	Probable WRKY transcription factor 40	-1.37	-1.6	-1.16	1.77	1.235	-1.09	1.295
gi|225166539	ACN81327.1	Prolycopene isomerase, chloroplastic	-1.38	1.39	-1.65	-1.63	-1.15	-2.18	-1.25
gi|41352687	AAS01050.1	Proteasome subunit beta type-5-B	1.165	1.145	-1.2	1.55	1.1	-2.11	1.275
gi|21592365	AAM64316.1	Proteasome subunit beta type-6	1.145	1.225	1.245	1.325	1.26	1.28	-1.36
gi|15235889	NP_194858.1	Proteasome subunit beta type-6	1.365	1.085	1.185	1.105	1.215	-1.25	1.165

gi|41352683	AAS01048.1	Proteasome subunit beta type-6	1.2	-1.33	1.19	1.125	1.32	-1.35	-1.06
gi|255553675	XP_002517878	Protein ARABIDOPSIS THALIANA ANTHER 7	-1.15	1.08	1.13	1.29	-1.37	1.185	-1.38
gi|29367477	AAO72594.1	Protein DA1-related 1-like	1.235	1.24	-1.07	-1.38	1.315	1.145	-1.22
gi|125548557	EAY94379.1	Protein EPIDERMAL PATTERNING FACTOR 2-like	-1.16	-1.67	1.345	1.67	-1.1	1.11	1.21
gi|270306970	ACZ71729.1	Protein FLUORESCENT IN BLUE LIGHT, chloroplastic isoform X1	1.095	-1.14	-1.29	1.085	1.255	-1.15	1.095
gi|1141784	AAB07225.1	Protein SLE2	-1.46	-1.86	-1.48	-1.79	-1.4	-1.33	-2.3
gi|212275286	NP_001130992.1	Protein WVD2-like 5	1.26	-1.28	1.085	1.345	1.155	1.205	1.095
gi|195652255	ACG45595.1	Protein WVD2-like 5	1.16	-1.11	1.17	1.04	1.225	-1.29	-1.83
gi|255564613	XP_002523301.1	Protein yippee-like At4g27745	-1.2	-1.16	-1.05	-1.02	1.165	1.12	1.195
gi|45533925	AAS67334.1	Protein YLS9-like	-1.3	-1.55	-1.13	1.325	-1.24	1.12	1.245
gi|222630446	EEE62578.1	Pseudo histidine-containing phosphotransfer protein 2	-1.58	1.265	1.095	-1.21	-1.29	1.115	-1.07
gi|168809271	ACA29392.1	Pseudo-response receiver	-1.35	-1.54	1.315	-1.91	1.075	1.095	1.34
gi|53791569	BAD52691.1	Putative Bowman Birk trypsin inhibitor	1.085	-1.25	-1.58	1.355	1.31	-1.22	1.33
gi|108796756	YP_636482.1	Putative chloroplast RF66 (chloroplast)	-1.18	-1.24	1.18	-1.88	-1.33	1.125	-1.02
gi|224132552	XP_002321348.1	Putative F-box/FBD/LRR-repeat protein At1g78840	-1.43	-1.33	-1.37	-1.43	-0.23	-2.42	-1.65
gi|213958295	ACJ54654.1	Putative methionyl-tRNA synthetase	0.42	-1.5	-1.64	1.53	1.535	-1.07	-0.05
gi|18423398	NP_568773.1	Putative rRNA 2'-O-methyltransferase fibrillarin 3	1.205	-1.21	1.125	-2.01	1.04	-1.16	1.27
gi|255542090	XP_002512109.1	Putative SNAP25 homologous protein SNAP30	-1.17	-1.2	-1.4	-1.45	-1.43	-1.36	-1.29
gi|15228199	ABA97802.2	Putative, Retrotransposon protein, Ty3-gypsy subclass	-1.1	-1.34	1.045	-1.2	-1.16	1.155	-1.12
gi|157086556	AAX96116.1	Putative, Retrotransposon, centromere-specific	-1.68	1.19	1.13	1.14	1.23	1.205	1.01

gi|51536238	ACU15849.1	Putative, Transmembrane protein	-1.79	1.63	1.39	1.58	1.425	-1.18	1.515
gi|149390755	AAX96588.1	Putative, Transposable element protein, Retrotrans_gag	1.405	-1.69	-1.41	-1.36	-1.53	-1.15	1.19
gi|108862524	ABA98441.1	Putative, Transposon protein, CACTA, En/Spm sub-class	-1.26	1.125	-1.12	-1.34	-1.36	1.17	-1.16
gi|62734007	NP_188264.1	Pyk10-binding protein 1	-1.25	1.035	-1.3	-1.07	-1.05	1.185	-1.21
gi|294864350	ABV21224.1	Pyrophosphate--fructose 6-phosphate 1-phosphotransferase subunit beta	-1.29	-1.14	1.055	-2.7	-1.05	1.15	1.36
gi|313183891	BAD38408.1	Receptor-like protein 2	1.22	1.145	-2.44	1.08	1.11	1.215	1.065
gi|56180897	ABR25395.1	Remorin	-1.18	-1.15	-1.22	-1.28	-1.09	1.195	-1.12
gi|148907015	ADF46049.1	Reverse transcriptase	1.245	-1.19	1.115	1.135	-1.24	-1.49	-1.47
gi|79325265	YP_004021745.1	Ribosomal protein L22 (chloroplast)	1.15	-1.1	-1.11	1.36	-1.15	1.305	-1.46
gi|255567135	AAV83543.1	Ribosomal protein S19 (chloroplast)	1.395	-1.49	-1.62	-1.57	-1.61	-1.76	-1.41
gi|256567906	ABR16651.1	Ribosomal RNA small subunit methyltransferase	1.245	1.3	1.085	1.125	-1.19	-1.15	-1.38
gi|154705504	NP_001031718.1	RNA binding Plectin/S10 domain-containing protein	1.175	-1.2	-1.12	1.29	1.24	1.315	1.135
gi|7209504	XP_002524549.1	RNA polymerase C (plastid)	-1.44	-1.94	1.355	-1.42	-1.48	1.065	-1.29
gi|148356707	ACU87438.1	RNA polymerase subunit (plastid)	1.22	1.07	-1.12	1.09	1.245	-1.15	-1.26
gi|257209021	ABS84178.1	RNase S6	-1.27	1.405	1.36	-1.51	1.46	1.125	1.295
gi|50251378	BAA92247.1	S locus protein 11	1.11	-1.61	1.46	1.1	1.465	-1.31	1.28
gi|115474139	BAF63026.1	Serine racemase	1.25	-1.21	-1.2	-1.37	-3.03	-1.35	-1.54
gi|4160416	CBB36498.1	Sorghum bicolor protein targeted either to mitochondria or chloroplast proteins T50848	1.18	1.285	-1.02	1.285	-1.18	-1.52	-1.15
gi|255565226	BAD28405.1	Splicing coactivator subunit-like protein	1.13	1.05	-1.23	-1.58	-1.16	-1.06	1.09
gi|218199733	NP_001060668.1	Stress responsive protein	-1.73	-1.95	-1.44	-1.35	-2.07	-1.37	-3.06

gi|226531284	AAD05231.1	Stylar self-incompatibility protein	1.28	1.055	-1.1	1.43	1.14	1.175	1.335
gi|159480794	XP_002523605.1	Subtilisin-like protease SBT1.9	1.195	1.205	-1.05	1.235	1.18	-0.11	1.29
gi|297852252	EEC82160.1	Succinate dehydrogenase subunit 3	-2.15	-1.44	-1.5	-1.49	-1.8	-1.18	-2.69
gi|15222488	NP_001147086.1	Thiol protease SEN102 precursor	1.255	-1.31	-1.56	-1.43	1.45	1.295	1.445
gi|255074655	XP_001698467.1	Thioredoxin	-1.18	-1.23	-1.56	1.225	-1.27	1.125	-1.42
gi|5230656	XP_002894007.1	Thioredoxin H5	-2.05	-0.33	-2.74	-1.34	-1.04	-1.64	-1.56
gi|195643542	NP_177146.1	Thioredoxin H8	-1.24	-1.55	-1.49	-1.21	1.12	1.075	-1.38
gi|302761140	XP_002501002.1	Thioredoxin-like 3-3	-1.07	1.405	1.17	-1.18	-1.19	1.215	1.235
gi|145346800	AAD40953.1	Transcription factor AS1	1.105	-1.13	1.055	1.25	1.155	-1.31	-1.22
gi|255630970	ACG41239.1	Transmembrane protein	-1.7	-1.57	1.18	-1.91	1.51	-1.18	-1.29
gi|62734479	XP_002963992.1	Transmembrane protein	1.15	1.355	-1.33	-1.24	1.17	1.085	1.18
gi|77555645	XP_001417870.1	Transmembrane protein 120 homolog	-1.08	1.36	-1.45	1.34	1.35	-1.4	-1.27
gi|224142047	XP_002324370.1	Transposon Tf2-12 polyprotein	-2.31	-1.77	-1.34	-1.34	-1.5	-1.25	-1.5
gi|147782013	CAN76654.1	Transposon Ty3-G Gag-Pol polyprotein	1.035	1.105	-1.2	1.17	1.14	1.18	1.14
gi|162459877	NP_001105107.1	Ubiquitin-conjugating enzyme E2 7	-1.31	-1.64	-1.47	-1.39	-1.78	-1.17	1.24
gi|31088843	sp|Q42540.1	Ubiquitin-conjugating enzyme E2 7	1.215	1.435	-1.36	1.345	1.635	-1.14	1.34
gi|18408206	NP_566884.1	Ubiquitin-conjugating enzyme E2 7	-2.05	-1.58	1.39	-1.46	-2.45	-1.04	-1.43
gi|302804260	XP_002983882.1	UBP1-associated protein 2C-like	-1.44	1.09	1.115	1.365	1.115	1.045	-1.11
gi|302784754	XP_002974149.1	Uncharacterized protein LOC9655997	1.13	1.21	1.355	1.07	1.195	1.325	-1.25
gi|302148438	BAJ14098.1	V-type proton ATPase catalytic subunit A	1.225	-1.1	1.075	1.22	1.32	-1.25	1.165
gi|222822683	ACM68454.1	Zinc finger A20 and AN1 domain-containing stress-associated protein 8-like	1.085	-1.31	-2.26	-1.56	1.275	1.16	-2.42
gi|12322419	AAG51230.1	Zinc finger CCCH domain-containing protein 4-like	-1.46	-1.54	-1.44	-1.63	-1.18	1.285	1.49

To further annotate the differentially expressed protein for its functions, the peptide sequences were subjected to functional enrichment analysis using MAPMAN. Prior to this, a mapping file of *S. fruticosa* was generated using Mercator. Out of the 177 peptide sequences that were analyzed, 45.1% (70 peptides) were not assigned (Figure 6.17). Majority of the peptides (13.7%) were found to play a role in protein metabolism which involves amino acid metabolism, protein translation, post-translational modification, degradation and protein stability (Figure 6.17 and 6.18). About 8% of the peptides were found to regulate RNA metabolism, 5.75% in secondary metabolism and, 5.1% in cell signaling and sensing.

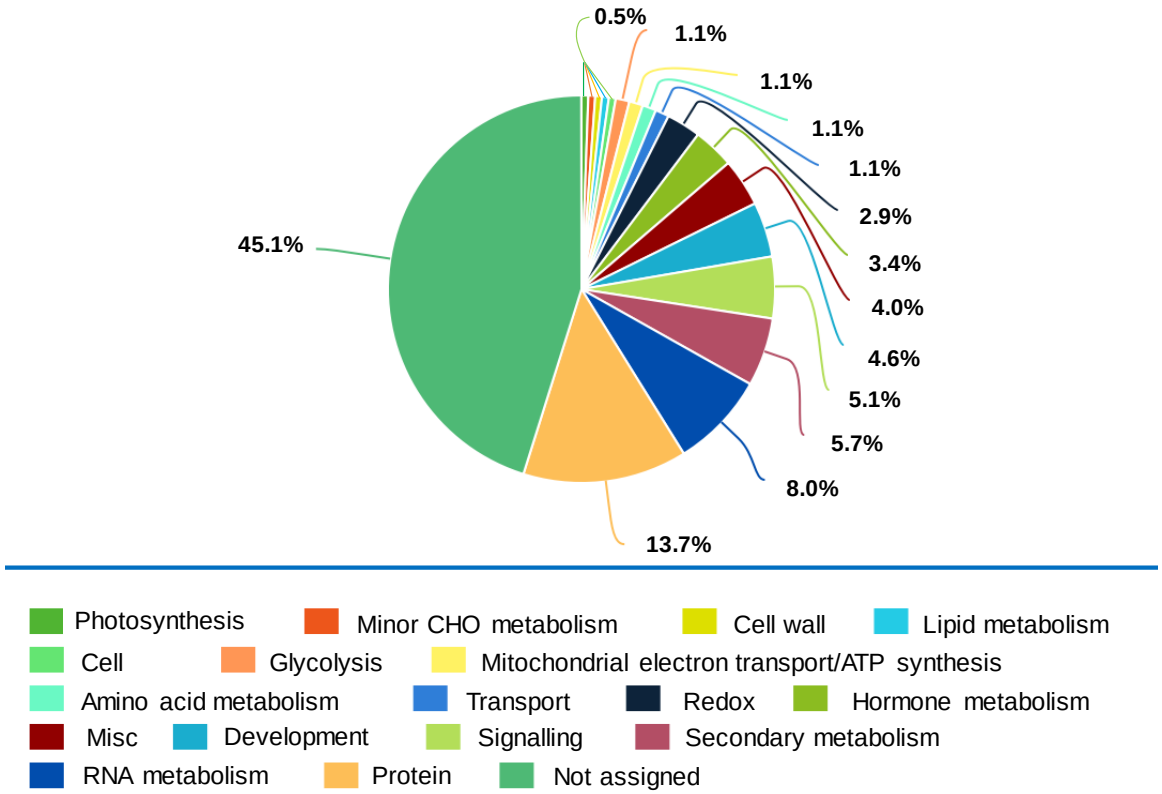

Figure 6.17: Mapping file as obtained from Mercator.The mapping file was used for functional enrichment analysis using MAPMAN.

6.4. Discussion

Suaeda fruticosa, a xero-halophytes, can survive and complete its life cycle under high salinity (Khan et al., 2000). Commercially, it is grown for its anticancer andanti-inflammatory property (Oueslati et al., 2012) and also for its hypoglycaemic and hypolipidaemic properties (Bennani-Kabchi et al., 1999). Over the years, scientists have studied its stress tolerance property by analyzing its transcriptome (Diray-Arce et al., 2015) and physiological and biochemical responses under heavy metal and nutritional stress (Bankaji et al., 2015). However, no work on proteomic studies has been done so far. In the present study, we have analyzed its proteome under different time points of the day and different seasons. To analyze the relative expression of proteins that are regulated by diurnal, protein accumulating at 8 am for each season was taken as control.

The state of circadian organization of an organism is reflected from its diurnal proteomic changes (Wang and Wang, 2011). A study of Arabidopsis proteomic changes as influenced by diurnal rhythm showed several changes in the core protein that are involved in photosynthesis, protein translation, metabolic regulator and cell transporter proteins (Uhrig et al., 2019). Proteomic study in rice also reveals the changes in expression of proteins that are involved in the regulation of redox homeostasis, carbohydrate flow, protein modification, nitrogen metabolism and photosynthesis (Wang and Wang, 2011). In wild halophytic genotype of rice, *Porteresia coarctata*, proteomic study showed regulation of the function of chaperone, higher expression of RuBisCO enzyme, expression of proteins that are involved in osmolyte synthesis and photosynthesis conferring to its adaptive mechanism under stress (Sengupta and Majumder 2009). In *S. fruticosa*, proteins related to the regulation of several biological roles ranging from physiological, molecular, and cellular was seen to be regulated by diurnal rhythm, seasonal changes, and stresses (Figure 6.19).

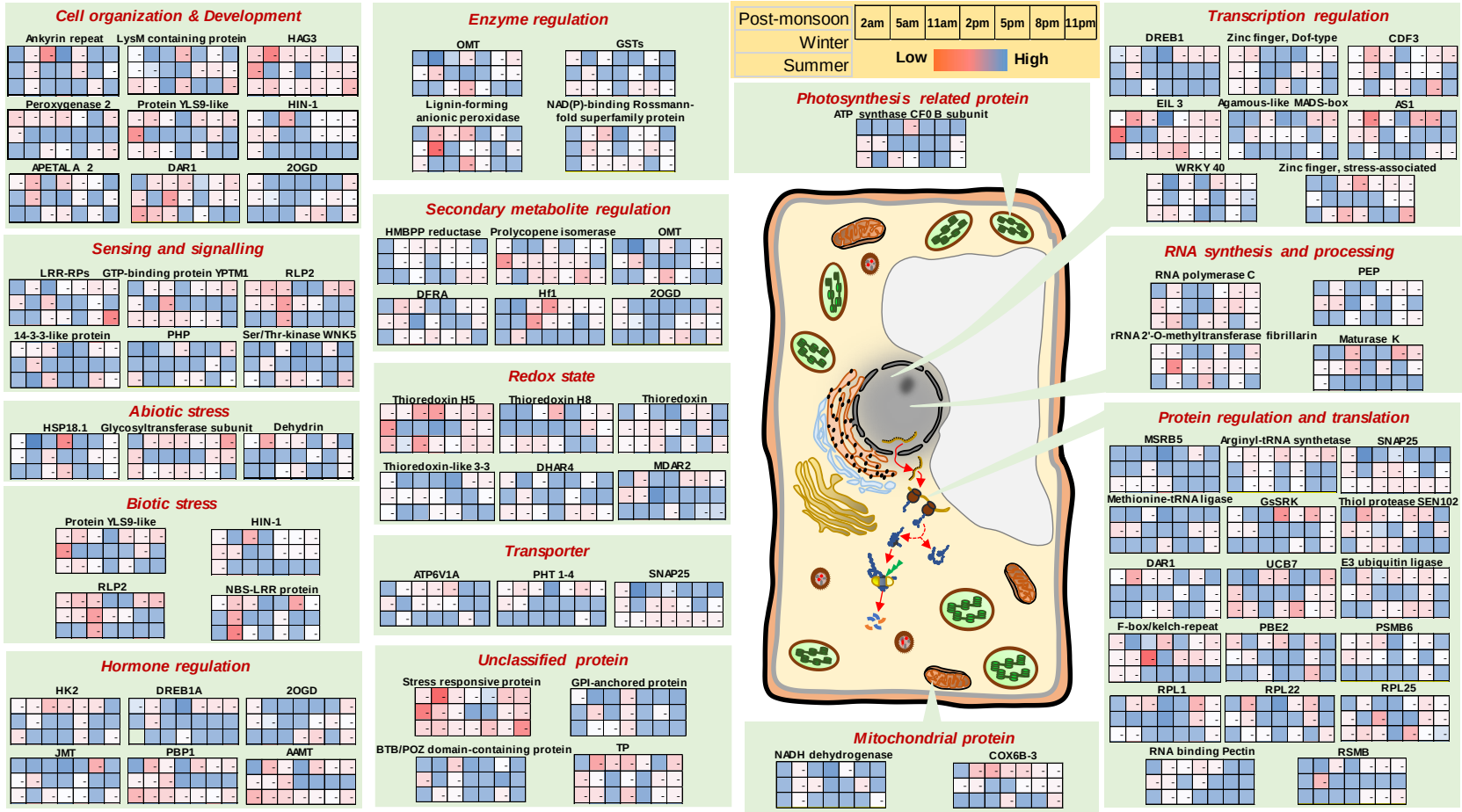

Figure 6.18: Overview of selected differentially expressed proteins on the biological, molecular, and cellular process in *S. fruticosa*. Proteins which showed differential expression during different time points and seasons were displayed on their corresponding functional enrichment category. Few proteins were found to be redundant in functions. The expression level is shown in a heatmap wherein; the blue color represents high expression and red as low expression. Each box in a column represents a different time point, and each row represents different seasons.

Using MAPMAN functional enrichment analysis, we identified 83 proteins that are functionally regulating in *S. fruticosa*. Out of which, 78 (some proteins such as Protein YLS9-like, Harpin inducing protein, Receptor-likeprotein-2, O-methyltransferase and 2-oxoglutarate-dependent dioxygenase shows redundant functions) show various functional role such as abiotic regulation, biotic stress, signaling, redox homeostasis, protein synthesis, post-translational modification, amino acid synthesis, cell development and organizations (Figure 6.18). Gene ontology for 4 proteins (out of 74), a transmembrane protein, GPI-anchored protein LLG1, BTB/POZ domain-containing protein and stress-responsive protein were not assigned. Of all the functional annotations, majority of the proteins (17 proteins) including SNAP-25, Methionine-tRNA ligase, an E3 ubiquitin ligase, and F-box/kelch-repeat were found to be those proteins accounting to the regulation of protein synthesis and post-translational modifications. Further, eight transcriptional regulating protein, four RNA synthesizing proteins, and four enzymes were also identified. Abiotic and biotic stress-related proteins such as HSP18.1, glycosyltransferase subunit, dehydrin, NBS-LRR resistance protein, Harpin inducing protein-1 (HIN-1), and SNAP-25 proteins were found to be differentially expressed. Proteins related to signaling such as Leucine-rich repeat protein kinase (LRR-RPs), GTP-binding protein YPTM1, Serine/threonine-protein kinase WNK5, and pseudo-histidine-containing phosphotransfer protein (PHP) were found abundantly expressed throughout the seasons. All the proteins detected were seen to be regulated diurnally as well as seasonally.

Cuticle layering in plants not only act as a barrier against water loss but also provide tensile strength and elasticity to the leaf (Onoda et al., 2012). In a succulent leaf, a thick layer of cuticle provides its ability to store a large volume of water by increasing the leaf elasticity and plasticity. It also further reduces the rate of transpiration (Boom et al., 2005). *In vitro* and *in planta* studies by expressing peroxygenase 2 protein in maize showed an increased biosynthesis of cutin monomer (Lequeu et al., 2003). In *S. fruticosa*, during winter and summer, as salinity increases, succulent leaf began to develop (Chapter 4).

During this season, the expression of peroxygenase 2 was seen to increase drastically throughout the day. This expression could have provided the tensile strength to develop into succulent leaf. Signal transferring molecules, 14-3-3-like protein, which interacts with MAPKK for regulating the activity of H^+-ATPases are known to express abundantly during salinity stress (Parihar et al., 2015). The expression of this protein was also found to increase under cold stress in *Physcomitrella patens* (Wang at al., 2009). In *S. fruticosa*, 14-3-3-like protein was seen to express throughout the year as salinity is a common phenomenon; however, the expression of which increases towards winter and summer as the level of salinity is high during the season. In between summer and winter, the expression was seen more during winter wherein, maximum expression was observed during 8 pm, 11 pm and 2 am as the temperature reduces. Non-lysine phosphorylating signaling protein, serine/threonine-protein kinase WNK5 has been reported to play a role in regulating flowering in Arabidopsis (Wang et al., 2008). In our study, the expression of serine/threonine-protein kinase WNK5 was found to be abundant during post-monsoon and winter season as the plants developed flowers.

Small heat shock protein such as HSP18.1 is known to be expressed in plants under heat stress (Sun et al., 2002), In the present study, the level of HSP18.1 was found to be high throughout the seasons, the expression for which was found to be most abundant during the noontime (between 11 am to 8 pm) during post-monsoon and summer seasons. Dehydrin protein, belonging to a large group of LEA (Late Embryogenesis Abundant) protein which is hydrophilic is known to play a significant role during dehydration (salinity and drought) and cold stress in plants (Close 1997; Rorat 2006). In the present study, as salinity and drought increase during winter and summer, the dehydrin protein was found to accumulate more during the seasons. In between the two seasons, the level of expression was found to be high during early and late hours of the day (8 pm to 5 am) in winter as the temperature is minimum and the plant is under the combination of both salinity and cold stress during this time. Collins et al. (2003)

found thatSynaptosome Associated Protein of molecular mass 25 kDa (SNAP-25) forms a binary SNAP receptor complex with ROR2 which exhibits resistance to powdery mildew in barley. In Arabidopsis, SNAP-25 is also found to give resistance to *Verticillium dahlia* (Wang et al., 2017). In *S. fruticosa*, expression of SNAP-25 protein was found to be abundant during post-monsoon and during the early and late hours (5 pm to 5 am) during winter. It was observed in our field survey that the population of aphids and other insects increases during post-monsoon. However, as winter and summer sets in, the harsh weather contributes to the suppression of insect population. To combat insects during post-monsoon, SNAP-25 level might have been expressed in abundance during the post-monsoon season.

Phytohormones such as abscisic acid, ethylene, and jasmonic acid play a crucial role in adapting plants to the changing environment and also help in mediating plants growth and development (Peleg and Blumwald 2011). Proteins mediated by cytokinin such as Histidine kinase 2 (HK2) (Hejátko et al., 2009), Dehydration-responsive element-binding protein 1A (DREB1A) and 2-oxoglutarate-dependent dioxygenase (2OGD) that mediates ethylene responses (Fukuda et al., 1992; Hsieh et al., 2002) and Jasmonic acid carboxyl methyltransferase (JMT) that regulates biosynthesis of jasmonic acid (Seo et al., 2001) are known to play a significant role in abiotic stress tolerance (Tran et al., 2007; Singh et al., 2015). In the present study, expression of HK2, DREB1A, 2OGD, and JMT was found throughout the seasons. The expression of HK2 was found maximum during winter and summer as salinity is maximum; however, JMT was found to be maximum during post-monsoon and winter seasons.

Plant thioredoxins are a group of ubiquitous disulfide reductases which regulate the redox homeostasis of proteins. In plants, 20 isoforms of thioredoxins have been identified (Gelhaye et al., 2005). These group of protein enhances the reducing property of reductase that detoxifies lipid hydroperoxides or repairs the

oxidized protein (Dos-Santos et al., 2006; Meyer et al., 2008). In *S. fruticosa*, four isoforms of thioredoxins were identified throughout the seasons in our study: thioredoxin, thioredoxin-like 3-3, thioredoxin H5, and thioredoxin H8. Expression of thioredoxin was seen maximum during 11 am, and 2 pm of post-monsoon, thioredoxin H5 between 5 am to 5 pm during winter, and thioredoxin H8 between 2 am to 5 pm during post-monsoon and winter. Two more proteins, probable glutathione S-transferase (DHAR4) and monodehydroascorbate reductase 2(MDAR2) that regulates the redox homeostasis in plants (Asada et al., 1997; Roxas et al., 1997) were seen to express abundantly during winter and summer in *S. fruticosa*.

Chloroplast protein, ATP synthase CF_0 β-subunit and mitochondrial protein, NADH dehydrogenase and cytochrome c oxidase subunit 6B-3 (COX6B-3) were the only proteins related to photosynthesis and respiration detected from our study. The expression for ATP synthase CF_0 β-subunit was found maximum during post-monsoon and least during summer. During post-monsoon, the expression for which was found minimum during 2 pm and between 11 pm and 2 pm during summer. However, respiration-related protein NADH dehydrogenase and COX6B-3 were found to be expressed more during summer. This may be an adaptive mechanism in *S. fruticosa* wherein plants generate ATP through respiration.

Proteins related to transcription regulation such as Agamous-like MADS-box (Pinyopich et al., 2003), WRKY 40; RNA synthesis and processing such as maturase K (Zoschke et al., 2010), RNA polymerase C; and protein regulation and translations such as Methionine-tRNA ligase (Kaminska et al., 2000) and E3 ubiquitin ligase (Rosebrock et al., 2007) which play direct and indirect role in abiotic and biotic stress were found to be expressed in *S. fruticosa* throughout the seasons at different time points.

6.5. Conclusions

In the present study, the proteome of *S. fruticosa* was analyzed to study the influence of diurnal rhythm as well as the changing seasons, for which, samples were harvested at different time points viz. 2 am, 5 am, 8 am, 2 pm, 5 pm, 8 pm, and 11 pm during three different seasons, i.e. post-monsoon, winter and summer. Differential accumulation of the proteins was analyzed using DIGE. From our study, we have identified 177 proteins that were differentially expressed at different time points and during different seasons. Filtering the redundant proteins, we got 147 proteins for which further analysis was made. Gene ontology of the proteins was also done using BLAST2GO and MAPMAN software. Functional enrichment and GO search showed that, maximum of the protein identified and those that shows statistical significance plays significant role in protein biosynthesis and modification. Some photosynthesis related proteins along with mitochondrial proteins which are involve in respiration were seen to be expressed throughout the seasons. Several stress-related proteins such as peroxygenase 2, chitinase, 14-3-3-like protein, dehydrin, and proteins that regulate PTM were found to alter as influenced by diurnal and with the change in seasons. This study provides useful knowledge on how *S. fruticosa*, a xero-halophyte, survive under harsh environmental conditions by regulating the expression of specific stress-related proteins that confers to its adaptation.

Chapter 7

Ionomics regulation in leaves of *S. fruticosa* as influenced by diurnal cycle and seasons

7.1. Introduction

Ionome refers to the mineral and trace elements present in an organism and represents the complete inorganic components of the cell (Salt et al., 2008). Phenotypic study through quantitative and qualitative analysis of the is called ionomics (Danku et al., 2013). Ionomics contribution in understanding the relationship between nutrient availability in the soil and the uptake of the minerals by plants. Ionomics can also be used to study the functional physiological state of the organism by integrating its outcome with the tools of genomics and bioinformatic (Salt et al., 2008; Watanabe et al., 2015). Some significant biochemical processes such as the deposition of suberin in the root (Baxter et al., 2009), biosynthesis of the sphingolipid in the root (Chao et al., 2011), sap transportation along the sieve tube element of phloem (Tian et al., 2010), and pathogen-genes responses and ion uptake (Borghi et al., 2011) which controls the accumulation of mineral ions and trace elements have been identified by integrating the tools of genomics and ionomics (Danku et al., 2013). Additionally, using these tools, genes that control the accumulation of ions such as sodium (Rus et al., 2006), molybdenum (Baxter et al., 2008), cobalt (Morrissey et al., 2009), copper (Kobayashi et al., 2008) and sulphur (Loudet et al., 2007) have also been identified.

Ionome of a plant can change under the influence of several environmental factors such as biotic and abiotic stress, physiological stimuli, genetic modification, and their developmental stage (Salt et al., 2008). In several cases, the mechanism of mineral and element homeostasis has been studied by monitoring the uptake of a single ion in plants (Clarkson and Hanson, 1980;

Marschner 1995; Sanders et al., 2002; Curie and Briat, 2003; Very and Sentenac 2003; Zhu 2003). However, mineral and elemental uptake by plants exist as a large multi elemental network which are interlinked with each other (Baxter et al., 2008). Therefore, to have a wholistic view of the physiology of a given plant, the study of complete ionome is essential rather than study of a specific ion under any conditions (Danku et al., 2013). In quantitative terms, after nitrogen, major elements required for plants' growth and development are in the order of potassium, phosphorus, calcium, and magnesium (Tränkner et al., 2018).

Soil is the largest reservoir for almost all the minerals (organic and inorganic) and elements which plants take up for its growth and development (Adler et al., 2009). However, the uptake of minerals and element by plants are affected by several factors of soil such as its crust (Harper and Belnap 2001), pH (Adamczyk-Szabela et al., 2015), density (Arvidsson 1999), alkalinity (Mengel and Geurtzen 1986), moisture (Baldwin 1975), porosity (Roose and Fowler 2004). Other factors such as rhizosphere temperature (Tindall et al., 1990; Bahuguna and Jagadish2015), drought (Salehi et al., 2006) and salinity (García-Caparrós et al., 2017) also influence the process. Several soil microflorae around the rhizosphere also have been known to help the plants in mineral uptake (Lin et al., 1983; Harper and Belnap 2001; Han and Lee 2005). Some plants growth promoting rhizobacteria (PGPR) such as *Serratia* sp. and *Rhizobium* sp. (Han and Lee 2005), *Bacillus megaterium* and *Bacillus mucilaginosus*(Han et al., 2006), *Azospirillum brasilens* (Lin et al., 1983), cyanobacteria and cyanolichens (Harper and Belnap 2001) are also reported to help in the uptake of copper, potassium, phosphorous,magnesium, zinc, nitric oxide, dihydrogen phosphate and nitrogen in plants such as pepper, cucumber, maize, lettuce, and *Coleogyne ramosissima*.

Heavy metal pollution (due to the mining activities), and soil erosion (driven by wind and water-diversion) have caused about 22 million hectares of land unsuitable for agriculture (Mendez and Maier, 2008; Ali et al., 2013;

Nsanganwimana et al., 2014). The best and most sustainable cost-effective tool to minimize heavy metal contaminations is through phytomanagement (an integrated system where the vegetation that is self-sustainable) (Tordoff et al., 2000; Parraga-Aguado et al., 2013; López-Orenes et al., 2017). Several plants are known to accumulate heavy metals and have been used for phytoremediation. About 45 plant families have been known for their hyper-accumulative ability for heavy metals including arsenic, cadmium, cobalt, copper, manganese, nickel, selenium, and zinc (Reeves & Baker, 2000; Guerinot & Salt, 2001; Galeas et al., 2007). During evolution, halophytes not only have evolved to combat high salinity but also have the mechanisms to tolerate heavy metals (Shevyakova et al., 2003; Lefevre et al., 2009; Nedjimi & Daoud, 2009). These plants can also be used to reclaim or clean up the saline soil or soil polluted with heavy metals (Manousaki & Kalogerakis, 2011b; Manousaki & Kalogerakis, 2011a).

In the present study, we have analyzed the ionomic changes in leaves of *S. fruticosa* under the influence of diurnal and seasonal changes. Diurnal regulation on the accumulation of ions has not been reported in any plants to date. However, seasonal changes leading to change in the accumulation of ions have been shown in plants such as Arabidopsis, *Populus nigra* and *Populus trichocarpa* (Arend et a., 2002; Moomaw and Maguire, 2008; Waters 2011). To investigate the changes in the ion accumulation pattern in leaves under the influence of diurnal rhythm as well as stresses, we harvested the leaf tissues of *S. fruticosa* during three seasons, i.e., post-monsoon, winter and summer at fixed time points viz. 2am, 5am, 8am, 11am, 2pm, 5pm, 8pm and 11pm. We have identified 18 elements using EDXRF and WDXRF from *S. fruticosa* harvested during different seasons at different time points. Strong correlations on the deposition of ions such as Na^+ and Cl^- on the leaf tissues of *S. fruticosa* was found as salinity in the soil changes dramatically over the seasons (winter and summer). However, the level of K^+ was found to be maintained at constant

values throughout the diverse seasons. From our study, we also found that diurnal changes do not regulate the micro-homeostasis of ions in *S. fruticosa*.

7.2. Material and Methods

7.2.1. Plant material and study conditions

Leaf samples of *S. fruticosa* growing naturally on the bank of the salt mining site in Sambhar Lake, Rajasthan were harvested during three seasons, i.e., post-monsoon, winter and summer. For every season, samples were harvested at an interval of three hours each, i.e., at 2 am, 5 am, 8 am, 11 am, 2 pm, 5 pm, 8 pm, and 11 pmto check for the diurnal ionomic changes. Harvested samples were brought to the laboratory in clean falcon tubes for further use (as described in the chapter 3).

7.2.2. Total ions estimation

Leaf samples of *S. fruticosa* harvested during the three seasons, i.e., post-monsoon, winter and summer were dried at 60^{o}C for three days in an oven and crushed into fine homogenous powder of less than 70 µm particle size. About 100 mg of the powdered leaf tissues were pressed to a pellet of 35 mm diameter with 4 mm thickness using hydraulic pressure of 15-tons. The pellet was then embedded on a sample cup of 40 mm diameter containing a tablet of boric acid. Elements from the samples were measured using EDXRF and WDXRF (PANalytical, Netherland), which have the X-ray source from Gadolinium tube under 100 keV for 5 minutes. A total of 18 elements (Na^{+}, K^{+}, Ca^{2+}, Mg^{2+}, Mn^{2+}, Cl^{-}, Al^{3+}, Fe^{3+}, Cu^{2+}, P^{3+}, Hg^{2+}, Br^{-}, Si^{2+}, Sr^{2+}, S^{2-}, W^{+}, Zn^{2+} and Ti^{3+}) were detected. Quantification of the elements detected this process was done using Epsilon software.

7.2.3. Statistical analysis

For each sample, three biological and three technical replicates (n = 6) was considered for analysis. ANOVA test for each ion detected at every time point was applied to check whether the variations were statistically significant (Fisher, 2002). The average value of each ion detected in every season was then represented in box plot that was developed using Sigma Plot version 12.0 (Hilbe, 2003). Further, the ion matrics represented in the form of heatmap was also generated using Multi Experiment Viewer (MeV) version 4.9 (Saeed et al., 2006).

7.3. Results

7.3.1. Ions detected from S. fruticosa during different seasons

Using EDXRF and WDXRF, a total of 18 elements (potassium, sodium, manganese, magnesium, chloride, aluminium, copper, calcium, phosphorus, aluminium, mercury, iron, bromide, silicon, sulfur, tungsten, zinc, titanium and strontium) were detected from the leaves of *Suaeda fruticosa* during the three seasons viz. post-monsoon, winter and summer (Table 7.1-7.3, Figure. 7.1, Figure. 7.2 and Figure. 7.3). The elements were further categorized broadly according to their physical properties, chemical nature, and importance in plants growth and development (Table 7.1-7.3). Of the eighteen elements detected, three were anionic (negatively charged), and fifteen were cationic (positively charged), ten were essential elements (elements that are necessary for growth and development of the plant) of which, four were heavy essential elements, and two were beneficial elements (elements that accelerate growth and development). Further, four micro and macro elements were also identified. Each of the elements detected was analyzed for its diurnal and seasonal changes.

Table 7.1: Ions detected from the leaves of *S. fruticosa* during post-monsoon season under diurnal condition

Elements	Time of the day							
	2 am	5am	8am	11am	2pm	5pm	8pm	11pm
CHNO	844877	845468.96	836854.13	842711.6	843084.7	844921.5	842381.8	847155.2
Sodium	64474.57	64710	65702.222	64067.78	66267.78	65842.22	64748.89	64152.22
Magnesium	4802.963	4736.6667	4747.7778	4639.366	4683.333	4705.556	4601.111	4762.858
Aluminium	3131.09	3123.3333	3132.2222	3189.556	3176.111	3113.222	3101.111	3098.667
Silicon	1271.694	1296.34	1197.3389	1222.222	1247.713	1259.445	1249.778	1271.311
Phosphorous	2142.84	3250	2178.8889	2103.248	2076.444	2307.3	2312.111	2200.817
Sulphur	4382.963	4250	4152.2222	4237.778	4233.111	4145.556	4391.111	4428.889
Chloride	52980.74	52606.667	52702.222	53067.78	52667.56	50572.22	53048.89	50881.11
Potassium	14131.91	14700	13868.889	14512.22	14506.89	14672.22	13808.89	14645.56
Calcium	5282.963	5080	5252.2222	5369.351	5243.556	5357.778	5250	5289.133
Titanium	19.17816	18.631	18.672222	19.26222	17.56989	17.88656	17.95111	18.48
Manganese	36.1871	35.252667	35.588222	34.985	38.47789	36.12878	34.408	35.68856
Iron	130.6358	137.80433	131.91311	131.9778	133.8186	132.7213	130.2221	130.0942
Copper	24.17927	21.850667	22.417	21.83822	21.23044	22.16078	23.54022	22.79911
Zinc	11.83111	12.804333	11.686667	11.95622	12.382	12.505	13.73722	11.83489
Bromide	211.4349	216.301	213.14856	206.6292	242.5276	206.5502	213.1557	227.9857
Strontium	77.51112	75.740333	90.816889	76.30178	75.18389	78.18778	76.67767	76.76578
Tungsten	138.6445	134.25	136.93911	138.3654	131.378	139.9752	139.0684	131.8623
Mercury	2.292765	2.7076667	2.8897778	2.131444	2.806333	2.093	2.243	2.139444

Table 7.2: Ions detected from the leaves of *S. fruticosa* during winter season under diurnal condition

Elements	Time of the day							
	2am	5am	8am	11am	2pm	5pm	8pm	11pm
CHNO	825310	822302	803090	816744	824443	830141	805557	828823
Sodium	65494	63680	63213	66859	63869	63364	65233	64390
Magnesium	4641.6	4917.8	5583.3	4487.8	4709.4	4807.7	4746.7	4963.3
Aluminium	3201.9	3320.6	3305.8	3355.3	3299.6	3253.8	3302.7	3312
Silicon	1733.1	1743.9	1760.1	1952.4	1729.1	1738.6	1740	1667.2
Phosphorous	960.66	980.26	965.6	982.01	935.68	930.71	942.57	943.18
Sulphur	8052.2	8206.9	8253.6	8371.1	8224.1	8330.3	8380	8373.3
Chloride	72214	76285	74182	75146	73233	72059	76619	75341
Potassium	13414	14398	14570	13981	13911	14134	14347	14247
Calcium	5336.3	5190	5161.1	5174.4	4967.8	4916.7	5210	4923.3
Titanium	14.053	14.327	15.272	14.341	14.552	13.664	15.062	14.914
Manganese	57.856	56.391	56.218	58.212	58.294	56.563	55.662	57.319
Iron	370.15	329.48	395.95	353.36	360.45	376.49	373.32	393.7
Copper	22.742	22.222	22.433	22.904	21.402	22.365	28.511	27.247
Zinc	11.726	10.398	11.126	11.059	11.488	11.212	11.171	11.098
Bromide	136.74	121.59	108.46	186.21	153.52	195.89	127.53	128.26
Strontium	28.519	21.5	25.626	22.126	21.955	22.696	24.922	21.576
Tungsten	155.55	138.44	168.84	156.21	152.22	184.75	168.65	165.65
Mercury	2.4301	2.5577	2.2976	2.7198	2.7417	2.7692	2.2453	2.6567

Table 7.3: Ions detected from the leaves of *S. fruticosa* during summer season under diurnal condition

Elements	Time of the day							
	2am	5am	8am	11am	2pm	5pm	8pm	11pm
CHNO	840553	841511	841591	842913	841369	845158	840682	843711
Sodium	45379	44623	41131	43926	45737	43331	45222	44637
Magnesium	3031.8	3141.5	3182	3100	3188.9	3298.9	3091.6	3123.3
Aluminium	3263.9	3294.9	3291.1	3361.8	3308.7	3217.7	3338.6	3254.5
Silicon	2715.3	2874.7	2939.6	2822.5	2884.1	2824.2	2888.8	2796.6
Phosphorous	1664.3	1545.3	1557.8	1601.1	1547.5	1516.7	1451.9	1677
Sulphur	7531.1	7531.1	7525.6	7525.6	7470	7301.1	7637	7631.5
Chloride	75621	74916	78466	74732	75831	76902	77348	75771
Potassium	14736	14755	13988	14267	13611	14259	13941	13839
Calcium	4120	4164.1	4007.8	4144.4	4244.4	4028.9	4073	4148.1
Titanium	30.703	31.344	30.563	30.047	30.007	30.168	29.951	30.208
Manganese	63.929	64.653	61.698	63.575	62.668	64.353	63.415	63.46
Iron	259.82	260.1	273.82	273.78	255.72	270.18	281.91	264.17
Copper	50.423	49.864	49.743	49.735	50.417	51.029	49.973	51.112
Zinc	8.2703	8.3148	8.1112	8.277	8.3629	8.0873	8.7684	8.0851
Bromide	183.8	184.37	187.46	185.87	183.5	181.92	175.93	183.64
Strontium	63.516	65.167	63.723	61.228	62.415	62.498	62.409	61.611
Tungsten	135.57	135.08	135.88	136.55	130.72	132.38	135.49	132.69
Mercury	4.2873	4.83	4.7044	3.7462	4.4157	4.4238	4.2385	4.0845

7.3.2. Diurnal regulation of the accumulation of ions in leaves of S. fruticosa growing under its natural habitat

To check for the influence of diurnal rhythm on the accumulation of ions in *S. fruticosa*, leaf samples of *S. fruticosa* were harvested at the different time points of the day (as discussed in the material and method section). The concentration of the ions accumulating in the leaves of *S. fruticosa* vary for each ion; however, no statistically significant variations of the ions detected as influenced by diurnal rhythm were found (Figure. 7.1, Figure. 7.2 and Figure. 7.3). Ions such as Cl^- ,Na^+,K^+, Mg^{2+}, Ca^{2+},and Al^{3+} were found to be abundant in *S. fruticosa* (Figure. 7.1a-f) of which, Cl^- and Na^+ (Figure. 7.1a and b) ions were found to be highest in their abundance. Macro and essential elements such as K^+, Mg^{2+}, and Ca^{2+} were also found to accumulate in abundance throughout the day, in leaves during all the seasons (Figure. 7.1c, d and e). The concentration of Al^{3+} was found to be high even though it is not under the category of essential or macro elements in the plant (Figure. 7.1f).

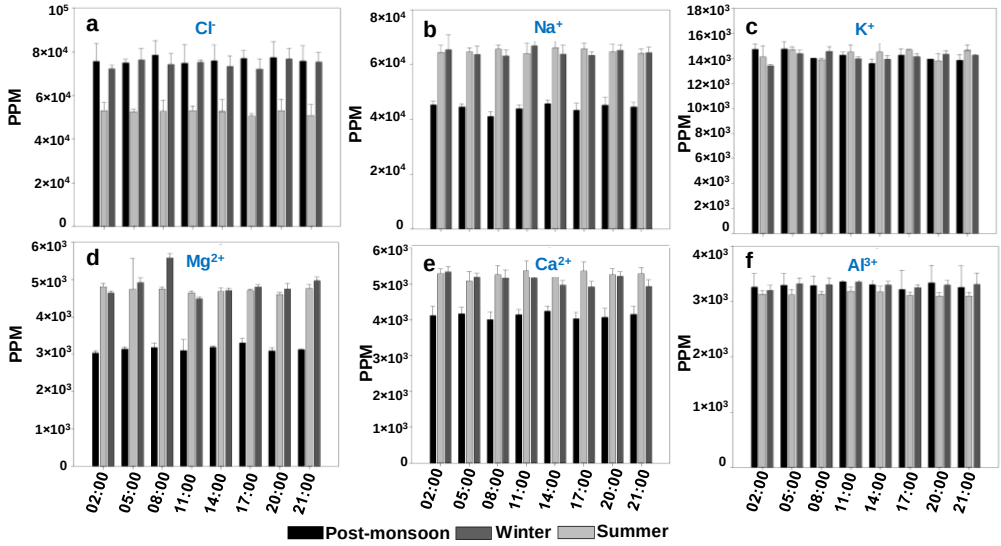

Figure 7.1: Ions identified from the leaves *S. fruticosa* at different time points of the day as influence by the diurnal rhythm. In the figure, the black bar represents ions identified during post-monsoon seasons, light grey during winter season and white during summer season. Each of the ion is represented in parts per million (PPM). A) Chloride. B) Sodium. C) Potassium. D) Magnesium. E) Calcium. F) Aluminum.

Some of the essential heavy elements such as S^{2-}, Si^{2+}, and P^{3+} were also found abundant in the leaves of *S. fruticosa* (Figure. 7.2a, b, and c) even though the concentration was lesser than that of the elements that were represented in Figure 7.1. The role of silicon in plants and its significance are still debatable as many of the conventional laboratory experiments conducted on plants are grown in liquid medium (hydroponics); however, its role in combating stress such as biotic and abiotic has been reported (Epstein 2009). Heavy metal ions such as Tungsten (W+), Bromide (Br-) and Iron (Fe3+) were also found to accumulate in abundance (Figure. 7.2d, e and f).

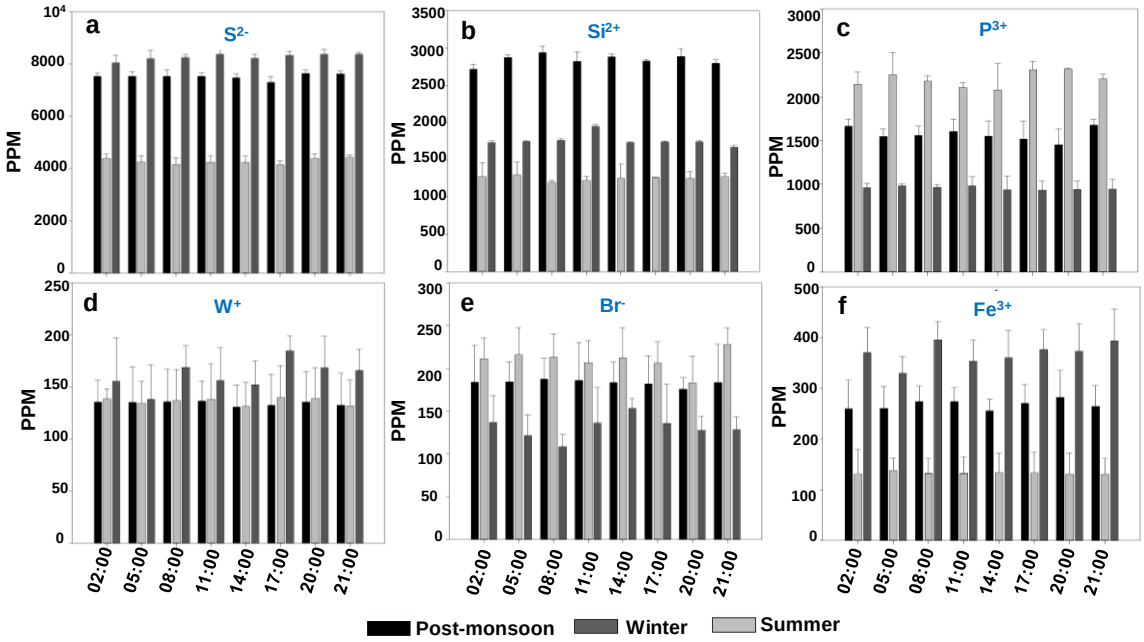

Figure 7.2: Ions identified from the leaves *S. fruticosa* at different time points of the day as influence by the diurnal rhythm. In the figure, the black bar represents ions identified during post-monsoon seasons, light grey during winter season and white during summer season. Each of the ion is represented in parts per million (PPM). A) Sulfur. B) Silicon. C) Phosphorus. D) Tungsten. E) Bromide. F) Ferric.

Unlike the above-mentioned elements (Figure. 7.1 and 7.2) whose concentrations ranges from few hundreds to thousands part-per-million (PPM) (Table 7.1-7.3), few elements such as Copper, Manganese, Titanium, Strontium, Mercury, and Zinc were also detected in trace amount (concentration at the range of 100 PPM) (Figure. 7.3). Among the trace elements identified, essential

heavy metal ions such as copper and Manganese were found to be the most accumulating ones on the leaves of *S. fruticosa* (Figure. 7.3a and b). Some heavy metal ions such as Titanium, Strontium, Mercury, and Zinc (Figure. 7.3c, d, e, and f) were found to accumulate only in trace quantities.

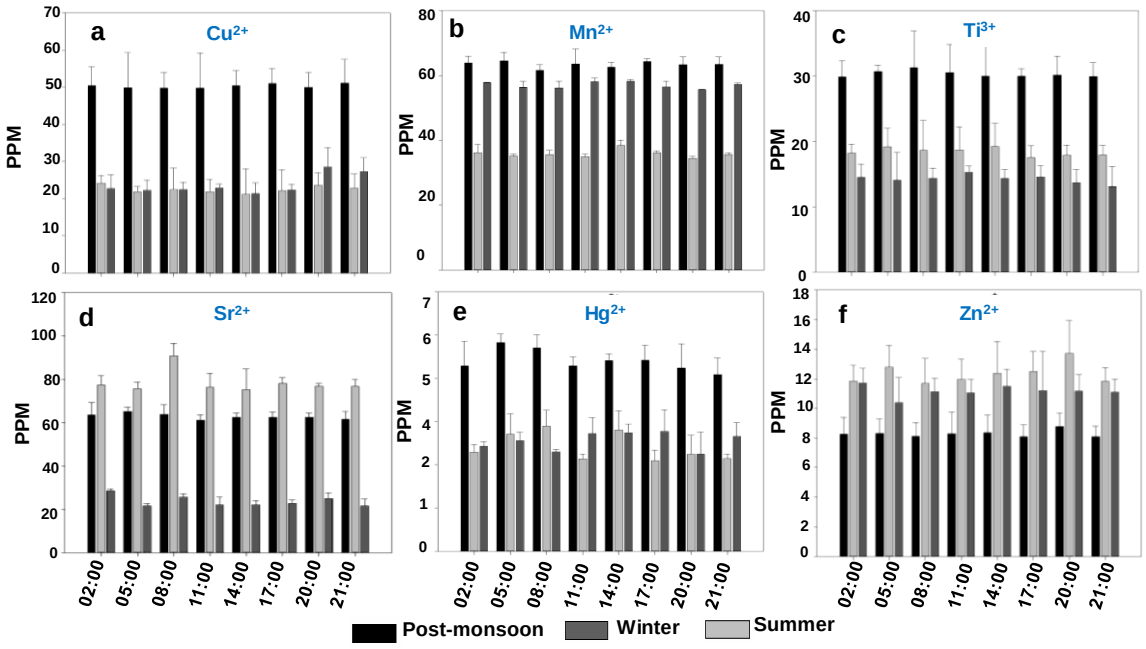

Figure 7.3: Ions identified from the leaves *S. fruticosa* at different time points of the day as influence by the diurnal rhythm. In the figure, the black bar represents ions identified during post-monsoon seasons, light grey during winter season and white during summer season. Each of the ion is represented in parts per million (PPM). A) Copper. B) Manganin ion. C) Titanium. D) Strontium. E) Mercury. F) Zinc.

7.3.3. Principle component analysis of the ions detected from the leaves of S. fruticosa

Principle component analysis (PCA) of the total ions detected from all the seasons showed a unique pattern of accumulation which are separated by PC1 and PC2 (Figure. 7.4). Two-dimensional PCA is a powerful statistical tool to identify maximum variance and also to find the correlation of the variance from any large data (Wold et al., 1987). PCA of the ions identified from each season at different time points to compare the pattern of variation of the ions across the seasons and also to provide an overview of the ionomics fingerprinting was done

using MetaboAnalyst 3.0. Whole ions detected at a specific time point is taken as one variance, which is then correlated with those ions' variant detected at different time points. Ions, from every season, identified from eight-time points i.e. 2 am, 5 am, 8 am, 11 am, 2 pm, 5 pm, 8 pm and 11 pm were clustered into eight variances. These are then statistically analyzed with the first two PCA, i.e., PC1 and PC2, to represent the total variance to and find their correlation. Both these components separate the variance into two vectors, with each having a positive and a negative axis. Seasonal variations were seen to have a direct impact on the pattern of ion accumulation, which is visible through PCA (Figure. 7.4).

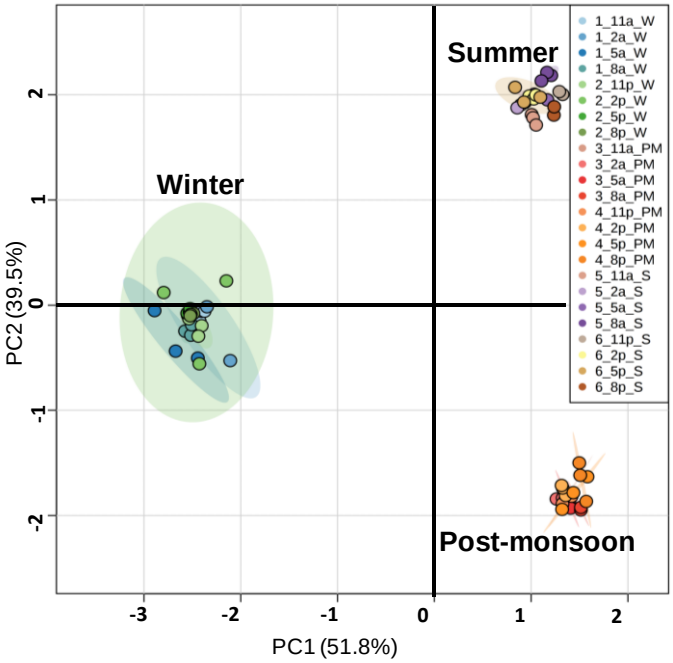

Figure 7.4: PCA showing the ionome of leaves of *S. fruticosa* as influenced by diurnal rhythm and seasonal variations. The PCA of the 18 ions identified during all the three seasons is represented by PC1 of 51.8% and PC2 of 39.5%**. The details of the samples are shown in an inset where 1_11a_ W represents the ionome of the leaves of *S. fruticosa* at 11am of winter, 1_2a_W for 2 am winter, 1_5a_W for 5 am winter, 2_11p_W for 11 pm winter, 2_2p_W for 2 pm winter, 2_5p_W for 5 pm winter, 2_8p_W for 8 pm winter, 3_11a_PM for 11 am post-monsoon, 3_2a_PM for 2 am post-monsoon, 3_5a_PM for 5 am post-monsoon, 4_11p_PM for 11 pm post-monsoon, 4_2p_PM for 2 pm post-monsoon, 4_5p_PM for 5 pm post-monsoon, 2_8p_PM for 8 pm post-monsoon, 5_11a_S for 11 am summer, 5_2a_S for 2 am summer, 5_5a_S for 5 am summer, 6_11p_S for 11 pm summer, 6_2p_PM for 2 pm summer, 6_5p_S for 5 pm summer, and 6_8p_S for 8 pm summer.**

PC1 and PC2 represent 91.3% of the seasonal variants wherein, PC1 separated the seasonal variations according to the atmospheric temperature wherein, the two hot seasons, i.e., post-monsoon and summer occupied the positive axis and winter occupied the negative axis. PC2 separated the three seasons according to salinity, wherein, the ions identified during post-monsoon, when the salinity is at its least, occupied the negative axis whereas the remaining two seasons, wherein salinity is at its peak, i.e., summer and winter were seen to occupy the positive and neutral axis.

Unlike the PCA that was obtained from the ions detected from all the seasons (Figure. 7.4) which showed distinct clustering, the PCA of the ions detected during different time point of the day for each season doesn't show any cyclic pattern (Figure. 7.5a-c). This also correlates the detailed accounts of ion accumulation as shown in Figure 7.1-7.3 where no significant changes in the pattern of ions were reported under the influence of diurnal rhythm (Figure 7.1-7.3). The non-rhythmic clustering of the PCA for each season indicates that the accumulation of ions was not regulated by the diurnal rhythm as micro homeostasis.

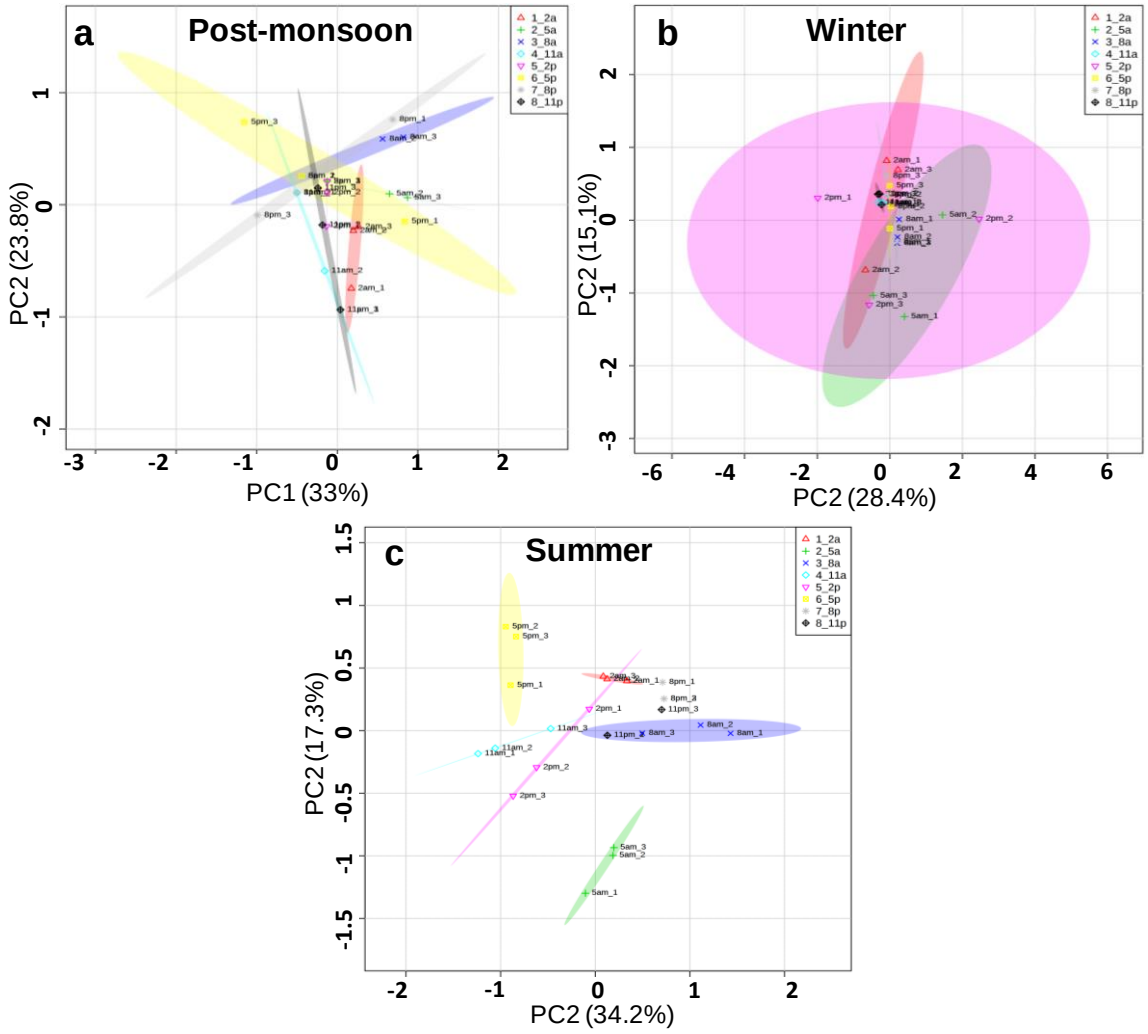

Figure 7.5: PCA showing the ionome of leaves of *S. fruticosa* as influenced by diurnal rhythm and seasonal variations. Influence of diurnal rhythm on the accumulation of ions was not observed in *S. fruticosa*. This is inferred as no distinct clustering of the ions detected at different time point was observed from the PCA that was obtained from the first two components of PCA, i.e., PC1 and PC2. A) PCA of the ions detected at a different time points of the day during post-monsoon. B) PCA of the ions identified at the different time points of the day during winter. C) PCA of the ions detected at a different time points of the day during summer.

7.3.4. Seasonal regulation of the accumulation of ions in leaves of S. fruticosa

Unlike the metabolic changes that were observed to be strongly influenced (chapter 5), ionomic changes under the influence of diurnal rhythm were not seen in *S. fruticosa* (Figure. 7.1-7.3 and Figure 7.4-7.5). To further check the influence of seasons on the accumulation of ions in *S. fruticosa*, each of the ions identified

at different time points in each season was averaged and was represented in the form of a box and whiskers plot (Figure 7.6-7.7). The ions detected are represented in parts-per-million (PPM). Significant changes in all the ions accumulating during different seasons could be observed. With the difference in the climatic condition, the level of salinity, availability of water, alkalinity, and the stage of the plant, the pattern of ions accumulating on the leaf of *S. fruticosa* was seen to vary. As described in chapter 5; the plant is under the stress of high temperature during the post-monsoon, combination of both cold stress and high salinity during winter and combination of both high temperature and salinity during summer. Additionally, the stage of the plant varies in each season, wherein, it germinates during monsoon, reaches the stage of escaping the harsh winter during winter and ultimately undergo senescence during summer. All these factors contribute to the pattern of ions accumulating in leaves of *S. fruticosa*.

The concentration of potassium ions accumulating in the leaves of *S. fruticosa* were found to be almost the same throughout the seasons (Figure. 7.6a). However, ions such as sodium, chloride, calcium, and magnesium increase as salinity and alkalinity of the soil increases, i.e., during winter and summer (Figure 7.6b-e). The concentration of phosphorous increases during winter as salinity increases and temperature reduces; however, as the temperature increases during summer, its concentration decreases (Figure. 7.6f). On the contrary, the concentration of iron and manganese is reduced with the reduction in temperature and attain the lowest value during winter. However, as the temperature increases, the concentration of ions gradually increases (Figure. 7.6g and h). In contrast, the concentration of copper ions decreases as salinity increases during winter and summer (Figure. 7.6i).

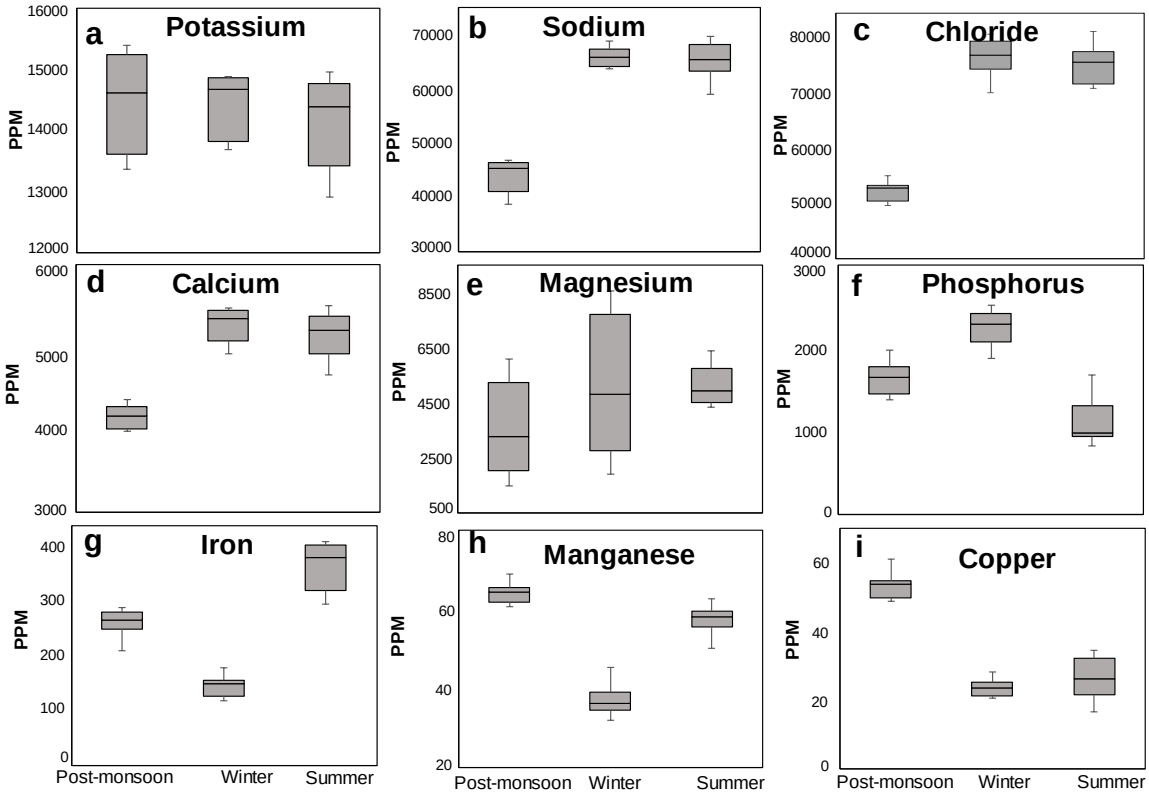

Figure 7.6: Ionic snapshots in the leaves of *S. fruticosa* as influenced by the change in seasons. The ions detected in each season at different time points were averaged and represented withbox and whiskers plot. The concentration of the ions accumulating in each season was found statistically varying. A) Potassium. B) Sodium. C) Chloride. D) Calcium. E) Magnesium. F) Phosphorous. G) Ferric. H) Manganese and I) Copper.

Like Iron, Manganese, and Copper, some of the trace and heavy metal elements such as Silicon, Sulfur, and Tungsten also were found to accumulate to higher levels during high temperature, i.e., post-monsoon and summer seasons (Figure. 7.7a-d). The concentration of these elements decreases during winter (cold stress). During post-monsoon and winter, the concentration of tungsten is maintained at the same level; however, as salinity and temperature increases during summer, the concentration increases (Figure. 7.7d). On the other hand, elements such as Zinc, Strontium, and Bromide accumulate more during cold stress (winter) as compared to that during high temperature (Figure 7.7e-g). The concentration of heavy metal elements such as mercury and Titanium is found to

be maximum during post-monsoon seasons as compared to that during winter and summer (Figure 7.7h and i).

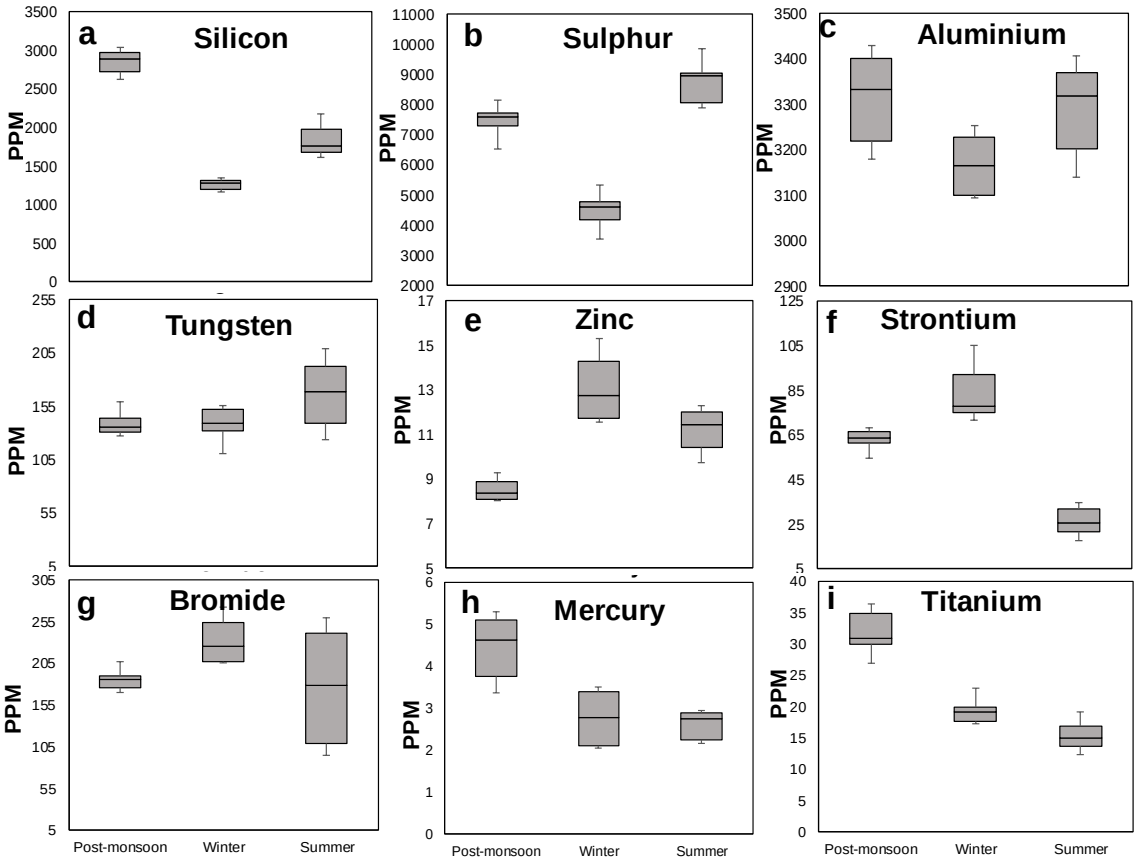

Figure 7.7: Ionic snapshots in the leaves of *S. fruticosa* as influenced by the change in seasons. The ions detected in each season at different time points were averaged and represented withbox and whiskers plot. The concentration of the ions accumulating in each season was found statistically varying. A) Silicon. B) Sulfur. C) Aluminum. D) Tungsten. E) Zinc. F) Strontium. G) Bromide. H) Mercury and I) Titanium.

The ion matrix of the complete ions identified from *S. fruticosa* at various time points and during different seasons is shown in Figure 7.8. The ion matrix, as represented in the form of a heatmap, shows that the accumulation of ions in all the three seasons showed significant changes. Some of the ions such as Chloride, Titanium, Manganese, Copper, and Mercury were seen to accumulate more during the post-monsoon season. During winter, sodium, Calcium, Zinc, Bromide, and Strontium were found to accumulate more. As summer sets in, ions such as Sodium, Magnesium, Aluminum, Magnesium, Sulfur, Chloride, Calcium,

Manganese and Iron were found to accumulate more on the leaf tissue of *Suaeda fruticosa*. However, some elements such as Potassium and Tungsten showed no change in their accumulation with the change in the seasons.

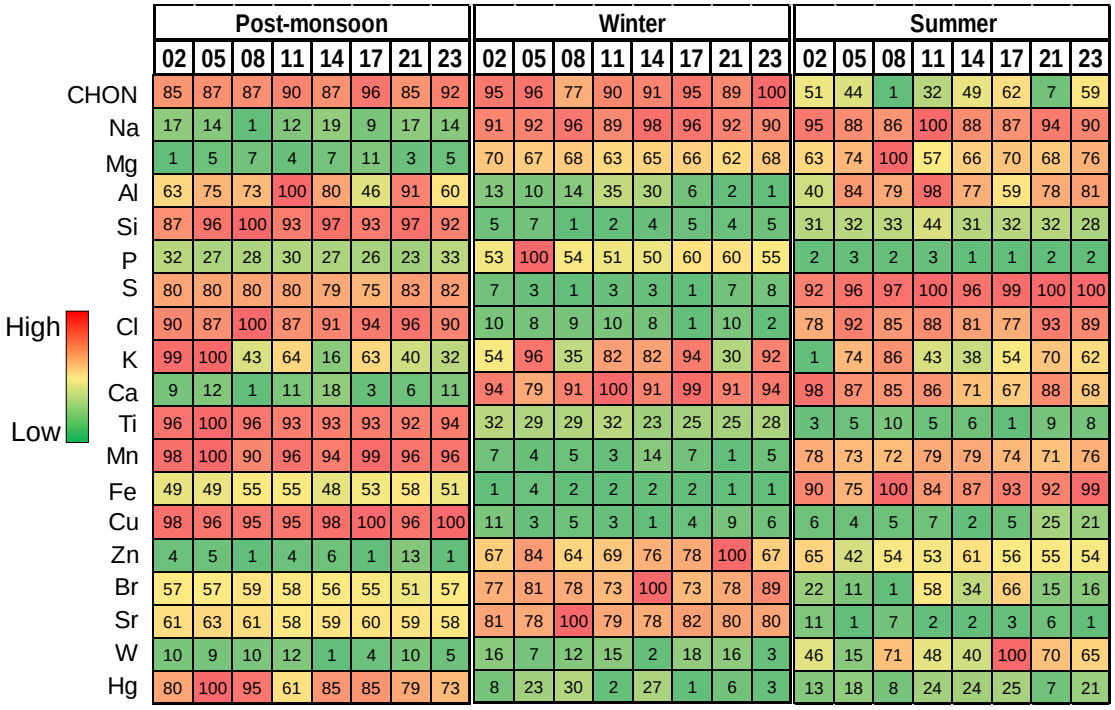

	Post-monsoon								Winter								Summer							
	02	05	08	11	14	17	21	23	02	05	08	11	14	17	21	23	02	05	08	11	14	17	21	23
CHON	85	87	87	90	87	96	85	92	95	96	77	90	91	95	89	100	51	44	1	32	49	62	7	59
Na	17	14	1	12	19	9	17	14	91	92	96	89	98	96	92	90	95	88	86	100	88	87	94	90
Mg	1	5	7	4	7	11	3	5	70	67	68	63	65	66	62	68	63	74	100	57	66	70	68	76
Al	63	75	73	100	80	46	91	60	13	10	14	35	30	6	2	1	40	84	79	98	77	59	78	81
Si	87	96	100	93	97	93	97	92	5	7	1	2	4	5	4	5	31	32	33	44	31	32	32	28
P	32	27	28	30	27	26	23	33	53	100	54	51	50	60	60	55	2	3	2	3	1	1	2	2
S	80	80	80	80	79	75	83	82	7	3	1	3	3	1	7	8	92	96	97	100	96	99	100	100
Cl	90	87	100	87	91	94	96	90	10	8	9	10	8	1	10	2	78	92	85	88	81	77	93	89
K	99	100	43	64	16	63	40	32	54	96	35	82	82	94	30	92	1	74	86	43	38	54	70	62
Ca	9	12	1	11	18	3	6	11	94	79	91	100	91	99	91	94	98	87	85	86	71	67	88	68
Ti	96	100	96	93	93	93	92	94	32	29	29	32	23	25	25	28	3	5	10	5	6	1	9	8
Mn	98	100	90	96	94	99	96	96	7	4	5	3	14	7	1	5	78	73	72	79	79	74	71	76
Fe	49	49	55	55	48	53	58	51	1	4	2	2	2	2	1	1	90	75	100	84	87	93	92	99
Cu	98	96	95	95	98	100	96	100	11	3	5	3	1	4	9	6	6	4	5	7	2	5	25	21
Zn	4	5	1	4	6	1	13	1	67	84	64	69	76	78	100	67	65	42	54	53	61	56	55	54
Br	57	57	59	58	56	55	51	57	77	81	78	73	100	73	78	89	22	11	1	58	34	66	15	16
Sr	61	63	61	58	59	60	59	58	81	78	100	79	78	82	80	80	11	1	7	2	2	3	6	1
W	10	9	10	12	1	4	10	5	16	7	12	15	2	18	16	3	46	15	71	48	40	100	70	65
Hg	80	100	95	61	85	85	79	73	8	23	30	2	27	1	6	3	13	18	8	24	24	25	7	21

Figure 7.8: Ion matrix of the various ions identified in leaves *S. fruticosa* during different time points in different seasons. The pattern of ions accumulating in *S. fruticosa* is represented in a heat map is shown. In the figure: red is for high, yellow for medium and green for the lowest values. All the data obtained were first normalized to bring the value of the parameters in the range of 1-100 to provide an unbiased color code.

7.4. Discussion

With the change in seasons, several edaphic and environmental factors parameters such as water availability, pH, minerals, elements and temperature around the rhizosphere vary (Hanc et al., 2017; Ouellette et al., 2017). These change in the parameters directly affect the plant mineral and elemental uptake. For example, in lotus, the osmotic pressure exhibited by the accumulation of sodium and potassium ions on the leaf was found to be maximum during September and October (Sánchez-Blanco et al., 1998). The nitrogen uptake in the alpine ecosystem was found to be maximum during the period from August to

October (Jaeger et al., 1999). In plants such as *Populus nigra* and *Populus trichocarpa* the plasma membrane H^+-ATPase was found to be most abundant during spring as compared to that during autumn which caused the accumulation of potassium on the plasma membrane and the tissue (Arend et al., 2002).

In Sambhar Lake, the natural habitat of *S, fruticosa*, changes significantly during seasons, viz. post-monsoon, winter and summer which results in change in the soil alkalinity, sodicity, water content and temperature (Chapter 5). Additionally, with the change in season, the anatomy and physiology of the leaves (Chapter 4), the metabolite content (Chapter 5) and the protein make up (Chapter 6) of *S. fruticosa* is also influenced. These change in the physical parameters, as well as the state of the plant, contributes to the pattern of ions accumulating in the leaf of *S. fruticosa*. Unlike the metabolites and proteins whose accumulation and expression were not only altered by the change in seasons but also are regulated diurnally, the ions that are accumulating in *S. fruticosa* were not regulated diurnally but only seasonally. In our study, we have been considering and analyzing the changes in the molecular make up such as proteins, metabolites, and ions of *S. fruticosa* under different time points, i.e., 2 am, 5 am, 8 am, 11 am, 2 pm, 5 pm, 8 pm, and 11 pm during three different seasons viz. post-monsoon, winter and summer. Diurnal, as well as seasonal regulation of metabolites and proteins, have been discussed in the previous two chapters (Chapter 5 and 6). However, diurnal ionomic changes identified in *S. fruticosa* was not observed (Figure. 7.1, 7.2 and 7.3). Principle component analysis of the ions detected during different time points for each season doesn't show any regular clustering or cyclic change like that of metabolites which infers that the accumulation of ions are not regulated significantly by the diurnal variations (Figure. 7.5). However, during different seasons, the changes in the pattern of ions accumulating in the leaves of *S. fruticosa* was quit evident (Figure. 7.6 and 7.7). A significant change of each ion was observed between different season. Principle component analysis of the ions accumulating in each season

shows distinct clustering wherein, each of the PC (PC1 and PC2) separated the clustering of the ions during the different seasons (Figure. 7.5).

Ion homeostasis is fundamental for all living organisms (Shcolnick et al., 2006). Over the years, many elements ranging from micro to macro levels, have been identified that play a role in the cellular protection mechanisms, however, accumulating beyond its threshold causes ion toxicity; therefore, plants possess strategies such as compartmentalization to adapt under heavy ionic stress (Zhu 2003). Through nutrient acquisition and ionic compartmentation, plants adapt under drought and saline stress (Bohnert et al., 1995; Acosta-Motos et al., 2017). As discussed in chapter 2, halophytes such as *Mesembryanthemum crystallinum*, *Aegiceras corniculatum*, and *Avicennia marina* can behave as accumulators, excluders or conductors (Bohnert et al., 1995; Yensen & Biel, 2006; Smaoui et al., 2011; Tan et al., 2013; Grigore et al., 2014) to survive under high saline environment. By accumulating salts such as Na^+ ions in the leaf and its organelles, halophytes reduce the water potential in the leaf as compared to that of the soil. This helps in water absorption from the saline soil (Hasegawa et al., 2000; Khan et al., 2000; Koyro et al., 2011). Compartmentalization of ions such as Na^+ and Cl^-between the mesophyll and epidermal layers have been reported in several plants such as sorghum (Boursier & Läuchli, 1989), wheat (Malone et al., 1991), barley and beans (Outlaw et al., 1984) of which, plants prefer the epidermal layers as, the ions accumulated in the epidermal cells layer help in buffering the pH of the leaf under saline environment (Outlaw et al., 1984). In addition, the ions that are accumulated on the epidermal leads to shrunken stomata that further reduces the rate of transpiration and water loss (Boursier & Läuchli, 1989; Malone et al., 1991). In *S. fruticosa*, as salinity and alkalinity increased, followed by a decrease in water availability leads to the accumulation of sodium and chloride ions in the leaf (Figure. 7.6b and c). This increase in the accumulation of sodium and chloride, which helps in water absorption and storage might have contributed to the succulent leaf development during winter and summer.

Among all the ions, Sodium ions are known to have the most detrimental effect on plant's physiology (Wakeel 2013). Sodium ions interfere with the homeostasis of potassium ions by hindering its uptake, which further alters the ratio of sodium and potassium (Na^+/K^+) in plants (Assaha et al., 2017). Increase in sodium/potassium ratio is lethal to plants as the core enzymatic activity of the cytosol gets disturbed, leading to plant death (Wakeel 2013). Potassium is known to play an important role in activation of over 60 enzymes involved in growth and development (Van Brunt and Sultenfuss, 1998), maintaining the turgidity of stomata for gas exchange and regulate stomatal activity for photosynthesis (Cochraneand Cochrane, 2009; Zhao et al., 2001), regulate enzymes for starch synthesis, and control the transportation of synthesized sugar molecules, water and nutrients in plants (Hawker et al., 1974; Kadam, 2011; Sze and Chanroj2018). Plants, therefore, need to maintain the level of potassium, irrespective of any condition, for its growth and development. In our study, we found that the level of potassium was maintained to same level in *S. fruticosa* even under high salinity and drought (Figure. 7.7a). This tight regulation of the potassium concentration under different stress that comes along with the change in seasons could confer to its highly tolerant character.

Calcium ions, apart from its role in activating enzymatic activities (Wallace et al., 1966; Jones and Lunt 1967), coordinating growth and development of roots, shoots, and leaves (Bush 1993; Johnson et al., 1995) are known to play a significant role in holding the plant cell wall component tightly which prevents the loss of water from the leaf tissues (White and Broadley 2003). In *S. fruticosa*, the concentration of calcium accumulating in the leaves ranged from, 4000-4500, 5000-5500, and 4800-5500 PPM during post-monsoon, winter and summer, respectively (Figure. 7.6d), maximum of which is during winter and summer when salinity is maximum. This could have helped the cell wall of *S. fruticosa* to hold together firmly preventing water loss conferring to its tolerance. Under salinity and temperature stress such as cold and high temperature, the photosynthesis machinery gets impaired due to degradation of thylakoid (Wungrampha et al.,

2018), this further generates ROS causing photo-oxidation and inhibit CO_2 uptake (Wang et al., 2003). Magnesium ions are compartmentalized mostly in the chloroplast as it is the primary ion for building the ultrastructure of the chloroplast. Magnesium also is the central core ion of the chlorophyll pigments. It also helps in the activation of RuBisCO (Carkman and Yaziri, 2010; Tränkner et al., 2018). Under high light intensity, magnesium ions protect the photosynthetic pigments from photodamage (Moomaw and Maguire, 2008) and also help in sucrose accumulation (Waters 2011). Accumulation of sucrose, an osmolyte, is known for its protection under salinity stress (Chapter 4; Rizhsky et al., 2004, Suzuki et al., 2014). *S. fruticosa* accumulate high amount of magnesium (range of 2800 to 4500 PPM) as compared to other glycophytes such as Arabidopsis which accumulate about 2500 PPM (Moomaw and Maguire, 2008; Waters 2011) in its leaf tissue throughout the seasons (Figure. 7.6e). The maximum concentration of magnesium was found during winter and summer as salinity and alkalinity was at its highest. This protects *S. fruticosa* from photodamage and regulates the photosynthesis under harsh conditions.

Phosphorus, a micronutrient which constitutes up to 0.2% of the dry weight, is involved in several biochemical reactions as well as genetic makeup in plants (Schachtman et al., 1998). It is also involved in controlling the enzyme activity (Theodorou and Plaxton 1993). In pea, phosphorous strongly influence the fixation of nitrogen from the soil (Jakobsen 1985). After nitrogen, phosphorus is the next most limiting macronutrient in plants (Schachtman et al., 1998). Deficiency of phosphorus leads to lowering of photosynthesis efficiency, impairs plant's growth and development finally reducing yield (Cakmak et al., 1994; Bonser et al., 1995; Hammond et al., 2004). Phosphorous deficiency is prevalent for the plants surviving in a dry climate as the root grows deep in search of water; however, the available phosphate for the plants are confined at the upper layer of the soil and reduces along with the depth (Bonser et al., 1995). In plants, the concentration of phosphorus varies between 1000-5000 PPM under normal conditions. However, the concentration may vary under stress (Epstein 1965). In

S. fruticosa, throughout the seasons, the concentration of phosphorus is tightly regulated and maintained within a range of 1500-1800, 2000-2500 and 1000-1500 PPM during post-monsoon, winter and summer respectively (Figure. 7.6f). At soil pH 5.5 or lower, the available manganese for the plants are in the di-ionic state (Mn^{2+}) however, as the pH increases to 6.5 or above, the di-ionic further gets reduced to Mn^{3+} or Mn^{4+} and Mn^{7+} which are not available for the plants (Ducic and Polle 2005). Manganese ions act as a cofactor for ROS scavenging enzymes such as the manganese superoxide dismutase also called the guardian of the powerhouse (Holley et al., 2011) and manganese catalase (Whittaker 2012). It also plays a vital role as a cofactor for the activation of pyruvate carboxylase (Burnell 1988) and phosphoenolpyruvate carboxykinase (Tanaka et al., 1995). Normally, plants accumulate 30 to 100 PPM of manganese on its tissues; however, some hyperaccumulators such as *Poa annua* L., *Cynodon dactylon L.,* and *Polygonum perfoliatum L*. can store up to 530 PPM (Edwards and Asher, 1982; Clarkson, 1988; Liu et al., 2010). In our study, we found that *S. fruticosa* is not a hyperaccumulator of manganese, however, even under different stress that the seasons bring, it still can maintain the level of Manganese at the range of 60-70, 35-40 and 55-60 PPM of dry weight during post-monsoon, winter and summer respectively (Figure. 7.6h). *Suaeda fruticosa* also accumulate 50-55, 20-25, and 20-30 PPM of copper per dry weight during post-monsoon, winter and summer seasons, respectively (Figure. 7.6i). In general, plants accumulate 20-30 PPM of Copper per dry mass under normal condition; however, the concentration may vary depending on the conditions to where it grows (Marschner, 1995; Ducic and Polle, 2005). Maintaining the level of Copper at its optimum is very crucial in plants as Copper ions are an essential component for various reactions involving the electron carrier such as; photosynthesis (plastocyanin), respiration (cytochrome c oxidase), superoxide dismutase, laccases and antioxidative defense (ascorbate oxidase) (Rodriguez et al., 1999).

Silicon, even though it is the second most abundant element, next to oxygen, in the earth crust, is not listed among the essential mineral elements in plants (Liang et al., 2007). However, the role of silicon ions as a critical element for stimulating growth in plants under salinity, drought, heavy metal toxicity and chilling stress by stimulating antioxidant species, co-precipitation with the toxic metals, acting as a barrier to prevent from uptake of salts, immobilizing the metal toxic and compartmentalizing the toxic elements have been debated by several scientists (Romero-Aranda et al., 2006; Liang et al., 2007; Lee et al., 2010; Zhu and Gong 2014). In *S. fruticosa*, throughout the seasons, silicon is accumulated in abundance at a concentration range of 1200-3000 PPM per dry weight (Figure. 7.7a).

Like many halophytes that are commercially used as heavy metal phytoremediation (Tordoff et al., 2000; Parraga-Aguado et al., 2013; López-Orenes et al., 2017) *S. fruticosa* also accumulate several heavy metals such aluminum, tungsten, zinc, strontium, mercury, and titanium throughout the seasons (Figure 7.7b-i).

7.5. Conclusions

With the change in seasons, salinity, alkalinity, soil pH and temperature vary in Sambhar lake. These changes in the parameters directly affect the ionic composition of the leaves of *S. fruticosa* growing in the region. As salinity and alkalinity increases during winter and summer, ions such as sodium, calcium, and chloride were found to accumulate in abundance. The accumulation of these ions further helped the plant in absorption and conservation of water from soil. On the other hand, the concentration of ions such as potassium, magnesium, and phosphorus that play a crucial role in growth and development as well as homeostasis of the plants were found to be accumulated in abundance throughout the seasons. Some heavy metals such as aluminum, tungsten, zinc, strontium, mercury, and titanium were also found to accumulate in *S. fruticosa*. These findings show how *S. fruticosa* regulates its ionic homeostasis that confers

to its adaptation. Secondly, because *S. fruticosa* can accumulate heavy metals throughout the seasons, it can potentially be used phytoremediation of heavy metal.

Chapter 8

Integration and correlation study of metabolomics, proteomics and ionomics data obtained from the leaves of *Suaeda fruticosa* as influenced by diurnal rhythm and seasonal variations

8.1 Introduction

With the advancements in high throughput technologies, research related to the understanding of global molecular structures of any organism has improved drastically over the past few years. The first global scale assessment to comprehensively identify the molecular make up of an organism (known as *omics* studies) is the *genomics* (Fleischmann et al., 1995). This also is the most advanced and matured omics studies till date. After the successful launch of genomics, several other omics studies such as *proteomics;* quantification and study of peptide abundance and modification (Mann and Jensen, 2003), *ionomics;* study on the accumulation of trace elements representing the inorganic components of an organism (Salt et al., 2008), *transcriptomics;* qualitative and quantitative study of the RNA in the whole genome (Trapnell et al., 2010), *metabolomics;* simultaneous analysis and quantification of small molecules such as amino acid, carbohydrates, fatty acids and other cellular metabolites at a given time (Patti et al, 2012), and *epigenomics*; genome-wide stud yon the reversible modifications of DNA and/or DNA-associated proteins (Piunti and Shilatifard, 2016) have been developed (Koboldt et al., 2013; Hasin et al., 2017).

Each of the omics study generates valuable information providing the global assessment of the molecular make up of an organism. However, in recent years, scientists are working on integrating each of the omics (multi omics studies) data generated from an organism to get the holistic framework of an

organism at the molecular level (Joyce and Palsson, 2006; Palsson and Zengler, 2010; Yizhak et al., 2010). The data generated by integrating multi omics are usually large; however, by supervising and targeting a particular pathway, several molecular functions and steps have been deciphered as all the measured omics platforms are connected, e.g. the integration study of genomics, transcriptomics and epigenetic had led to the understanding of cis-regulation network involve in cancer development (Huang et al., 2017; Wu et al., 2019). Two aspects of integration of multi omics have been widely practiced: a) integrating same types of omics data generated from different studies for the same species, and, b) integrating different omics data sets generated from the same cohort samples of a species (Wu et al., 2019).

In the recent past, targeted studies such as lipidomics to identify the diversity in lipid contents (Patel et al., 2019), measurement of essential element contents (Khan et al., 2000), estimation of phenolic contents under stress (Oueslati et al., 2012), transcriptomics analysis (Diray-Arce et al., 2015) have been done for the xerohalophyte *Suaeda fruticosa*. However, no work has been done on integrating the multi OMICS data obtained from this plant. In the present chapter, we performed an attempt to integrate the three data sets (metabolomics, proteomics and ionomics from the previous chapters of this thesis) that were generated from *S. fruticosa*. This has been achieved through Weight Gene Co-expression Network Analysis (WGCNA), an algorithm designed in R-studio for correlational study of independent datasets (Langfelder and Horvath, 2008; Wanichthanarak et al., 2015; Zierer et al., 2015; Rodriguez et al., 2019). There is a need to comprehensively understand the correlation between the metabolites accumulating, proteome expressing and ions accumulating at a set time point and season with respect to the environmental factors such as salinity, pH and atmospheric temperature (in our study). From our correlation study, we found that the molecular framework of *S. fruticosa* is largely governed by the changes in atmospheric temperature rather than the changes in soil pH and salinity. We also found through hierarchical clustering of the ‘multi-omics’ datasets that the

pattern of metabolites, proteins and ions accumulating in *S. fruticosa* also differs in each season.

8.2 Material and methods

8.2.1 Omics data sets

From *S. fruticosa*, three independent omics datasets; metabolomics (Chapter 5), proteomics (Chapter 6) and ionomics (Chapter 7) were generated. As described in the material and methods section for each chapter, independent omics study of *S. fruticosa* was done eight at different time points (2am, 5am, 8am, 11am, 2pm, 5pm, 8pm and 11pm) to check for diurnal regulation and during three different seasons viz. post-monsoon, winter and summer to study the influence of changing seasons to *S. fruticosa*. So, in total we had 96 (8×3×4) datasets from the same plants. Most importantly, the strength of experiments lies in the fact that it is the same tissue harvested at the same time and used for the OMICS analysis. Hence the datasets are quite robust in nature.

8.2.2. Correlation module identification

For the correlational studies of the multi-omics data available with us, the algorithm for Weighted Correlation Network Analysis (WGCNA) developed by Langfelder and Horvath (2008) was used in R-studio (Team, 2010). Adjacent matrix (adjacent value, a_{ijk}) between the three omics datasets were calculated through Pearson correlation co-efficiency (PCC) using the formula:

$$a_{ijk} = \left| 1+ \{cor(x_i, x_j, x_k)\}/3 \right|^{\beta}$$

Where, i, j and p represent compile data of metabolomics, proteomics and ionomics respectively. The power factor, β (18 in our study, Figure 8.1), in the equation represents the weight value which is generated from the scale-free network using pickSoftThreshold function that is available in WGCNA package (Langfelder and Horvath, 2012). To further convert the adjacent matrix (a_{ijk}) into

topological overlap matrix (TOM), hierarchical clustering was done using dissimilarity matrix (cf. Yip and Horvath, 2007). Each of the modules identified after generating TOM were represented by hierarchical clustering through cutting branches tree clustering using dynamic tree-cut algorithm (Langfelder and Horvath, 2008).

8.3 Results and discussion

8.3.1 Construction of weighted co-expression network

To arrange the three independent omics datasets obtained from *S. fruticosa* into a single suitable set for analyzing with WGCNA, all the identified metabolites, proteins and ions were arranged in one file and the single data generated was normalized step wise (Khojasteh et al., 2005) after imputing the missing value completely at random (MCAR) with the lowest observed value (Karpievitch et al., 2012). Following which, weighted co-expression network was calculated by applying key parameters assigned as soft-thresholding power (Cf. Zhang and Horvath, 2005; Pei et al., 2017). As recommended by Langfelder et al. (2008), the soft-thresholding power was chosen based on the criteria of scale-free topology. Using the formulae given in the material and method section, the power 18 was chosen (Figure 8.1) to find the correlation. The value was chosen as it represents the lowest power point at which the curve for the scale-free topology index fit and fall flat (Figure 8.1a). It is also true that it is at this value that the index reaches the highest value above 0.85 (Figure 8.1a), and also shows moderate median, mean and maximum connectivity (Figure 8.1b, c and d).

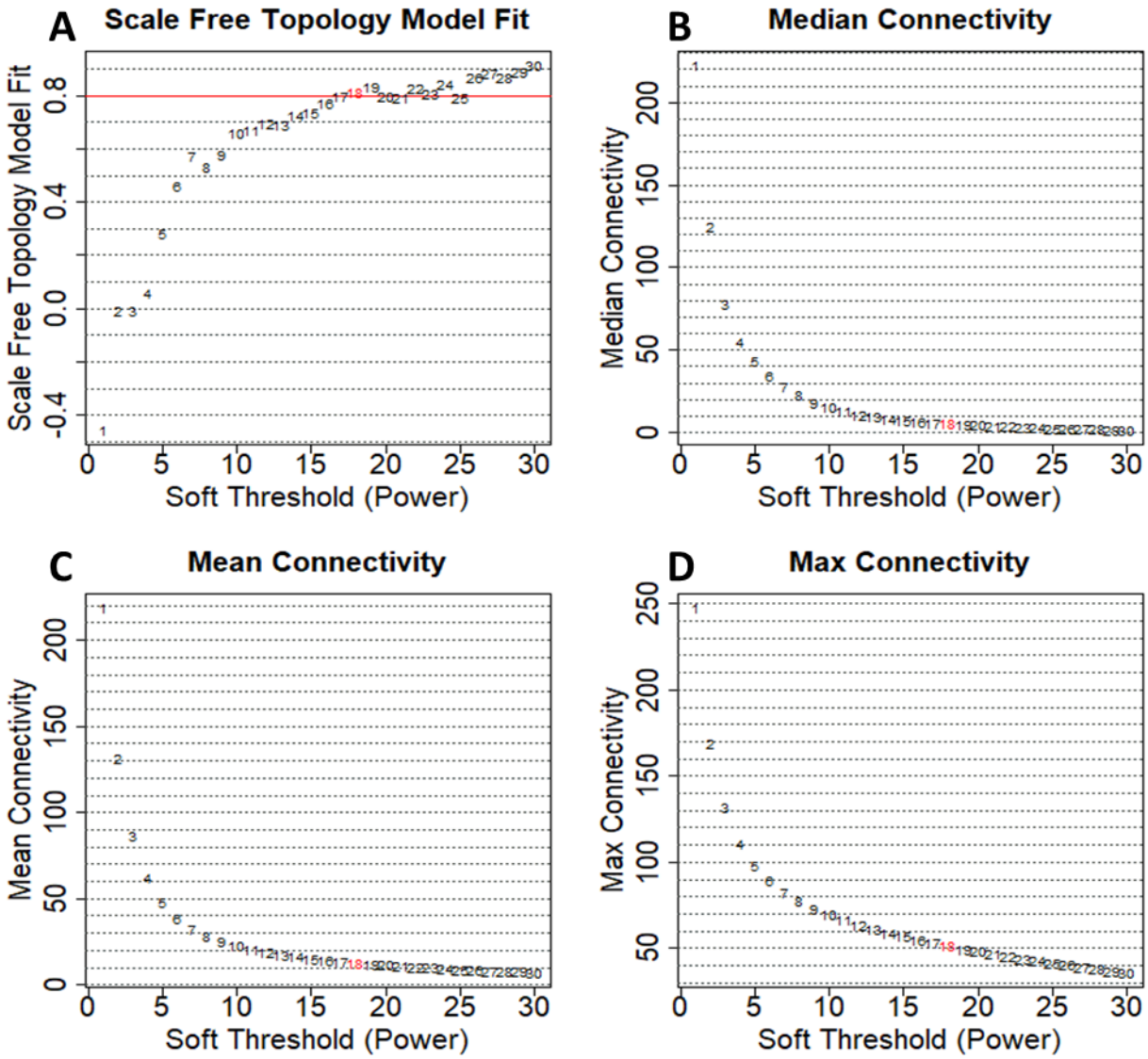

Figure 8.1: Summary of the network indices (y-axis) to the functions of soft thresholding power (x-axis). Numbers in the plots indicate the corresponding soft thresholding powers. The plots indicate that approximate scale-free topology is attained around the soft-thresholding power of 18 for the three sets of data. This value is chosen as the summary connectivity measures decline steeply with increasing soft-thresholding power; it is advantageous to choose the lowest power that satisfies the approximate scale-free topology criterion. A) Scale-free topology criterion plot for choosing the power β for the signed weighted correlation network. Left-hand side: the SFT index R^2 (*y*-axis) as a function of different powers β (*x*-axis). B) Scatterplots of mean connectivity vs. soft thresholding power. C) Scatterplots of Median connectivity vs. soft thresholding power. D) Scatterplots of Max connectivity vs, soft thresholding power.

8.3.2 Identifying the functional module of the three datasets through WGCNA

One principle parameters of weighted co-expression gene network analysis (WGCNA) is to find the correlation direction for both signed and/or unsigned networks (Pei et al., 2017). In general, the nodes that are negatively correlating in the *signed correlation* network are usually considered as unconnected. This is assigned as; the connection strength between the nodes in signed correlation modules is found to be almost zero, or, zero in most cases (Lawyer, 2015). However, in the correlation network of *unsigned modules*, the nodes that are negatively correlated are considered to have higher connection strength. The values of correlation in this module are based on the absolute values therefore, the positive or negatively correlated parameters were considered as equal correlation (Langfelder and Horvath, 2008; Langfelder, 2015). As the correlation assigned to both positive and negatively correlated parameters are considered as same, unsigned modules was not considered for the network construction through WGCNA. The functional network constituting the block-wise modules that are from the signed modules was therefore set in our studies.

In an attempt to understand the molecular adaptations of *S. fruticosa* under different seasons viz. post-monsoon, winter and summer and during different time points of the day, we have analyzed the physiological adaptation (Chapter 4), change in the metabolomics (Chapter 5), proteomics (Chapter 6) and ionomics (Chapter 7) which are described in the previous chapters. To further find the correlations of the metabolites, proteins and ions accumulating during different time points of the day in different seasons, we performed WGCNA and constructed the network with those metabolites/proteins/ions that shows Pearson correlation of $r \geq 0.8$ and $p \leq 0.05$ (as described in Langfelder and Hovarth, 2008) using the three datasets we have of *S. fruticosa* (Chapter 5, 6 and 7). In our study, we have measured few parameters that directly influence the molecular construct of *S. fruticosa* viz. soil salinity, pH and atmospheric temperature (as described in Chapter 3). Taking these three parameters as three

independent traits, a module was generated through WGCNA to find the influence of the traits in metabolites/proteins/ions of *S. fruticosa*. Each module was indicated by color codes wherein brown represents the metabolites/proteins/ions that shows correlational expression under the influence of soil salinity, blue by soil pH, turquoise by atmospheric temperature, and grey for those metabolites/proteins/ions that were not influenced by the three parameters taken into account (Figure 8.2). List of the metabolites, proteins and ions that showed correlation with respect to the traits (temperature, pH and salinity) are listed in Table 8.1.

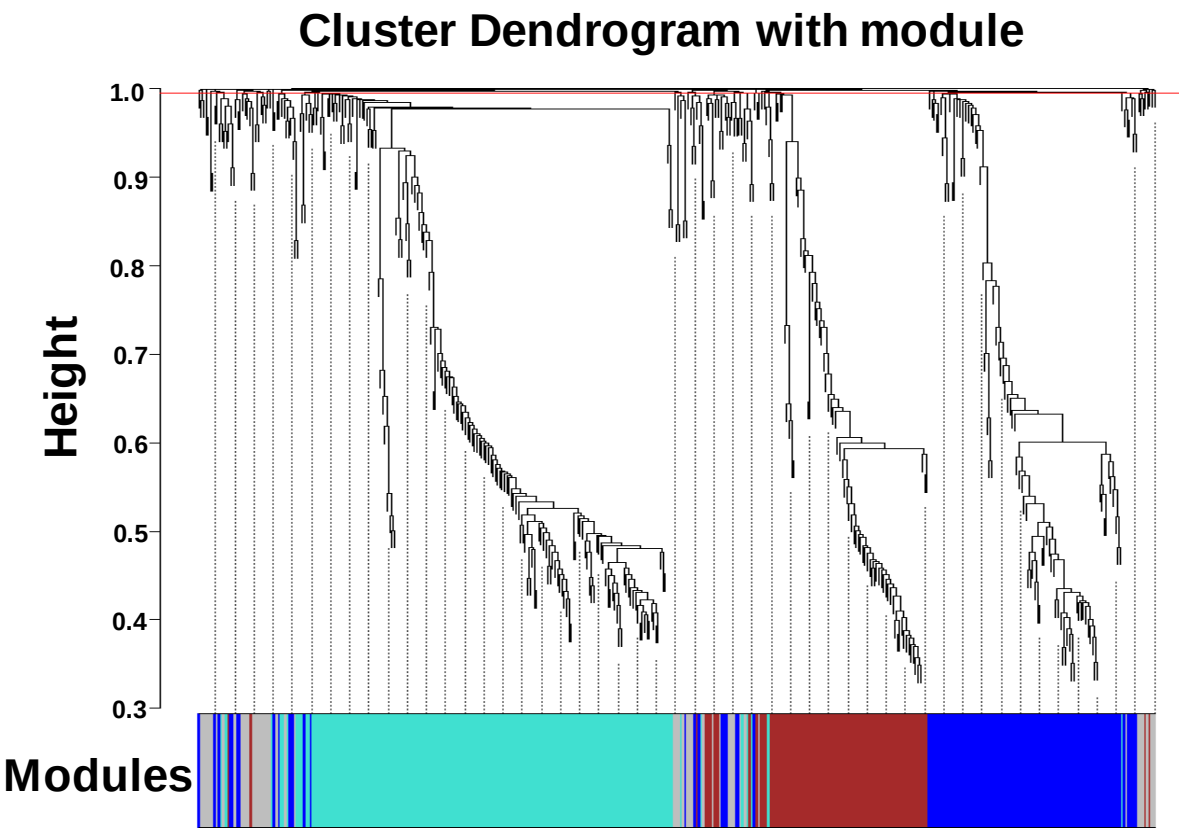

Figure 8.2: Hierarchical clustering dendrogram of metabolites/proteins/ions for identifying consensus modules under the influence of soil salinity, pH and atmospheric temperature. Branches of the dendrogram, cut at the red line, correspond to consensus modules. Metabolites/proteins/ions in each module are assigned the same color, shown in the color band below the dendrogram. Metabolites/proteins/ions under the influence of salinity, pH and temperature are assigned by brown, blue and turquoise respectively. Metabolites/proteins/ions not assigned to any of the modules are colored grey**.**

Table 8.1 List of the top metabolites, proteins and ions that showed positive correlation with the change in traits (temperature, pH and salinity) in the leaves of *S. fruticosa*. Metabolites are listed in the blue box, ions in pink box and proteins in green box

pH regulated (Module: blue in Figure 8.2)	Salinity regulated (Moducle: brown in Figure 8.2)	Temperature regulated (Module: turquoise in Figure 8.2)	Unassigned (Module: grey in Figure 8.2)
Vinyloxyethanol	Thiophenethiol	Citrulline	ETHYLENE INSENSITIVE3 LIKE 1
Methylpropantriol	Phytol	Glutamine	Transposable element protein
Threonine	Glycine	Homocystine	Dehydrin
Valine	Tyrosine	Alanine	Os01g0593500 Oryza sativa Japonica Group
Ornithine	N N Dimethylglycine	L Asparagine	Conserved hypothetical protein Ricinus communis
Penicillamine	Pyroglutamic acid	L Aspartic acid	DNA directed RNA polymerase beta chain
Hydroxyisocaproic acid	Tyramine	L Cysteine	ASR
Methylvaline	Myristic acid	L Glutamic acid	14 3 3 like protein
Anthracene	Ricinoleic acid	L Isoleucine	Peptidyl prolyl cis trans isomerase
Palmitoleic acid	Phosphoric acid	L Leucine	Dof type zinc finger protein
Inositol	L-chiro inositol	L Lysine	Defensin like protein
Alloxanic acid	Stigmasterol	L Norleucine	Remorin
Butyric acid	Hydroxystearic acid	L Norvaline	Dihydrodipicolinate synthase
Citraconic acid	Dodecandioic acid	L Phenylalanine	WRKY transcription factor
Gluconic acid	Formic acid	L Proline	Hypothetical protein VITISV_012456 Vitis vinifera
Ribonic acid	Glucuronic acid	L Serine	Hypothetical protein ARALYDRAFT_478970 Arabidopsis lyrata subsp lyrata
Isothiocyanic acid	Glycolic acid	N Acetylglutamine	O methyltransferase
Tartaric acid	Gulonic acid	Alanine	Hypothetical protein Vitis vinifera
Methanoic acid	Lactic acid	Hydroxylamine	Ppi phosphofructokinase
Propionic acid	Maleic acid	Matairesinol	Unnamed protein product
Ribonic acid	Mesaconic acid	Glycerol	Dihydroflavonol 4 reductase
Shikimic acid	Aminoisobutyric acid	Glycerol-3-phosphate	APETALA2 protein
Fe	Al	Na	Caffeic acid 3 O methyltransferase
W	Si	Mg	Predicted protein Populus

			trichocarpa
Predicted protein Populus trichocarpa	S	P	Heat shock protein
Metallothionein 1	Cl	K	Phosphoenolpyruvate carboxylase
GTP binding protein	Ti	Ca	Terminal flower 1
Ubiquitin conjugating enzyme E2 7	Mn	Zn	Flavanone 3 hydroxylase
Hypothetical protein OsI_16144	Cu	Br	WDL1
CLAVATA3	Hg	Sr	Maturase K
S locus pollen protein	Predicted protein	Defensin like protein 1	ABC transporter family protein
B1340F09 22 Oryza sativa Japonica Group	L protein of photosystem II	Em protein	Gbberellin regulated protein 2 precursor
ORF60b	Putative methionyl tRNA synthetase	Stress responsive protein	psbR PSII R photosystem II polypeptide
DNAJ heat shock N terminal domain containing protein	Pseudo response regulator 7	Hypothetical protein VITISV_006719	Dihydroflavonol 4 reductase 1
Self incompatibility S26 RNase	Hypothetical protein SORBIDRAFT_01g031120 Sorghum bicolor	F box family protein	Hypothetical protein SORBIDRAFT_06g028410
unknown Glycine max	Carotenoid isomerase	Cytochrome P450	Ribosomal protein L22
Maturase	LOC100286242 Zea mays	Predicted protein Micromonas pusilla	hypothetical protein CHLNCDRAFT_143905
Thiol protease SEN102	Synaptosomal associated protein	Hypothetical protein OsI_26228	Hypothetical protein ARALYDRAFT_473326 Arabidopsis lyrata subsp lyrata
Putative F Box protein	Predicted protein Ostreococcus lucimarinus CCE9901	Thioredoxin H type 5	Tyrosine N monooxygenase
Bowman Birk trypsin inhibitor	ribulose 1 5 bisphosphate carboxylase oxygenase large subunit	Predicted protein Arabidopsis lyrata subsp lyrata	Nonspecific lipid transfer protein 3 precursor
Trypsin inhibitor MCI 3	Thioredoxin y	ATP synthase beta chain	Hypothetical protein VITISV_009746
Polynucleotidyl transferase	Vf14 3 3d protein	Metallothionein like protein	p23
Putative DNA binding protein	GPI anchored protein	Os02g0793150 *Oryza sativa* Japonica Group	RNA polymerase.subunit

To further define the block-wise modules in WGCNA analysis, several parameters such as TOMType, the signed module that defines the counts which directly connects with Topological overlap Matrix (TOM), and minModules Size, that defines the minimum module of size 30 connecting with the node are taken into account (Pei et al., 2017). In most of the case study, the default value 30 for calculating the minModules Size that is given in the package is used (Liu et al., 2014; Broadbent et al., 2017; Vignato et al., 2019). Similarly, we also used 30 to calculate the minModules Size in our study. In addition, several modules are available to identify group of parameters whose expression/accumulations profiles are highly correlated. Those modules which shows positive correlation can be summarized into one representative gene, also known as eigengene (Langfelder and Hovarth, 2007). From our study, we identified four eigengenes from the three omics datasets of *Suaeda fruticosa* which are assigned with different color code (Figure 8.3). The four eigengenes module identified are further clustered to visualized the relationship between the modules.

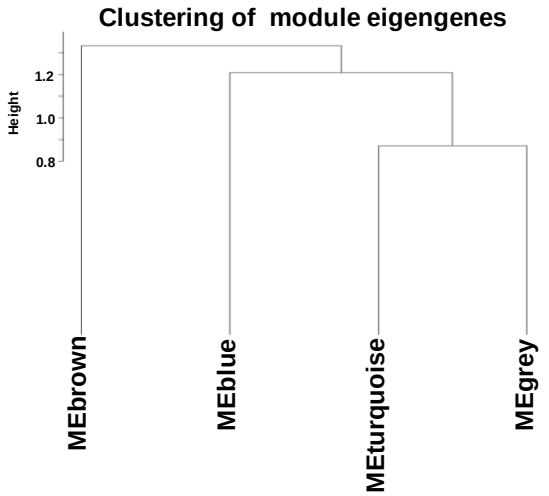

Figure 8.3: Clustering dendrograms of consensus module eigengenes for identifying meta-modules. To visualize the eigengene network representing the relationships among the modules i.e. the traits (salinity, pH and temperature) to the correlation of the change in metabolites/proteins/ions a hierarchical clustering dendrogram of the eigengenes based on the dissimilarity was performed. The branches of the dendrogram group together the parameters that are positively correlated. The color code module brown represents the soil salinity parameter, blue the pH, turquoise the temperature, and grey the non-correlated parameters.

We identified three clusters from the four eigengenes of which, the grey modules which has the metabolites/proteins/ions that are not correlated with the change in seasons and time are found to cluster closely with those that show correlation with atmospheric temperature. Those that show correlation with respect to pH (blue) and salinity (brown) were seen to cluster separately and independently (Figure 8.3).

8.3.3 Dendrogram clustering of the three Omics datasets obtained from S. fruticosa shows the influence of atmospheric temperature in its molecular construct

As mentioned in the material and methods section in Chapter 5, 6 and 7, the complete sets of Omics were obtained by harvesting *S. fruticosa* at different time point to check the influence of diurnal rhythm and also during three different seasons viz. post-monsoon, winter and summer to check the influence of changing seasons on the molecular construct of *S. fruticosa* growing in a xerophytic condition. To further check the correlation of the complete sets of metabolites/proteins/ions accumulating/expressing in *Suaeda fruticosa* during different seasons at different time points, clustering using *hclust* function matrix of the compiled omics was done (Figure 8.4).

We observed three distinct clusters from the complete datasets of omics through hierarchical clustering corresponding to the three different seasons. However, clusters of post-monsoon and summer were observed to be closer and also the two-cluster merge earlier than that of the winter in the hierarchical clustering (Figure 8.4). The site from where *S. fruticosa* was harvested has longer summer with extreme heat and very short winter. In addition, salinity and pH of the area remains high throughout the year even though during post-monsoon it gets relatively lower (Chapter 3). These phenomena were seen to have an impact on the molecular framework of *Suaeda fruticosa* as observed through clustering wherein; hierarchical clustering of the complete metabolites, proteins and ions were seen to be largely influenced by the change in

atmospheric temperature rather than the change in salinity. This is observed as; post-monsoon and summer, the two seasons that experiences hot weather, were seen to cluster closer and merge earlier however, the cluster during winter were seen further apart. This shows that, the molecular construct of *S. fruticosa* is largely monitored by the change in atmospheric temperature.

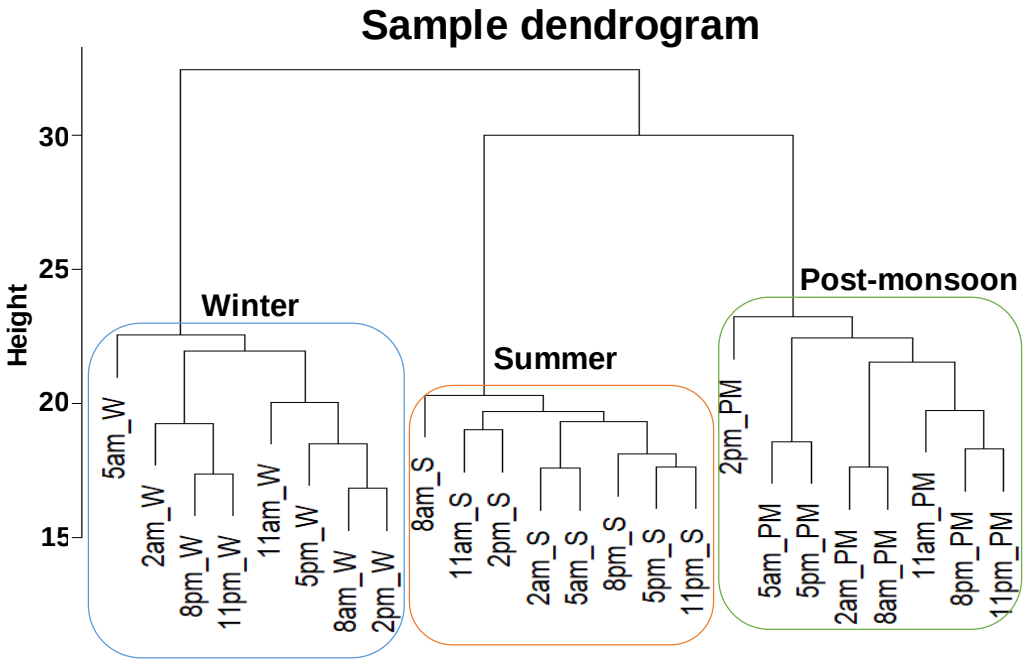

Figure 8.4: Sample dendrogram as calculated from the three omics datasets showing the hierarchical clustering of the time when *Suaeda fruticosa* was harvested. The complete sample composition level based on a Pearson correlation matrix allowed the identification of three main clustering groups showing the correlation of the three omics datasets at different time point. Different seasons were clustered separately.

During each season, the molecular framework of one particular time point was seen to separate uniquely from the cluster; 5am, 8am and 2pm for winter, summer and post-monsoon respectively. The coldest time point (~5^{o}C) during winter was observed between 4am-5am, the most favorable temperature (~30^{o}C) and PAR unit (~1000 µmoles photons $m^{-2}s^{-1}$) was observed at 8am during summer, and, highest temperature (~45^{o}C) was observed at 2pm during post-monsoon (Chapter 3). These three-time points which are the most extreme (during winter and post-monsoon) and most favorable (during summer) were

seen to cluster uniquely from the rest. These suggest that the change in environmental factors such as atmospheric temperature and light intensity play a major role in the change in diurnal molecular framework of *S. fruticosa*.

8.4 Conclusions

From our previous chapters, we found that change in physiology, metabolite accumulation, protein expression and ion accumulation were strongly influenced by the change in seasons. We also observed that the metabolome and proteome of *S. fruticosa* were influenced by diurnal rhythm. To further find the correlation of the three omics dataset from *S. fruticosa* under the influence of changing season and diurnal rhythm, WGCNA was performed. We found that, the environmental factors, such as atmospheric temperature, salinity and pH largely influence the change in not just the independent omics platform but the complete holistic molecular framework in *S. fruticosa*. We also found that, atmospheric temperature plays a crucial role in the regulation of the accumulation of metabolites, ions and expression of protein in *S. fruticosa*. However, the change in pH and salinity does not show significant alterations in the molecular construct. This may be due to *S. fruticosa* being halophytic and more tolerant to salinity and pH but is more susceptible to change in atmospheric temperature. Further analysis is being done to finetune the correlation module for *S. fruticosa*.

Chapter 9

Summary and Conclusions

Plants are exposed to several combinations of stress in their natural environment. Being sessile, they need to adjust to these changes by adopting several modes of temporary and/or permanent mechanisms at the molecular, physiological, and anatomical levels. Depending on the mode of adaptations, plants are categorized as *extremophiles*- those plants that can survive and reproduce under stress such as salinity, alkalinity, cold and hot weather, and *glycophytes*- those plants that are sensitive to even mild stress. Halophytes are a group of plant species falling under the category of extremophiles that can complete their life cycle even at a salinity above the concentration of seawater (500 mM). Halophytes evolve through unique modes of adaptive mechanisms to combat salinity. Anatomically, they develop modified root system, viviparous seeds, salt glands, vesiculated trichomes, and succulent leaves. Physiologically, they adapt by accumulating several stress-responsive molecules such as sucrose, beta-glycine, proline, and GABA. They also have the ability to switch the mode of carbon assimilation through photosynthesis from C3 to CAM or, C3 to C4 under stress. At molecular level, they regulate the expression of several stress-related genes such as HSP 18.1, APX, NHX, SOS, NAC, DREB, HKT and many others (Kumari et al., 2009).

Suaeda, belonging to the family Chenopodiaceae, consists of about 110 species spreading around the coastal tropic as well as the sub-tropical areas. Most of the species are annual halophytes growing in saline or alkaline wetlands and dessert by developing succulent leaves. In India, about four species of *Suaeda* have been listed, one of which is *S. fruticosa*. *S. fruticosa* (L.) Forssk. is an evergreen succulent obligate halophyte shrub that grows to about 1 m in height. It is usually seen to flourish well in sandy, alkaline and highly saline soil and produce numerous seeds. Flowering begin from September till May. This

plant can tolerate salt as high as 1000 mM NaCl; however, its optimum growth is seen between 200-400mM.

In recent years, attempts have been made to understand the adaptations in *S. fruticosa* to harsh environmental conditions such as high temperature, heavy metal, and salinity stress. Several laboratories have reported the physiological, morphological and transcriptome-based studies of this plant under stress. However, little or no work has been done to understand the physiological or molecular changes this plant during different seasons.

In the present work, we have analyzed the changes in the diurnal metabolic, proteomics and ionomics profile of *S. fruticosa* growing naturally around the Salt Lake in Rajasthan for three major seasons (post-monsoon, winter, and summer). Apart from the morphological changes of the leaf tissues wherein, it developed succulent and smaller leaves during winter and summer, along with tight regulation of photosynthetic activity, we identified several changes in the distribution of metabolites, proteins, and ions in each season which may be contributing to its survival, growth, and tolerance under extreme condition (Figure 9.1). During the post-monsoon season, temperature, pH and salinity around the lake were found to be moderate. However, during winter and summer seasons, temperature, pH and salinity gets extreme which leads to several change in the plant morphology such as development of lesser leaves that are highly succulent to store water and produce seeds (both black and brown), to escape from the harsh climatic conditions. Along with this development, plants also accumulate several osmolytes such as proline, sucrose, glycine and GABA. Some stress regulating proteins such as glycosyltransferase, HSP 18.1, G-type lectin S-receptor-like serine/threonine proteins and Proteasome subunit beta type-5-B precursor were also found to be expressed.

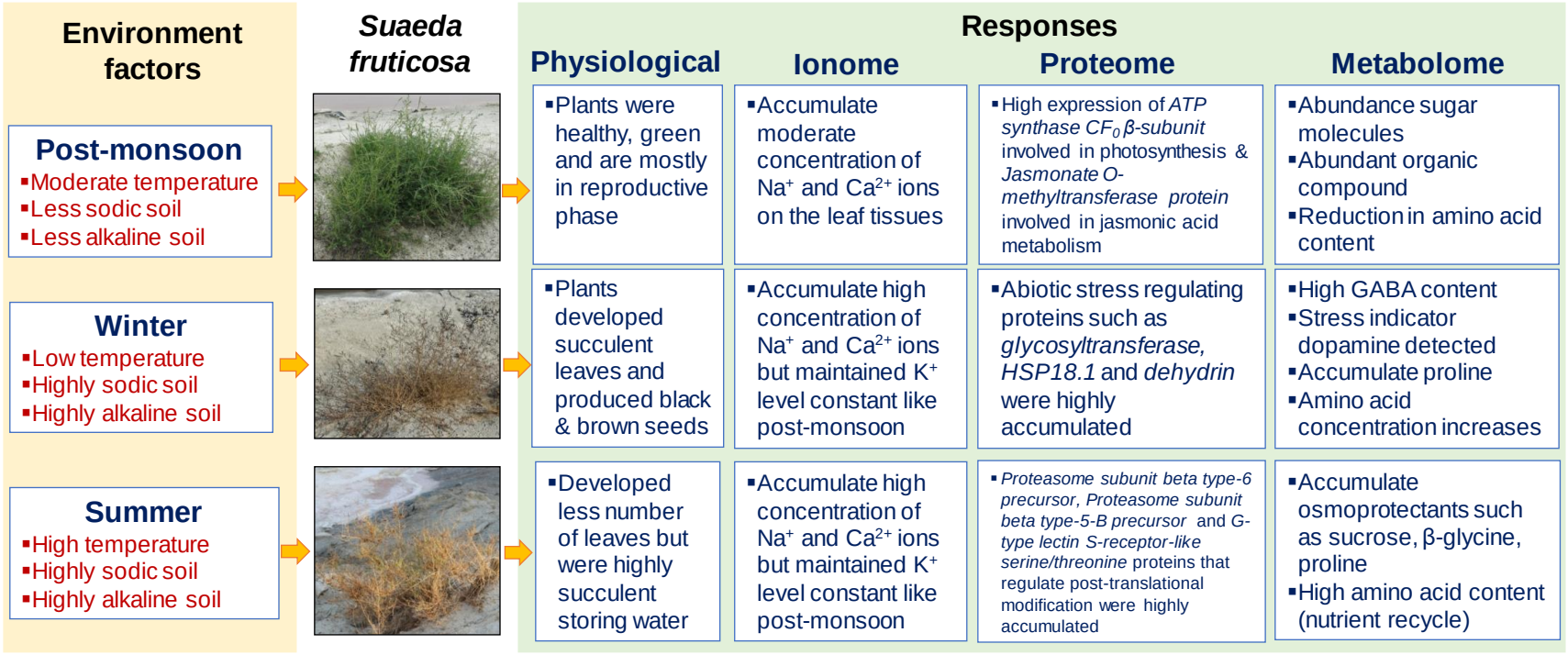

Figure 9.1. Overview of the diverse environmental factors predominant at the salt lake which the habitat of *S. fruticosa* and the strategic responses adopted by the plant to survive under the harsh conditions. During the post -monsoon season, temperature, soil salinity and alkalinity were found to be moderate however, during winter season, temperature reduces up to 3^{o}C in the night and salinity as well as alkalinity increases. During the summer season, the temperature increases to roughly 50^{o}C, soil salinity and pH reaches up to 65 dS/m and 10.5 respectively. *S. fruticosa* strategically adapts these harsh environmental factors by changing its physiology and also by altering the ionome, proteome and metabolome profile which attributes to its adaptation.

Some of the key findings from the present work are:

- From the CO_2 gas exchange analysis using IRGA and measurement of fluorescence kinetics of Chl *a* using Handy-PEA, we inferred that the maximum rate of photosynthesis was found to be at 8 am. The maximum quantum yield of PSII photochemistry (Fv/Fm), as inferred from the ratio of the variable (Fv) to maximum (Fm) chlorophyll *a* fluorescence measurement, in *S. fruticosa* was highest between 11 pm to 5 am. This increase in Fv/Fm during the night suggests that *S. fruticosa* overcomes the photodamage of PSII experienced during the day. Further, the total photosynthesis performance index was highest at dawn and dusk. This study demonstrated that the prime strategy enabling the halophyte *S. fruticosa* to grow in the extremely saline environment was by maintaining structural integrity and electron flow through PSI and PSII along with the protection of photosynthesis machinery from photoinhibition during high irradiance at midday.

- From our metabolomics analysis, we inferred that accumulation of metabolites in *S. fruticosa* is regulated both by diurnal rhythm as well as seasonal changes. Several vital metabolites such as sucrose, GABA, glycine, proline, myo-inositol, inositol, valine, ornithine, caprylic acid, and citrulline and α-Linolenic, which are known to play a significant role in stress tolerance, were seen to accumulate abundantly in *S. fruticosa*. Moreover, dopamine, a stress indicator metabolite, was also seen to accumulate during winter and summer seasons. Among the osmolytes that *S. fruticosa* accumulated, sucrose was found to be accumulated most abundantly during post-monsoon and summer seasons, the concentrations for which was also found to be higher than that of proline. The choice of accumulating sucrose rather than proline further helped *S. fruticosa* to combat the combinations of salinity and high temperature, as under the combination of these stresses, proline causes proline toxicity.

- Proteomics study using 2D-DIGE of *S. fruticosa* revealed several stress-related proteins such as peroxygenase 2, chitinase, 14-3-3-like protein, dehydrin, HSP18.1, HK, DREB and HIN proteins that were expressed in abundant throughout the season for its survival. Some other proteins that regulate PTM such as E3 ubiquitin ligase, MSRB5, methionine tRNA ligase, and RNA binding pectin were also found to alter as influenced by diurnal and seasonal variations. Through gene ontology analysis of the proteins identified using BLAST2GO, we observed that maximum of the proteins which showed differential expression throughout the seasons and diurnally were involved in protein translation, post-translation, and modifications.

- *Suaeda fruticosa*, a halophyte species growing not only in a place where the temperature reaches up to 50^{o}C during summer and as low as 4^{o}C during winter but also on a saline environment of soil salinity 65 dSm^{-1} during summer shows several modes of adaptions on its metabolite accumulation, photosynthetic regulation and protein expression as discussed earlier. In addition to these, one primary mode of adaptations that *S. fruticosa* undertake to adapt to a saline environment is by accumulating salt to absorb and conserve water. As salinity and soil pH increases during winter and summer, the concentration of Na^+ and Cl^- ions increases drastically in the leaf of *S. fruticosa*. These further help by lowering the water potential of the leaf, which further help in water uptake from the saline soil. Additionally, accumulation of these salts, especially Na^+, leads to closure of stomata, which further helps in the conservation of water. Plants such as Pokkali have been shown to accumulate K^+ ions along with the increase in soil salinity to maintain Na^+/K^+ ratio for its homeostasis. However, in *S. fruticosa*, we found that the level of K^+ was

maintained at the same level irrespective of the increase in salinity of the soil.

- Correlational study of the independent multi-OMICS datasets (metabolomics, proteomics and ionomics) along with the different traits i.e. temperature, pH and salinity was done using R-program by performing Weighted Correlation Network Analysis (WGCNA). From the preliminary work that we have done, we could identify the key metabolites, proteins and ions from the leaves of *S. fruticosa* that showed positive correlation with the change in temperature, pH and salinity.

9.1 Limitation of the work

From the literature, we found that *Suaeda fruticosa* develops two types of seeds, black and brown seeds. Wherein, the brown is more tolerant and can germinate even under high saline environment whereas, the black seeds are sensitive and remain dormant until the salinity of the soil lowers during monsoon. We proposed to analyzed the metabolomics, ionomics, and proteomics for the dimorphic seeds (black and brown seeds) that *Suaeda fruticosa* developed in the present thesis. However, due to the less availability of the brown seeds, the proposed experiments could not be done.

9.2 Future work

In depth-correlation studies of the multi-omics data that have been generated from our studies of metabolomics, proteomics, and ionomics can provide us a better understanding of the adaptive mechanism operative in *S. fruticosa*. Transcriptomic studies to check for transcript abundance under the influence of diurnal and seasonal variations will add to the knowledge of stress adaptations in *S. fruticosa*. Multi-OMICS study of both the root and shoot can further add to the wholistic understanding on stress adaption in *S. fruticosa*. Further, all the multi-OMICS studies done in the present work were from the complete leaf tissues of *S. fruticosa*. However, with the increase in

understanding of the cellular compartmentalization in plant, cell specific OMICS studies can further strengthen the knowledge on the mode of adaptations that *S. fruticosa* undergo to survive under harsh xerophytic condition. We expect these investigations will further help researchers in identifying essential genes and pathways for raising crops for saline and dry areas.

References

Abideen Z, Ansari R, Gul B, Khan AM. (2012). The place of halophytes in Pakistan's biofuel industry. *Biofuels* 3(2): 211-220.

Abideen Z, Ansari R, Khan MA. (2011). Halophytes: Potential source of ligno-cellulosic biomass for ethanol production. *Biomass and Bioenergy* 35(5): 1818-1822.

Acosta-Motos J, Ortuño M, Bernal-Vicente A, Diaz-Vivancos P, Sanchez-Blanco, M, Hernandez J. (2017). Plant responses to salt stress: adaptive mechanisms. *Agronomy* 7(1): 18.

Adamczyk-Szabela D, Markiewicz J, Wolf WM. (2015). Heavy metal uptake by herbs. IV. Influence of soil pH on the content of heavy metals in *Valeriana officinalis* L. *Water, Air, & Soil Pollution* 226(4): 106.

Adams P, Thomas JC, Vernon DM, Bohnert HJ, Jensen RG. (1992). Distinct cellular and organismic responses to salt stress. *Plant and Cell Physiology* 33(8): 1215-1223.

Adler PR, Cumming JR, Arora R. (2009). Nature of Mineral Nutrient Uptake by Plants. *Agricultural Sciences*, 1: 355-371.

Agarwal PK, Shukla PS, Gupta K, Jha B. (2013). Bioengineering for salinity tolerance in plants: state of the art. *Molecular Biotechnology* 54(1): 102-123.

Aggarwal K, Choe LH, Lee KH. (2006) Shotgun proteomics using the iTRAQ isobaric tags. *Briefings in Functional Genomics* 5(2): 112-120.

Aggarwal SC. (1951). The Sambhar lake salt source. In Directorate of printing GoI. Delhi: Government of India Press. 365.

Ahmed D, Huchzermeyer B, Abdelly C, Koyro HW. (2010). Current challenges and future opportunities for a sustainable utilization of halophytes. In: Öztürk M, Böer B, Barth HJ, Clüsener-Godt M, A. KM, W. BS eds. Sabkha Ecosystems. Netherlands: Springer Netherlands 59-77.

Ahuja I, De-Vos RCH, Bones AM, Hall RD. (2010). Plant molecular stress responses face climate change. *Trends in Plant Science* 15: 664-74.

Akçay N, Bor M, Karabudak T, Özdemir F, Türkan I. (2012). Contribution of gamma amino butyric acid (GABA) to salt stress responses of *Nicotiana sylvestris* CMSII mutant and wild type plants. *Journal of plant physiology* 169: 452-458.

Aleman F, Nieves-Cordones M, Martinez V, Rubio F. (2009). Differential regulation of the HAK5 genes encoding the high-affinity K+ transporters of *Thellungiella halophila* and *Arabidopsis thalian*. Environmental and Experimental Botany 65: 263-269.

Alemzadeh A, Fujie M, Usami S, Yoshizaki T, Oyama K, Kawabata T, Yamada T. (2006). ZMVHA-B1, the gene for subunit B of vacuolar H+-ATPase from the eelgrass *Zostera marina* L. Is able to replace vma2 in a yeast null mutant. *Journal of Bioscience and Bioengineering* 102(5): 390-395.

Ali H, Khan E, Sajad MA. (2013). Phytoremediation of heavy metals—concepts and applications. *Chemosphere* 91(7): 869-881.

Alongi DM. (2014). Carbon cycling and storage in mangrove forests. *Annual Review of Marine Science* 6(1-487): 195-219.

Alqahtani M, Roy SJ, Tester M. (2019). Increasing Salinity Tolerance of Crops. *Crop Science* 245-267.

Amtmann A, Bohnert HJ, Bressan RA. (2005). Abiotic stress and plant genome evolution. Search for new models. *Plant Physiology* 138(1): 127-130.

Amtmann A. (2009). Learning from evolution: *Thellungiella* generates new knowledge on essential and critical components of abiotic stress tolerance in plants. *Molecular Plant* 2(1): 3-12.

An D, Yang J, Zhang P. (2012). Transcriptome profiling of low temperature treated cassava apical shoots showed dynamic responses of tropical plant to cold stress. *BMC Genomics* 13.

An Y, Wang Y, Lou L, Zheng T, Qu GZ. (2011). A novel zinc-finger-like gene from Tamarix hispida is involved in salt and osmotic tolerance. *Journal of Plant Research* 124: 689–697.

Anderson M. (2014). Enter halophytes We are running out of land for traditional agriculture. Time to figure out what saltwater plants can do for us. aeon.

Araujo WL, Tohge T, Ishizaki K, Leaver CJ, Fernie AR. (2011). Protein degradation - an alternative respiratory substrate for stressed plants. *Trends in Plant Science* 16: 489-98.

Ardie SW, Xie L, Takahashi R, Liu S, Takano T. (2009). Cloning of a high-affinity K+ transporter gene PutHKT2;1 from *Puccinellia tenuiflora* and its functional comparison with OsHKT2;1 from rice in yeast and *Arabidopsis*. *Journal of Experimental Botany* 60(12): 3491-3502.

Arend M, Weisenseel MH, Brummer M, Osswald W, Fromm JH. (2002). Seasonal changes of plasma membrane H+-ATPase and endogenous ion current during cambial growth in poplar plants. *Plant physiology* 129(4): 1651-1663.

Arunkumar R, Sairam RK, Deshmukh PS, Pal MA, Khetarpal SA, Pandey SK, Kushwaha SR, Singh TP. (2012). High temperature stress and accumulation of compatible solutes in chickpea (*Cicer arietinum* L.). *Indian Journal of Plant Physiology* 17: 145-150.

Arvidsson J. (1999). Nutrient uptake and growth of barley as affected by soil compaction. *Plant and soil* 208(1): 9-19.

Asad MZ, Bai B, Lan C, Yan J, Xia X, Zhang Y, He Z. (2014). Identification of QTL for adult-plant resistance to powdery mildew in Chinese wheat landrace Pingyuan 50. *The Crop Journal* 2(5): 308-314.

Asada K. (1997). The role of ascorbate peroxidase and monodehydroascorbate reductase in H_2O_2 scavenging in plants. *Cold Spring Harbor Monograph Archive* 34: 715-735.

Asada K. (2006). Production and scavenging of reactive oxygen species in chloroplasts and their functions. *Plant Physiology* 141(2): 391-396.

Ashburner M, Ball CA, Blake JA, Botstein D, Butler H, Cherry JM, Davis AP, Dolinski K, Dwight SS, Eppig JT, Harris MA. (2000). Gene ontology: tool for the unification of biology. *Nature genetics* 25(1): 25.

Ashraf M, Akram NA. (2009). Improving salinity tolerance of plants through conventional breeding and genetic engineering: An analytical comparison. *Biotechnology Advances* 27(6): 744-752.

Ashraf M, Foolad M. (2007). Roles of glycine betaine and proline in improving plant abiotic stress resistance. *Environmental and Experimental Botany* 59: 206-216.

Ashraf MF, Foolad M. (2007) Roles of glycine betaine and proline in improving plant abiotic stress resistance. *Environmental and Experimental botany* 59(2): 206-216.

Askari H, Edqvist J, Hajheidari M, Kafi M, Salekdeh GH. (2006). Effects of salinity levels on proteome of *Suaeda aegyptiaca* leaves. *Proteomics* 6(8): 2542-2554.

Assaha DV, Ueda A, Saneoka H, Al-Yahyai R, Yaish MW. (2017). The role of Na+ and K+ transporters in salt stress adaptation in glycophytes. *Frontiers in physiology* 8: 509.

Atia A, Debez A, Barhoumi Z, Abdelly C, Smaoui A. (2010). Localization and composition of seed oils of *Crithmum maritimum* L. (Apiaceae). *African Journal of Biotechnology* 9(39): 6482-6485.

Attri SD, Tyagi A. (2010). Climate profile of India. In Department IM. New Delhi: Environment Monitoring and Research Centre. 122.

Ayyappan D, Sanjiviraja K, Balakrishnan V, Ravindran KC. (2013). Impact of halophytic compost on growth and yield characteristics of *Vigna radiata* L. *African Journal of Agricultural Research* 8(22): 2663-2672.

Bacarin MA, Martinazzo EG, Cassol D, Falqueto AR, Silva DM. (2016). Daytime variations of chlorophyll a fluorescence in Pau D'alho seedlings. *Revista Árvore* 40(6): 1023-1030.

Bagchi S, Goyal SP, Sankar K. (2003). Prey abundance and prey selection by tigers (*Panthera tigris*) in a semi-arid, dry deciduous forest in western India. *Journal of Zoology* 260(3): 285-290.

Bagri J, Yadav A, Anwar K, Dkhar J, Singla-Pareek SL, Pareek A. (2017). Metabolic shift in sugars and amino acids regulates sprouting in Saffron corm. *Scientific Report* 7: 11904.

Bahuguna RN, Jagadish KS. (2015). Temperature regulation of plant phenological development. *Environmental and Experimental Botany* 111: 83-90.

Baisakh N, RamanaRao MV, Rajasekaran K, Subudhi P, Janda J, Galbraith D, Vanier C, Pereira A. (2012). Enhanced salt stress tolerance of rice plants expressing a vacuolar H+ -ATPase subunit c1 (SaVHAc1) gene from the halophyte grass *Spartina alterniflora* Loisel. *Plant Biotechnology Journal* 10(4): 453-464.

Balakrishnan V, Venkatesan K, Ravindran KC. (2007). The influence of halophytic compost, farmyard manure and phosphobacteria on soil microflora and enzyme activities. *Plant Soil Environment* 53(4): 186–192.

Baldwin JP. (1975). A quantitative analysis of the factors affecting plant nutrient uptake from some soils. *Journal of Soil Science* 26(3): 195-206.

Ban Q, Liu G, Wang Y. (2011). A DREB gene from Limonium bicolor mediates molecular and physiological responses to copper stress in transgenic tobacco. *Journal of Plant Physiology* 168(5): 449-458.

Bankaji I, Caçador I, Sleimi N. (2015). Physiological and biochemical responses of Suaeda fruticosa to cadmium and copper stresses: growth, nutrient uptake, antioxidant enzymes, phytochelatin, and glutathione levels. *Environmental Science and Pollution Research* 22(17) 13058-13069.

Bankaji I, Pérez-Clemente RM, Caçador I, Sleimi N. (2019). Accumulation potential of *Atriplex halimus* to zinc and lead combined with NaCl: Effects on physiological parameters and antioxidant enzymes activities. *South African Journal of Botany* 123: 51-61.

Barbour MG. (1970). Is any Angiosperm an obligate halophyte? *The American Midland Naturalist* 84(1): 105-120.

Bareen FE, Tahira SA. (2011). Metal accumulation potential of wild plants in tannery effluent contaminated soil of Kasur, Pakistan: field trials for toxic metal clean-up using *Suaeda fruticosa*. *Journal of hazardous materials* 186: 443-450.

Barhoumi Z. (2019). Physiological response of the facultative halophyte, *Aeluropus littoralis*, to different salt types and levels. Plant Biosystems-An *International Journal Dealing with all Aspects of Plant Biology* 153(2): 298-305.

Barkla BJ, Vera-Estrella R, Pantoja O. (2012). Protein profiling of epidermal bladder cells from the halophyte *Mesembryanthemum crystallinum*. *Proteomics* 12(18): 2862-2865.

Barkla BJ, Vera-Estrella R, Raymond C. (2016). Single-cell-type quantitative proteomic and ionomic analysis of epidermal bladder cells from the halophyte model plant *Mesembryanthemum crystallinum* to identify salt-responsive proteins. *BMC plant biology* 6(1): 110.

Barnes CR. (1898). Plant life, considered with special reference to form and function. New York: New York,H. Holt & company.

Barrett-Lennard EG. (2003). The interaction between waterlogging and salinity in higher plants: causes, consequences and implications. *Plant and Soil* 253: 35-54.

Bashir A, Hoffmann T, Smits SH, Bremer, E. (2014). Dimethylglycine provides salt and temperature stress protection to *Bacillus subtilis*. *Applied and Environmental Microbiology* 80(9): 2773-2785.

Bassham JA, Benson AA, Celvin M. 1950. The path of carbon in photosynthesis: VIII. The role of malic acid. *The Journal of Biological Chemistry* 185: 781-787.

Basyuni M, Oku H, Inafuku M, Baba S, Iwasaki H, Oshiro K, Okabe T, Shibuya M, Ebizuka Y. (2006). Molecular cloning and functional expression of a multifunctional triterpene synthase cDNA from a mangrove species Kandelia candel (L.) Druce. *Phytochemistry* 67(23): 2517-2524.

Bates LS, Waldren RP, Teare ID. (1973). Rapid determination of free proline for water-stress studies. *Plant and soil* 39: 205-207.

Baxter I, Hosmani PS, Rus A, Lahner B, Borevitz JO, Muthukumar B, Mickelbart MV, Schreiber L, Franke RB, Salt DE. (2009). Root suberin forms an extracellular barrier that affects water relations and mineral nutrition in Arabidopsis. *PLoS genetics* 5(5): e1000492.

Baxter I, Muthukumar B, Park, HC, Buchner P, Lahner B, Danku J, Zhao K, Lee J, Hawkesford MJ, Guerinot ML. Salt DE. (2008). Variation in molybdenum content across broadly distributed populations of Arabidopsis thaliana is controlled by a mitochondrial molybdenum transporter (MOT1). *PLoS Genetics* 4(2): p.e1000004.

Baxter IR, Vitek O, Lahner B, Muthukumar B, Borghi M, Morrissey J, Guerinot ML, Salt DE. (2008). The leaf ionome as a multivariable system to detect a plant's physiological status. *Proceedings of the National Academy of Sciences* 105(33): 12081-12086.

Becker VI, Goessling JW, Duarte B, Caçador I, Liu F, Rosenqvist E, Jacobsen SE. (2017). Combined effects of soil salinity and high temperature on photosynthesis and growth of quinoa plants (Chenopodium quinoa). *Functional Plant Biology* 44: 665-678.

Bedre R, Mangu VR, Srivastava S, Sanchez LE, Baisakh N. (2016). Transcriptome analysis of smooth cordgrass (*Spartina alterniflora* Loisel), a monocot halophyte, reveals candidate genes involved in its adaptation to salinity. *BMC Genomics* 17(1): 657.

Bell HL, O'Leary JW. (2003). Effects of salinity on growth and cation accumulation of *Sporobolus virginicus* (poaceae). *American Journal of Botany* 90(10): 1416-1424.

Bendix C, Marshall CM, Harmon FG. (2015). Circadian clock genes universally control key agricultural traits. *Molecular plant* 8(8): 1135-1152.

Bennani-Kabchi N, Kehel L, Fdhil H, Marquie G. (1999). Effect of Suaeda fruticosa aqueous extract in the hypercholesterolaemic and insulin-resistant sand rat. *Therapie* 54: 725-30.

Benwahhoud M, Jouad H, Eddouks M, Lyoussi B. (2001). Hypoglycemic effect of *Suaeda fruticosa* in streptozotocin-induced diabetic rats. *Journal of ethnopharmacology* 76: 35-38.

Bhalani H, Thankappan R, Mishra GP, Sarkar T, Bosamia TC, Dobaria JR. (2019). Regulation of antioxidant mechanisms by AtDREB1A improves soil-moisture deficit stress tolerance in transgenic peanut (*Arachis hypogaea* L.). *PloS one* 14(5): e0216706.

Bhuyan P, Khan ML, Tripathi RS. (2003). Tree diversity and population structure in undisturbed and human-impacted stands of tropical wet evergreen forest in Arunachal Pradesh, Eastern Himalayas, India. *Biodiversity & Conservation* 12(8): 1753-1773.

Binzel ML, Hess FD, Bressan RA, Hasegawa PM. (1988). Intracellular compartmentation of ions in salt adapted tobacco cells. *Plant Physiology* 86: (607-614).

Bita C, Gerats T. (2013) Plant tolerance to high temperature in a changing environment: scientific fundamentals and production of heat stress-tolerant crops*. Frontiers in plant science*. 31(4): 273.

Böhner HJ. (2006). General climatic controls and topoclimatic variations in Central and High Asia. *Boreas* 35(2): 279-295.

Bohnert HJ, Nelson DE, Jensen RG. (1995). Adaptations to environmental stresses. *The Plant Cell* 7: 1099-1111.

Bomani BMM, Hendricks RC, Elbuluk M, Okon M, Lee E, Gigante B. (2011). NASA's GreenLab Research Facility: A guide for a self-sustainable renewable energy ecosystem*. NASA/TP* 217208.

Bonser AM, Lynch J, Snapp S. (1996). Effect of phosphorus deficiency on growth angle of basal roots in *Phaseolus vulgaris*. *New Phytologist*, 132(2): 281-288.

Boom A, Damsté JS, De-Leeuw JW. (2005). Cutan, a common aliphatic biopolymer in cuticles of drought-adapted plants. *Organic Geochemistry* 36(4): 595-601.

Borges N, Gonçalves LG, Rodrigues MV, Siopa F, Ventura R, Maycock C, Lamosa P, Santos H. (2006). Biosynthetic pathways of inositol and glycerol phosphodiesters used by the hyperthermophile *Archaeoglobus fulgidus* in stress adaptation. *Journal of Bacteriology* 188: 8128-8135.

Borghi M, Rus A, Salt DE. (2011). Loss-of-function of constitutive expresser of pathogenesis related genes5 affects potassium homeostasis in *Arabidopsis thaliana*. *PLoS One*, 6(10), e26360.

Bose J, Munns R, Shabala S, Gilliham M, Pogson B, Tyerman SD. (2017). Chloroplast function and ion regulation in plants growing on saline soils: lessons from halophytes. *Journal of Experimental Botany* 68: 3129-3143.

Bose J, Rodrigo-Moreno A, Shabala S. (2014). ROS homeostasis in halophytes in the context of salinity stress tolerance. *Journal of Experimental Botany* 65(5): 1241-1257.

Bourrié G, Salhi N, Slimani R, Douaoui A, Hamdi-aïssa B, Mohammed G, Trolard F. (2018). Irrigation, Water and Soil Quality. Soils as a Key Component of the Critical Zone 4: *Soils and Water Quality* 4:73-125.

Boursier P, Läuchli A. (1989). Mechanisms of chloride partitioning in the leaves of salt-stressed Sorghum bicolor L. *Physiologia Plantarum* 77: 537–544.

Boyle WJ, van der Geer P, Hunter T. (1991). Phosphopeptide mapping and phosphoamino acid analysis by two-dimensional separation on thin-layer cellulose plates. *Methods in enzymology* 201: 110-149.

Broadbent J, Sampson D, Sabapathy S, Haseler LJ, Wagner KH, Bulmer AC, Peake JM, Neubauer O. (2017). Gene networks in skeletal muscle following endurance exercise are coexpressed in blood neutrophils and linked with blood inflammation markers. *Journal of Applied Physiology* 122(4): 752-766.

Brock MA. (1981). Accumulation of proline in a submerged aquatic halophyte, *Ruppia* L. *Oecologia* 51(2): 217–219.

Brosse N, Dufour A, Meng X, Sun Q, Ragauskas A. (2012). Miscanthus: a fast-growing crop for biofuels and chemicals production. *Biofuels, Bioproducts and Biorefining* 6(5): 580-598.

Broun P, Somerville C. (1997). Accumulation of ricinoleic, lesquerolic, and densipolic acids in seeds of transgenic Arabidopsis plants that express a fatty acyl hydroxylase cDNA from castor bean. *Plant Physiology* 113: 933-942.

Brown JJ, Glenn EP, Fitzsimmons KM, Smith SE. (1999). Halophytes for the treatment of saline aquaculture effluent. *Aquaculture* 175: 255-268.

Bundy JG, Davey MP, Viant MR. (2008). Environmental metabolomics: a critical review and future perspectives. *Metabolomics* 5: 3-21.

Burley SK, Almo SC, Bonanno JB, Capel M, Chance MR, Gaasterland T, Lin D, Šali A, Studier FW, Swaminathan S. (1999). Structural genomics: beyond the human genome project. *Nature genetics* 23(2): 151.

Burn DH, Whitfield PH. (2018). Changes in flood events inferred from centennial length streamflow data records. *Advances in water resources* 121:333-349.

Burnell JN. (1988). The biochemistry of manganese in plants. In Manganese in soils and plants (pp. 125-137). Springer, Dordrecht.

Burt CC. (2014). Warmest places on earth: Average annual temperature. Weather Underground. Georgia, USA.

Bush DS. (1993). Regulation of cytosolic calcium in plants. *Plant Physiology* 103(1): 7.

Bussotti F, Desotgiu R, Pollastrini M, Cascio C. (2010). The JIP test: a tool to screen the capacity of plant adaptation to climate change. Scandinavian Journal of *Forest Research* 25(S8): 43-50.

Bustan A, Pasternak D, Pirogova I, Durikov M, Devries TT, El-Meccawi S, Degen AA. (2005). Evaluation of saltgrass as a fodder crop for livestock. *Journal of the Science of Food and Agriculture* 85(12): 2077-2084.

Cabello-Hurtado F, Ramos J. (2004). Isolation and functional analysis of the glycerol permease activity of two new nodulin-like intrinsic proteins from salt stressed roots of the halophyte *Atriplex nummularia*. *Plant Science* 166(3): 633-640.

Cakmak I, Hengeler C, Marschner H. (1994). Partitioning of shoot and root dry matter and carbohydrates in bean plants suffering from phosphorus, potassium and magnesium deficiency. *Journal of Experimental Botany* 45(9): 1245-1250.

Cakmak I, Yazici AM. (2010). Magnesium: a forgotten element in crop production. *Better Crops* 94(2): 23-25.

Cano-Ramirez DL, Dodd AN. (2018). New connections between circadian rhythms, photosynthesis, and environmental adaptation. *Plant, Cell & Environment* 41(11): 2515-2517.

Cao D, Gao X, Liu J, Wang X, Geng S, Yang C, Liu B, Shi D. (2012). Root-specific DNA methylation in Chloris virgata, a natural alkaline-resistant halophyte, in response to salt and alkaline stresses. *Plant Molecular Biology Reporter* 30(5): 1102-1109.

Cassaniti C, Leonardi C, Flowers TJ. (2009). The effects of sodium chloride on ornamental shrubs. *Scientia Horticulturae* 122(4): 586-593.

Cecconi D. (2016). Comparative evaluation of software features and performances. In 2-D PAGE Map Analysis (pp. 69-78). Humana Press, New York, NY.

Celis JE, Gromov P. (1999). 2D protein electrophoresis: can it be perfected? *Current Opinion in Biotechnology* 10(1): 16-21.

Chao DY, Gable K, Chen M, Baxter I, Dietrich CR, Cahoon EB, Guerinot ML, Lahner B, Lü S, Markham JE, Morrissey J. (2011). Sphingolipids in the root play an important role in regulating the leaf ionome in *Arabidopsis thaliana*. *The Plant Cell* 23(3): 1061-1081.

Chapin III FS, Autumn K, Pugnaire F. (1993). Evolution of suites of traits in response to environmental stress. *The American Naturalist* 142: S78-S92.

Chapman RL, Buchheim MA. (1992). Green algae and the evolution of land plants: inferences from nuclear-encoded rRNA gene sequences. *BioSystems* 28: 127-137.

Chaturvedi AK, Patel MK, Mishra A, Tiwari V, Jha B. (2014). The SbMT-2 gene from a halophyte confers abiotic stress tolerance and modulates ROS scavenging in transgenic tobacco. *PLoS One* 9(10): e111379.

Chen AP, Wang GL, Qu ZL, Lu CX, Liu N, Wang F, Xia GX. (2007). Ectopic expression of ThCYP1, a stress-responsive cyclophilin gene from *Thellungiella halophila*, confers salt tolerance in fission yeast and tobacco cells. *Plant Cell Reports* 26(2): 237-245.

Chen J, Cheng T, Wang P, Liu W, Xiao J, Yang Y, Hu X, Jiang Z, Zhang S, Shi J. (2012). Salinity-induced changes in protein expression in the halophytic plant *Nitraria sphaerocarpa*. *Journal of Proteomics* 75(17): 5226-5243.

Chen P, He WS. (2011). The effects of different fertilization structure on yields of sunflower in saline alkali soil. *Agricultural Research in the Arid Areas* 29: 108-114.

Chen SH, Guo SL, Wang ZL, Zhao JQ, Zhao YX, Zhang H. (2007). Expressed sequence tags from the halophyte *Limonium sinense*. *DNA Sequence* 18(1): 61-67.

Chen X, Han H, Jiang P, Nie L, Bao H, Fan P, Lv S, Feng J, Li Y. (2011). Transformation of beta-lycopene cyclase genes from *Salicornia europaea* and Arabidopsis conferred salt tolerance in Arabidopsis and tobacco. *Plant and Cell Physiology* 52(5): 909-921.

Chen Y, Li L, Zong J, Chen J, Guo H, Guo A, Liu J. (2015). Heterologous expression of the halophyte *Zoysia matrella* H (+)-pyrophosphatase gene improved salt tolerance in *Arabidopsis thaliana*. *Plant Physiology and Biochemistry* 91: 49-55.

Cheng L, Fuchigami LH, Breen PJ. (2001). The relationship between photosystem II efficiency and quantum yield for CO_2 assimilation is not

affected by nitrogen content in apple leaves. *Journal of Experimental Botany* 52(362): 1865–1872.

Cheng T, Chen J, Zhang J, Shi S, Zhou Y, Lu L, Wang P, Jiang Z, Yang J, Zhang S, Shi J. (2015). Physiological and proteomic analyses of leaves from the halophyte *Tangut nitraria* reveals diverse response pathways critical for high salinity tolerance. *Frontiers in Plant Science* 6: 30.

Chiang JM, Lin TC, Luo YC, Chang CT, Cheng JY, Martin CE. (2013). Relationships among rainfall, leaf hydrenchyma, and Crassulacean acid metabolism in *Pyrrosia lanceolata* (L.) Fraw. (Polypodiaceae) in central Taiwan. *Flora - Morphology, Distribution, Functional Ecology of Plants* 208(5-6): 343-350.

Chinnusamy V, Zhu J, Zhu JK. (2007). Cold stress regulation of gene expression in plants. *Trends in Plant Science* 12(10): 444-451.

Chopra RN, Nayar SL, Chopra IC. (1986). Glossary of Indian medicinal plants (including the supplement). In: Research CO SaI, ed. New Delhi, 2-79.

Clarkson DT, Hanson JB. (1980). The mineral nutrition of higher plants. *Annual review of plant physiology* 31(1): 239-298.

Clarkson DT. (1988). The uptake and translocation of manganese by plant roots. In Manganese in soils and plants (pp. 101-111). Springer, Dordrecht.

Close TJ. (1997). Dehydrins: a commonalty in the response of plants to dehydration and low temperature. *Physiologia Plantarum* 100(2): 291-296.

Cochrane TT, Cochrane TA. (2009). The vital role of potassium in the osmotic mechanism of stomata aperture modulation and its link with potassium deficiency. *Plant signaling and behavior* 4(3): 240-243.

Collins NC, Thordal-Christensen H, Lipka V, Bau S, Kombrink E, Qiu JL, Hückelhoven R, Stein M, Freialdenhoven A, Somerville SC, Schulze-Lefert P. (2003). SNARE-protein-mediated disease resistance at the plant cell wall. *Nature* 425(6961): 973.

Colmer TD, Munns R, Flowers TJ. (2005). Improving salt tolerance of wheat and barley: future prospects. *Australian Journal of Experimental Agriculture* 45(11): 1425-1443.

Cota-Sanchez JH, Reyes-Olivas A, Sanchez-Soto B. (2007). Vivipary in coastal cacti: A potential reproductive strategy in halophytic environment. *American Journal of Botany* 94(9): 1577-1581.

Cramer GR, Urano K, Delrot S, Pezzotti M, Shinozaki K. (2011). Effects of abiotic stress on plants: a systems biology perspective. *BMC plant biology* 11(163).

Crozier AA. (1892). A dictionary of botanical terms. New York: New York, H. Holt.

Cruz RPD, Golombieski JI, Bazana MT, Cabreira C, Silveira TF, Silva LPD, (2010). Alterations in fatty acid composition due to cold exposure at the vegetative stage in rice. *Brazilian Journal of Plant Physiology* 22: 199-207.

Cuin TA, Shabala S. (2007). Amino acids regulate salinity-induced potassium efflux in barley root epidermis. *Planta* 225: 753-61.

Curie C, Briat JF. (2003). Iron transport and signalling in plants. *Annual Review of Plant Biology* 54(1): 183-206.

Cushman JC, Tillett RL, Wood JA, Branco JM, Schlauch KA. (2008). Large-scale mRNA expression profiling in the common ice plant, *Mesembryanthemum crystallinum*, performing C3 photosynthesis and Crassulacean acid metabolism (CAM). *Journal of Experimental Botany* 59(7): 1875-1894.

Danku JM, Lahner B, Yakubova E, Salt DE. (2013). Large-scale plant ionomics. In Plant Mineral Nutrients (pp. 255-276). Humana Press, Totowa, NJ.

Das P, Nutan KK, Singla-Pareek SL, Pareek A. (2015). Oxidative environment and redox homeostasis in plants: dissecting out significant contribution of major cellular organelles. *Frontiers in Environmental Science* 2(70).

Das P, Nutan KK, Singla-Pareek SL, Pareek A. (2015). Understanding salinity responses and adopting 'omics-based' approaches to generate salinity tolerant cultivars of rice. *Frontiers in Plant Science* 6: 712.

Dassanayake M, Oh DH, Haas JS, Hernandez A, Hong H, Ali S, Yun DJ, Bressan RA, Zhu JK, Bohnert HJ, Cheeseman JM. (2011). The genome of the extremophile crucifer *Thellungiella parvula*. *Nature Genetics* 43(9): 913-918.

Davidar P, Rajagopal B, Mohandass D, Puyravaud JP, Condit R, Wright SJ, Leigh Jr EG. (2007). The effect of climatic gradients, topographic variation and species traits on the beta diversity of rain forest trees. *Global Ecology and Biogeography* 16(4): 510-518.

De Caluwé J, Melo JRF, Tosenberger A, Hermans C, Verbruggen N, Leloup JC, Gonze D. (2017). Modelling the photoperiodic entrainment of the plant circadian clock. *Journal of theoretical biology* 420: 220-231.

De US, Dube RK, Rao GSP. (2005). Extreme weather events over India in the last 100 years. *The Journal of Indian Geophysical Union* 9(3): 173-187.

Debez A, Braun HP, Pich A, Taamalli W, Koyro HW, Abdelly C, Huchzermeyer B. (2012). Proteomic and physiological responses of the halophyte *Cakile maritima* to moderate salinity at the germinative and vegetative stages. *Journal of Proteomics* 75(18): 5667-5694.

Deivanai SR, Xavier V, Vinod V, Timalata K, Lim OF. (2011). Role of exogenous proline in ameliorating salt stress at early stage in two rice cultivars. *Journal of Stress Physiology & Biochemistry* 7(4): 157-174

Díaz-Troya S, Pérez-Pérez ME, Florencio FJ, Crespo JL. (2008). The role of TOR in autophagy regulation from yeast to plants and mammals. *Autophagy* 4: 851-65.

Diez R, Herbstreith M, Osorio C, Alzate O. (2010). 2-D fluorescence difference gel electrophoresis (DIGE) in neuroproteomics. CRC Press/Taylor & Francis: Boca Raton, FL.

Diray-Arce J, Clement M, Gul B, Khan MA, Nielsen BL. (2015). Transcriptome assembly, profiling and differential gene expression analysis of the halophyte *Suaeda fruticosa* provides insights into salt tolerance. *BMC Genomics* 16: 353.

Dkhar J, Pareek A. (2019). ASYMMETRIC LEAVES1 and REVOLUTA are the key regulatory genes associated with pitcher development in *Nepenthes khasiana*. *Scientific reports* 9(1): 6318.

Dodd AN, Salathia N, Hall A, Kévei E, Tóth R, Nagy F, Hibberd JM, Millar AJ, Webb AA. (2005). Plant circadian clocks increase photosynthesis, growth, survival, and competitive advantage. *Science* 309(5734): 630-633.

Dong Y, Fan G, Zhao Z, Deng M. (2014). Transcriptome expression profiling in response to drought stress in *Paulownia australis*. *International Journal of Molecular Sciences* 15: 4583-4607.

Dos Santos CV, Rey P. (2006). Plant thioredoxins are key actors in the oxidative stress response. *Trends in plant science* 11(7): 329-334.

Downton WJS, Grant WJR, Loveys BR. (1987). Diurnal changes in the photosynthesis of field-grown grape vines. *New Phytologist* 105(1): 71-80.

Draper SR. (1972). Amino acid changes associated with low temperature treatment of *Lolium perenne*. *Phytochemistry* 11: 639-641.

Du X, P. L, Guan FC. (2009). The efficient cultivation techniques of Suaeda glauca bunge in protected field. *Jilin Agricultural Science and Technology College* 34: 52–53.

Duarte B, Cabrita MT, Gameiro C, Matos AR, Godinho R, Marques JC, Cacador I. (2017). Disentangling the photochemical salinity tolerance in *Aster tripolium* L.: connecting biophysical traits with changes in fatty acid composition. *Plant Biology* 19(2): 239-248.

Duarte B, Santos D, Marques JC, Cacador I. (2013). Ecophysiological adaptations of two halophytes to salt stress: photosynthesis, PS II photochemistry and anti-oxidant feedback--implications for resilience in climate change. *Plant Physiology and Biochemistry* 67: 178-188.

Duarte P, Ferreira JG. 1995. Seasonal adaptation and short-term metabolic responses of *Gelidium sesquipedale* to varying light and temperature. *Marine Ecology Progress Series* 121: 289-300.

Ducic T, Polle A. (2005). Transport and detoxification of manganese and copper in plants. *Brazil Journal of Plant Physiology* 17: 103-112.

Dunn MJ. (2000). Studying heart disease using the proteomic approach. *Drug Discovery Today* 5(2): 76-84.

Edwards DG, Asher CJ. (1982). Tolerance of crop and pasture species to manganese toxicity. In Plant nutrition 1982: proceedings of the ninth International Plant Nutrition Colloquium, Warwick University, England, August 22-27, 1982/edited by A. Scaife. Slough, UK: Commonwealth Agricultural Bureaux, c1982.

Edwards DM, Reed RH, Chudek JA, Foster R, Stewart WD. (1987) Organic solute accumulation in osmotically-stressed *Enteromorpha intestinalis*. *Marine Biology* 95(4): 583-592.

El-Kereamy A, Bi YM, Ranathunge K, Beatty PH, Good AG, Rothstein SJ. (2012). The rice R2R3-MYB transcription factor OsMYB55 is involved in the tolerance to high temperature and modulates amino acid metabolism. *PLoS One* 7(12): e52030.

Ellison AM, Farbsworth EJ. (1990). The ecology of Belizean mangrove-root fouling communities. I. Epibenthic fauna are barriers to isopod attack of red mangrove roots. *Journal of Experimental Marine Biology and Ecology* 142: 91-104.

El-Sayed AI, Rafudeen MS, Golldack D. (2014) Physiological aspects of raffinose family oligosaccharides in plants: protection against abiotic stress. *Plant Biology* 16(1):1-8.

Endo T, Yamamoto S, Larrinaga JA, Fujiyama H, Honna T. (2011). Status and causes of soil salinization of irrigated agricultural lands in Southern Baja California, Mexico. *Applied and Environmental Soil Science* (2011): 1-12.

Epstein E. (1965). Typical concentrations sufficient for plant growth. *Plant Biochemistry* 438-466.

Epstein E. (2009). Silicon: its manifold roles in plants. *Annals of Applied Biology* 155(2): 155-160.

Ezawa S, Tada Y. (2009). Identification of salt tolerance genes from the mangrove plant *Bruguiera gymnorhiza* using Agrobacterium functional screening. **Plant Science** 176(2): 272-278.

Falasca A, Melck D, Paris D, Saviano G, Motta A, Iorizzi M, (2013). Seasonal changes in the metabolic fingerprint of *Juniperus communis* L. berry extracts by 1H NMR-based metabolomics. *Metabolomics* 10: 165-74.

Fan L, Wang A, Miao Y, Liao S, Ye C, Lin Q. (2016). Comparative proteomic identification of the hepatopancreas response to cold stress in white shrimp, *Litopenaeus vannamei*. *Aquaculture* 1(454): 27-34.

Fan P, Feng J, Jiang P, Chen X, Bao H, Nie L, Jiang D, Lv S, Kuang T, Li Y. (2011). Coordination of carbon fixation and nitrogen metabolism in *Salicornia europaea* under salinity: Comparative proteomic analysis on chloroplast proteins. *Proteomics* 11(22): 4346-4367.

FAO, IFAD, UNICEF, WFP & WHO. (2018). The State of Food Security and Nutrition in the World 2018. Building climate resilience for food security and nutrition. Rome, FAO. License: CC BY-NC-SA 3.0 IGO. (http://www.fao.org/state-of-food-security-nutrition/en/).

Feng D, Wang Y, Lu T, Zhang Z, Han X. (2017). Proteomics analysis reveals a dynamic diurnal pattern of photosynthesis-related pathways in maize leaves. *PloS one* 12(7): e0180670.

Fisher DD, Schenk HJ, Thorsch JA, Ferren WRJ. (1997). Leaf anatomy and subgeneric affiliations of C3 and C4 species of *Suaeda* (Chenopodiaceae) in North America. *American Journal of Botany* 84: 1198-210.

Fisher RA. (2006). Statistical methods for research workers. Genesis Publishing Pvt Ltd.

Fleischmann RD, Adams MD, White O, Clayton RA, Kirkness EF, Kerlavage AR, Bult CJ, Tomb JF, Dougherty BA, Merrick JM. (1995). Whole-genome random sequencing and assembly of *Haemophilus influenzae* Rd. *Science* 269(5223): 496-512.

Flowers TJ, Colmer TD. (2008). Salinity tolerance in halophytes. *New Phytologist* 179(4): 945-963.

Flowers TJ, Colmer TD. (2015). Plant salt tolerance: adaptations in halophytes. *Annals of Botany* 115: 327-31.

Flowers TJ, Galal HK, Bromham L. (2010). Evolution of halophytes multiple origins of salt tolerance in land plants. *Functional Plant Biology* 37: 604-612.

Flowers TJ, Hajibagheri MA, Clipson NJW. (1986). Halophytes. *The Quarterly Review of Biology* 61(3): 313-337.

Flowers TJ. (2004). Improving crop salt tolerance. *Journal of Experimental Botany* 55(396): 307-319.

Fortmeier R, Schubert S. (1995). Salt tolerance of maize (*Zea mays* L.) the role of sodium exclusion. *Plant, Cell and Environment* 18: 1041-1047.

Foyer CH. (2005). Redox homeostasis and antioxidant signalling a metabolic interface between stress perception and physiological responses. *The Plant Cell* 17: 1866-1875.

Francoz E, Ranocha P, Nguyen-Kim H, Jamet E, Burlat V, Dunand C. (2015). Roles of cell wall peroxidases in plant development. *Phytochemistry* 112: 15-21.

Freitas DDS, Nunes WDS, Do Prado Apparecido R, Lopes TIB, Alcantara GB, (2018). NMR-based approach reveals seasonal metabolic changes in mate (Ilex paraguariensis A..). *Magnetic Resonance in Chemistry* 1-10.

Fu X, Huang Y, Deng S, Zhou R, Yang G, Ni X, Li W, Shi S. (2005). Construction of a SSH library of *Aegiceras corniculatum* under salt stress and expression analysis of four transcripts. *Plant Science* 169(1): 147-154.

Fujita M, Fujita Y, Noutoshi Y, Takahashi F, Narusaka Y, Yamaguchi-Shinozaki K, Shinozaki K. (2006). Crosstalk between abiotic and biotic stress responses: a current view from the points of convergence in the stress signaling networks. *Current Opinion in Plant Biology* 9(4): 436-442.

Fukuda H, Ogawa T, Tazaki M, Nagahama K, Fujiil T, Tanase S, Morino Y. (1992). Two reactions are simultaneously catalyzed by a single enzyme: the arginine-dependent simultaneous formation of two products, ethylene and succinate, from 2-oxoglutarate by an enzyme from *Pseudomonas syringa*e. *Biochemical and biophysical research communications* 188(2): 483-489.

Gago C, Sousa AR, Juliao M, Miguel G, Antunes DC, Panagopoulos T. (2011). Sustainable use of energy in the storage of halophytes used for food. *International Journal of Energy and Environment* 5(4): 592-599.

Galeas, M. L., Zhang, L. H., Freeman, J. L., Wegner, M., & Pilon-Smits, E. A. (2007). Seasonal fluctuations of selenium and sulfur accumulation in selenium hyperaccumulators and related non accumulators. *New Phytologist* 173(3): 517-525.

Gao C, Wang Y, Jiang B, Liu G, Yu L, Wei Z, Yang C. (2010). A novel vacuolar membrane H+-ATPase c subunit gene (ThVHAc1) from *Tamarix hispida* confers tolerance to several abiotic stresses in Saccharomyces cerevisiae. Molecular Biology Reports 38: 957–963.

Gao F, Gao Q, Duan X, Yue G, Yang A, Zhang J. (2006). Cloning of an H+-PPase gene from *Thellungiella halophila* and its heterologous expression to improve tobacco salt tolerance. *Journal of Experimental Botany* 57(12): 3259-3270.

Gao N, Zhou J, Zhang X, Cai W, Guan T, Jiang L, Du H, Yang D, Cong Z, Zheng Y. (2017). Correlation between vegetation and environment at different levels in an arid, mountainous region of China. *Ecology and Evolution* 7(14): 5482-5492.

García-Caparrós P, Llanderal A, Pestana M, Correi, PJ, Lao MT. (2017). *Lavandula multifida* response to salinity: growth, nutrient uptake, and

physiological changes. *Journal of Plant Nutrition and Soil Science* 180(1): 96-104.

García-Plazaola JI, Fernández-Marín B, Ferrio JP, Alday JG, Hoch G, Landais D, Milcu A, Tissue DT, Voltas J, Gessler A, Roy J. (2017). Endogenous circadian rhythms in pigment composition induce changes in photochemical efficiency in plant canopies. *Plant, Cell & Environment* 40(7): 1153-1162.

Garg R, Verma M, Agrawal S, Shankar R, Majee M, Jain M. (2014). Deep transcriptome sequencing of wild halophyte rice, *Porteresia coarctata*, provides novel insights into the salinity and submergence tolerance factors. *DNA Research* 21(1): 69-84.

Gautam A, Agrawal D, V. SPS, Jajoo A. (2014). A quick method to screen high and low yielding wheat cultivars exposed to high temperature. *Physiology and Molecular Biology of Plants* 20(4): 533-537.

Gelhaye E, Rouhier N, Navrot N, Jacquot JP. (2005). The plant thioredoxin system. *Cellular and Molecular Life Sciences CMLS* 62(1): 24-35.

Georgiadou EC, Kowalska E, Patla K, Kulbat K, Smolinska B, Leszczynska J, Fotopoulos V. (2018). Influence of heavy metals (Ni, Cu and Zn) on nitro-oxidative stress responses, proteome regulation and allergen production in basil (*Ocimum basilicum* L.) plants. *Frontiers in plant science* 9: 862.

Gibson F, Anderson L, Babnigg G, Baker M, Berth M, Binz PA, Borthwick A, Cash P, Day BW, Friedman DB, Garland D. (2008) Guidelines for reporting the use of gel electrophoresis in proteomics. *Nature biotechnology* 26(8): 863.

Gil R, Bautista I, Boscaiu M, Lidon A, Wankhade S, Sanchez H, Llinares J, Vicente O. (2014). Responses of five Mediterranean halophytes to seasonal changes in environmental conditions. *AoB Plants* 6.

Gil R, Boscaiu M, Lull C, Bautista I, Lidon A, Vicente O. (2013). Are soluble carbohydrates ecologically relevant for salt tolerance in halophytes? *Functional Plant Biology* 40(9): 805-818.

Gillman GP, Sumpter EA. (1986). Modification to the compulsive exchange method for measuring exchange characteristics of soils. *Australian Journal of Soil Research* 24: 61-66.

Glenn EP, Brown JJ. (1999). Salt tolerance and crop potential of halophytes. *Critical Reviews in Plant Sciences* 18(2): 227–255

Godbole NN. (1952). The salinity of Sambhar lake.In India BoNIoSo. *Proceedings of symposium on Rajputana Desert* 89–93.

Goldstein A, Annor G, Vamadevan V, Tetlow I, Kirkensgaard JJ, Mortensen K, Blennow A, Hebelstrup KH, Bertoft E. (2017). Influence of diurnal photosynthetic activity on the morphology, structure, and

thermal properties of normal and waxy barley starch. *International journal of biological macromolecules* 98: 188-200.

Golldack D, Luking I, Yang O. (2011). Plant tolerance to drought and salinity: stress regulating transcription factors and their functional significance in the cellular transcriptional network. *Plant Cell Reports* 30(8): 1383-1391.

Gosa SC, Lupo Y, Moshelion M. (2019). Quantitative and comparative analysis of whole-plant performance for functional physiological traits phenotyping: New tools to support pre-breeding and plant stress physiology studies. *Plant science* 282: 49-59.

Goussi R, Manaa A, Derbali W, Cantamessa S, Abdelly C, Barbato R. (2018). Comparative analysis of salt stress, duration and intensity, on the chloroplast ultrastructure and photosynthetic apparatus in *Thellungiella salsuginea*. *Journal of Photochemistry & Photobiology, B: Biology* 183: 275-287.

Gowik U, Westhoff P. (2011). The path from C3 to C4 photosynthesis. *Plant Physiology* 155(1): 56-63.

Graham LE, Cook ME, Busse JS. (2000). The origin of plants: body plan changes contributing to a major evolutionary radiation. *Proceedings of the National Academy of Sciences* 97(9): 4535-4540.

Grattan SR, Grieve CM. (1998). Salinity–mineral nutrient relations in horticultural crops. *Scientia Horticulturae* 78(1-4): 127-157.

Graves PR, Haystead TA. (2002). Molecular biologist's guide to proteomics. *Microbiology and Molecular Biology Reviews* 66(1):39-63.

Greenham K, McClung CR. (2015). Integrating circadian dynamics with physiological processes in plants. *Nature Reviews Genetics* 16(10): 598.

Griffiths H. (2013). Plant venation: from succulence to succulents. *Current Biology* 23(9): R340-341.

Grigore MN, Ivanescu L, Toma C. (2014). Halophytes: An integrative anatomical study. Switzerland: Springer International Publishing.

Guan B, Hu Y, Zeng Y, Wang Y, Zhang F. (2011). Molecular characterization and functional analysis of a vacuolar Na+/H+ antiporter gene (HcNHX1) from *Halostachys caspica. Molecular Biology Reports* 38: 1889–1899.

Guerinot ML. Salt DE. (2001). Fortified foods and phytoremediation. Two sides of the same coin. *Plant physiology* 125(1): 164-167.

Gul B, Khan MA. (2003). Saline agriculture: promises and prospects for future agriculture in degraded saline lands. Technology & Development in the New Millennium: 149-156.

Guo R, Shi L, Yan C, Zhong X, Gu F, Liu Q, Xia X, Li H. (2017). Ionomic and metabolic responses to neutral salt or alkaline salt stresses in maize (*Zea mays* L.) seedlings. *BMC plant biology* 17(1): 41.

Guo S, Yin H, Zhang X, Zhao F, Li P, Chen S, Zhao Y, Zhang H. (2006). Molecular cloning and characterization of a vacuolar H+ -pyrophosphatase gene, SsVP, from the halophyte *Suaeda salsa* and its overexpression increases salt and drought tolerance of Arabidopsis. *Plant Molecular Biology* 60(1): 41-50.

Gupta AK, Kaur N. (2005). Sugar signalling and gene expression in relation to carbohydrate metabolism under abiotic stresses in plants. *Journal of biosciences* 30: 761-76.

Gupta B, Huang B. (2014). Mechanism of salinity tolerance in plants: physiological, biochemical, and molecular characterization. *International Journal of Genomics* (2014): 701596.

Gupta HP, Khandelwal A. (1989). Mangroves of India: History and palynostratigraphy of Chilka lake, Orissa. *The Palaeobotanist* 379-393.

Gururani MA, Venkatesh J, Ganesan M, Strasser RJ, Han Y, Kim JI, Lee HY, Song PS. (2015). In vivo assessment of cold tolerance through chlorophyll-a fluorescence in transgenic Zoysia grass expressing mutant phytochrome a. *PLoS One* 10(5): e0127200.

Gutterman Y. (1993). Seed Germination in Desert Plants: Springer-Verlag Berlin Heidelberg.

Gygi SP, Corthals GL, Zhang Y, Rochon Y, Aebersold R. (2000). Evaluation of two-dimensional gel electrophoresis-based proteome analysis technology. *Proceedings of the National Academy of Sciences* 97(17): 9390-9395.

Hajiboland R. (2014). Reactive oxygen species and photosynthesis. Oxidative damage to plants. Academic Press 2014: 1-63.

Hamada A, Shono M, Xia T, Ohta M, Hayashi Y, Tanaka A, Hayakawa T. (2001). Isolation and characterization of a Na+/H+ antiporter gene from the halophyte *Atriplex gmelini*. *Plant Molecular Biology* 46: 35-42.

Hameed A, Hussain T, Gulzar S, Aziz I, Gul B, Khan MA. (2012). Salt tolerance of a cash crop halophyte *Suaeda fruticosa*: biochemical responses to salt and exogenous chemical treatments. *Acta Physiologiae Plantarum* 34: 2331-2340.

Hammond JP, Broadley MR, White PJ. (2004). Genetic responses to phosphorus deficiency. *Annals of botany* 94(3): 323-332.

Han HS, Lee KD. (2005). Plant growth promoting rhizobacteria effect on antioxidant status, photosynthesis, mineral uptake and growth of lettuce under soil salinity. *Journal: Research Journal of Agriculture and Biological Sciences* 1(3): 210-215.

Han HS, Supanjani, Lee KD. (2006). Effect of co-inoculation with phosphate and potassium solubilizing bacteria on mineral uptake and growth of pepper and cucumber. *Plant soil and Environment* 52(3): 130.

Hanc A, Ochecova P, Vasak F. (2017). Changes of parameters during composting of bio-waste collected over four seasons. *Environmental technology* 38(13-14): 1751-1764.

Harper KT, Belnap J. (2001). The influence of biological soil crusts on mineral uptake by associated vascular plants. *Journal of arid environments* 47(3): 347-357.

Hasanuzzaman M, Nahar K, Alam MM, Bhowmik PC, Hossain MA, Rahman MM, Prasad MN, Ozturk M, Fujita M. (2014). Potential use of halophytes to remediate saline soils. *BioMed Research International* (2014): 589341.

Hasegawa PM, Bressan RA, Zhu JK, Bohnert HJ. (2000). Plant cellular and molecular responses to high salinity. *Annual review of plant physiology and plant molecular biology* 51: 463-499.

Hasin Y, Seldin M, Lusis A. (2017). Multi-omics approaches to disease. *Genome biology* 18(1): 83.

Hawker JS, Marschner H, Downton WJS. (1974). Effects of sodium and potassium on starch synthesis in leaves. *Functional Plant Biology* 1(4): 491-501.

Hayashi T, Yoshida T, Fujii K, Mitsuya S, Tsuji T, Okada Y, Hayashi E, Yamauchi A. (2013). Maintained root length density contributes to the waterlogging tolerance in common wheat (*Triticum aestivum* L.). *Field Crops Research* 152: 27-35.

He Z, Ruan C, Qin P, Seliskar DM, Gallagher JL. (2003). Kosteletzkya virginica, a halophytic species with potential for agroecotechnology in Jiangsu Province, China. *Ecological Engineering* 21(4-5): 271-276.

Heidari B, Saeidi G, Tabatabaei BES, Suenaga K. (2012). QTLs involved in plant height, Peduncle length and heading date of Wheat (*Triticum aestivum* L.). *Journal of Agricultural Science and Technology* 14: 1093-1104.

Hejátko J, Ryu H, Kim GT, Dobešová R, Choi S, Choi SM, Souček P, Horák J, Pekárová B, Palme K, Brzobohatý B. (2009). The histidine kinases CYTOKININ-INDEPENDENT1 and ARABIDOPSIS HISTIDINE KINASE2 and 3 regulate vascular tissue development in Arabidopsis shoots. *The Plant Cell* 21(7): 2008-2021.

Hendricks RC, Bushnell DM. (2008). Halophytes energy feedstocks: Back to our roots. The 12th International Symposium on Transport Phenomena and Dynamics of Rotating Machinery. Honolulu, Hawaii. 1-8.

Hennessey TL, Field CB. (1991). Circadian rhythms in photosynthesis: oscillations in carbon assimilation and stomatal conductance under constant conditions. *Plant Physiology* 96(3): 831-836.

Hennessey TL, Freeden AL, Field CB. (1993). Environmental effects on circadian rhythms in photosynthesis and stomatal opening. *Planta* 189(3): 369-376.

Hennion F, Bouchereau A. (1998). Accumulation of organic and inorganic solutes in the subantarctic cruciferous species *Pringlea antiscorbutica* in response to saline and cold stresses*. Polar Biology* 20(4): 281-291.

Hilbe JM. (2003). A review of current SPSS products: SPSS 12, SigmaPlot 8.02, SigmaStat 3.0, Part 1. *The American Statistician* 57(4): 310-315.

Hildebrandt TM, Nunes Nesi A, Araujo WL, Braun HP, (2015). Amino acid catabolism in plants. *Molecular Plant* 8: 1563-1579.

Hirota T, Izumi M, Wada S, Makino A, Ishida H. (2018). Vacuolar protein degradation via autophagy provides substrates to amino acid catabolic pathways as an adaptive response to sugar starvation in *Arabidopsis thaliana*. *Plant & Cell Physiology* 59(7): 1363-1376.

Hoberg J. (2011). Economic analysis of mangrove forests: A case study in Gazi Bay, Kenya: United Nations Environment Programme; ISBN: 978-92-807-3187-3.

Hoffmann AA, Hercus MJ. (2000). Environmental stress as an evolutionary force. *Bio Science* 50(3): 217-226.

Hoffmann AA, Willi Y. (2008). Detecting genetic responses to environmental change. *Nature Reviews Genetics* 9(6): 421-432.

Holland TH, Christie WAK. 1909. The origin of the salt deposits of Rajputana. *Records of the Geological Survey of India* 38(2): 154-186.

Holley AK, Bakthavatchalu V, Velez-Roman JM, St-Clair DK. (2011). Manganese superoxide dismutase: guardian of the powerhouse. *International journal of molecular sciences* 12(10): 7114-7162.

Holmstrom KO, Somersalo S, Mandal A, Palva TE, Welin B. (2000). Improved tolerance to salinity and low temperature in transgenic tobacco producing glycine betaine. *Journal of Experimental Botany* 51(343): 117-185.

Hoque MA, Banu MN, Nakamura Y, Shimoishi Y, Murata Y. (2008). Proline and glycinebetaine enhance antioxidant defense and methylglyoxal detoxification systems and reduce NaCl-induced damage in cultured tobacco cells. *Journal of Plant Physiology* 165(8): 813-824.

Hsieh TH, Lee J., Yang PT, Chiu LH, Charng YY, Wang YC, Chan MT. (2002). Heterology expression of the Arabidopsis C-repeat/dehydration response element binding Factor 1 gene confers elevated tolerance to chilling and oxidative stresses in transgenic tomato*. Plant physiology* 129(3): 1086-1094.

Hu Y, Wu Q, Sprague SA, Park J, Oh M, Rajashekar CB, Koiwa H, Nakata PA, Cheng N, Hirschi KD, White FF. (2015). Tomato expressing *Arabidopsis glutaredoxin* gene AtGRXS17 confers tolerance to chilling

stress via modulating cold responsive components. *Horticulture research* 11(2):15051.

Hu YZ, Zeng YL, Guan B, Zhang FC. (2012). Overexpression of a vacuolar H+-pyrophosphatase and a B subunit of H+-ATPase cloned from the halophyte Halostachys caspica improves salt tolerance in *Arabidopsis thaliana*. *Plant cell Tissue and Organ Culture* 108: 63-71.

Huang J, Lu X, Yan H, Chen S, Zhang W, Huang R, Zheng Y. (2012). Transcriptome characterization and sequencing-based identification of salt-responsive genes in *Millettia pinnata*, a semi-mangrove plant. *DNA Research* 19(2): 195-207.

Huang S, Chaudhary K, Garmire LX. (2017). More is better: recent progress in multi-omics data integration methods. *Frontiers in genetics* 16(8): 84.

Huang W, Yang YJ, Hu H, Cao KF, Zhang SB. (2016). Sustained diurnal stimulation of cyclic electron flow in two tropical tree species *Erythrophleum guineense* and *Khaya ivorensis*. *Frontiers in Plant Science* 7: 1068.

Huchzermeyer B, Hausmann N, Hausmann N, Paquet-durant F, Koyro HW. (2004). Biochemical and physiological mechanisms leading to salt tolerance. *Tropical Ecology* 45(1): 141-150.

Hugly S, Somerville C. 1992. A role for membrane lipid polyunsaturation in chloroplast biogenesis at low temperature. *Plant Physiology* 99: 197-202.

Hulskamp M. (2004). Plant trichomes: a model for cell differentiation. *Nature Reviews Molecular Cell Biology* 5(6): 471-480.

Ikkonen EN, Shibaeva TG, Rosenqvist E, Ottosen CO. (2015). Daily temperature drop prevents inhibition of photosynthesis in tomato plants under continuous light. *Photosynthetica* 53(3): 389-394.

Inada M, Ueda A, Shi W, Takabe T. (2005). A stress-inducible plasma membrane protein 3 (AcPMP3) in a monocotyledonous halophyte, *Aneurolepidium chinense*, regulates cellular Na(+) and K(+) accumulation under salt stress. *Planta* 220(3): 395-402.

Inukai T, Nagashima S, Kato M. (2019). Pid3-I1 is a race-specific partial-resistance allele at the Pid3 blast resistance locus in rice. *Theoretical and Applied Genetics* 132(2): 395-404.

Ishihama Y. (2005) Proteomic LC–MS systems using nanoscale liquid chromatography with tandem mass spectrometry. *Journal of Chromatography A* 1067(1-2): 73-83.

Jacob JM, Karthik C, Saratale RG, Kumar SS, Prabakar D, Kadirvelu K, Pugazhendhi A. (2018). Biological approaches to tackle heavy metal pollution: A survey of literature. *Journal of environmental management* 217: 56-70.

Jaeger CH, Monson RK, Fisk MC, Schmidt SK. (1999). Seasonal partitioning of nitrogen by plants and soil microorganisms in an alpine ecosystem. *Ecology* 80(6): 1883-1891.

Jakher GR, Bhargava SC, Sinha RK. (1990). Comparative limnology of Sambhar and Didwana lakes (Rajasthan, NW India). Springer, Dordrecht.

Jakobsen I. (1985). The role of phosphorus in nitrogen fixation by young pea plants (Pisum sativum). *Physiologia Plantarum* 64(2): 190-196.

Jespersen D, Xu C, Huang B. (2015). Membrane proteins associated with heat-induced leaf senescence in a cool-season grass species. *Crop Science* 55(2): 837-850.

Jha B, Agarwal PK, Reddy PS, Lal S, Sopory SK, Reddy MK. (2009). Identification of salt-induced genes from *Salicornia brachiata*, an extreme halophyte through expressed sequence tags analysis. *Genes & Genetic Systems* 84: 111-120.

Jha B, Lal S, Tiwari V, Yadav SK, Agarwal PK. (2012a). The SbASR-1 gene cloned from an extreme halophyte *Salicornia brachiata* enhances salt tolerance in transgenic tobacco. *Marine Biotechnology* 14: 782-792.

Jha B, Mishra A, Jha A, Joshi M. (2013). Developing transgenic Jatropha using the SbNHX1 gene from an extreme halophyte for cultivation in saline wasteland. *PLoS One* 8(8): e71136.

Jha B, Sharma A, Mishra A. (2011). Expression of SbGSTU (tau class glutathione S-transferase) gene isolated from *Salicornia brachiata* in tobacco for salt tolerance. *Molecular Biology Reports* 38: 4823-4832.

Jha B, Singh NP, Mishra A. (2012b). Proteome profiling of seed storage proteins reveals the nutritional potential of *Salicornia brachiata* Roxb., an extreme halophyte. *Journal of Agricultural and Food Chemistry* 60(17): 4320-4326.

Jia YL, Chen H, Zhang C, Gao LJ, Wang XC, Qiu LL, Wu JF. (2016). Proteomic analysis of halotolerant proteins under high and low salt stress in *Dunaliella salina* using two-dimensional differential in-gel electrophoresis. *Genetics and molecular biology* 39(2): 239-247.

Jin H, Dong D, Yang Q, Zhu D. (2016). Salt-responsive transcriptome profiling of *Suaeda glauca* via RNA sequencing. *PLoS One* 11(3): e0150504.

Jithesh MN, Prashanth SR, Sivaprakash KR, Parida AK. (2006). Antioxidative response mechanisms in halophytes: their role in stress defence. *Journal of Genetics* 85(3): 237-254.

Joët T, Genty B, Josse EM, Kuntz M, Cournac L, Peltier G. (2002). Involvement of a plastid terminal oxidase in plastoquinone oxidation as evidenced by expression of the Arabidopsis thaliana enzyme in tobacco. *Journal of Biological Chemistry* 277(35): 31623-31630.

Johnson CH, Knight MR, Kondo T, Masson P, Sedbrook J, Haley A, Trewavas A. (1995). Circadian oscillations of cytosolic and chloroplastic free calcium in plants. *Science* 269(5232): 1863-1865.

Joseph S, Reddy SC, Pattanaik C, Sudhakar S. (2008). Distribution of plant communities along climatic and topographic gradients in Mudumalia Wildlife Sanctuary (Southern India). *Biological Letter* 45: 29-41.

Joshi R, Karan R, Singla-Pareek SL, Pareek A. (2016). Ectopic expression of Pokkali phosphoglycerate kinase-2 (OsPGK2-P) improves yield in tobacco plants under salinity stress. *Plant Cell Reports* 35(1): 27-41.

Joshi R, Ramanarao MV, Baisakh N. (2013). Arabidopsis plants constitutively overexpressing a myo-inositol 1-phosphate synthase gene (SaINO1) from the halophyte smooth cordgrass exhibits enhanced level of tolerance to salt stress. *Plant Physiology and Biochemistry* 65: 61-66.

Joshi R, Sahoo KK, Tripathi AK, Kumar R, Gupta BK, Pareek A, Singla-Pareek SL. (2018). Knockdown of an inflorescence meristem-specific cytokinin oxidase–OsCKX2 in rice reduces yield penalty under salinity stress condition. *Plant, Cell & Environmen*t 41(5): 936-946.

Joyce AR, Palsson BØ. (2006). The model organism as a system: integrating 'omics' data sets. *Nature reviews Molecular cell biology* 7: 198–210.

Jun ZY, Fei G, Feng LX, Jun Z, Fa ZG. (2010). Alterations in phosphoproteome under salt stress in *Thellungiella* roots. *Chinese Science Bulletin* 55(32): 3673-3679.

Kadam AS, Wadje SS, Patil R. (2011). Roll of potassium humate on growth and yield of soybean and black gram. *International Journal of Pharma and Bio Sciences* 1: 243-246.

Kadukova J, Manousaki E, Kalogerakis N. (2008). Pb and Cd accumulation and phyto-excretion by salt cedar (*Tamarix smyrnensis* Bunge). *International Journal of Phytoremediation* 10(1): 31-46.

Kalaji HM, Schansker G, Brestic M, Bussotti F, Calatayud A, Ferroni L, Goltsev V, Guidi L, Jajoo A, Li P, et al. (2017). Frequently asked questions about chlorophyll fluorescence, the sequel. *Photosynthesis research* 132(1): 13-66.

Kalamaki MS, Merkouropoulos G, Kanellis AK. (2009). Can ornithine accumulation modulate abiotic stress tolerance in Arabidopsis? *Plant Signalling & Behaviour* 4: 1099-1101.

Kaminska M, Deniziak M, Kerjan P, Barciszewski J, Mirande M. (2000). A recurrent general RNA binding domain appended to plant methionyl-tRNA synthetase acts as a cis-acting cofactor for aminoacylation. *The EMBO journal* 19(24): 6908-6917.

Kane J. (2018). List of deserts in India. Sciencing. Santa Monica, Californi: Leaf Group Ltd.

Kant S, Bi YM, Weretilnyk E, Barak S, Rothstein SJ. (2008). The Arabidopsis halophytic relative *Thellungiella halophila* tolerates nitrogen-limiting conditions by maintaining growth, nitrogen uptake, and assimilation. Plant Physiology 147(3): 1168-1180.

Kaplan F, Guy CL. (2004) β-Amylase induction and the protective role of maltose during temperature shock. *Plant Physiology* 135: 1674–1684

Karimi M. (2019) Wheat (Bam variety) responses to interactive effects of irrigation water salinity and different rates of potassium sulphate fertilizer. *AGRIS since.*

Karpievitch YV, Dabney AR, Smith RD. (2012). Normalization and missing value imputation for label-free LC-MS analysis. *BMC bioinformatics* 13(16): S5.

Kassanis B. (1952). Some effects of high temperature on the susceptibility of plants to infection with viruses. *Annals of Applied Biology* 39(3): 358-369.

Katschnig D, Bliek T, Rozema J, Schat H. (2015). Constitutive high-level SOS1 expression and absence of HKT1;1 expression in the salt-accumulating halophyte *Salicornia dolichostachya*. *Plant Science* 234: 144-154.

Kavitha K, George S, Venkataraman G, Parida A. (2010). A salt-inducible chloroplastic monodehydroascorbate reductase from halophyte *Avicennia marina* confers salt stress tolerance on transgenic plants. *Biochimie* 92(10): 1321-1329.

Kazerani B, Navabpour S, Sabouri H, Ramezanpour SS, Zaynali Nezhad K, Eskandari A. (2019). Evaluation of proline content and enzymatic defense mechanism in response to drought stress in rice. *Plant Physiology* 9(2): 2749-2757.

Khan MA, Ansari R, Ali H, Gul B, Nielsen BL. (2009). Panicum turgidum, a potentially sustainable cattle feed alternative to maize for saline areas. *Agriculture, ecosystems & environment* 129: 542-546.

Khan MA, Gul B. (1998). High salt tolerance in germinating dimorphic seeds of *Arthrocnemum indicum*. *International Journal of Plant Sciences* 159(5): 826-832.

Khan MA, Musharaf S, Shinwari ZK. (2011). Ethnobotanical importance of halophytes of Noshpho salt mine, District Karak, Pakistan. *Research in Pharmaceutical Biotechnology* 3(4): 46-52.

Khan MA, Ungar IA, Guan B. (1998). Action of compatible osmotica and growth regulators in alleviating the effect of salinity on the germination of dimorphic seeds of *Arthrocnemum indicum* L. *International Journal of Plant Sciences* 159(2): 313-317.

Khan MA, Ungar IA, Showalter AM, (2000). The effect of salinity on the growth, water status, and ion content of a leaf succulent perennial

halophyte, *Suaeda fruticosa* (L.) Forssk. *Journal of Arid Environments* 45: 73-84.

Khan MA, Ungar IA, Showalter AM. (2000). Effects of salinity on growth, water relations and ion accumulation of the subtropical perennial halophyte, *Atriplex griffithi*i var. stocksii. *Annals of Botany* 85: 225-232.

Khan MA, Ungar IA, Showalter AM. (2000). The effect of salinity on the growth, water status, and ion content of a leaf succulent perennial halophyte, Suaeda fruticosa (L.) Forssk. *Journal of Arid Environments* 45(1): 73-84.

Khan MA, Ungar IA, Showalter AM. (2000). The effect of salinity on the growth, water status, and ion content of a leaf succulent perennial halophyte, *Suaeda fruticosa* (L.) Forssk. *Journal of Arid Environments* 45(1): 73-84.

Khan MA., Ungar IA, Showalter AM. (2000). The effect of salinity on the growth, water status, and ion content of a leaf succulent perennial halophyte, *Suaeda fruticosa* (L.) Forssk. *Journal of Arid Environments* 45: 73-84.

Khojasteh M, Lam WL, Ward RK, MacAulay C. (2005). A stepwise framework for the normalization of array CGH data. *BMC bioinformatics* 6(1): 274.

Kim HK, Choi YH, Verpoorte R (2011). NMR-based plant metabolomics: where do we stand, where do we go? *Trends in Biotechnology* 29: 267-275.

Kim SW, Lee SK, Jeong HJ, An G, Jeon JS, Jung KH. (2017). Crosstalk between diurnal rhythm and water stress reveals an altered primary carbon flux into soluble sugars in drought-treated rice leaves. *Scientific reports* 7(1): 8214.

Kobayashi Y, Kuroda K, Kimura K, Southron-Francis JL, Furuzawa A, Kimura K, Iuchi S, Kobayashi M, Taylor GJ Koyama H. (2008). Amino acid polymorphisms in strictly conserved domains of a P-type ATPase HMA5 are involved in the mechanism of copper tolerance variation in Arabidopsis. *Plant Physiology* 148(2): 969-980.

Koboldt DC, Steinberg KM, Larson DE, Wilson RK, Mardis ER. (2013). The next-generation sequencing revolution and its impact on genomics. *Cell* 155:27–38.

Kore-eda S, Cushman MA, Akselrod I, Bufford D, Fredrickson M, Clark E, Cushman JC. (2004). Transcript profiling of salinity stress responses by large-scale expressed sequence tag analysis in *Mesembryanthemum crystallinum*. *Gene* 341: 83-92.

Kosova K, Prail IT, Vitamvas P. (2013). Protein contribution to plant salinity response and tolerance acquisition. *International Journal of Molecular Sciences* 14(4): 6757-6789.

Kosová K, Vítámvás P, Urban MO, Prášil IT, Renaut J. (2018). Plant abiotic stress proteomics: The major factors determining alterations in cellular proteome. *Frontiers in plant science* 9: 122.

Koyro HW, Helmut L, Bilquees G, Raziuddin A, Bernhard H, Zainul A, Tabassum H, Ajmal KM. (2014). Importance of the diversity within the halophytes to agriculture and land management in arid and semiarid countries. In: Khan MA, Böer B, Öztürk M, Abdessalaam TZA, Clüsener-Godt M, Gul B eds. Sabkha Ecosystems. Netherlands: Springer Netherlands: 175-198.

Koyro HW, Hussain T, Huchzermeyer B, Khan AM. (2013). Photosynthetic and growth responses of a perennial halophytic grass *Panicum turgidum* to increasing NaCl concentrations. *Environmental and Experimental Botany* 91: 22-29.

Koyro HW, Khan MA, Lieth H. (2011). Halophytic crops: A resource for the future to reduce the water crisis? *Emirates Journal of Food and Agriculture* 23(1): 1-16.

Koyro HW. (2006). Effect of salinity on growth, photosynthesis, water relations and solute composition of the potential cash crop halophyte *Plantago coronopus* (L.). *Environmental and Experimental Botany* 56(2): 136-146.

Krasensky J, Jonak C. (2012). Drought, salt, and temperature stress-induced metabolic rearrangements and regulatory networks. *Journal of Experimental Botany* 63(4): 1593-1608.

Krauss KW, Allen JA, Cahoon DR. (2003). Differential rates of vertical accretion and elevation change among aerial root types in Micronesian mangrove forests. *Estuarine, Coastal and Shelf Science* 56(2): 251-259.

Krishna PH, Reddy CS, Meena SL, Katewa SS. (2014a). Pattern of plant species diversity in grasslands of Rajasthan, India. *Taiwania* 59(2): 111–118.

Krishnamurthy P, Tan XF, Lim TK, Lim TM, Kumar PP, Loh CS, Lin Q. (2014). Proteomic analysis of plasma membrane and tonoplast from the leaves of mangrove plant *Avicennia officinalis*. *Proteomics* 14(21-22): 2545-2557.

Ksouri R, Ksouri WM, Jallali I, Debez A, Magné C, Hiroko I, Abdelly C. (2012). Medicinal halophytes: potent source of health promoting biomolecules with medical, nutraceutical and food applications. *Critical Reviews in Biotechnology* 32(4): 289-326.

Kudo M, Kidokoro S, Yoshida T, Mizoi J, Kojima M, Takebayashi Y, Yamaguchi-Shinozaki K. (2019). A gene-stacking approach to overcome the trade-off between drought stress tolerance and growth in Arabidopsis. *The Plant Journal* 97(2): 240-256.

Kumar GR, Sakthivel K, Sundaram RM, Neeraja CN, Balachandran SM, Rani NS, Madhav MS. (2010). Allele mining in crops: prospects and potentials. *Biotechnology advances* 28(4): 451-461.

Kumari S, Sabharwal VP, Kushwaha HR, Sopory SK, Singla-Pareek SL, Pareek A. (2009). Transcriptome map for seedling stage specific salinity stress response indicates a specific set of genes as candidate for saline tolerance in *Oryza sativa* L. *Functional & Integrative Genomics* 9: 109–123.

Kumari S, Singh P, Singla-Pareek SL, Pareek A. (2009). Heterologous expression of a salinity and developmentally regulated rice cyclophilin gene (OsCyp2) in E. coli and *S. cerevisiae* confers tolerance towards multiple abiotic stresses. *Molecular Biotechnology* 42: 195–204.

Kusvuran S, Dasgan HY, Abak K, (2013). Citrulline is an important biochemical indicator in tolerance to saline and drought stresses in melon. *Scientific World Journal* (2013): 253414.

Kutyshenko VP, Budantsev AY, Uversky VN, (2015). Analysis of seasonal changes in plants by high-resolution NMR spectroscopy: Looking at the aqueous extracts from different plant tissues. *Journal of Nature and Science* 1: e88.

Labidi N, Ammari M, Mssedi D, Benzerti M, Snoussi S, Abdelly C. (2010). Salt excretion in *Suaeda fruticosa*. *Acta Biologica Hungarica* 61, 299-312.

Lakra N, Kaur C, Anwar K, Singla-Pareek SL, Pareek A. (2018). Proteomics of contrasting rice genotypes: identification of potential targets for raising crops for saline environment. *Plant, cell & environment* 41(5): 947-969.

Lakra N., Kaur C, Singla-Pareek SL, Pareek A. (2019). Mapping the 'early salinity response'triggered proteome adaptation in contrasting rice genotypes using iTRAQ approach. *Rice* 12(1): 3.

Lan T, Duan Y, Wang B, Zhou Y, Wu W. (2011). Molecular cloning and functional characterization of a Na+ antiporter gene from halophyte *Spartina anglica*. *Turkish Journal of Agriculture and Forestry* 35: 535-543.

Lang'at JKS, Kairo JG, Mencuccini M, Bouillon S, Skov MW, Waldron S, Huxham M. (2014). Rapid losses of surface elevation following tree girdling and cutting in tropical mangroves. *PLoS One* 9(9): e107868.

Langfelder P, and Horvath S. (2012). Identification of consensus modules in aging-related methylation data.

Langfelder P, Horvath S. (2007). Eigengene networks for studying the relationships between co-expression modules. *BMC systems biology* 1(1): 54.

Langfelder P, Horvath S. (2008) WGCNA: an R package for weighted correlation network analysis. *BMC Bioinformatics* 9: 559.

Langfelder P, Zhang B, Horvath S. (2008). Defining clusters from a hierarchical cluster tree: The dynamic tree cut package for R. *Bioinformatics* 24(5): 719–720.

Langfelder P. (2015). Signed vs. Unsigned Topological Overlap Matrix Technical Report.

Larkindale J, Huang B. (2004). Changes of lipid composition and saturation level in leaves and roots for heat-stressed and heat-acclimated creeping bentgrass (*Agrostis stolonifera*). *Environmental and Experimental Botany* 51(1): 57-67.

Laslett GM, McBratney AB, Pahl PJ, Hutchinson MF. (1897). Comparison of several spatial prediction methods for soil pH. *Journal of Soil Science* 38: 325-341.

Lawyer G. (2015). Understanding the influence of all nodes in a network. *Scientific reports* 2(5): 8665.

Leakey ADB, Bernacchi CJ, Dohleman FG, Ort DR, Long SP. (2004). Will photosynthesis of maize (*Zea mays*) in the US corn belt increase in future [CO_2] rich atmospheres? An analysis of diurnal courses of CO_2 uptake under free-air concentration enrichment (FACE). *Global Change Biology* 10(6): 951-962.

Lee G, Carrow RN, Duncan RR. (2004). Photosynthetic responses to salinity stress of halophytic seashore paspalum ecotypes. *Plant Science* 166(6): 1417-1425.

Lee SK, Sohn EY, Hamayun M, Yoon JY, Lee IJ. (2010). Effect of silicon on growth and salinity stress of soybean plant grown under hydroponic system. *Agroforestry systems* 80(3): 333-340.

Lee YP, Giorgi FM, Lohse M, Kvederaviciute K, Klages S, Usadel B, Meskiene I, Reinhardt R, Hincha DK. (2013). Transcriptome sequencing and microarray design for functional genomics in the extremophile Arabidopsis relative *Thellungiella salsuginea* (Eutrema salsugineum). *BMC Genomics* 14: 793.

Leegood RC. (2007). A welcome diversion from photorespiration. *Nature Biotechnology* 25: 359-340.

Lefevre I, Marchal G, Meerts P, Correal E, Lutts S. (2009). Chloride salinity reduces cadmium accumulation by the Mediterranean halophyte species *Atriplex halimus* L. *Environmental and Experimental Botany* 65(1): 142-152

Lequeu J, Fauconnier ML, Chammaï A, Bronner R, Blée E. (2003). Formation of plant cuticle: evidence for the occurrence of the peroxygenase pathway. The *Plant Journal* 36(2): 155-164.

Levine B, Klionsky DJ. (2004). (Development by self-digestion: molecular mechanisms and biological functions of autophagy. *Developmental cell* 6: 463-77.

Li B, Wei A, Song C, Li N, Zhang J. (2008). Heterologous expression of the TsVP gene improves the drought resistance of maize. *Plant Biotechnology Journal* 6(2): 146-159.

Li C, Sun X, Chang C, Jia D, Wei Z, Li C, Ma F. Dopamine. (2015). Dopamine alleviates salt-induced stress in *Malus hupehensis*. *Physiologia Plantarum* 153: 584-602.

Li J, Sun X, Yu G, Jia C, Liu J, Pan H. (2014). Generation and analysis of expressed sequence tags (ESTs) from halophyte *Atriplex canescen*s to explore salt-responsive related genes. *International Journal of Molecular Sciences* 15(6): 11172-11189.

Li M, Yin X, Sakata K, Yang P, Komatsu S. (2015). Proteomic analysis of phosphoproteins in the rice nucleus during the early stage of seed germination. *Journal of proteome research* 14(7): 2884-2896.

Li QL, Gao XR, Yu XH, Wang XZ, An LJ. (2003a). Molecular cloning and characterization of betaine aldehyde dehydrogenase gene from *Suaeda liaotungensis* and its use in improved tolerance to salinity in transgenic tobacco. *Biotechnology letters* 25(17): 1431-1436.

Li QL, Liu DW, Gao XR, Su Q, An LJ. (2003b). Cloning of cDNA encoding choline monooxygenase from *Suaeda liaotungensis* and salt tolerance Tobacco. *Acta Botanica Sinica* 45(2): 242-247.

Li W, Wang D, Jin T, Chang Q, Yin D, Xu S, Liu B, Liu L. (2011a). The Vacuolar Na+/H+ antiporter gene SsNHX1 from the halophyte *Salsola soda* confers salt tolerance in transgenic Alfalfa (*Medicago sativa* L.). *Plant Molecular Biology Reporter* 29: 278-290.

Li W, Zhang C, Lu Q, Wen X, Lu C. (2011b). The combined effect of salt stress and heat shock on proteome profiling in *Suaeda salsa*. *Journal of Plant Physiology* 168(15): 1743-1752.

Liang B, Li C, Ma C, Wei Z, Wang Q, Huang D, Chen Q, Li C, Ma F. (2017). Dopamine alleviates nutrient deficiency-induced stress in *Malus hupehensis*. *Plant Physiology and Biochemistry* 119: 346-59.

Liang S, Chao ZR, Sui DS, Hua SS. (2008). Adaptation to salinity in mangroves: Implication on the evolution of salt-tolerance. *Science Bulletin* 53(11): 1708-1715.

Liang Y, Sun W, Zhu YG, Christie P. (2007). Mechanisms of silicon-mediated alleviation of abiotic stresses in higher plants: a review. *Environmental pollution* 147(2): 422-428.

Lilley KS, Friedman DB. (2004). All about DIGE: quantification technology for differential-display 2D-gel proteomics. *Expert review of proteomics* 1(4): 401-409.

Lim JH, Yang HJ, Jung KH, Yoo SC, Paek NC. (2014). Quantitative trait locus mapping and candidate gene analysis for plant architecture traits using whole genome re-sequencing in rice. *Molecules and Cells* 37(2): 149-160.

Lin W, Okon Y, Hardy RW. (1983). Enhanced mineral uptake by Zea mays and Sorghum bicolor roots inoculated with *Azospirillum brasilense*. *Applied and Environmental Microbiology* 45(6): 1775-1779.

Liu J, Zhang Q, Liu M, Ma L, Shi Y, Ruan J, (2016). Metabolomic analyses reveal distinct change of metabolites and quality of green tea during the short duration of a single spring season. *Journal of Agricultural and Food Chemistry* 64: 3302-9.

L**iu J, Zhou Y, Luo C, Xiang Y, An L**. (2016). De novo transcriptome sequencing of desert herbaceous *Achnatherum splendens* (Achnatherum) seedlings and identification of salt tolerance genes. *Genes (Basel)* 7(4).

Liu L, Wang Y, Wang N, Dong YY, Fan XD, Liu XM, Yang J, Li HY. (2011). Cloning of a vacuolar H(+)-pyrophosphatase gene from the halophyte *Suaeda corniculata* whose heterologous overexpression improves salt, saline-alkali and drought tolerance in Arabidopsis. *Journal of Integrative Plant Biology* 53(9): 731-742.

Liu P, Tang X, Gong C, Xu, G. (2010). Manganese tolerance and accumulation in six Mn hyperaccumulators or accumulators. *Plant and soil* 335(1-2): 385-395.

Liu Q, Liu R, Ma Y, Song J. (2018). Physiological and molecular evidence for Na+ and Cl− exclusion in the roots of two *Suaeda salsa* populations. Aquatic Botany: 146, 1-7.

Liu W, Li L, Li W. (2014). Gene co-expression analysis identifies common modules related to prognosis and drug resistance in cancer cell lines. *International journal of cancer* 135(12): 2795-2803.

Loewith R, Hall MN. (2011). Target of rapamycin (TOR) in nutrient signalling and growth control. *Genetics* 189: 1177-1201.

López-Orenes A, Bueso MC, Conesa HM, Calderón AA, Ferrer MA. (2017). Seasonal changes in antioxidative/oxidative profile of mining and non-mining populations of Syrian beancaper as determined by soil conditions. *Science of The Total Environment* 575: 437-447.

Loudet O, Saliba-Colombani V, Camilleri, C, Calenge F, Gaudon V, Koprivova, A, North KA, Kopriva S, Daniel-Vedele F. (2007). Natural variation for sulfate content in *Arabidopsis thaliana* is highly controlled by APR2. *Nature genetics* 39(7): 896.

Lu A, Jiang G, Wang B, Kuang T. (2003). Photosystem II photochemistry and photosynthetic pigment composition in salt-adapted halophyte *Artimisia anethifolia* grown under outdoor conditions. *Journal of Plant Physiology* 160: 403-4008.

Luo HH, Merope TM, Zhang YL, Zhang WF. (2016). Combining gas exchange and chlorophyll a fluorescence measurement to analyze the photosynthetic activity of drip-irrigated cotton under different soil water deficits. *Journal of Integrative Agriculture* 15(6): 1256–1266.

Lv S, Zhang K, Gao Q, Lian L, Song Y, Zhang J. (2008). Overexpression of an H+-PPase gene from *Thellungiella halophila* in cotton enhances salt tolerance and improves growth and photosynthetic performance. *Plant and Cell Physiology* 49(8): 1150-1164.

Lynch DV, Steponkus PL. (1987). Plasma membrane lipid alterations associated with cold acclimation of winter rye seedlings (*Secale cereale* L. cv Puma). *Plant Physiology* 83: 761-767.

Ma J, Zhang M, Xiao X, You J, Wang J, Wang T, Yao Y, Tian C. (2013). Global transcriptome profiling of *Salicornia europaea* L. shoots under NaCl treatment. *PLoS One* 8(6): e65877.

Mahajan S, Tuteja N. (2005). Cold, salinity and drought stresses: an overview. *Archives of Biochemistry and Biophysics* 444(2): 139-158.

Mahmood A, Amaya R, Turgay OC, Yaprak AE, Taniguchi T, Kataoka R. (2019). High salt tolerant plant growth promoting rhizobacteria from the common ice-plant *Mesembryanthemum crystallinum* L. *Rhizosphere* 9: 10-17.

Majee M, Maitra S, Dastidar KG, Pattnaik S, Chatterjee A, Hait NC, Das KP, Majumder AL. (2004). A novel salt-tolerant L-myo-inositol-1-phosphate synthase from *Porteresia coarctata* (Roxb.) Tateoka, a halophytic wild rice. *The Journal of Biological Chemistry* 279(27): 28539-28552.

Malone M, Leigh RA, Tomos AD. (1991). Concentrations of vacuolar inorganic ions in individual cells of intact wheat leaf epidermis. *Journal of Experimental Botany* 42: 305–309.

Mann M, Jensen ON. (2003). Proteomic analysis of post-translational modifications. *Nature Biotechnology* 21: 255–261.

Manousaki E, Kadukova J, Papadantonakis N, Kalogerakis N. (2008). Phytoextraction and phytoexcretion of Cd by the leaves of *Tamarix smyrnensis* growing on contaminated non-saline and saline soils. *Environmental Research* 106(3): 326-332.

Manousaki E, Kalogerakis N. (2011a). Halophytes-an emerging trend in phytoremediation. *International Journal of Phytoremediation* 13(10): 959-969.

Manousaki E, Kalogerakis N. (2011b). Halophytes present new opportunities in phytoremediation of heavy metals and saline soils. *Industrial & Engineering Chemistry Research* 50: 656-660.

Marcińska I, Czyczyło-Mysza I, Skrzypek E, Grzesiak MT, Popielarska-Konieczna M, Warchoł M, Grzesiak S. (2017). Application of

photochemical parameters and several indices based on phenotypical traits to assess intraspecific variation of oat (*Avena sativa* L.) tolerance to drought. *Acta Physiologiae Plantarum* 39(7).

Marschner H. (1995). Mineral nutrition of higher plants, 2nd edn London Academic Press

Marschner H. (2011). Marschner's mineral nutrition of higher plants. Academic press.

Masi A, Trentin AR, Agrawal GK, Rakwal R. (2015). Gamma-glutamyl cycle in plants: a bridge connecting the environment to the plant cell?. *Frontiers in plant science* 6: 252.

Mathur S, Jajoo A, Mehta P, Bharti S. (2011). Analysis of elevated temperature-induced inhibition of photosystem II using chlorophyll a fluorescence induction kinetics in wheat leaves (*Triticum aestivum*). *Plant Biology* 13(1): 1-6.

McCusker A. 1971. Knee Roots in *Avicennia marina* (Forsk.) Vierh. *Annals of Botany* 35: 707-712.

Megdiche W, Hessini K, Gharbi F, Jaleel CA, Ksouri R, Abdelly C. (2008). Photosynthesis and photosystem 2 efficiency of two salt-adapted halophytic seashore *Cakile maritima* ecotypes. *Photosynthetica* 46(3): 410-419.

Mehta PA, Sivaprakash K, Parani M, Venkataraman G, Parida AK. (2005). Generation and analysis of expressed sequence tags from the salt-tolerant mangrove species *Avicennia marina* (Forsk) Vierh. *Theoretical and Applied Genetics* 110(3): 416-424.

Mendez MO, Maier RM. (2007). Phytostabilization of mine tailings in arid and semiarid environments—an emerging remediation technology. *Environmental health perspectives* 116(3): 278-283.

Mengel K, Geurtzen G. (1986). Iron chlorosis on calcareous soils. Alkaline nutritional condition as the cause for the chlorosis. *Journal of Plant Nutrition* 9(3-7): 161-173.

Meyer Y, Siala W, Bashandy T, Riondet C, Vignols F, Reichheld JP. (2008). Glutaredoxins and thioredoxins in plants. *Biochimica et Biophysica Acta (BBA)-Molecular Cell Research* 1783(4): 589-600.

Michalowski CB, Bohnert HJ. (1992). Nucleotide sequence of a root-specific transcript encoding a Germin-like protein from the halophyte *Mesembryanthemum crystallinum*. *Plant Physiology* 100: 537-538.

Mikolajczyk S, Brody S. (1990). De novo fatty acid synthesis mediated by acyl-carrier protein in *Neurospora crassa* mitochondria. *The FEBS Journal* 187, 431-7.

Ming Y, Genxing P, Lianqing L, Jianwen Z. (2010). An overview of the potential role of reed (Phragmites australis) wetlands in terrestrial carbon sequestration of *China hinese Agricultural Science Bulletin* 18: 72.

Mishra A, Tanna B, (2017). Halophytes: Potential resources for salt stress tolerance genes and promoters. *Frontiers in Plant Science* 8: 829.

Mittler R, Vanderauwera S, Gollery M, Van Breusegem F. (2004). Reactive oxygen gene network of plants. *Trends in Plants Science* 9(10): 490-498.

Miyama M, Hanagata N. (2007). Microarray analysis of 7029 gene expression patterns in burma mangrove under high-salinity stress. *Plant Science* 172(5): 948-957.

Mo X-Q, Li H-Y. (2010). Application of wild halophytes in Tianjin coastal wetland. Urban Environ. *Urban Ecology* 2: 14–17.

Mocali S, Chiellini C, Fabiani A, Decuzzi S, de Pascale D, Parrilli E, Tutino ML, Perrin E, Bosi E, Fondi M, Giudice AL. (2017). Ecology of cold environments: new insights of bacterial metabolic adaptation through an integrated genomic-phenomic approach. *Scientific reports* 7: 839.

Moomaw AS, Maguire ME. (2008). The unique nature of Mg^{2+} channels. *Physiology* 23(5): 275-285.

Moon J, Parry G, Estelle M. (2004). The ubiquitin-proteasome pathway and plant development. *The Plant Cell* 16: 3181-95.

Mora-García S, de Leone MJ, Yanovsky M. (2017). Time to grow: circadian regulation of growth and metabolism in photosynthetic organisms. *Current opinion in plant biology* 35: 84-90.

Morrissey J, Baxter IR, Lee J, Li L, Lahner B, Grotz N, Kaplan J, Salt DE, Guerinot M.L. (2009). The ferroportin metal efflux proteins function in iron and cobalt homeostasis in Arabidopsis. *The Plant Cell* 21(10): 3326-3338.

Mounzer O, Pedrero-Salcedo F, Nortes PA, Bayona JM, Nicolás-Nicolás E, Alarcón JJ. (2013). Transient soil salinity under the combined effect of reclaimed water and regulated deficit drip irrigation of Mandarin trees. *Agricultural water management* 31(120): 23-29.

Muller BJ, Hocking M. (2002). Salinity change in the west Wimmera. In; Centre for Land Protection Research, Department of Natural Resources & Environment, Cnr Midland Highway and Taylor St, Epsom. Vic. 3551.

Müller NA, Wijnen CL, Srinivasan A, Ryngajllo M, Ofner I, Lin T, Ranjan A, West D, Maloof JN, Sinha NR, Huang S. (2016). Domestication selected for deceleration of the circadian clock in cultivated tomato. *Nature genetics* 48(1): 89.

Munns R, Gilliham M. (2015). Salinity tolerance of crops - what is the cost? *New Phytologist* 208(3): 668-673.

Munns R, Tester M. (2008). Mechanisms of salinity tolerance. *Annual Review of Plant Biology* 59: 651-81.

Munns R. (2002). Comparative physiology of salt and water stress*. Plant, Cell and Environment* 25: 239–50.

Murali KS, Sukumar R. (1993). Leaf flushing phenology and herbivory in a tropical dry deciduous forest, southern India. *Oecologia* 94(1): 114-119.

Naidoo G, Somaru R, Achar P. (2008). Morphological and physiological responses of the halophyte, *Odyssea paucinervis* (Staph) (Poaceae), to salinity. *Flora* 203(5): 437-447.

Nath S. (2012). Explore these 3 deserts of India. World Nomads. Australia.

Nazir F, Hussain A, Fariduddin Q. (2019). Interactive role of epibrassinolide and hydrogen peroxide in regulating stomatal physiology, root morphology, photosynthetic and growth traits in *Solanum lycopersicum* L. under nickel stress*. Environmental and Experimental Botany* 162: 479-495.

Nedjimi B, Daoud Y. (2009). Cadmium accumulation in *Atriplex halimus* subsp. schweinfurthii and its influence on growth, proline, root hydraulic conductivity and nutrient uptake. *Flora - Morphology, Distribution, Functional Ecology of Plants* 204(4): 316-324.

Nevo E. (2011). Evolution under environmental stress at macro- and microscales. *Genome Biology and Evolution* 3: 1039-1052.

Newete SW, Mayonde S, Byrne MJ. (2019). Distribution and abundance of invasive *Tamarix* genotypes in South Africa. *Weed Research*. doi.org/10.1111/wre.12356

Niinemets Ü, Kull O. (2011). Sensitivity of photosynthetic electron transport to photoinhibition in a temperate deciduous forest canopy: Photosystem II center openness, non-radiative energy dissipation and excess irradiance under field conditions. *Tree Physiology* 21(12-13): 899-891.

Nimmo HG. (2000). The regulation of phosphoenolpyruvate carboxylase in CAM plants. *Trends in Plants Science* 5(2): 75-80.

Nisbet RE, Fisher R, Nimmo RH, Bendall DS, Crill PM, Gallego-Sala AV, Hornibrook ER, Lopez-Juez E, Lowry D, Nisbet PB, Shuckburgh EF. (2009). Emission of methane from plants. *Proceedings of the Royal Society B: Biological Sciences* 276: 1347-54.

Nishida I, Murata N. (1996). Chilling sensitivity in plants and cyanobacteria: the crucial contribution of membrane lipids. *Annual Review of Plant Biology* 47: 541-68.

Nitschke S, Cortleven A, Iven T, Feussner I, Havaux M, Riefler M, Schmülling T. (2016). Circadian stress regimes affect the circadian clock and cause jasmonic acid-dependent cell death in cytokinin-deficient Arabidopsis plants. *The Plant Cell* 28(7): 1616-1639

Nongpiur R, Singla-Pareek SL, Pareek A. (2016). Genomics approaches for improving salinity stress tolerance in crop plants. *Current Genomics* 17: 343-357.

Nongpiur R, Singla-Pareek SL, Pareek A. (2019). The quest for 'osmosensors' in plants. *Journal of Experimental Botany* erz263

Norman HC, Masters DG, Barrett-Lennard EG. (2013). Halophytes as forages in saline landscapes: Interactions between plant genotype and environment change their feeding value to ruminants. *Environmental and Experimental Botany* 92: 96-109.

Novitskaya GV, Suvorova TA, Trunova TI. (2000). Lipid composition of tomato leaves as related to plant cold tolerance. *Russian Journal of Plant Physiology* 47: 728-733.

Nsanganwimana F, Pourrut B, Mench M, Douay F. (2014). Suitability of Miscanthus species for managing inorganic and organic contaminated land and restoring ecosystem services. A review. *Journal of Environmental Management* 143: 123-134.

Nublat A, Desplans J, Casse F, Berthomieu P. (2001). SAS1, an Arabidopsis mutant over accumulating sodium in the shoot, shows deficiency in the control of the root radial transport of sodium. *The Plant Cell* 13: 125-137.

Nuccio ML, Rhodes D, McNeil SD, Hanson AD. (1999) Metabolic engineering of plants for osmotic stress resistance. *Current opinion in plant biology* 2(2): 128-134.

Nyffeler R, Eggli U, Ogburn M, Edwards E. (2008). Variations on a theme: Repeated evolution if succulent life forms in the *Portulacineae* (Caryophyllales). *Haseltonia* 14: 26-36.

Obata T, Witt S, Lisec J, Palacios-Rojas N, Florez-Sarasa I, Yousfi S, Araus JL, Cairns JE, Fernie AR. (2015). Metabolite profiles of maize leaves in drought, heat, and combined stress field trials reveal the relationship between metabolism and grain yield. *Plant Physiology* 169: 2665-2683.

Ogawa D, Yamamoto E, Ohtani T, Kanno N, Tsunematsu H, Nonoue Y, Yonemaru JI. (2018). Haplotype-based allele mining in the Japan-MAGIC rice population. *Scientific reports* 8(1): 4379.

Oh DH, Dassanayake M, Bohnert HJ, Cheeseman JM. (2012). Life at the extreme: lessons from the genome. *Genome Biology* 13(241): 1-9.

Oh DH, Dassanayake M, Haas JS, Kropornika A, Wright C, d'Urzo MP, Hong H, Ali S, Hernandez A, Lambert GM, **Inan G**. (2010). Genome structures and halophyte-specific gene expression of the extremophile *Thellungiella parvula* in comparison with *Thellungiella salsuginea* (*Thellungiella halophila*) and Arabidopsis. *Plant Physiology* 154(3): 1040-1052.

Ohta M, Hayashi Y, Nakashima A, Hamada A, Tanaka A, Nakamura T, Hayakawa T. (2002). Introduction of a Na+/H+ antiporter gene from *Atriplex gmelini* confers salt tolerance to rice. *FEBS Letters* 532: 279-282.

Ong SE, Blagoev B, Kratchmarova I, Kristensen DB, Steen H, Pandey A, Mann M. (2002) Stable isotope labeling by amino acids in cell culture, SILAC, as a simple and accurate approach to expression proteomics. *Molecular & cellular proteomics* 1(5): 376-386.

Onoda Y, Richards L, Westoby M. (2012). The importance of leaf cuticle for carbon economy and mechanical strength. *New Phytologist* 196(2): 441-447.

Orgogozo V, Broman KW, Stern DL. (2006). High-resolution quantitative trait locus mapping reveals sign epistasis controlling ovariole number between two Drosophila species. *Genetics* 173(1): 197-205.

Ouellette JD, Johnson JT, Balenzano A, Mattia F, Satalino G, Kim SB, Dunbar RS, Colliander A, Cosh MH, Caldwell TG, Walker JP. (2017). A time-series approach to estimating soil moisture from vegetated surfaces using L-band radar backscatter. *IEEE Transactions on Geoscience and Remote Sensing* 55(6): 3186-3193.

Oueslati S, Ksouri R, Falleh H, Pichette A, Abdelly C, Legault J. (2012). Phenolic content, antioxidant, anti-inflammatory and anticancer activities of the edible halophyte *Suaeda fruticosa* Forssk. *Food Chemistry* 132(2): 943-947.

Oueslati S, Ksouri R, Falleh H, Pichette A, Abdelly C, Legault J. (2012). Phenolic content, antioxidant, anti-inflammatory and anticancer activities of the edible halophyte *Suaeda fruticosa* Forssk. *Food Chemistry* 132(2): 943-947.

Outlaw WH, Tarczynski MC, Miller WI. (1984). Histological compartmentation of phosphate in Vicia faba L. Leaflet: Possible significance to stomatal functioning. Plant Physiology 74(2): 430-433.

Ozheredova IP, Parnikoza IY, Poronnik OO, Kozeretska IA, Demidov SV, Kunakh VA. (2015). Mechanisms of Antarctic vascular plant adaptation to abiotic environmental factors. *Cytology and Genetics* 49(2): 139-145.

Palanivelu R, Brass L, Edlund AF, Preuss D. (2003). Pollen tube growth and guidance is regulated by POP2, an Arabidopsis gene that controls GABA levels. *Cell* 114: 47-59.

Palsson B, Zengler K. (2010). The challenges of integrating multi-omic data sets. *Nature chemical biology* 6: 787-789.

Pan WJ, Wang X, Deng YR, Li JH, Chen W, Chiang JY, Yang JB, Zheng L. (2015). Nondestructive and intuitive determination of circadian chlorophyll rhythms in soybean leaves using multispectral imaging. *Scientific reports* 5: 11108.

Pandey SP, Somssich IE. (2009). The role of WRKY transcription factors in plant immunity. *Plant Physiology* 150(4): 1648-1655.

Pang Q, Chen S, Dai S, Chen Y, Wang Y, Yan X. (2010). Comparative proteomics of salt tolerance in Arabidopsis thaliana and *Thellungiella halophi*. *Journal of Proteome Research* 9: 2584–2599.

Papageorgiou GC. (2011). Photosystem II fluorescence: slow changes–scaling from the past. *Journal of Photochemistry and Photobiology B: Biology* 104(1-2): 258-270.

Pardo-Domènech LL, Tifrea A, Grigore MN, Boscaiu M, Vicente O. (2015). Proline and glycine betaine accumulation in two succulent halophytes under natural and experimental conditions. *Plant Biosystems - An International Journal Dealing with all Aspects of Plant Biology* 150(5): 904-915.

Pareek A, Sopory SK, Bohnert HJ. (2010). Abiotic stress adaptation in plants. Springer.

Parihar P, Singh S, Singh R, Singh VP, Prasad SM. (2015). Effect of salinity stress on plants and its tolerance strategies: a review. *Environmental Science and Pollution Research* 22(6): 4056-4075.

Park EJ, Jeknic Z, Pino MT, Murata N, Chen TH. (2007). Glycinebetaine accumulation is more effective in chloroplasts than in the cytosol for protecting transgenic tomato plants against abiotic stress. *Plant Cell and Environment* 30(8): 994-1005.

Parraga-Aguado I, Gonzalez-Alcaraz MN, Alvarez-Rogel J, Jimenez-Carceles FJ, Conesa HM. (2013). The importance of edaphic niches and pioneer plant species succession for the phytomanagement of mine tailings. *Environmental pollution* 176: 134-143.

Patakas A, (2012). Abiotic stress-induced morphological and anatomical changes in plants. In: P. A, M. P, eds. Abiotic Stress Responses in Plants. New York, NY: Springer, 21-39.

Patel MK, Pandey S, Brahmbhatt HR, Mishra A, Jha B. (2019). Lipid content and fatty acid profile of selected halophytic plants reveal a promising source of renewable energy. *Biomass and Bioenergy* 124: 25-32.

Patti GJ, Yanes O, Siuzdak G. (2012). Innovation: Metabolomics: the apogee of the omics trilogy. *Nature Reviews Molecular Cell Biology* 13: 263–269.

Pei G, Chen L, Zhang W. (2017). WGCNA application to proteomic and metabolomic data analysis. *Methods in enzymology* 585: 135-158.

Peleg Z, Blumwald E. (2011). Hormone balance and abiotic stress tolerance in crop plants. *Current opinion in plant biology* 14(3): 290-295.

Peng L, Yi Y, Fu-li G, Ze-qu L. (1997). A preliminary study on the introduction of *Descurainia sophia*, an oil plant species for industrial uses. *Acta Botanica Sinica* 39(5): 447-479.

Peter AJ, Shanower TG. (1998). Plant glandular trichomes chemical factories with many potential uses. *Resonance* 3(3): 41-45.

Peterson A, Murphy K. (2015). Tolerance of lowland quinoa cultivars to sodium chloride and sodium sulfate salinity. *Crop Science* 55(1): 331-338.

Phadtare S, Alsina J, Inouye M. (1999). Cold-shock response and cold-shock proteins. *Current opinion in microbiology* 2(2): 175-180.

Pinyopich A, Ditta GS, Savidge B, Liljegren SJ, Baumann E, Wisman E, Yanofsky MF. (2003). Assessing the redundancy of MADS-box genes during carpel and ovule development. *Nature* 424(6944): 85.

Piunti A, Shilatifard A. (2016). Epigenetic balance of gene expression by Polycomb and COMPASS families. *Science* 352: aad9780.

Prasad VK, Badarinath KVS, Eaturu A. (2008). Effects of precipitation, temperature and topographic parameters on evergreen vegetation greenery in the Western Ghats, India. *International Journal of Climatology* 28(13): 1807-1819.

Priyashree S, Jha S, Pattanayak SP. (2010). A review on Cressa cretica Linn.: A halophytic plant. Pharmacognosy Review 4(8): 161–166.

Purnobasuki H, Siuzuki M. (2005). Functional anatomy of air conducting network on the Pneumatophores of a Mangrove plant, *Avicennia marima* (Forsk.) Vierh. *Asian Journal of Plant Sciences* 4(4): 334-347.

Purty RS, Kumar G, Singla-Pareek SL, Pareek A. (2008). Towards salinity tolerance in Brassica: an overview. *Physiology and Molecular Biology of Plants* 14(1&2): 39-49.

Qadir M, Quillérou E, Nangia V, Murtaza G, Singh M, Thomas RJ, Drechsel P, Noble AD. (2014). Economics of salt-induced land degradation and restoration. *Natural Resources Forum* 38(4): 282-295.

Qi X, Xu W, Zhang J, Guo R, Zhao M, Hu L, Wang H, Dong H, Li Y. (2017). Physiological characteristics and metabolomics of transgenic wheat containing the maize C4 phosphoenolpyruvate carboxylase (PEPC) gene under high temperature stress. *Protoplasma* 254: 1017-1030.

Qin Y, Druzhinina IS, Pan X, Yuan Z. (2016). Microbially mediated plant salt tolerance and microbiome-based solutions for saline agriculture. *Biotechnology Advances* 34(7): 1245-1259.

R Development Core Team. (2010). R: A Language and Environment for Statistical Computing. Vienna, Austria: R Foundation for Statistical Computing. 11: Accessed from http://www.r-project.org/verified 10/5/

Raiten DJ, Combs GF. (2019). Nutritional ecology: Understanding the intersection of climate/environmental change, food systems and health. *Agriculture for Improved Nutrition: Seizing the Momentum* 28:68.

Ramakrishna A, Ravishankar GA. (2011). Influence of abiotic stress signals on secondary metabolites in plants. *Plant Signalling and Behaviour* 6(11): 1720-1731.

Ramesh R, Jani RA, Bhushan R. (1993). Stable isotopic evidence for the origin of salt lakes in the Thar desert. *Journal of Arid Environments* 25(1): 117-123.

Ramesh SA, Tyerman SD, Xu B, Bose J, Kaur S, Conn V, Domingos P, Ullah S, Wege S, Shabala S, Feijó JA. (2015). GABA signalling modulates plant growth by directly regulating the activity of plant-specific anion transporters. *Nature Communications* 6: 7879.

Rathore LS, Attri SD, Jaswal AK. (2013). State level climate change trends in India.In Department IM. New Delhi: India Meteorological Department, Lodi Road. 147.

Rausch C, Bucher M. (2002). Molecular mechanisms of phosphate transport in plants. *Planta* 216(1): 23-37.

Ravindran KC, Venkatesan K, Balakrishnan V, Chellappan KP, Balasubramanian T. (2007). Restoration of saline land by halophytes for Indian soils. *Soil Biology and Biochemistry* 39(10): 2661-2664.

Redondo-Gomez S, Mateos-Naranjo E, Cambrolle J, Luque T, Figueroa ME, Davy AJ. (2008). Carry-over of differential salt tolerance in plants grown from dimorphic seeds of *Suaeda splendens*. *Annals of Botany* 102(1): 103-112.

Reeves RD, Baker AJ. (2000). Metal-accumulating plants. In 'Phytoremediation of toxic metals: using plants to clean up the environment'. (Eds I Raskin, BD Ensley) 193–229.

Reginato MA, Castagna A, Furlan A, Castro S, Ranieri A, Luna V. (2014). Physiological responses of a halophytic shrub to salt stress by Na_2SO_4 and NaCl: oxidative damage and the role of polyphenols in antioxidant protection. *AoB Plants* 6.

Reid RW, Luo Y, Yan S, Miller TE, Song BH. (2016). Transcriptome dataset of halophyte Beach Morning Glory, a close wild relative of sweet potato. *Frontiers in Plant Science* 7: 1267.

Rejeb IB, Pastor V, Mauch-Mani B. (2014). Plant responses to simultaneous biotic and abiotic stress: Molecular mechanisms. *Plants* 3(4): 458-475.

Ricciardi A, Palmer ME, Yan ND. (2011). Should biological invasions be managed as natural disasters? *BioScience* 61(4): 312-317.

Richards PW. 1952. The tropical rain forest; an ecological study. U. K.: The University Press; Cambridge.

Ricklefs RE. 1977. Environmental heterogeneity and plant species diversity: A hypothesis. *The American Naturalist* 111(978): 376–381.

Rivas-Ubach A, Sardans J, Perez-Trujillo M, Estiarte M, Penuelas J, (2012). Strong relationship between elemental stoichiometry and metabolome in plants. *Proceedings of the National Academy of Sciences* 109: 4181-6.

Rizhsky L, Liang H, Shuman J, Shulaev V, Davletova S, Mittler R. (2004). When defense pathways collide. The response of Arabidopsis to a combination of drought and heat stress. *Plant Physiology and Biochemistry* 134: 1683–1696.

Roach T, Miller R, Aigner S, Kranner I. (2015). Diurnal changes in the xanthophyll cycle pigments of freshwater algae correlate with the environmental hydrogen peroxide concentration rather than non-photochemical quenching. *Annals of Botany* 116(4): 519-527.

Rodrıguez Fl, Esch JJ, Hall A., Binder BM, Schaller GE, Bleecker AB. (1999). A copper cofactor for the ethylene receptor ETR1 from Arabidopsis. *Science* 283(5404): 996-998.

Rodriguez PA, Rothballer M, Chowdhury SP, Nussbaumer T, Gutjahr C, Falter-Braun P. (2019). Systems biology of plant microbiome interactions. *Molecular plant* 22.

Romero-Aranda MR, Jurado O, Cuartero, J. (2006). Silicon alleviates the deleterious salt effect on tomato plant growth by improving plant water status. *Journal of plant physiology* 163(8): 847-855.

Roose T, Fowler AC. (2004). A mathematical model for water and nutrient uptake by plant root systems. *Journal of theoretical biology* 228(2): 173-184.

Rorat T. (2006). Plant dehydrins—tissue location, structure and function. *Cellular & molecular biology letters* 11(4): 536.

Rosa M, Prado C, Podazza G, Interdonato R, González JA, Hilal M, Prado FE. (2009). Soluble sugars—Metabolism, sensing and abiotic stress. *Plant Signaling & Behavior* 4(5): 388-393.

Rosebrock TR, Zeng L, Brady JJ, Abramovitch RB, Xiao F, Martin GB. (2007). A bacterial E3 ubiquitin ligase targets a host protein kinase to disrupt plant immunity. *Nature* 448(7151): 370.

Roxas VP, Smith RK, Allen ER, Allen RD. (1997). Overexpression of glutathione S-transferase/glutathioneperoxidase enhances the growth of transgenic tobacco seedlings during stress. *Nature biotechnology* 15(10): 988.

Roy AB. (1999). Evolution of saline lakes in Rajasthan. *Current Science* 76(3): 290-295.

Rozema J, Schat H. (2013). Salt tolerance of halophytes, research questions reviewed in the perspective of saline agriculture. *Environmental and Experimental Botany* 92: 83-95.

Rus A, Baxter I, Muthukumar B, Gustin J, Lahner B, Yakubova E, Salt DE. (2006). Natural variants of AtHKT1 enhance Na^+ accumulation in two wild populations of Arabidopsis. *PLoS genetics* 2(12): e210.

Saad RB, Fabre D, Mieulet D, Meynard D, Dingkuhn M, Al-Doss A, Guiderdoni E, Hassairi A. (2012). Expression of the *Aeluropus littoralis* AlSAP gene in rice confers broad tolerance to abiotic stresses through maintenance of photosynthesis. *Plant Cell and Environment* 35: 626-643.

Saad RB, Zouari N, Ramdhan WB, Azaza J, Meynard D, Guiderdoni E, Hassairi A. (2010). Improved drought and salt stress tolerance in transgenic tobacco overexpressing a novel A20/AN1 zinc-finger ‘‘AlSAP’’ gene isolated from the halophyte grass *Aeluropus littoralis*. *Plant Molecular Biology* 72: 171-190.

Sabovljević M, Sabovljević A. (2007). Contribution to the coastal bryophytes of the Northern Mediterranean: Are there halophytes among bryophytes? *Phytologia Balcanica* 13(2): 131-135.

Saeed AI, Bhagabati NK, Braisted JC, Liang W, Sharov V, Howe EA, Li J, Thiagarajan M, White JA, Quackenbush J. (2006). [9] TM4 microarray software suite. *Methods in Enzymology* 411: 134-193.

Saiki ST, Ishida A, Yoshimura K, Yazaki K, (2017). Physiological mechanisms of drought-induced tree die-off in relation to carbon, hydraulic and respiratory stress in a drought-tolerant woody plant. *Scientific Report* 7: 2995.

Sakho I, Mesnage V, Copard Y, Deloffre J, Faye G, Lafite R, Niang I. (2015). A cross-section analysis of sedimentary organic matter in a mangrove ecosystem under dry climate conditions: The Somone estuary, Senegal. *Journal of African Earth Sciences* 101: 220-231.

Salehi A, Tasdighi H, Gholamhoseini M. (2016). Evaluation of proline, chlorophyll, soluble sugar content and uptake of nutrients in the German chamomile (*Matricaria chamomilla* L.) under drought stress and organic fertilizer treatments. *Asian Pacific journal of tropical biomedicine* 6(10): 886-891.

Salt DE, Baxter I, Lahner B. (2008). Ionomics and the study of the plant ionome. *Annual Review of Plant Biology* 59: 709-733.

Sánchez-Blanco MJ, Morales MA, Torrecillas A, Alarcón JJ. (1998). Diurnal and seasonal osmotic potential changes in *Lotus creticus* plants grown under saline stress. *Plant science* 136(1): 1-10.

Sanders D, Pelloux J, Brownlee C, Harper JF. (2002). Calcium at the crossroads of signaling. *The Plant Cell* 14: S401-S417.

Sandilyan S, Kathiresan K. (2014). Decline of mangroves – A threat of heavy metal poisoning in Asia. *Ocean & Coastal Management* 102: 161-168.

Satake T, Yoshida S. 1978. High temperature-induced sterility in indica rices at flowering*. Japanese Journal of Crop Science* 47(1): 6-17.

Schachtman DP, Reid RJ, Ayling SM. (1998). Phosphorus uptake by plants: from soil to cell. *Plant physiology* 116(2): 447-453.

Schreiber U, Schliwa UWB. (1986). Continuous recording of photochemical and non-photochemical chlorophyll fluorescence quenching with a new type of modulation fluorometer. *Photosynthesis research* 10(1-2): 51-62.

Schuback N, Flecken M, Maldonado MT, Tortell PD. (2016). Diurnal variation in the coupling of photosynthetic electron transport and carbon fixation in iron-limited phytoplankton in the NE subarctic Pacific. *Biogeosciences* 13(4): 1019-1035.

Scognamiglio M, D'abrosca B, Fiumano V, Golino M, Esposito A, Fiorentino A, (2014). Seasonal phytochemical changes in *Phillyrea angustifolia* L.: Metabolomic analysis and phytotoxicity assessment. *Phytochemistry Letters* 8: 163-170.

Sengupta S, Majumder AL. (2009). Insight into the salt tolerance factors of a wild halophytic rice, *Porteresia coarctata*: a physiological and proteomic approach. *Planta* 229: 911–929.

Seo HS, Song JT, Cheong JJ, Lee YH, Lee YW, Hwang I, Lee JS, Do-Choi, Y. (2001). Jasmonic acid carboxyl methyltransferase: a key enzyme for jasmonate-regulated plant responses. *Proceedings of the National Academy of Sciences* 98(8): 4788-4793.

Serba DD, Daverdin G, Bouton JH, Devos KM, Brummer EC, Saha MC. (2015). Quantitative Trait Loci (QTL) underlying biomass yield and plant height in switchgrass. *Bioenergy Research* 8: 307-324.

Shaar-Moshe L, Blumwald E, Peleg Z. (2017) Unique physiological and transcriptional shifts under combinations of salinity, drought, and heat. *Plant physiology* 174(1): 421-434.

Shadforth IP, Dunkley TP, Lilley KS, Bessant C. (2005). i-Tracker: For quantitative proteomics using iTRAQ™. *BMC genomics* 6(1): 145.

Shahi M, Saaghari M, Esfahan EZ, Jaimand K. (2013). Investigation on potential of Suaeda fruticosa as a source of edible oil. *Journal of Biodiversity and Environmental Sciences* 3(12): 2222-3045

Shahid SA, Zaman M, Heng L. (2018). Soil Salinity: Historical Perspectives and a World Overview of the Problem. In Guideline for Salinity Assessment, Mitigation and Adaptation Using Nuclear and Related Techniques. Springer, Cham. 43-53.

Sharma DK, Anshuman S. (2015). Salinity research in India achievements, challenges and future Prospects. In; W & E (Water Resource Section). ICAR-Central Soil Salinity Research Institute, Karnal, Haryana.

Sharma P, Jha AB, Dubey RS, Pessarakli M. (2012). Reactive oxygen species, oxidative damage, and antioxidative defense mechanism in plants under stressful conditions. *Journal of Botany* (2012): 1-26.

Sharma PK, Hall DO. (1991). Interaction of salt stress and photoinhibition on photosynthesis in Barley and Sorghum. *Journal of Plant Physiology* 138(5): 614-619.

Sharma R, Wungrampha S, Singh V, Pareek A, Sharma MK. (2016). Halophytes as bioenergy crops. *Frontiers in Plant Science* 7: 1372.

Shcolnick S, Keren N. (2006). Metal homeostasis in cyanobacteria and chloroplasts. Balancing benefits and risks to the photosynthetic apparatus. *Plant physiology* 141(3): 805-810.

Shen YG, Zhang WK, Yan DQ, Du BX, Zhang JS, Che NSY. (2002). Overexpression of proline transporter gene isolated from halophyte confers salt tolerance in Arabidopsis. *Acta Botanica Sinica* 44(8): 956－962.

Shen YG, Zhang WK, Yan DQ, Du BX, Zhang JS, Liu Q, Chen SY. (2003). Characterization of a DRE-binding transcription factor from a halophyte *Atriplex hortensis*. *Theoretical and Applied Genetics* 107: 155-161.

Shevchenko A, Jensen ON, Podtelejnikov AV, Sagliocco F, Wilm M, Vorm O, Mortensen P, Shevchenko A, Boucherie H, Mann M. (1996) Linking genome and proteome by mass spectrometry: large-scale identification of yeast proteins from two dimensional gels. *Proceedings of the National Academy of Sciences* 93(25):14440-14445.

Shevchenko A, Tomas H, Havli J, Olsen JV, Mann M. (2006). In-gel digestion for mass spectrometric characterization of proteins and proteomes. *Nature protocols* 1(6): 2856.

Shevyakova NI, Netronina IA, Aronova EE, Kuznetsov VV. (2003). Compartmentation of cadmium and iron in *Mesembryanthemum crystallinum* plants during the adaptation to cadmium stress. *Russian Journal of Plant Physiology* 50(5): 678-685.

Shillinger K, Globe B. (2001). Saltwater farm irrigates desert on Eritrea coast seeds, oil, seafood expected as harvest. SFGATE. San Francisco.

Singh A, Kushwaha HR, Soni P, Gupta H, Singla-Pareek SL, Pareek A. (2015). Tissue specific and abiotic stress regulated transcription of histidine kinases in plants is also influenced by diurnal rhythm. *Frontiers in Plant Science* 6: 711.

Singh A, Kushwaha HR, Soni P, Gupta H, Singla-Pareek SL, Pareek A. (2015). Tissue specific and abiotic stress regulated transcription of histidine kinases in plants is also influenced by diurnal rhythm. *Frontiers in plant science* 6: 711.

Singh G, Rathod TR. (2002). Plant growth, biomass production and soil water dynamics in a shifting dune of Indian desert. *Forest Ecology and Management* 171(3): 309-320.

Singh JS, Singh SP. (1987). Forest vegetation of the Himalaya. The Botanical Review 53(1): 80-192.

Singh N, Mishra A, Jha B. (2014a). Ectopic over-expression of peroxisomal ascorbate peroxidase (SbpAPX) gene confers salt stress tolerance in transgenic peanut (*Arachis hypogaea*). *Gene* 547(1): 119-125.

Singh N, Mishra A, Jha B. (2014b). Over-expression of the Peroxisomal Ascorbate Peroxidase (SbpAPX) gene cloned from halophyte *Salicornia brachiata* confers salt and drought stress tolerance in transgenic tobacco. *Marine Biotechnology* 16: 321-332.

Singh RL. (1971). India; a regional geography. Varanasi, India: National Geographical Society of India.

Singh S, Parihar P, Singh R, Singh VP, Prasad SM. (2016). Heavy metal tolerance in plants: role of transcriptomics, proteomics, metabolomics, and ionomics. *Frontiers in plant science* 6: 1143.

Sinha R, Raymahashay BC. (2004). Evaporite mineralogy and geochemical evolution of the Sambhar Salt Lake, Rajasthan, India. *Sedimentary Geology* 166(1-2): 59-71.

Smaoui A, Barhoumi Z, Rabhi M, Abdelly C. (2011). Localization of potential ion transport pathways in vesicular trichome cells of *Atriplex halimus* L. *Protoplasma* 248(2): 363-372.

Sobhanian H, Motamed N, Jazii FR, Nakamura T, Komatsu K. (2010). Salt stress induced differential proteome and metabolome response in the shoots of *Aeluropus lagopoides* (Poaceae), a Halophyte C4 plant. *Journal of Proteomics Research* 9: 2882-2897.

Soda N, Gupta BK, Anwar K, Sharan A, Govindjee., Singla-Pareek SL, Pareek A. (2018). Rice intermediate filament, OsIF, stabilizes photosynthetic machinery and yield under salinity and heat stress. *Scientific Report* 8(1): 4072.

Soda N, Sharan A, Gupta BK, Singla-Pareek SL, Pareek A. (2016). Evidence for nuclear interaction of a cytoskeleton protein (OsIFL) with metallothionein and its role in salinity stress tolerance. *Scientific Report* 6: 34762.

Stein A, Gerstner K, Kreft H. (2014). Environmental heterogeneity as a universal driver of species richness across taxa, biomes and spatial scales. *Ecology letters* 17(7): 866-880.

Stein A, Kreft H. (2015). Terminology and quantification of environmental heterogeneity in species-richness research. *Biological Reviews* 90(3): 815-836.

Steindal AL, Rødven R, Hansen E, Mølmann J. (2015) Effects of photoperiod, growth temperature and cold acclimatisation on glucosinolates, sugars and fatty acids in kale. *Food chemistry* 1(174) :44-51.

Stepien P, Johnson GN. (2009). Contrasting responses of photosynthesis to salt stress in the glycophyte Arabidopsis and the halophyte *Thellungiella*: role of the plastid terminal oxidase as an alternative electron sink. *Plant Physiology* 149(2): 1154-1165.

Steward GR, Lee JA. 1974. The role of proline accumulation in halophytes. *Planta* 120(3): 279-289.

Steward GR, Rhodes D. 1978. Niteogen metabolism of Halophytes. III. Enzymes of ammonia assimilation. *New Phytologist* 80: 307-316.

Stirbet A, Riznichenko GY, Rubin AB. (2014). Modeling chlorophyll a fluorescence transient: relation to photosynthesis. *Biochemistry* (Moscow) 79(4): 291-323.

Stirbet A. (2011). On the relation between the Kautsky effect (chlorophyll a fluorescence induction) and photosystem II: basics and applications of the OJIP fluorescence transient. *Journal of Photochemistry and Photobiology B: Biology* 104(1-2): 236-257.

Stirbet A. (2012). Chlorophyll a fluorescence induction: a personal perspective of the thermal phase, the J–I–P rise. *Photosynthesis research* 113(1-3): 15-61.

Stoop JM, Williamson JD, Pharr DM. (1996). Mannitol metabolism in plants: a method for coping with stress. *Trends in Plant Science* 1: 139-44.

Strasser RJ, Srivastava A, Govindjee. (1995). Polyphasic chlorophyll a fluorescence transient in plants and cyanobacteria. *Photochemistry and photobiology* 61(1): 32-42.

Strasser RJ, Srivastava A, Tsimilli-Michael M. (2000). The fluorescence transient as a tool to characterize and screen photosynthetic samples. *Probing photosynthesis: mechanisms, regulation and adaptation*: 445-483.

Strasser RJ, Tsimilli-Michael M, Srivastava A. (2004). Analysis of the chlorophyll a fluorescence transient. In: Papageorgiou GCG ed. Chlorophyll a fluorescence. Springer, Dordrecht.

Strasser RJ. (1999). "The Fo and the OJIP fluorescence rise in higher plants and algae." Regulation of Chloroplast Biogenesis. Springer, Boston, MA, 423-426.

Suji KK, Biji KR, Poornima R, Prince KS, Amudha K, Kavitha S, Mankar S, Babu RC. (2012). Mapping QTLs for plant phenology and production traits using indica rice (*Oryza sativa* L.) lines adapted to rainfed environment. *Molecular Biotechnology* 52(2): 151-160.

Sultana S, Khew CY, Morshed MM, Namasivayam P, Napis S, Ho CL. (2012). Overexpression of monodehydroascorbate reductase from a mangrove plant (AeMDHAR) confers salt tolerance on rice. *Journal of Plant Physiology* 169(3): 311-318.

Sun W, Van MM, Verbruggen N. (2002). Small heat shock proteins and stress tolerance in plants. *Biochimica et Biophysica Acta (BBA)-Gene Structure and Expressio*n 1577(1): 1-9.

Suzuki N, Rivero RM, Shulaev V, Blumwald E, Mittler R. (2014). Abiotic and biotic stress combinations. *New Phytologist* 203: 32-43.

Swain A, Kutzbach JE, Hastenrath S. (1983). Estimates of holocene precipitation for Rajasthan, India, based on pollen and lake-level data. *Quaternary Research* 19(1): 1-17.

Sze H, Chanroj S. (2018). pH and Ion Homeostasis on Plant Endomembrane Dynamics: Insights from structural models and mutants of K+/H+ antiporters. *Plant Physiology* 142. doi:10.1104/pp.18.00142

Tada Y, Kashimura T. (2009). Proteomic analysis of salt-responsive proteins in the mangrove plant, *Bruguiera gymnorhiza*. *Plant and Cell Physiology* 50(3): 439-446.

Taji T, Sakurai T, Mochida K, Ishiwata A, Kurotani A, Totoki Y, Toyoda A, Sakaki Y, Seki M, Ono H, Sakata Y. (2008). Large-scale collection and annotation of full-length enriched cDNAs from a model halophyte, *Thellungiella halophila*. *BMC Plant Biology* 8: 115.

Tan WK, Lin Q, Lim TM, Kumar P, Loh CS. (2013). Dynamic secretion changes in the salt glands of the mangrove tree species *Avicennia officinalis* in response to a changing saline environment. *Plant Cell and Environment* 36(8): 1410-1422.

Tanaka K, Takio S, Satoh T. (1995). Inactivation of the cytosolic Cu/Zn-superoxide dismutase induced by copper deficiency in suspension-cultured cells of *Marchantia paleacea* var. diptera. *Journal of Plant Physiology* 146(3): 361-365.

Tang R, Li C, Xu K, Du Y, Xia T. (2009). Isolation, functional characterization, and expression pattern of a vacuolar Na+/H+ antiporter gene TrNHX1 from *Trifolium repens* L. *Plant Molecular Biology Reporter* 28(1): 102-111.

Theodorou ME, Plaxton WC. (1993) Metabolic adaptations of plant respiration to nutritional phosphate deprivation. *Plant Physiology* 101:339–344.

Thieringer HA, Jones PG, Inouye, M. (1998). Cold shock and adaptation. *Bioessays* 20(1): 49-57.

Thomson WW, Berry WL, Liu LL. (1969). Localization and secretion of salt by the salt glands of *Tamarix aphylla*. *Botany* 63: 310-317.

Tian H, Baxter IR, Lahner B, Reinders A, Salt DE, Ward JM. (2010). Arabidopsis NPCC6/NaKR1 is a phloem mobile metal binding protein necessary for phloem function and root meristem maintenance. *The Plant Cell* 22(12): 3963-3979.

Tindall JA, Mills HA, Radcliffe DE. (1990). The effect of root zone temperature on nutrient uptake of tomato. *Journal of Plant Nutrition* 13(8): 939-956.

Tiwari V, Chaturvedi AK, Mishra A, Jha B. (2014). The transcriptional regulatory mechanism of the peroxisomal ascorbate peroxidase (pAPX) gene cloned from an extreme halophyte, *Salicornia brachiata*. *Plant and Cell Physiology* 55(1): 201-217.

Tiwari V, Chaturvedi AK, Mishra A, Jha B. (2015). Introgression of the SbASR-1 gene cloned from a halophyte Salicornia brachiate enhances salinity and drought endurance in transgenic groundnut (*Arachis hypogaea*) and acts as a transcription factor. *PLoS One* 10(7): e0131567.

Tordoff GM, Baker AJM, Willis AJ. (2000). Current approaches to the revegetation and reclamation of metalliferous mine wastes. *Chemosphere* 41(1-2): 219-228.

Tounekti T, Mahdhi M, Al-Turki TA, Khemira H. (2018). Physiological Responses of the Halophyte *Salvadora persica* to the Combined Effect of Salinity and Flooding. *International Journal of Agriculture and Biology* 20(10): 2211-2220.

Towhidi A, Saberifar T, Dirandeh E. (2011). Nutritive value of some herbage for dromedary camels in the central arid zone of Iran. *Tropical animal health and production* 43: 617-622.

Tran LSP, Urao T, Qin F, Maruyama K, Kakimoto T, Shinozaki K, Yamaguchi-Shinozaki K. (2007). Functional analysis of AHK1/ATHK1 and cytokinin receptor histidine kinases in response to abscisic acid, drought, and salt stress in Arabidopsis. *Proceedings of the National Academy of Sciences* 104(51): 20623-20628.

Tränkner M, Tavakol E, Jákli B. (2018). Functioning of potassium and magnesium in photosynthesis, photosynthate translocation and photoprotection. *Physiologia plantarum* 163(3): 414-431.

Trapnell C, Williams BA, Pertea G, Mortazavi A, Kwan G, van Baren MJ. (2010). Transcript assembly and quantification by RNA-Seq reveals unannotated transcripts and isoform switching during cell differentiation. *Nature Biotechnology* 28: 511–515.

Tripathi AK, Pareek A, Sopory SK, Singla-Pareek SL. (2012). Narrowing down the targets for yield improvement in rice under normal and abiotic stress conditions via expression profiling of yield-related genes. *Rice* 5(37).

Tsiatsiani L, Heck AJ. (2015). Proteomics beyond trypsin. *The FEBS journal* 282(14): 2612-2626.

Tsukagoshi H, Suzuki T, Nishikawa K, Agarie S, Ishiguro S, Higashiyama T. (2015). RNA-seq analysis of the response of the halophyte, *Mesembryanthemum crystallinum* (ice plant) to high salinity. *PLoS One* 10(2): e0118339.

Türkan I, Demiral T. (2009). Recent developments in understanding salinity tolerance. *Environmental and Experimental Botany* 67(1): 2-9.

Tyers M, Mann M. (2003). From genomics to proteomics. *Nature* 422(6928): 193.

Uarrota VG, Fuentealba C, Hernández I, Defilippi-Bruzzone B, Meneses C, Campos-Vargas R, Lurie S, Hertog M, Carpentier S, Poblete-Echeverría C, Pedreschi R. (2019). Integration of proteomics and metabolomics data of early and middle season Hass avocados under heat treatment*. Food Chemistry*.

Uhrig RG, Schläpfer P, Roschitzki B, Hirsch-Hoffmann M, Gruissem W. (2019). Diurnal changes in concerted plant protein phosphorylation and acetylation in Arabidopsis organs and seedlings. *The Plant Journal*.

UN news. (2013). World must sustainably produce 70 per cent more food by mid-century – UN report. (https://news.un.org/en/story/2013/12/456912)

United Nations. (2017). World Population Prospects: The 2017 Revision. United Nations Department of Economic and Social Affairs. (https://www.un.org/development/desa/en/news/population/world-population-prospects-2017.html) ; (https://population.un.org/wpp/.)

Ünlü M, Morgan ME, Minden JS. (1997) Difference gel electrophoresis. A single gel method for detecting changes in protein extracts. *Electrophoresis* 18(11): 2071-2077.

Upasani V, Desai S. (1990). Sambhar salt lake. *Archives of microbiology* 154(6): 589-593.

Upchurch RG. (2008). Fatty acid unsaturation, mobilization, and regulation in the response of plants to stress. *Biotechnology Letter* 30: 967-977.

Vargas R, Pankova EI, Balyuk SA, Krasilnikov PV, Khasankhanova GM. (2018). Handbook for saline soil management. FAO/LMSU: 2018.

Vega AS, Rúgolo de Agrasar ZE. (2006). Vivipary and pseudovivipary in the Poaceae, including the first record of pseudovivipary in *Digitaria* (Panicoideae: Paniceae). *South African Journal of Botany* 72(4): 559-564.

Vega SE, Del Rio AH, Bamberg JB, Palta JP. (2004). Evidence for the up-regulation of Stearoyl-ACP (Δ9) Desaturase gene expression during cold acclimation. *American Journal of Potato Research* 81: 125-35.

Ventura Y, Eshel A, Pasternak D, Sagi M. (2015). The development of halophyte-based agriculture: past and present. *Annals of Botany* 115(3): 529-540.

Ventura Y, Sagi M. (2013). Halophyte crop cultivation: The case for Salicornia and Sarcocornia. *Environmental and Experimental Botany* 92: 144-153.

Ventura Y, Wuddineh WA, Ephrath Y, Shpigel M, Sagi M. (2010). Molybdenum as an essential element for improving total yield in seawater-grown *Salicornia europaea* L. *Scientia Horticulturae* 126(3): 395-401.

Vera-Estrella R, Barkla BJ, Pantoja O. (2014). Comparative 2D-DIGE analysis of salinity responsive microsomal proteins from leaves of salt-sensitive Arabidopsis thaliana and salt-tolerant *Thellungiella salsuginea*. *Journal of Proteomic*s 111: 113-127.

Very AA, Sentenac H. (2003). Molecular mechanisms and regulation of K+ transport in higher plants. *Annual review of plant biology* 54(1): 575-603.

Vignato BS, Coutinho LL, Cesar AS, Poleti MD, Regitano LC, Balieiro JC. (2019). Gene Co-Expression Network Analysis Associated with Carcass Traits in Nellore Steers. *Meat and Muscle Biology* 1(3): 143.

Viswanath NMK, Ramachandran S. (2018). Unobservable components modelling of monthly average maximum and minimum temperature patterns in India 1981–2015. *Pure and Applied Geophysics*: 1-20.

Wakeel A, Asif AR, Pitann B, Schubert S. (2011). Proteome analysis of sugar beet (Beta vulgaris L.) elucidates constitutive adaptation during the first phase of salt stress. *Journal of Plant Physiology* 168(6): 519-526.

Wakeel A. (2013). Potassium–sodium interactions in soil and plant under saline-sodic conditions. *Journal of Plant Nutrition and Soil Science* 176(3): 344-354.

Wallace A, Frolich E, Lunt OR. (1966). Calcium requirements of higher plants. *Nature* 209(5023): 634.

Wang B, Luttge U, Ratajczak R. (2004). Specific regulation of SOD isoforms by NaCl and osmotic stress in leaves of the C3 halophytes *Suaeda salsa* L. *Journal of Plant Physiology* 161: 285-293.

Wang H, Schauer N, Usadel B, Frasse P, Zouine M, Hernould M, Latché A, Pech JC, Fernie AR, Bouzayen M. (2009). Regulatory features underlying pollination-dependent and-independent tomato fruit set revealed by transcript and primary metabolite profiling. *The Plant Cell* 21: 1428-1452.

Wang J, Meng Y, Li B, Ma X, Lai Y, Si E, Yang K, Xu X, Shang X, Wang H. (2015). Physiological and proteomic analyses of salt stress response in

the halophyte *Halogeton glomeratus*. *Plant Cell and Environment* 38(4): 655-669.

Wang L, Baskin JM, Baskin CC, Cornelissen JHC, Dong M, Huang Z. (2012). Seed dimorphism, nutrients and salinity differentially affect seed traits of the desert halophyte *Suaeda aralocaspica* via multiple maternal effects. *BMC Plant Biology* 12(1): 170.

Wang L, Huang Z, Baskin CC, Baskin JM, Dong M. (2008). Germination of dimorphic seeds of the desert annual halophyte *Suaeda aralocaspica* (Chenopodiaceae), a C4 plant without Kranz anatomy. *Annals of Botany* 102(5): 757-769.

Wang L, Liang W, Xing J, Tan F, Chen Y, Huang L, Cheng CL, Chen W. (2013). Dynamics of chloroplast proteome in salt-stressed mangrove *Kandelia candel* (L.) Druce. *Journal of Proteome Research* 12(11): 5124-5136.

Wang L, Liu X, Liang M, Tan F, Liang W, Chen Y, Lin Y, Huang L, Xing J, Chen W. (2014). Proteomic analysis of salt-responsive proteins in the leaves of mangrove *Kandelia candel* during short-term stress. *PLoS One* 9(1): e83141.

Wang L, Pan D, Li J, Tan F, Hoffmann-Benning S, Liang W, Chen W. (2015). Proteomic analysis of changes in the *Kandelia candel* chloroplast proteins reveals pathways associated with salt tolerance. *Plant Science* 231: 159-172.

Wang L, Sun X, Weiszmann J, Weckwerth W. (2017). System-level and granger network analysis of integrated proteomic and metabolomic dynamics identifies key points of grape berry development at the interface of primary and secondary metabolism. *Frontiers in plant science* 8: 1066.

Wang P, Zhang X, Ma X, Sun Y, Liu N, Li F, Hou Y. (2017). Identification of CkSNAP33, a gene encoding synaptosomal-associated protein from *Cynanchum komarovii*, that enhances Arabidopsis resistance to *Verticillium dahliae*. *PloS one* 12(6): e0178101.

Wang W, Vinocur B, Altman A. (2003). Plant responses to drought, salinity and extreme temperatures: towards genetic engineering for stress tolerance. *Planta* 218(1): 1-14.

Wang W, Yan Z, You S, Zhang Y, Chen L, Lin G. (2011). Mangroves: obligate or facultative halophytes? A review. *Trees* 25(6): 953-963.

Wang X, Chang L, Wang B, Wang D, Li P, Wang L, Yi X, Huang Q, Peng M, Guo A. (2013). Comparative proteomics of *Thellungiella halophila* leaves from plants subjected to salinity reveals the importance of chloroplastic starch and soluble sugars in Halophyte salt tolerance. *Molecular & Cellular Proteomics* 12(8): 2174-2195.

Wang X, Fan P, Song H, Chen X, Li X, Li Y. (2009). Comparative proteomic analysis of differentially expressed proteins in shoots of *Salicornia*

europaea under different salinity. *Journal of Proteomics Research* 8: 3331-3345.

Wang X, Li X, Deng X, Han H, Shi W, Li Y. (2007). A protein extraction method compatible with proteomic analysis for the euhalophyte *Salicornia europaea*. *Electrophoresis* 28(21): 3976-3987.

Wang X, Yang P, Zhang X, Xu Y, Kuang T, Shen S, He, Y. (2009). Proteomic analysis of the cold stress response in the moss, *Physcomitrella patens*. *Proteomics* 9(19): 4529-4538.

Wang Y, Chu Y, Liu G, Wang MH, Jiang J, Hou Y, Qu G, Yang C. (2007). Identification of expressed sequence tags in an alkali grass (*Puccinellia tenuiflora*) cDNA library. *Journal of Plant Physiology* 164(1): 78-89.

Wang Y, Liu K, Liao H, Zhuang C, Ma H, Yan X. (2008). The plant WNK gene family and regulation of flowering time in Arabidopsis. *Plant Biology* 10(5): 548-562.

Wang Z, Wang T. ((2011)). Dynamic proteomic analysis reveals diurnal homeostasis of key pathways in rice leaves. *Proteomics* 11(2): 225-238.

Wang ZL, Li PH, Fredricksen M, Gong ZZ, Kim CS, Zhang C, Bohnert HJ, Zhu JK, Bressan RA, Hasegawa PM. (2004). Expressed sequence tags from *Thellungiella halophila*, a new model to study plant salt-tolerance. *Plant Science* 166(3): 609-616.

Wanichthanarak K, Fahrmann JF, Grapov D. (2015). Genomic, proteomic, and metabolomic data integration strategies. *Biomarker insights* 10: BMI-S29511.

Warnock JW. The politics of hunger: the global food system. Routledge. doi.org/10.4324/9780429296826.

Wasternack C. (2007). Jasmonates: an update on biosynthesis, signal transduction and action in plant stress response, growth and development. *Annals of Botany* 100: 681-697.

Watanabe T, Urayama M, Shinano T, Okada, R, Osaki M. (2015). Application of ionomics to plant and soil in fields under long-term fertilizer trials. *Springer Plus* 4(1): 781.

Waters BM. (2011). Moving magnesium in plant cells. *New Phytologist* 190(3): 510-513.

Weber DJ, Ansari R, Gul B, Khan MA. (2007). Potential of halophytes as source of edible oil. *Journal of Arid Environments* 68: 315-321.

Weis E, Berry JA. (1998). Plants and high temperature stress. *Symposia of the Society for Experimental Biology* 42: 329-346.

Wen X, Qiu N, Lu Q, Lu C. (2005). Enhanced thermotolerance of photosystem II in salt-adapted plants of the halophyte *Artemisia anethifolia*. *Planta* 220(3): 486-497.

Werner AK, Witte CP. (2011). The biochemistry of nitrogen mobilization: purine ring catabolism. *Trends in Plants Science* 16(7): 381-387.

White PJ, Broadley MR. (2003). Calcium in plants. *Annals of botany* 92(4): 487-511.

Whittaker JW. (2012). Non-heme manganese catalase–the 'other' catalase. *Archives of biochemistry and biophysics* 525(2): 111-120.

Williams DG, Hultine KR, Dettman DL. (2014). Functional trade-offs in succulent stems predict responses to climate change in columnar cacti. *Journal of Experimental Botany* 65(13): 3405-3413.

Winter K, Holtum JA. (2007). Environment or development? Lifetime net CO_2 exchange and control of the expression of Crassulacean acid metabolism in *Mesembryanthemum crystallinum*. *Plant Physiology* 143(1): 98-107.

Wise RR, Olson AJ, Schrader SM, Sharkey TD. (2004). Electron transport is the functional limitation of photosynthesis in field-grown pima cotton plants at high temperature. *Plant, Cell & Environment* 27(6): 717-724.

Wold S, Esbensen K, Geladi P. (1987). Principal component analysis. *Chemometrics and intelligent laboratory systems* 2: 37-52.

Wu C, Gao X, Kong X, Zhao Y, Zhang H. (2008). molecular cloning and functional analysis of a Na+/H+ Antiporter gene ThNHX1 from a halophytic plant *Thellungiella halophila*. *Plant Molecular Biology Reporter* 27(1): 1-12.

Wu C, Zhou F, Ren J, Li X, Jiang Y, Ma S. (2019). A Selective review of multi-level omics data integration using variable selection. *High-throughput* 8(1): 4.

Wu HJ, Zhang Z, Wang JY, Oh DH, Dassanayake M, Liu B, Huang Q, Sun HX, Xia R, Wu Y. (2012). Insights into salt tolerance from the genome of *Thellungiella salsuginea. Proceedings of the National Academy of Sciences* 109(30): 12219-12224.

Wu S, Su Q, An LJ. (2010). Isolation of choline monooxygenase (CMO) gene from *Salicornia europaea* and enhanced salt tolerance of transgenic tobacco with CMO genes. *Indian Journal of Biochemistry & Biophysics* 47(5): 298-305.

Wu X, Xiong E, Wang W, Scali M, Cresti M. (2014). Universal sample preparation method integrating trichloroacetic acid/acetone precipitation with phenol extraction for crop proteomic analysis. *Nature protocols* 9(2): 362.

Wungrampha S, Joshi R, Singla-Pareek SL, Pareek A. (2018). Photosynthesis and salinity: are these mutually exclusive? *Photosynthetica* 56(1): 366-381.

Xia J, Wishart DS. (2016). Using MetaboAnalyst 3.0 for comprehensive metabolomics data analysis. *Current Protocols in Bioinformatics* 55: 14-10.

Xian-Zhao L, Chun-zhi W, Qing S, Chao-kul L. (2012). The potential resource of halophytes for developing bio-energy in China coastal zone. *Journal of Agricultural and Food Chemistry* 1(3): 44-51.

Xie X, Pu L, Zhu M, Xu Y, Wang X. (2019). Linkage between soil salinization indicators and physicochemical properties in a long-term intensive agricultural coastal reclamation area, Eastern China. *Journal of Soils and Sediments* 1-9.

Xiong Y, Contento AL, Bassham DC. (2005). AtATG18a is required for the formation of autophagosomes during nutrient stress and senescence in Arabidopsis thaliana. *The Plant Journal* 42: 535-546.

Yadav DN, Sarin MM. (2009). Geo-chemical behaviour of uranium in the Sambhar Salt Lake, Rajasthan (India): Implications to "source" of salt and uranium "sink". *Aquatic Geochemistry* 15(4): 529-545.

Yadav DN. (1997). Oxygen isotope study of evaporating brines in Sambhar Lake, Rajasthan (India). *Chemical Geology* 138(1-2): 109-118.

Yadav NS, Shukla PS, Jha A, Agarwal PK, Jha B. (2012). The SbSOS1 gene from the extreme halophyte *Salicornia brachiata* enhances Na+ loading in xylem and confers salt tolerance in transgenic tobacco. *BMC Plant Biology* 12(188): 1-18.

Yang G, Wang Y, Xia D, Gao C, Wang C, Yang C. (2014). Overexpression of a GST gene (ThGSTZ1) from Tamarix hispida improves drought and salinity tolerance by enhancing the ability to scavenge reactive oxygen species. *Plant Cell, Tissue and Organ Culture* 117(1): 99-112.

Yang XS, Chen GX. (2015). Diurnal changes in gas exchange and chlorophyll fluorescence in Ginkgo leaves under field conditions. *Journal of Animal and Plant Sciences* 25: 309-313.

Yen SK, Chung MC, Chen PC, Yen HE. (2001). Environmental and developmental regulation of the wound-induced cell wall protein WI12 in the halophyte Ice plant. *Plant Physiology* 127(2): 517-528.

Yensen NP, Biel KY. (2006). Soil remediation via salt-conduction and the hypotheses of halosynthesis and photoprotection. In: Khan MA, Weber DJ eds. Ecophysiology of High Salinity Tolerant Plants: Springer Netherlands, 313-344.

Yi X, Sun Y, Yang Q, Guo A, Chang L, Wang D, Tong Z, Jin X, Wang L, Yu J. (2014). Quantitative proteomics of *Sesuvium portulacastrum* leaves revealed that ion transportation by V-ATPase and sugar accumulation in chloroplast played crucial roles in halophyte salt tolerance. *Journal of Proteomics* 99: 84-100.

Yin J, Zhan X, Hain CR, Liu J, Anderson MC. (2018). A method for objectively integrating soil moisture satellite observations and model simulations toward a blended drought index. *Water Resources Research* 54(9):6772-6791.

Yip AM, Horvath S. (2007). Gene network interconnectedness and the generalized topological overlap measure. *BMC Bioinformatics* 8(1): 22.

Yizhak K, Benyamini T, Liebermeister W, Ruppin E, Shlomi T. (2010). Integrating quantitative proteomics and metabolomics with a genome-scale metabolic network model. *Bioinformatics* 26(12): i255–i260.

Yoshizumi T, Tsumoto Y, Takiguchi T, Nagata N, Yamamoto YY, Kawashima M, Ichikawa T, Nakazawa M, Yamamoto N, Matsui M. (2006). Increased level of polyploidy1, a conserved repressor of CYCLINA2 transcription, controls endoreduplication in Arabidopsis. *The Plant Cell* 18(10): 2452-2468.

Yu J, Chen S, Zhao Q, Wang T, Yang C, Diaz C, Sun G, Dai S. (2011). Physiological and proteomic analysis of salinity tolerance in *Puccinellia tenuiflora*. *Journal of Proteome Research* 10(9): 3852-3870.

Yuan F, Lyu MJ, Leng BY, Zhu XG, Wang BS. (2016). The transcriptome of NaCl-treated Limonium bicolor leaves reveals the genes controlling salt secretion of salt gland. *Plant Molecular Biology* 91(3): 241-256.

Yuanyuan M, Yali Z, Jiang L, Hongbo S. (2009). Roles of plant soluble sugars and their responses to plant cold stress. *African Journal of Biotechnology* 8(10): 2004-2010.

Zandalinas SI, Mittler R, Balfagon D, Arbona V, Gomez-Cadenas A. (2018). Plant adaptations to the combination of drought and high temperatures. *Physiologia Plantarum* 162: 2-12.

Zandalinas SI, Sales C, Beltran J, Gomez-Cadenas A, Arbona V, (2016). Activation of secondary metabolism in citrus plants Is associated to sensitivity to combined drought and high temperatures. *Frontiers in Plant Science* 7: 1954.

Zhang B, Horvath S. (2005). A general framework for weighted gene co-expression network analysis. *Statistical Applications in Genetics and Molecular Biology* 4: 17.

Zhang L, Ma XL, Zhang Q, Ma CL, Wang PP, Sun YF, Zhao YZ, Zhng H. (2001). Expressed sequence tags from a NaCl-treated *Suaeda salsa* cDNA library. *Gene* 267: 193-200.

Zhang S, Li N, Gao F, Yang A, Zhang J. (2010). Over-expression of TsCBF1 gene confers improved drought tolerance in transgenic maize. *Molecular Breeding* 26: 455-465.

Zhang X, Liao M, Chang D, Zhang F. (2014a). Comparative transcriptome analysis of the Asteraceae halophyte *Karelinia caspica* under salt stress. *BMC Research Notes* 7: 927.

Zhang X, Lu G, Long W, Zou X, Li F, Nishio T. (2014b). Recent progress in drought and salt tolerance studies in Brassica crops. *Breeding Science* 64(1): 60-73.

Zhang XY, Liang C, Wang GP, Luo Y, Wang W. (2010). The protection of wheat plasma membrane under cold stress by glycine betaine overproduction. *Biologia Plantarum* 54(1): 83-88.

Zhang Y, Lai J, Sun S, Li Y, Liu Y, Liang L, Chen M, Xie Q. (2008). Comparison analysis of transcripts from the halophyte *Thellungiella halophila*. *Journal of Integrative Plant Biology* 50(10): 1327-1335.

Zhao D, Oosterhuis DM, Bednarz CW. (2001). Influence of potassium deficiency on photosynthesis, chlorophyll content, and chloroplast ultrastructure of cotton plants*. Photosynthetica* 39(1): 103-109.

Zhao SJ, Zhang J, Xu YM. (2004). Monitoring of processes with multiple operating modes through multiple principle component analysis models. *Industrial & engineering chemistry research* 43(22): 7025-7035.

Zheng LL, Gao Z, Wang J, Zhang HR, Wang YC. (2014). Molecular cloning and functional characterization of a novel CBL-interacting protein kinase NtCIPK2 in the halophyte *Nitraria tangutorum*. *Genetics and Molecular Research* 13(3): 4716-4728.

Zhou G, Ma BL, Li J, Feng C, Lu J, Qin P. (2010). Determining salinity threshold level for castor bean emergence and stand establishment. *Crop science* 50(5): 2030-2036.

Zhou S, Chen X, Zhang X, Li X. (2008). Improved salt tolerance in tobacco plants by co-transformation of a betaine synthesis gene BADH and a vacuolar Na+/H+ antiporter gene SeNHX1. *Biotechnology letters* 30: 369-376.

Zhu JK. (2003). Regulation of ion homeostasis under salt stress. *Current opinion in plant biology* 6(5): 441-445.

Zhu JQ, Zhang JT, Tang RJ, Lv QD, Wang QQ, Yang L, Zhang HX. (2009). Molecular characterization of ThIPK2, an inositol polyphosphate kinase gene homolog from *Thellungiella halophila*, and its heterologous expression to improve abiotic stress tolerance in *Brassica napus*. *Physiologia Plantarum* 136(4): 407-425.

Zhu Y, Gong H. (2014). Beneficial effects of silicon on salt and drought tolerance in plants. *Agronomy for Sustainable Development* 34(2): 455-472.

Zhu Z, Chen J, Zheng HL. (2012). Physiological and proteomic characterization of salt tolerance in a mangrove plant, *Bruguiera gymnorrhiza* (L.) Lam. *Tree Physiology* 32(11): 1378-1388.

Zierer J, Menni C, Kastenmüller G, Spector TD. (2015). Integration of 'omics' data in aging research: from biomarkers to systems biology. *Aging cell* 14(6): 933-944.

Zor T, Selinger Z. (1996). Linearization of the Bradford protein assay increases its sensitivity: theoretical and experimental studies. *Analytical biochemistry* 236(2): 302-308.

Zoschke R, Nakamura M, Liere K, Sugiura M, Börner T, Schmitz-Linneweber C. (2010). An organellar maturase associates with multiple group II introns. *Proceedings of the National Academy of Sciences* 107(7): 3245-3250.

Zouari N, Ben Saad R, Legavre T, Azaza J, Sabau X, Jaoua M, Masmoudi K, Hassairi A. (2007). Identification and sequencing of ESTs from the halophyte grass *Aeluropus littoralis*. *Gene* 404(1-2): 61-69.

Zrenner R, Stitt M, Sonnewald U, Boldt R. (2006). Pyrimidine and purine biosynthesis and degradation in plants. *Annual Review of Plant Biology* 57: 805-836.